LIVRO DE RESUMOS

EnBraER

VII Encontro Brasileiro de Espectroscopia Raman

Hotel Fonte Colina Verde **São Pedro – SP, 05-08/12/2022**

FabNS HORIBA UNICAMP

FAPESP CytoViva NOWLAB

CAPES CNPq Agilent | Trusted Answers Anton Paar

SUMÁRIO

VII Encontro Brasileiro de Espectroscopia Raman

EnBraER

APRESENTAÇÃO

VII Encontro Brasileiro de Espectroscopia Raman

EnBraER

É com especial prazer que damos as boas-vindas a todos os participantes do VII Encontro Brasileiro de Espectroscopia Raman (EnBraER), realizado em São Pedro, de 05 a 08 de dezembro de 2022!

O Encontro Brasileiro de Espectroscopia Raman (EnBraER) surgiu com o propósito de reunir especialistas, usuários e iniciantes na técnica, em ambiente propício para discussões sobre os desenvolvimentos recentes e perspectivas futuras da técnica e seus desdobramentos.

O I EnBraER foi realizado em dezembro de 2009 em São Pedro, SP, e reuniu pesquisadores de todo o país, contando também com a participação de pesquisadores estrangeiros de renome. O II EnBraER ocorreu em Belo Horizonte, MG, em dezembro de 2011, com grande sucesso e participação de um número significativo de pesquisadores e participantes estrangeiros de prestígio.

Em outubro de 2013, III EnBraER, ocorreu em Fortaleza, CE, e preservando uma característica importante dos eventos anteriores: a grande participação de estudantes, tanto de pós-graduação quanto de graduação, que enriqueceram a discussão dos mais diversos pontos envolvidos no uso da técnica. O IV EnBraER foi realizado em 2015 em Juiz de Fora, MG, e o V EnBraER foi realizado, em 2017, em Campos do Jordão, onde grandes temas da fronteira da espectroscopia Raman foram discutidos para fomentar a interação entre os diferentes grupos de pesquisas no Brasil, na viabilização de compartilhamento de equipamentos e desenvolvimento conjunto de pesquisas e pós-graduação.

O VI EnBraER foi realizado em Belém, PA, em dezembro de 2019, contou com uma expressiva participação de estudantes e pesquisadores e com ampla discussão a respeito dos fundamentos, aplicações e efeitos de intensificação da espectroscopia Raman em problemas de interesse de toda a comunidade científica brasileira.

O VII EnBraER, realizado em dezembro de 2022, retorna a sua sede inicial, em São Pedro, SP, após 13 anos, com uma comunidade científica consolidada e um parque instrumental bastante ampliado, tornando, ainda mais imperioso resgatar os propósitos da criação do evento, ou seja, de *reunir especialistas, usuários e iniciantes na técnica, em ambiente propício para discussões sobre os desenvolvimentos recentes e perspectivas futuras da técnica e seus desdobramentos*. O VII EnBraER, inicialmente previsto para ocorrer em dezembro de 2021, foi adiado em função das restrições impostas pela pandemia de COVID-19 e com a certeza de podermos nos reunir de forma presencial para ampliar e fortalecer as interações entre os pesquisadores, estudantes e expositores.

O interstício entre o VI e VII EnBraER foi marcado por uma pandemia global sem precedentes nos últimos 100 anos, impondo grandes desafios às universidades e institutos de pesquisa, tanto no

sentido da manutenção da formação de qualidade dos estudantes como na manutenção das atividades de pesquisa e pós-graduação. O ensino superior e o sistema de ciência e tecnologia também enfrentaram, junto a pandemia, um severo ataque ao conhecimento científico e contingenciamento de recursos. O corpo docente e de pesquisadores brasileiros fizeram um esforço hercúleo para se adaptar e superar todos e tantos desafios impostos. Tais adversidades prejudicaram o financiamento e o apoio a participação de muitos membros da comunidade Raman, mas a realização do VII EnBraER, com mais de 110 trabalhos apresentados, 5 conferências plenárias (sendo 2 com palestrantes do exterior), 10 palestras longas, 6 palestras técnicas (sendo 3 de palestrantes do exterior) demonstram a resiliência e sucesso da dedicação de toda a comunidade científica brasileira.

Não podemos deixar de registrar a perda, em abril de 2020, do Prof. Ronei Jesus Poppi (UNICAMP), pesquisador atuante na área Raman com abordagem na área analítica e de quimiometria, vítima da COVID-19. Também perdemos, em julho de 2021, o Prof. Oswaldo Luiz Alves (UNICAMP), cujo início da carreira foi fortemente dedicado a espectroscopia, particularmente a espectroscopia Raman. Em 07 de dezembro de 2021, a comunidade científica brasileira perdeu o Prof. Oswaldo Sala, um dos pioneiros da espectroscopia Raman. Como forma de reconhecimento perene ao legado e contribuição do Prof. Sala, o Comitê Organizador propôs, e foi aceito pelo Comitê Científico, a criação do Prêmio “Oswaldo Sala” para “homenagear personalidades que se destacaram em suas contribuições para o desenvolvimento da espectroscopia Raman, em nosso país, e por importantes contribuições à Ciência brasileira”.

Gostaríamos de agradecer aos nossos patrocinadores que tornaram este evento possível! Agradecer ao nosso *staff* por todo suporte na organização e condução do evento e, principalmente, agradecer a todos os participantes que atenderam ao convite (ou puderam atender) e estão presentes abrilhantando o evento. Desejamos a todos, pesquisadores, alunos, cientistas de aplicação e patrocinadores, um excelente evento. Acreditamos que é momento para celebrarmos a superação dos desafios e nos revigorarmos para os desafios que virão!

Um excelente e muito produtivo VII EnBraER à tod@s!

Comitê Organizador do VII EnBraER

Comissão Organizadora Local

VII Encontro Brasileiro de Espectroscopia Raman

EnBraER

Italo Odone Mazali - UNICAMP (Presidente)

Fernando Aparecido Sigoli - UNICAMP

Diego Pereira dos Santos - UNICAMP

Milene Heloisa Martins - UNICAMP

Carlos José Leopoldo Constantino – UNESP

Comitê Científico

VII Encontro Brasileiro de Espectroscopia Raman

EnBraER

Alejandro Pedro Ayala - UFC

Antônio Gomes Souza Filho – UFC

Carlos José Leopoldo Constantino – UNESP

Cristiano Fantini Leite - UFMG

Dalva Lúcia Araújo de Faria – USP

Erlon Henrique Martins Ferreira – INMETRO

Gustavo Fernandes Souza Andrade – UFJF

Herculano da Silva Martinho – UFABC

Italo Odone Mazali – UNICAMP

Luiz Fernando Cappa de Oliveira – UFJF

Marcia Laudelina Arruda Temperini – USP

Paulo Sérgio Pizani – UFSCar

Rômulo Augusto Ando - USP

Sebastião Silva – UnB

Waldeci Paraguassu Feio – UFPA

Realização

VII Encontro Brasileiro de Espectroscopia Raman

EnBraER

UNICAMP

Instituto de Química

Patrocinadores

VII Encontro Brasileiro de Espectroscopia Raman

EnBraER

HORIBA

FabNS

CytoViva®

NOW LAB

Agilent | Trusted Answers

Anton Paar

APOIO

VII Encontro Brasileiro de Espectroscopia Raman

EnBraER

FAPESP

CAPES

CNPq

UNICAMP

PRINCIPAIS TEMAS ABORDADOS

EnBraER

- Desenvolvimentos teóricos, cálculos e simulações.
- Instrumentação e aplicações industriais.
- Espectroscopia Raman não linear.
- Efeitos de intensificação: Raman ressonante, SERS, TERS, campo próximo.
- Espectroscopia Raman resolvida no tempo.
- Microscopia Raman e imagens.
- Atividade óptica Raman.
- Aplicações em ciência dos materiais.
- Aplicações em ciências biomédicas, biológicas e biomoléculas.
- Aplicações em geociências, património cultural, criminalística, meio ambiente e astrobiologia.
- Aplicações em química analítica.
- Técnicas acopladas: LIBS, AFM, EDS, FTIR, STM, etc.
- Controle de qualidade e métodos quimiométricos.

PROGRAMAÇÃO

VII Encontro Brasileiro de Espectroscopia Raman

05 DE DEZEMBRO - SEGUNDA	
14:00 h às 17:00 h	**Entrega do material e registro de participantes (Salão Florestal)**.
16:00 h às 18:00 h	Jogo da Copa do Mundo – Brasil nas Oitavas de Final (Salão Arena Colina).
19:00 h	**ABERTURA do VII EnBraER (Anfiteatro)**
19:20 h	**Plenária 1 (Abertura): Prof. Dr. Antônio Gomes Souza Filho (UFC) –** "A Espectroscopia Raman no Brasil: aspectos históricos e impactos".
20:10 h	**HOMENAGENS**
20:40 h	**JANTAR DE ABERTURA** **oferecido a todos os inscritos**

06 DE DEZEMBRO - TERÇA	
Coordenador Sessão 1: Diego Pereira dos Santos	
8:30 h às 9:20 h	**Plenária 2 – Prof. Alexandre G. Brolo (University of Victoria, Canadá) -** "Ultra-high speed single-particle and single-molecule SERS spectroscopy and imaging".
9:20 h – 9:50 h	**Apresentação Longa 1 – Alejandro Pedro Ayala (UFC) –** "Structure-property relationships in metal halide perovskites".
9:50 h às 10:20 h	**COFFEE-BREAK**
10:20 h às 10:50 h	**Apresentação Longa 2 – Luiz Gustavo Cançado (UFMG) - "**On the development of new Raman spectroscopy technologies for measurement and data analysis of mass-produced graphene".
10:50 h às 11:20 h	**Palestra Técnica 1** – **Thibault Brulé (Horiba, França)** – "New tendencies in Raman Microscopy: Innovative sample scanning methods, artificial intelligence chemometrics and chemical microgeoprocessing".
11:20 h às 11:40 h	**Comunicação Oral 1 - Lucas Carvalho (UFMG) -** "O espalhamento Raman correlacionado Stokes-anti-Stokes: um estudo da influência da largura temporal do pulso de excitação".
11:40 h às 12:00 h	**Comunicação Oral 2 - Anerise de Barros (UNICAMP) -** "Silicon microchannel-driven Raman scattering enhancement to improved gold nanorod functions as a SERS substrates toward single molecule detection of R6G and Thiram".
12:00 h às 14:00 h	**ALMOÇO**
Coordenador Sessão 2: Celly Mieko Shinohara Izumi	
14:00 h às 14:30h	**Palestra Técnica 2** - **Vitor Pena Monken (FabNS)** – "Inovação tecnológica como plataforma habilitadora de novos avanços científicos – o caso do nanoscópio Porto".
14:30 h às 14:50h	**Comunicação Oral 3 - Isabela Santos (USP) - "**Uso combinado de Microscopia Raman e SEM-EDS na análise de obras de arte: Independência ou morte".
14:50 h às 15:10 h	**Comunicação Oral 4 -Niklaus Wetter (IPEN) - "**From micro to nano Raman: new developments in the detection of micro and nanoplastics of marine origin from the Amazon basin to Santos".
15:10 h às 15:30 h	**Comunicação Oral 5 -Mariana Gibin (UEM) - "**Effect of storage solutions on the mineral and organic content of dentin and enamel: a Raman spectroscopy study".
15:30 h às 16:00 h	**COFFEE-BREAK**
16:00 h às 16:30 h	**Apresentação Longa 3 – Airton Abrahão Martin (Universidade Brasil e DermoProbes) - "**Influência de Fatores Endógenos e Exógenos na Pele Humana: Espectroscopia Raman Confocal".
16:30 h às 17:00 h	**Palestra Técnica 3 – José Martins (Anton-Paar, Nanotimize) -"**Determinações quantitativas de excipientes farmacêuticos em comprimidos - estudo comparativo NIR x Raman".
17:00 h às 17:30 h	**Apresentação Longa 4 – Mónica Benicia Mamián López (UFABC) –** "Espectroscopia SERS e Raman aliadas à Quimiometria".
17:30 h às 17:50 h	**Comunicação Oral 6 - Wallance Pazin (UNESP) - "**Direct detection of SARS-CoV-2 antigen based on surface-enhanced Raman scattering (SERS) using machine learning".
17:50 h	**FOTO OFICIAL DO EVENTO**
18:00 h às 19:30 h	**SESSÃO DE PAINÉIS**
19:30 h	**Reunião do Comitê Científico - EnBraER**

07 DE DEZEMBRO - QUARTA	
Coordenador Sessão 3: Carlos José Leopoldo Constantino	
8:30 h às 9:20 h	**Plenária 3 – Prof. Stephanie Reich (Freie Universität Berlin, Alemanha)** –"Raman scattering to probe the interaction of one-dimensional nanostructures".
9:20 h às 9:50 h	**Apresentação Longa 5 – Gustavo Fernandes Souza Andrade (UFJF) – "**Proteção superficial de nanopartículas plasmônicas por óxidos e polímeros naturais para aplicações em SERS".
9:50 h às 10:20 h	**COFFEE-BREAK**
10:20 h às 10:50 h	**Apresentação Longa 6 – Eduardo Granado (UNICAMP) -** "Spin-phonon coupling: Raman scattering as a powerful probe of magnetic materials".
10:50 h às 11:20 h	**Palestra Técnica 4** – **Thibault Brulé (Horiba, França)** – "Strategies to correlate Raman spectroscopy with other techniques for a complete sample characterization".
11:20 h às 11:40 h	**Comunicação Oral 7 - Angela Raba (UFPS, Colômbia) - "**Raman spectroscopic study towards the growth of $CuO/CuWO_4$ heterostructure".
11:40 h às 12:00 h	**Comunicação Oral 8 -Leonardo Furini (UFSC) - "**Detection of thiabendazole pesticide in matrix of food by surface-enhanced Raman scattering (SERS)".
12:00 h às 14:00 h	**ALMOÇO**
Coordenador Sessão 4: Luiz Fernando Cappa de Oliveira	
14:00h às 14:30 h	**Apresentação Longa 7 – Herculano da Silva Martinho (UFABC) –** "Vibrational Spectroscopy and biofluids investigation: from biomarkers to real-time diagnosis".
14:30 h às 15:00h	**Palestra Técnica 5** - **Luciana Pataro (Agilent).** "Identificação Química sem abertura de embalagem utilizando a Espectroscopia Raman com Compensação Espacial (SORS)".
15:00 h às 15:20h	**Comunicação Oral 9 - Quesle Martins (UNIR) -** "Raman and FTIR spectra in nanoemulsion from Carapa guianensis Aubl. oil".
15:20 h às 15:40 h	**Comunicação Oral 10 -Paulo Pizani (UFSCar)-** "$PbO.SiO_2$ glass under high pressure: ex-situ and in-situ Raman analysis".
15:40 h às 16:00 h	**Comunicação Oral 11 -Jéssica Viegas (UFMG) -** "Polarized Raman spectroscopy of monoclinic $(In,Sc)_2Ge_2O_7$ ceramics".
16:00 h às 16:30 h	**COFFEE-BREAK**
16:30 h às 17:00 h	**Apresentação Longa 8 – Rômulo Ando (USP) –** "Espectroscopia Vibracional na Caracterização de Pares Frustrados de Lewis".
17:00 h às 17:30 h	**Palestra Técnica 6 –Sam Lawrence (Cytoviva**). "Multi-modal imaging and analysis - combining darkfield hyperspectral microscopy with confocal Raman microscopy".
17:30 h às 18:00 h	**Apresentação Longa 9 – Javier Erick Lobatón Villa (UNICAMP) –** "Ultrasensitive SERS immunoassay for stress biomarker monitoring and diagnosis".
18:00 h às 19:30 h	**SESSÃO DE PAINÉIS**
20:30 h	**Jantar de Confraternização** **oferecido a todos os inscritos**

08 DE DEZEMBRO - QUINTA	
Coordenador Sessão 5: Fernando Aparecido Sigoli	
8:30 h às 9:20 h	**Plenária 4 – Ado Jorio (UFMG) –** “Nano-Raman Spectroscopy: development, applications and perspectives”.
9:20 h às 9:50 h	**Apresentação Longa 10 – Sebastião William da Silva (UnB) –** “Uso da Espectroscopia vibracional no estudo das interações entre moléculas bioativas e sistemas nanoestruturados aplicados a saúde humana”.
9:50 h às 10:20 h	**COFFEE-BREAK**
10:20 h às 10:40 h	**Comunicação Oral 12 - Antonio Sant'Ana (UFJF) -** "SERS monitoring of the photocatalytic degradation of the fungicide Tebuconazole by hybrid catalyst AgNP/TiO_2".
10:40 h às 11:00 h	**Comunicação Oral 13 - Waldeci Paraguassu (UFPA) -** "High-pressure properties of $(CH_3)_2NH_2PbBr_3$ lead halide perovskite".
11:00 h às 11:50 h	**Plenária 5 (Encerramento) – Prof. Mauro Carlos Costa Ribeiro (USP) –** “Espectroscopia Raman e Transições de Fases de Líquidos Iônicos”.
11:50 h	**Encerramento/Premiação**

PRÊMIO "OSWALDO SALA"

VII Encontro Brasileiro de Espectroscopia Raman

EnBraER

Nascido em Bauru em 29 de junho de 1926, **Oswaldo Sala** fez licenciatura e bacharelado em Física pela Faculdade de Filosofia Ciências e Letras da USP (FFCH-USP) tendo obtido esses graus em 1948. Em 1949 foi contratado como Professor Assistente pelo Instituto Astronômico e Geofísico da USP. No ano seguinte, após um estágio de curta duração no Departamento de Física da Faculdade de Filosofia, Ciências e Letras, foi indicado para contratação pelo Prof. Hans Stammreich, com quem iniciou o doutoramento. A tese de doutorado "*Espectros Raman, Análise Vibracional e Constantes de Força de alguns Compostos de Cromo Hexavalente*" foi defendida em 1961. Começou a trabalhar em regime de dedicação integral à docência e à pesquisa (RDIDP) em 1959; mas antes disso (1955-1958) foi Professor contratado pela Faculdade de Filosofia São Bento (PUC). Torna-se Professor Regente do Departamento de Física da FFCL-USP (1968-1970) e Professor Assistente Doutor agora no Instituto de Química da USP em 1970, assim permanecendo até 1986 quando tornou-se Livre-Docente, título obtido pelo Departamento de Química Fundamental do Instituto de Química da USP. No ano seguinte (1987) ascendeu à posição de Professor Adjunto na mesma Instituição e em 1988 torna-se Professor Titular por concurso realizado no Instituto de Química da USP. Fez estágio de pós-doutoramento no Mellon Institute (Pittsburgh, USA) em 1962/1963.

Foi Vice-Chefe do Departamento de Química Fundamental no período de 1990 a 1993 e Vice-Diretor do IQUSP no período 1994-1996.

É autor do livro *"Fundamentos da Espectroscopia Raman e no Infravermelho", Ed. UNESP, 1996,* que é referência em espectroscopia vibracional, e é organizador e coautor do livro "*Espectroscopia Raman. Princípios e Aplicações*", São Paulo, 1984, 242 páginas (O. Sala, D. Bassi, P.S. Santos, Y. Hase, R.I.M.G. Forneris, M.L.A. Temperini e Y. Kawano), com patrocínio do CNPq. Ainda no âmbito de sua preocupação com a formação de estudantes, publicou alguns artigos sobre espectros atômicos e espectroscopia Raman e também de divulgação: O. Sala, P.S. Santos e M.L.A. Temperini, "*Resultados de alguns estudos sobre o efeito Raman ressonante"*, Química Nova, 1, 3 (1978); O. Sala, Y. Kawano, P.S. Santos e M.L.A. Temperini, "*O Laboratório de Espectroscopia Vibracional Hans Stammreich na Universidade de São Paulo"*, Química Nova, 7, 320 (1984); O. Sala, "*Uma introdução à espectroscopia atômica: o átomo de hidrogênio*", Química Nova, 30, 1773 (2007); O. Sala, *"Uma introdução à espectroscopia atômica: II - o espectro do sódio"*, Química Nova, 30, 2057 (2007); O. Sala. "I_2*: uma molécula didática*". Química Nova, 31, 914 (2008).

Orientou 11 doutorados e 13 mestrados além de incontáveis alunos de Iniciação Científica. Foi membro da Sociedade Brasileira de Química e membro titular da Academia de Ciências da Estado de São Paulo e da Academia Brasileira de Ciências (1996). Recebeu do IQUSP o *"Prêmio Rheinboldt-Hauptmann"* em 1992 e do governo federal

recebeu em 1998 o título de "*Comendador da Ordem Nacional do Mérito Científico"*. Foi também homenageado com a *Medalha "Simão Mathias"* (2000), honraria concedida pela Sociedade Brasileira de Química àqueles que se destacam por suas atividades acadêmicas.

Foi homenageado na ocasião de seu 70º Aniversário com o workshop "*Modern Aspects of Vibrational Spectroscopy*", IQUSP 1996, que originou um número especial no *Journal of the Brazilian Chemical Society* (JBCS) e 10 anos depois foi homenageado com o Curso de Espectroscopia Vibracional Prof. Oswaldo Sala (Vibros I).

As contribuições de Oswaldo Sala para a implantação e desenvolvimento da espectroscopia vibracional no Brasil e América Latina, em especial a espectroscopia Raman, são inquestionavelmente significativas e tiveram impacto determinante na expansão dessa área em nosso país. Junto de Hans Stammreich, fez parte do grupo que desenvolveu uma metodologia capaz de permitir o uso rotineiro da excitação de espectros Raman com comprimentos de onda mais longos, por meio de lâmpadas de hélio e do uso de redes de difração. Após o falecimento do Prof. Stammreich (1969), tornou-se responsável pelo laboratório e a fim de fazer frente às novas demandas de pesquisa, adquiriu em 1970 o primeiro instrumento que operava não mais com lâmpadas, mas sim com lasers. Do ponto de vista da técnica, teve papel pioneiro em investigações sobre o efeito Raman ressonante e, posteriormente, sobre o efeito SERS (*Surface-enhanced Raman Scattering*), além de ter introduzido o uso de matrizes criogênicas de gases inertes em espectroscopia vibracional no Brasil.

Prof. Oswaldo Sala foi um exemplo de dedicação e competência, contribuindo decisivamente para a nucleação de diversos grupos de pesquisa no país, mas, além de tudo isso, foi um exemplo como ser humano. Aqueles que tiveram o prazer de desfrutar de sua companhia sabem que o Homem foi tão grande quanto o Cientista.

Prof. Oswaldo Sala faleceu em 07/12/2021, quase exatos 12 anos após proferir a conferência de abertura do I EnBraER, em 06/12/2009, intitulada "*Os primeiros tempos da espectroscopia Raman no Brasil*", abrindo a série histórica deste encontro. O VII EnBraER estava previsto justamente para ocorrer na primeira semana de dezembro/2021, sendo adiado devido a pandemia de COVID-19. Quis assim o destino, que o pioneiro da espectroscopia Raman no Brasil, partisse no período que tradicionalmente a comunidade Raman brasileira se reúne.

O *"Prêmio Oswaldo Sala" do Encontro Brasileiro de Espectroscopia Raman* tem por objetivo reconhecer o legado do Prof. Sala homenageando personalidades que se destacaram em suas contribuições para o desenvolvimento da espectroscopia Raman, em nosso país, e por importantes contribuições à Ciência brasileira.

O *"Prêmio Oswaldo Sala" do Encontro Brasileiro de Espectroscopia Raman* será outorgado por indicação do Comitê Científico do EnBraER.

Na 1ª. Edição do Prêmio "Oswaldo Sala" do Encontro Brasileiro de Espectroscopia Raman, foram contemplados, por indicação do Comitê Científico:

Prof. Dr. Roberto Ignazio Maria Guglielmo Forneris (USP)

É Bacharel em Física pela Faculdade de Filosofa, Ciência e Letras da Universidade de São Paulo (FFCH-USP, 1949) e Licenciado pela mesma Instituição em 1950, ano em que também fez especialização em Física na mesma unidade da USP. Em 1961 defendeu tese de doutoramento pela Universidade de São Paulo (1961), intitulada "Sobre a espectroscopia Raman na região de comprimentos de onda longos. Os espectros Raman das moléculas halogênicas e inter-halogênicas diatômicas". Foi Prof. Pleno do Centro Estadual de Educação Tecnológica Paula Souza, *Senior Research Associate* da Vanderbilt University, Pesquisador Senior do Centro Técnico Aeroespacial (CTA, São José dos Campos) e *Visiting Research Fellow* da University of Pittsburgh.

A época em que Roberto Forneris iniciou sua carreira na USP (final da década de 1950) não poderia ser mais propícia. De 1942 a 1965, o Depto. de Física da FFCL-USP funcionava em um sobrado na Av. Brigadeiro Luis Antônio e durante o período da Segunda Guerra Mundial as atividades estavam voltadas à pesquisa sobre radiação cósmica e ao esforço de guerra em geral. Hans Stammreich, orientador de Forneris, aproximou-se da USP em 1944 quando o Depto. de Física criou uma equipe envolvida no desenvolvimento de um sonar para a Marinha, e há relatórios dele descrevendo a construção de válvulas de mercúrio e o desenvolvimento de papéis especiais para serem usados em registradores de sonares. Devido, porém, à declaração de guerra à Alemanha, Stammreich só pode ser contratado em 1945, quando a guerra foi encerrada. Tornou-se responsável pela cadeira de Física Superior em 1947, ano em que o Depto. de Física adquiriu um espectrógrafo Raman comercial (Lane-Wells com lâmpada de mercúrio e três prismas de 10 cm de base), com o qual publicou o primeiro artigo usando lâmpada de He em 1950 (Stammreich, H.; Sala, O.; Forneris, R.; An. Acad. Bras. Ciênc. 1950, 22, 307). O comprimento de onda 587,6 nm foi usado para estudar a relação de intensidade entre as bandas Stokes e anti-Stokes do CCl_4 e o mesmo arranjo experimental foi utilizado em um estudo sobre azobenzenos também publicado em 1950 (Stammreich, H.; Experientia 1950, 6, 224) e em 1952 (Stammreich, H.; Forneris, R.I.M.G., Das Raman Spektrumedes P-Benzochingns. Zeitschrift fur Naturforschng, 1952, 7A, 576). No caso do azobenzeno, um trabalho anterior da literatura reportava o estudo dessa substância empregando as linhas amarelas da lâmpada de Hg em 577,0 nm e 579,1 nm (dubleto). Esses comprimentos de onda haviam sido tentados em outros trabalhos do grupo de Stammreich, sem sucesso por causa da fraca intensidade dessas linhas e da absorção da radiação incidente e espalhada pela amostra, no caso de amostra intensamente colorida; além disso, a dispersão recíproca reportada no artigo da literatura era muito baixa (160 Å/mm) e devido a todos esses fatores os autores observaram apenas três bandas Raman para o azobenzeno. A equipe de Stammreich usou então uma lâmpada de He (linha amarela em

578,6 nm) e investigou o azobenzeno como uma solução de concentração 2,5% (volume) em CCl_4; usando tempo de exposição de 20 minutos, ele e sua equipe registraram 12 bandas Raman, duas das quais haviam sido observadas no trabalho anteriormente publicado. A partir daí, o grupo de Stammreich nele incluído Roberto Forneris, instalado no porão do sobrado da Av Brigadeiro Luis Antônio, começou a trabalhar arduamente no desenvolvimento de lâmpadas cada vez mais estáveis e de um espectrógrafo que usasse redes de difração no lugar de prismas devido à sua maior dispersão no vermelho. Em 1955 Stammreich, Forneris e Sone publicam um artigo pioneiro sobre o espectro Raman de dicloreto de enxofre no qual é empregado pela primeira vez um espectrógrafo dotado de redes de difração de transmissão da Bausch & Lomb com brilho (blaze), que apresentava resolução espectral comparável ao do instrumento comercial Lane-Wells com lâmpada de Hg (Stammreich, H.; Forneris, R.; Sone, K.; J. Phys. Chem. 1955, 23, 972. 49). Poucos anos depois (1961), Stammreich e Forneris, usando uma rede de difração adequada (2160 linhas/mm com brilho em 600 nm na primeira ordem da rede) e uma lâmpada de He (587,6 nm) obtiveram o espectro Raman de cloro líquido com resolução espectral entre 0,3 cm^{-1} e 1,5 cm^{-1} o que permitiu separar as contribuições das espécies isotópicas de cloro $^{35}Cl_2$, $^{37}Cl_2$ e $^{35}Cl^{37}Cl$) (Stammreich, H.; Forneris, R.; Spectrochim. Acta 1961, 17, 775).

A partir de 1966, com a conclusão dos laboratórios dos recém criados Institutos de Física e Química foi dada a Stammreich a oportunidade de escolher em qual das duas Unidades gostaria de continuar suas atividades e ele fez sua optou pelo Instituto de Química. Roberto I. M. G. Forneris, entretanto, preferiu continuar ligado ao Instituto de Física, criando lá seu próprio grupo de pesquisa.

Profa. Dra. Márcia Laudelina Arruda Temperini (USP)

Possui graduação em Bacharel em Química pela Universidade de São Paulo (1971), mestrado em Química (Físico-Química) pela Universidade de São Paulo (1974) e doutorado em Química (Físico-Química) pela Universidade de São Paulo (1977). Estagiou na Universidade de Yale com Prof. R. K. Chang (1985) e no Departamento de Química Inorgânica da Universidade De La Plata (1988) com Prof. P.J. Aymonino. Desde 2002 é professora titular da Universidade de São Paulo. Atua principalmente no campo da Espectroscopia Vibracional. Utiliza o efeito Raman ressonante para estudar as propriedades de polímeros condutores e filmes de nanomateriais poliméricos não conjugados naturais, o efeito SERS (Surface Enhanced Raman Scattering) para o entendimento do comportamento de moléculas em sistemas eletroquímicos e em condição de uma única molécula em sistema contendo nanopartículas metálicas. Foi pesquisadora 1A do CNPq, coordenou projetos de pesquisa temático e de infraestrutura FAPESP do Laboratório de Espectroscopia Molecular (LEM).

É membro da Academia de Ciências do Estado de São Paulo e Comendador (2008) da Ordem de Mérito Científico. Entre 2006-2009 foi Presidente da Comissão de Cultura e Extensão do IQUSP e membro titular dessa mesma Comissão entre 2010 a 2012.

Prof. Dr. Marcos Assunção Pimenta (UFMG)

Marcos A. Pimenta possui graduação (1980) e mestrado (1983) em Física pela Universidade Federal de Minas Gerais (1980), doutorado (1987) em Ciências pela Université dOrléans, França, e pós-doutorado (1997-98) no Massachusetts Institute of Technology (MIT), EUA. É pesquisador 1A do CNPq e tem experiência em propriedades ópticas de materiais, atuando principalmente nos seguintes temas: nanomateriais, grafeno, nanotubos, espectroscopia Raman, cristais bi-dimensionais e transições de fase estruturais. É professor titular e atua como professor convidado no Departamento de Física da Universidade Federal de Minas Gerais, onde criou o Laboratório de Espectroscopia Raman em 1992 e introduziu as áreas de pesquisa de nanotubos de carbono e grafeno. Foi um dos criadores e o coordenador geral do Centro de Tecnologia em Nanomateriais e Grafeno (CTNano) da UFMG de 2010 a 2020. É atualmente o coordenador do Instituto Nacional de Ciência e Tecnologia (INCT) de Nanomateriais de Carbono.

É membro titular da Academia Brasileira de Ciências e da "The World Academy of Sciences" (TWAS). Recebeu as seguintes distinções: prêmio Scopus-CAPES 2008, Somyia award de 2009 da IUMRS (International Union of Materials Research Society), prêmio da TWAS em Física de 2013; prêmio Marcos Mares-Guia de 2014 da FAPEMIG/SESTEC; Comendador (2010) e Grã-Cruz (2018) da Ordem de Mérito Científico; Prêmio de Teses CAPES como orientador em Física (2007 e 2018) e em Engenharias IV (2018). Entre 2017 e 2019 foi o presidente da Sociedade Brasileira de Física.

FOTO OFICIAL

VII Encontro Brasileiro de Espectroscopia Raman

CONFERÊNCIAS PLENÁRIAS

VII Encontro Brasileiro de Espectroscopia Raman

“A Espectroscopia Raman no Brasil: aspectos históricos e impactos”

Prof. Dr. Antônio Gomes Souza Filho
Universidade Federal do Ceará

A história da espectroscopia Raman no Brasil acompanha o desenvolvimento da ciência brasileira a partir de 1947. Nessa palestra mostraremos alguns eventos que marcaram a atuação da comunidade brasileira de espectroscopia Raman destacando suas contribuições na formação de recursos humanos, no avanço da ciência e no desenvolvimento de instrumentação.

"Ultra-high speed single-particle and single-molecule SERS spectroscopy and imaging"

Prof. Dr. Alexandre G. Brolo
University of Victoria, Canada

Surface enhanced Raman spectroscopy (SERS) is a well-known and highly-studied effect that effectively represents both the challenges and opportunities inherent to nanophotonics and nanotechnology. This is due to the extremely localized nature of SERS, where intense plasmonic "hotspots" increase Raman scattering by orders of magnitude, generating signals from single molecules. These signals often show significant fluctuations, both in intensity and spectral features due to the dynamic nature of light-matter interaction at the atomic scale. These SERS intensity fluctuations (SIFs) occur over an extremely wide range of timescales, from seconds to micro-seconds. While many mechanisms have been proposed for these fluctuations, such as molecular diffusion or transient plasmonic hotspot generation, the underlying source of these fluctuations are likely to be a complex interplay of several different effects. In this work, we will discuss our results on the measurements of high-speed intensity fluctuations and imaging at the single particle and single molecule level. High-speed spectral information was also obtained using a fast acquisition system capable of taking more than 100,000 spectra per second. Characterization of SERS fluctuations at these speeds can provide further clues as to the source of these fluctuation events.

"Raman scattering to probe the interaction of one-dimensional nanostructures"

Prof. Stephanie Reich
Freie Universität Berlin, Germany

Raman scattering is a powerful tool to study the electronic, vibrational, and optical states of nanoscale materials and the interaction between the various excitations. In my talk I will present an overview over recent experiments in my group on the Raman spectra of single-walled, double-walled and filled carbon nanotubes.I will show how we can quantify the shielding of the hollow core by the nanotube wall and its effect on confined nanosystems such as inserted molecules or a second, inner tube. The combination of two nanotubes in a double-walled species can also be viewed as a one-dimensional Moiré structure. I will consider the effect of the Moiré-like tube-tube interaction on the vibrational and excitonic states of carbon nanotubes. If time permits, I will introduce the concept of exciton-polaritons in carbon nanotubes and examine the role such hybrid light-matter states play in Raman scattering by the tubes. Many puzzling and conflicting observations that have been reported for Raman scattering on nanotubes can be explained naturally when considering polaritons instead of uncoupled excitons as the mediating excitations for resonant Raman scattering in carbon nanotubes.

"Nano-Raman spectroscopy: development, applications and perspectives"

Prof. Ado Jorio
Universidade Federal de Minas Gerais

In this presentation the nano-Raman spectroscopy will be discussed broadly, from the historical development [1] to applications and perspectives. Together with the worldwide picture, the contributions from our group will be addressed, with achievements in areas like single defects [2], spatial field coherence [3,4] and phonon localization in twisted bilayer graphene [5]. Besides the scientific perspective, instrumental development will also be addressed, including our efforts to offer the community a ready-to-use nano-Raman spectrometer.

[1] M.D.D. Costa, L. G. Cançado and A. Jorio. J. of Raman Spectr. 52, 587 - 599 (2021).
[2] I. Maciel et al. Nature Materials 7, 878 - 883 (2008).
[3] R. Beams, L. G. Cancado, A. Jorio and L. Novotny. Phys. Rev. Lett. 113, 186101 (2014).
[4] L. G. Cancado, R. Beams, A. Jorio and L. Novotny. Phys. Rev. X 4, 031054 (2014).
[5] A. C. Gadelha et al. Nature, 590, 405 - 409 (2021)..

“Espectroscopia Raman e transições de fases de líquidos iônicos”

Prof. Mauro Carlos Costa Ribeiro
Universidade de São Paulo

Líquidos iônicos, i.e. sais fundidos em temperatura ambiente (por convenção, Tm < 100 C), apresentam complexa fenomenologia de transição de fases, incluindo cristalização, polimorfismo, eventos antecipando a fusão (*pre-melting*), ou vitrificação e cristalização sob aquecimento do vidro (*cold-crystallization*). Nesta palestra mostraremos como espectroscopia Raman tem sido utilizada em estudos de transições de fases de líquidos iônicos em função da temperatura e pressão. Discutiremos as regiões de frequências baixas do espectro Raman (assim como o espectro far-IR), a qual é devida à dinâmica intermolecular do líquido, e de frequências altas que indicam, por exemplo, mudanças conformacionais das estruturas moleculares dos íons normalmente usados na preparação de líquidos iônicos. No caso de ânion simples e simétrico, a dependência da frequência vibracional com a pressão é reproduzida com modelo de esfera dura e extrapolações de equações de estado empíricas propostas para líquidos iônicos. Curvas de temperaturas de fusão e de transição vítrea em função da pressão, Tm(P) e Tg(P), foram obtidas por espectroscopia Raman usando cela de diamantes (DAC, *diamond anvil cell*) em criostato. A similaridade dTm/dP ≈ dTg/dP observada experimentalmente será discutida com argumentos baseados em termodinâmica de não-equilíbrio. Exemplos serão dados para ilustrar como eventos complexos de *pre-melting* ou transição sólido-sólido, que muitas vezes não são aparentes em medidas calorimétricas, por outro lado são revelados pelos espectros Raman de líquidos iônicos obtidos com diferentes taxas de variação de temperatura e pressão.

Apresentações Longas

VII Encontro Brasileiro de Espectroscopia Raman

"Structure-property relationships in metal halide perovskites"

Prof. Alejandro Pedro Ayala
Universidade Federal do Ceará

The energy conversion efficiency of halide perovskite-based solar cells, which rapidly increased from 3.8% in 2009 to 25.5% in 2021, has drawn attention to a new family of materials for photovoltaic and optoelectronic applications. Among its advantages we can highlight its ease of manufacture, abundance of raw materials, low cost and, in particular, ideal optoelectronic properties. On the other hand, the main disadvantages are the low stability under real working conditions and the predominance of lead in the compositions. Due to this, the search for new materials that allow the development of devices that meet market requirements has been intense. Thus, the term "metal halide organic-inorganic perovskites" has come to describe a large number of structural families, many of which bear little resemblance to the ideal perovskite structure. A prevalent feature in these structures are the metal halide octahedral networks of different dimensionalities (sharing vertices, edges, faces or isolated) responsible for the confinement effects that give rise to the excellent optoelectronic properties. In all cases, the crystal structure determines the properties that can be controlled through induced phase transitions when subjected to various types of perturbations, such as chemical modifications or variation in temperature and/or pressure. In this presentation, several structures based on metal halide networks will be discussed, with special emphasis on the use of Raman spectroscopy in its characterization and study of phase transitions, as well as its correlation with properties relevant to applications, such as photoluminescence.

“On the development of new Raman spectroscopy technologies for measurement and data analysis of mass-produced graphene”

Prof. Luiz Gustavo Cançado
Universidade Federal de Minas Gerais

The advent of nanomaterials has brought several challenges on the materials' characterization framework. These challenges open for opportunities on the development of instruments capable of overcoming today's technological limitations. In Raman spectroscopy, diffraction mimics the capacity of conventional setups to extract spectral information at the nanoscale. In this talk, recent advances on the development of a metrological framework for the characterization of mass-produced graphene based on Raman spectroscopy will be presented. The goal is to create a robust quality control process for assisting the mass production of graphene, in a reproducible and scalable way, following the route of mechanically-assisted chemical exfoliation of natural graphite. The talk will cover the development of new technologies, automation of data analysis and processing, establishment of new protocols and standard operating procedures, and the creation of a real-time analysis Raman system to be incorporated along the production line of a pilot plant. Combined with tip-enhanced Raman spectroscopy (TERS) analysis, the real-time monitoring system revealed that as the average number of layers decreases, more structural defects are introduced in the nanoflakes.

“Influência de fatores endógenos e exógenos na pele humana: espectroscopia Raman confocal”

Prof. Airton Abrahão Martin
Universidade Brasil e DermoProbes

A pele é uma das principais barreiras naturais que impedem a entrada de microrganismos, poluentes e toxinas no corpo humano. A sua composição é determinante para mitigar os efeitos de processos endógenos ou exógenos que causam o envelhecimento cutâneo. Entre os principais componentes que garantem a saúde da pele, podemos destacar o colágeno, que uma vez degradado por inúmeros fatores levam ao processo de envelhecimento de forma mais acelerada. Por isso, atualmente diversos estudos têm proposto a utilização de suplementos com a finalidade de diminuir os efeitos da degradação das fibras colágenas na pele, além dos efeitos hidratantes e imunológicos. Entretanto, grande parte dos resultados de pesquisa apresentados na literatura atualmente utilizam modelos animais e/ou testes invasivos não específicos para verificar estes possíveis efeitos de suplementos. Neste contexto, o objetivo do presente estudo é avaliar por espectroscopia Raman confocal in vivo as mudanças bioquímicas na pele de pessoas diabéticas e saudáveis, antes, durante e após a suplementação contínua.

VII Encontro Brasileiro de Espectroscopia Raman
VII EnBraER
05 a 08/12/2022, São Pedro – SP

"Espectroscopia SERS e Raman aliadas à quimiometria"

Prof. Mónica Benicia Mamián López
Universidade Federal do ABC

A espectroscopia Raman amplificada por superfície (SERS), permite aumentar significativamente a detectabilidade em aplicações analíticas. Do ponto de vista analítico, SERS passou de uma técnica reconhecida pela baixa reprodutibilidade (associada principalmente à síntese de nanopartículas metálicas), até o *status* atual como excelente alternativa analítica, tendo a quimiometria como sua principal aliada. Os métodos e ferramentas quimiométricas têm sido protagonistas quando o problema envolve matrizes complexas com múltiplos componentes ou contribuintes ao espectro SERS e Raman (misturas, matrizes biológicas, processos cinéticos ou imagens), pois além de utilizar o sinal completo ao invés de bandas específicas, modela interferências presentes nas mesmas, e minimiza significativamente procedimentos de preparo de amostra em bancada. Nesta palestra serão mostradas algumas aplicações que combinam a espectroscopia SERS e Raman com métodos quimiométricos.

“Proteção superficial de nanopartículas plasmônicas por óxidos e polímeros naturais para aplicações em SERS”

Prof. Gustavo Fernandes Souza Andrade
Universidade Federal de Juiz de Fora

Apesar das potencialidades da técnica SERS nas mais diversas áreas da química e da ciência de materiais, algumas aplicações são fortemente limitadas pelas variações de intensidade com a agregação descontrolada de nanopartículas usadas como substratos para a técnica. Uma abordagem que vem sendo muito estudada na última década é a utilização de nanopartículas protegidas por óxidos dielétricos ou semicondutores ou polímeros naturais ou sintéticos, que apresentam muito menor tendência à agregação descontrolada, como substratos SERS. Nessa apresentação vão ser discutidos resultados SERS de substratos de nanoesferas e nanobastões recobertas com óxidos de silício e manganês ou por quitosana como substratos, tanto com relação à caracterização do nanomateriais obtidos quanto ao desempenho espectroscópico para o estudo de corantes com diferentes cargas e estruturas químicas. Os resultados indicaram a necessidade de entender diferentes aspectos dos sistemas estudados, como espessura do recobrimento e interações específicas com os modificadores, assim como caminhos para a otimização da intensidade SERS.

"Spin-phonon coupling: Raman scattering as a powerful probe of magnetic materials"

Prof. Eduardo Granado Monteiro da Silva
Universidade Estadual de Campinas

The magnetic exchange energy is highly dependent on the bond distances and angles in a given material, meaning that lattice vibrations are capable of modulating such energy. This leads to temperature-dependent phonon shifts associated with magnetic ordering/correlations that depends not only on the detailed microscopic magnetic arrangement but also on the nature of the magnetic coupling mechanism. Over the last 25 years, spin-phonon spectroscopy has become a powerful probe of magnetic materials in a microscopic level. In this talk, I will show how this technique has been employed to gain insight into a number of quantum magnetic materials, from colossal magnetoresistance manganites to multiferroic oxides, double perovskites and spin-orbit iridates, also showing some prospects on how the spin-phonon coupling can contribute to the investigation of heterogeneous magnetic materials from the nano to the mesoscale.

"Vibrational spectroscopy and biofluids investigation: from biomarkers to real-time diagnosis"

Prof. Herculano da Silva Martinho
Universidade Federal do UFABC

In this talk we will revise some key concepts related to the potential of liquid biopsy as a valuable tool for implementation of precision medicine. It will be discussed some recent advances obtained in our research group related to infectious and cardiovascular diseases.

VII Encontro Brasileiro de Espectroscopia Raman
VII EnBraER
05 a 08/12/2022, São Pedro – SP

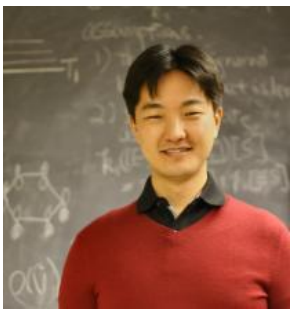

“Espectroscopia vibracional na caracterização de pares frustrados de Lewis”

Prof. Rômulo Ando
Universidade de São Paulo

Um aduto clássico de Lewis é formado quando há uma ligação covalente entre um ácido e uma base de Lewis. Quando a formação do aduto é impedida por efeitos estéricos, o sistema molecular é denominado de par frustrado de Lewis. Os pares frustrados de Lewis (FLPs) tem ganhado destaque na área de catálise, pois são sistemas não metálicos capazes de ativar moléculas pequenas como H_2 e CO_2. Devido às fracas interações entre as espécies, evidências experimentais para comprovar a existência dos FLPs são bastante limitadas. Neste seminário será demonstrada a aplicação da espectroscopia vibracional na caracterização de pares frustrados de Lewis, tanto via espectroscopia Raman ressonante como por infravermelho (IR). Além disso, serão apresentados resultados de cálculos computacionais baseados na teoria do funcional da densidade (DFT) para auxiliar a interpretação dos dados experimentais.

"Ultrasensitive SERS immunoassay for stress biomarker monitoring and diagnosis"

Prof. Javier Erick Lobatón Villa
Universidade Estadual de Campinas

Globalization, living style, work competition, and pandemic, are some the main reasons of the alarming increased levels of human stress worldwide. Accordingly, reliable methods capable to routinely monitor stress are necessary to improve the global life quality. Cortisol is a steroid hormone that plays an important role to trigger the human stress response in challenging, threatening, or startling situations, and is therefore considered the main stress biomarker. In this presentation, the rational design of a cortisol biosensor by combining a highly sensitive analytical technique (surface-enhanced Raman spectroscopy, SERS) and a specific assay (competitive immunoassay) will be described. Special attention will be devoted to the synthesis and surface modification of sensitive SERS nanotags (stars, spheres and rods), the use of different capture agents and the influence of plasmonic coupling on the performance of the sensor. A critical comparison among the proposed SERS immunoassay and well-developed analytical techniques, such as high-performance liquid chromatography coupled to mass spectrometry (HPLC-MS) and ELISA, will be addressed. Finally, the applicability of this SERS-based technology for monitoring human stress levels, cortisol-related disorders (Cushing's syndrome and Addison's disease) and other potential analytical applications will be discussed.

"Uso da Espectroscopia vibracional no estudo das interações entre moléculas bioativas e sistemas nanoestruturados aplicados a saúde humana"

Prof. Sebastião William da Silva
Universidade de Brasília

A ciência e a tecnologia em escala nanométrica compõem atualmente um campo de fronteira multi- e interdisciplinar com grande potencial tecnológico. A medicina atual vem empregando esforços para desenvolver sistemas nanoestruturados a serem utilizados no diagnóstico, tratamento e cura dos mais variados tipos de cânceres e infecções. Estes sistemas são geralmente construídos a partir do acoplamento de drogas ou biomoléculas a materiais nanoestruturados. No entanto, para tornar essas aplicações (marcadores biológicos e sistema para entrega de drogas, por exemplo) tão eficazes quanto possível, é essencial conhecer as propriedades físico-químicas da interface partículas/cobertura. As espectroscopias vibracionais, como as espectroscopias Raman e FTIR, são particularmente sensíveis às mudanças decorrentes das interações inter- e intramoleculares, pois estas interações levam a mudanças nas propriedades físicas e químicas do sistema nanoparticulado. As informações adquiridas nos espectros vibracionais permitem correlacionar as alterações químicas, conformacionais e estruturais sofridas pelas moléculas decorrentes do seu processo de interação. Portanto, as alterações espectrais podem ser usadas para estudar os efeitos diretos ou indiretos da interação molecular em virtudes de ligações inter- ou intramolecular de grupos químicos tais como hidroxila ou amino, bem como alterações mediadas por cátions ou ânions presentes na superfície das nanopartículas. Neste trabalho apresentaremos alguns resultados envolvendo a adsorção de moléculas bioativas em diferentes sistemas nanoparticulados. Por exemplo, os dados espectroscópicos evidenciam que moléculas lipídicas exercem papel importante no arranjo espacial das cadeias de hidrocarbonetos que compõem nanoemulsões à base de lecitina. Em complemento, o estudo da bioconjugação de anticorpos na superfície de nanopartículas de ouro, utilizadas na detecção do vírus SARS-CoV-2, indicaram que o efeito doador de elétrons dos grupos NH_2 livres, assim como os íons carboxilato, são responsáveis por acoplar o anticorpo ao terminal éster succinimidil, presentes na superfície da NP de ouro, de modo a formar uma ligação amida pelo ataque nucleofílico da amina no carbono carbonílico do éster.

Palestras Técnicas

VII Encontro Brasileiro de Espectroscopia Raman

"New tendencies in raman microscopy : innovative sample scanning methods, artificial intelligence chemometrics and chemical microgeoprocessing"

Dr. Thibault Brulé

Global Product Specialist / Raman Influencer, HORIBA, France

In this talk you will learn the basic principles of applied Raman spectroscopy and Raman imaging (the importance of spectral and spatial resolutions for image generation) and discover the new tendencies applied on Raman microscopy. Theory, application and instrumentation will be the main topics for a wide range of materials characterization, including polymers, drugs, biomaterials, life sciences and two-dimensional (2D) materials. Raman microscopy is one of the only techniques capable of providing accurate, non-destructive analysis combined with high resolution images. Raman spectroscopy provides valuable information about the sample studied, such as chemical and structural composition. Based on the light-matter interaction, the Raman technique can perform characterizations through mapping measurements, obtaining relevant information, such as: particle distribution, homogeneity, grain size, phase changes and several other characteristics of the sample through the chemical evaluation of the material. The effects of chemical bonding, deformation and crystal size will be covered and we will show you how to measure and image these features. In addition, we will discuss combined laser-excited photoluminescence and Raman scattering images of two-dimensional (2D) crystals to reveal the spatially variable solid-state structure of these materials. The topics and content will be valuable to researchers in industry and academia, materials scientists, characterization chemists and physicists, professors and graduate students.

VII Encontro Brasileiro de Espectroscopia Raman
VII EnBraER
05 a 08/12/2022, São Pedro – SP

"Inovação tecnológica como plataforma habilitadora de novos avanços científicos – o caso do nanoscópio Porto"

Vitor Pena Monken
FabNS

Inovação em equipamentos científicos e ferramentas de software são não apenas grandes catalisadores do avanço da fronteira na pesquisa de base, mas fundamentais para o avanço na indústria e de aplicações, e com impactos diretos em toda sociedade. Assim como o microscópio óptico expandiu o conhecimento humano para o mundo da microbiologia, sistemas capazes de realizar imagens ópticas abaixo do limite de difração da luz têm demonstrado potencial disruptivo. A espectroscopia Raman melhorada por sonda (TERS, do inglês tip-enhanced Raman spectroscopy) viabiliza a aplicação dessa importante técnica espectroscópica a sistemas em escala nanométrica, possibilitando resolvê-los opticamente com resolução que ultrapassa o limite de difração da luz. Avanços recentes na instrumentação, na produção de nanoantenas ressonantes de alto desempenho e em ferramentas de software para análise de dados podem, em conjunto, fomentar pesquisas em nanociência e na nanotecnologia. O presente trabalho tem como objetivo aprofundar nos avanços tecnológicos que viabilizaram o uso robusto da técnica TERS e apresentar alguns resultados obtidos com esse sistema na análise de grafeno, nanodispositivos e materiais biológicos.

VII Encontro Brasileiro de Espectroscopia Raman
VII EnBraER
05 a 08/12/2022, São Pedro – SP

“Determinações quantitativas de excipientes farmacêuticos em comprimidos - estudo comparativo NIR x Raman”

Dr. José Martins
Antor-Paar, Nanotimize

Uma das tendências no processo de inovação da indústria de equipamentos tem sido a miniaturização, um dos desafio das últimas décadas. Essas iniciativas têm trazido muitas possibilidades de aplicação desse novos instrumentos em muitos mercados, traduzindo-se numa avalanche de dados químicos que precisam ser analisados de forma criteriosa. Existe nesse sentido a necessidade de observar as normativas regulatórias para cada segmento de mercado de forma específica e o segmento farmacêutico oferece amplas possibilidades de aplicação, objetivando atender ao desenvolvimento de novos produtos farmacêuticos de maneira rápida, segura e a menor custo. Esse trabalho tem por objetivo apresentar um racional de modelagem, por técnicas de análise multivariada, aplicado a dados obtidos por dois instrumentos distintos para o mesmo conjunto amostral. Os resultados obtidos demonstram equivalência e convergência para o caso aplicado e em total aderência às normas regulatórias vigentes (Famacopeia Brasileira, United State Pharmacopeia, European Pharmacopeia, etc.). O racional abrange o atendimento das normativas, suas condições de restrição as quais foram aplicadas desde a concepção do planejamento amostral (por Design of Experiment - DoE) bem como no tratamento dos dados, a modelagem propriamente dita, na busca de métodos de predição validáveis e de fácil aplicação na rotina laboratorial.

"Strategies to correlate Raman spectroscopy with other techniques for a complete sample characterization"

Dr. Thibault Brulé
Global Product Specialist / Raman Influencer, HORIBA, France

In this talk you will learn how the information from Raman spectroscopy can be linked to information provided by other techniques like AFM, X-Ray Fluorescence or SEM, using different strategies of colocalization. Theory, application and instrumentation will be the main topics for a wide range of materials characterization, including polymers, biomaterials, life sciences and two-dimensional (2D) materials. Raman imaging is one of the only techniques capable of providing a non-destructive molecular analysis with no or very low sample preparation with high resolution images. Raman spectroscopy provides valuable information about the sample studied, such as chemical and structural composition. Based on the light-matter interaction, the Raman technique can perform characterizations through mapping measurements, obtaining relevant information, such as: particle distribution, homogeneity, grain size, phase changes and several other characteristics of the sample through the chemical evaluation of the material. All of these information are very valuable especially when they are combined with elemental or physical information provided by other techniques. Thus, it can be applied in several areas of knowledge, such as pharmaceuticals, photovoltaics, graphene, cells, nanoparticles, microplastics, among others. The topics and content will be valuable to researchers in industry and academia, materials scientists, characterization chemists and physicists, professors and graduate students.

HORIBA

"Identificação Química sem abertura de embalagem utilizando a Espectroscopia Raman com compensação espacial (SORS)"

Dra. Luciana Foltram Pataro
Molecular Spectroscopy Product Specialist at Agilent Technologies

Nessa apresentação, apresentaremos a Espectroscopia Raman com Compensação Espacial (SORS) e como ela permite realizar análises Raman através de diferentes tipos de embalagens, de frascos de vidro transparente a embalagens de papel multicamada. A tecnologia SORS trabalha através de muitos milímetros de material, permitindo análises químicas precisas por meio de barreiras como papel, vidro, plástico, tecido e até pele. O método não requer conhecimento prévio da embalagem ou material de superfície e não requer contato físico direto. Essa tecnologia permite a análise das amostras sem necessidade de abertura de embalagens, reduzindo o tempo e o custo das análises.

Agilent | Trusted Answers

"Multi-modal imaging and analysis - combining darkfield hyperspectral microscopy with confocal Raman microscopy"

Dr. Sam Lawrence
C.E.O. at CytoViva, USA

This talk will explore the unique advantages offered by the multi-modal combination of Enhanced Darkfield Hyperspectral microscopy and Confocal Raman microscopy. Enhanced Darkfield optical imaging allows users to observe nano-scale entities as small as 10 nm. When combined with Hyperspectral image analysis, these entities can be spectrally characterized and mapped at the pixel level, with pixels as small as 128 nm2, in a variety of translucent matrices. Combining this technique with Confocal Raman microscopy on the same imaging platform leverages the optical and spectral clarity of Enhanced Darkfield Hyperspectral imaging with the molecular specificity of Confocal Raman microscopy while allowing data collection, analysis and compositional verification to occur in minutes rather than hours. Various applications of this multi-modal capability will be discussed with a special emphasis on life sciences.

Comunicações Orais

VII Encontro Brasileiro de Espectroscopia Raman

Comunicação Oral 1 - - "O espalhamento Raman correlacionado Stokes-anti-Stokes: um estudo da influência da largura temporal do pulso de excitação".

Lucas Valente de Carvalho (UFMG)

Comunicação Oral 2 – "Silicon microchannel-driven Raman scattering enhancement to improved gold nanorod functions as a SERS substrates toward single molecule detection of R6G and Thiram".

Anerise de Barros Riul (UNICAMP)

Comunicação Oral 3 - "Uso combinado de Microscopia Raman e SEM-EDS na análise de obras de arte: Independência ou morte".

Isabela Ferreira Sodré dos Santos (USP)

Comunicação Oral 4 – "From micro to nano Raman: new developments in the detection of micro and nanoplastics of marine origin from the Amazon basin to Santos".

Niklaus Ursus Wetter (IPEN)

Comunicação Oral 5 – "Effect of storage solutions on the mineral and organic content of dentin and enamel: a Raman spectroscopy study".

Mariana Sversut Gibin (UEM)

Comunicação Oral 6 – "Direct detection of SARS-CoV-2 antigen based on surface-enhanced Raman scattering (SERS) using machine learning".

Wallance Moreira Pazin (UNESP)

Comunicação Oral 7 – "Raman spectroscopic study towards the growth of CuO/$CuWO_4$ heterostructure".

Angela Mercedes Raba Paez (UFPS, Colômbia)

Comunicação Oral 8 – "Detection of thiabendazole pesticide in matrix of food by surface-enhanced Raman scattering (SERS)".

Leonardo Negri Furini (UFSC)

Comunicação Oral 9 – "Raman and FTIR spectra in nanoemulsion from Carapa guianensis Aubl. oil".

Quesle da Silva Martins (UNIR)

Comunicação Oral 10 – "$PbO.SiO_2$ glass under high pressure: ex-situ and in-situ Raman analysis".

Paulo Sérgio Pizani (UFSCar)

Comunicação Oral 11 – Polarized Raman spectroscopy of monoclinic $(In,Sc)_2Ge_2O_7$ ceramics".

Jéssica Ivone Viegas (UFMG)

Comunicação Oral 12 – "SERS monitoring of the photocatalytic degradation of the fungicide Tebuconazole by hybrid catalyst $AgNP/TiO_2$".

Antonio Carlos Sant'Ana (UFJF)

Comunicação Oral 13 – "High-pressure properties of $(CH_3)_2NH_2PbBr_3$ lead halide perovskite".

Waldeci Paraguassu Feio (UFPA)

Trabalhos Premiados

VII Encontro Brasileiro de Espectroscopia Raman

Au nanostars as inkjet printing SERS substrate for the detection of molecules of biological and environmental interest

Edison H. Montoya (PG) *[1], Lucas F. Oliveira Fernando[1], A. Sigoli (PQ)[1], Italo O. Mazali (PQ)[1]

Investigação SERS do inseticida fosmete em superfícies de Ag e Au

Larissa A. B. Ferreira (IC), Clara de Jesus Rangel (PG), Mari F. Nicolas (PG), Rômulo A. Ando (PQ)*

Silicon microchannel-driven Raman scattering enhancement to improved gold nanorod functions as a SERS substrate toward single molecule detection of R6G and Thiram

Jaciara Bär (PG), [1] Anerise de Barros (PQ),[1*] Davi H. S. de Camargo (PQ),[2] Mariane P. Pereira (PQ),[3] Leandro Merces (PQ),[3] Flavio M. Shimizu (PQ),[3] Fernando A. Sigoli(PQ),[1] Carlos C. B. Bufon (PQ),[2] Italo O. Mazali (PQ)[1,*]

SERS detection of acephate pesticide degradation product: methamidophos

Maíza S. Ozório* (PQ), Rafael J. G. Rubira (PQ), Cibely S. Martin (PQ), Luis F. C. Morato (PG) and Carlos J. L. Constantino (PQ)

Espectroscopia vibracional e reologia de solventes eutéticos profundos baseados em ureia e sais de colina

Ícaro F. T. de Souza (PG)[1]*, Mauro C. C. Ribeiro (PQ)[1]

Porous liquids of ZIF-67 with gemini ionic liquids based on benzylammonium acetate for CO_2 adsorption.

Ahmed D. Páez (PG),[1] Nicolas Keppeler (PG),[2] Omar A. El Seoud (PQ),[2] Rômulo A. Ando (PQ)[1,*].

Defect Engineering Control on Lanthanum-Doped Ceria Nanoparticles for the Oxidative Coupling of Methane

Fabiane J. Trindade (PQ), Bria Cisi (IC),[1] Daniele C. Ferreira (PQ),[1] Andre S. Ferlauto,[1]

O espalhamento Raman correlacionado Stokes-anti-Stokes: um estudo da influência da largura temporal do pulso de excitação.

Lucas V. Carvalho (PG),[1] Tiago A. Freitas (PG),[2] Paula D. Machado (PG),[1] Raul Corrêa (PG),[1] Carlos H. Monken (PQ),[1] Marcelo F. Santos (PQ),[3] Ado Jorio (PQ)[1,*]

Trabalhos Apresentados

VII Encontro Brasileiro de Espectroscopia Raman

VII Encontro Brasileiro de Espectroscopia Raman
VII EnBraER
05 a 08/12/2022, São Pedro – SP

Oswaldo Sala e o desenvolvimento da espectroscopia Raman no Brasil e na América Latina

Dalva L. A. de Faria (PQ), Marcia L. A. Temperini (PQ)

mlatempe@iq.usp.br

Departamento de Química Fundamental, Instituto de Química, USP

Palavras Chave: *Oswaldo Sala, Raman ressonante, SERS*

Highlights

Oswaldo Sala and the development of Raman spectroscopy in Brazil and Latin America. The history of Raman spectroscopy in Brazil goes back to the 1940's and in the 1970's landmark contributions in the study of resonance Raman and SERS effects were given, orchestrated by Oswaldo Sala.

Resumo/Abstract

As contribuições de Oswaldo Sala para a implantação e desenvolvimento da espectroscopia vibracional no Brasil e América Latina, em especial a espectroscopia Raman, são inquestionavelmente significativas e tiveram impacto determinante na expansão dessa área em nosso país. Junto de Hans Stammreich, fez parte do grupo que desenvolveu uma metodologia capaz de permitir o uso rotineiro da excitação de espectros Raman com comprimentos de onda mais longos, por meio de lâmpadas de hélio estáveis e do uso de redes de difração. Após o falecimento do Prof. Stammreich (1969), tornou-se responsável pelo Laboratório de Espectroscopia Molecular (LEM) e, a fim de fazer frente às novas demandas de pesquisa, adquiriu em 1970 o primeiro instrumento que operava não mais com lâmpadas, mas sim com lasers (Jarrell-Ash 25-300). Com isso o grupo de pesquisa por ele comandado, teve papel pioneiro em investigações sobre o efeito Raman ressonante e, posteriormente, sobre o efeito SERS (Surface Enhanced Raman Scattering), além de ter introduzido o uso de matrizes criogênicas de gases inertes em espectroscopia vibracional no Brasil.

Os estudos envolvendo o efeito Raman ressonante foram iniciados em 1974 com a observação da variação na intensidade relativa de algumas bandas nos espectros Raman do Cu_3PS_4, no estado sólido, obtidos com radiações de comprimentos de onda distintos. A análise dos resultados obtidos mostrou que as intensidades das bandas dependiam tanto da frequência da radiação excitante como da espalhada.

O acaso teve papel importante para o início das investigações sobre o efeito SERS, uma vez que o tubo de laser de Ar^+ deixou de funcionar comprometendo as atividades do laboratório, na ocasião bastante focadas no efeito Raman ressonante. Na época, a literatura apontava para um novo efeito de intensificação de espalhamento Raman, denominado efeito SERS, promovido pela interação de determinadas moléculas com superfícies rugosas de Au, Cu e Ag. As superfícies de cobre e ouro eram convenientemente estudadas com linhas laser no vermelho, como a 647,1 nm disponível no LEM. A partir daí importantes contribuições foram dadas à compreensão do efeito, principalmente através de superfícies geradas eletroquimicamente. Um dos pontos verificados foi a dependência do potencial de máxima intensidade das bandas do adsorbato com a radiação excitante e a sua conformação de adsorção.

Oswaldo Sala foi um exemplo de dedicação e competência, contribuindo decisivamente para a nucleação de diversos grupos de pesquisa no país mas, além de tudo isso, foi um exemplo como ser humano. Aqueles que tiveram o prazer de desfrutar de sua companhia sabem que se o cientista foi grande, o homem foi ainda maior.

Agradecimentos/Acknowledgments

À Fundação de Amparo à Pesquisa do Estado de São Paulo (FAPESP), processo nº 2016/21070-5.

Raman and FTIR spectra in nanoemulsion from *Carapa guianensis Aubl.* oil

Quesle S. Martins(PQ)[1*], Laffert G.F. Silva(PQ)[2], Roberta L. Cristina(IC)[1], Asaf Ribas(IC)[1], Duíllio L.L. de Oliveira(IC)[1]

quesle.martins@unir.br

[1]*Fundação Universidade Federal de Rondônia, UNIR.*
[2]*Instituto Federal de Educação de Rondônia - IFRO*

Palavras Chave: Nanoemulsion, Amazonian Oil, Vibrational spectroscopy, DFT method

Highlights

Nanoemulsion based on andiroba oil (*Carapa guianensis Aubl.)*;
Carapa Guianensis Raman and FTIR;
Raman and FTIR nanoemulsion;
DFT vibrational signatures of the oleic acid molecule.

Resumo/Abstract

Raman spectroscopy (RS) and Fourier transform infrared (FTIR) as a proposal for a vibrational characterization of *Carapa Guianensis Aubl*. essential oil in natura (CGEO) and polymerized (CGPO) and of magnetic nanoemulsion (CGNE) (Figura 1). Calculation of computational chemistry based on the method Density Functional Theory (DFT) with B3LYP/6-311+G(d,p) was used to obtain theoretical frequencies and vibrational signatures of the oleic acid molecule. Results of RS and FTIR confirm bands of CGEO present in CGPO and CGNE studied. DFT method shows that the bands 1099 cm^{-1}, 1714 cm^{-1} and 1812 cm^{-1} explain the presence of vibrational modes of oleic acid in the samples [1-3].

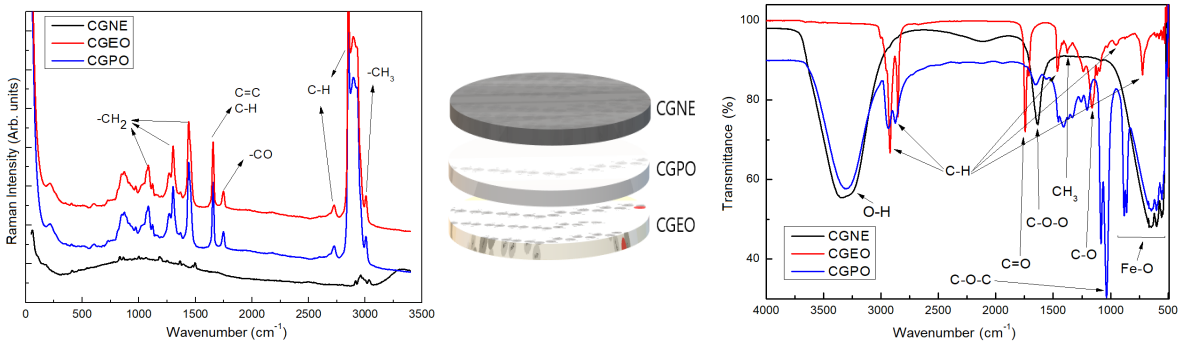

Figura 1: À esquerda: Espectros Raman Raman (Labram HR 800/633.5 nm/UFMT); Centro: Resumo gráfico; À direita: Espectros Infravermelho (SHIMADZU FTIR-IR-Prestige-2/GON - UFAL).

[01] Q.S. Martins, L.M.S. Santos, J.L.B. Faria, Vib. Spectrosc., (2020) https://doi.org/10.1016/j.vibspec.2019.102986
[02] P. Larkin (Peter J.), Infrared and Raman spectroscopy. Elsevier Inc. (2011)
[03] L.G. Silva, T.A. Beleza, J.G. Santos, L.B. Silveira, Int. J. Inn. Education and Research, (2020) 418–425. https://doi.org/10.31686/ijier.vol8.iss6.2435

Agradecimentos/Acknowledgments

The authors acknowledges the Program in Nanoscience Nanobiotechnology – UnB, Optics and Nanoscopy Group (GON) - UFAL, Laboratório de Espalhamento de Luz - UFMT, Federal Institute of Education of Rondônia – IFRO. The Grupo de Pesquisa em Física Experimental e Aplicada - UNIR and Estrutura da Matéria e Física Computacional - DAF/JP - UNIR.

Raman em óleo de castanha-do-Brasil: introdução ao estudo de ácidos graxos

Roberta L. Cristina (IC)[1*], Asaf Ribas(IC)[1], Duíllio L.L. de Oliveira(IC)[1], Quesle S. Martins (PQ)[1]

robertajpro@gmail.com

[1] *Fundação Universidade Federal de Rondônia, UNIR.*

Palavras Chave: Espectro Raman, método DFT, óleo vegetal, ácidos graxos

Highlights

DFT in oleic acid: Introduction to vibrational spectroscopy and conformational analysis of fatty acids. Raman spectrum of vegetable oil from the amazon; Study of fatty acids in vegetable oils; Calculation ab initio: DFT method

Resumo/Abstract

O estudo reúne Raman experimental em óleo de castanha-do-Brasil (Brazil nuts oil - BNO) e Raman teórico de ácido oleico. A proposta introduz o processo de análise vibracional de amostras ricas em ácidos graxos, comuns em óleos vegetais. Uma identificação dos modos vibracionais experimentais e teóricos foi efetuada. Espectro experimental foi obtido com Raman Labram HR 800 (Instituto de Física - UFMT) e teórico, no programa Gaussian 09. Otimização da geometria com conjunto de base 6-31g e funcional de densidade (B3LYP) foram utilizados. A energia de conformação foi de -855.407645 Hartree. Os resultados obtidos foram espectro vibracional do material estudado, a energia de conformação, frequência teórica ou calculadas, otimização, modos vibracionais, fórmula de estrutura molecular.

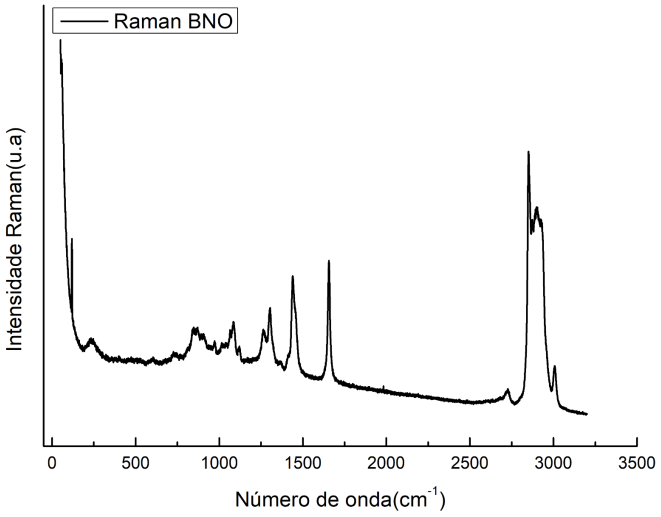

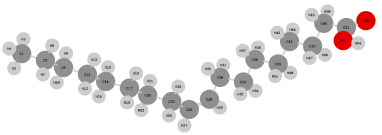

Molécula ácido oleico

[01] Q.S. Martins, L.M.S. Santos, J.L.B. Faria, Vib Spectros, (2020) https://doi.org/10.1016/j.vibspec.2019.102986
[02] P. Larkin (Peter J.), Infrared and Raman spectroscopy. Elsevier Inc. (2011)
[03] Mariko; I. S. Menezes; H. S. Barroso; S. P. Zanotto; C. R. F. Carioca. Acta Amaz. 43, 4 (2013) https://doi.org/10.1590/S0044-59672013000400012

Agradecimentos/Acknowledgments

Agradecemos ao PIBIC/UNIR. Ao Laboratório de Espalhamento de Luz - UFMT e Laboratório Estrutura da Matéria e Física Computacional DAF/JP - UNIR. À INOVAM BRASIL LTDA pela amostra cedida.

DFT em glicerol: Introdução a espectroscopia vibracional e análise conformacional

Duíllio L.L. de Oliveira (IC)[1*], Roberta L. Cristina (IC)[1], Asaf Ribas(IC)[1], Quesle S. Martins (PQ)[1]

duillio.lopes@gmail.com

[1] *Fundação Universidade Federal de Rondônia, UNIR.*

Palavras Chave: Espectro Raman, Métodos DFT, Análise conformacional, Lipídios.

Highlights

DFT in glycerol: Introduction to vibrational spectroscopy and conformational analysis.
Ab initio calculations: Geometry optimization and frequency calculation;
Study of the lowest energy conformer of each molecule performed at DFT/B3LYP/6–311G (d,p)

Resumo/Abstract

O estudo permite a aplicação do nível DFT (Density Functional Theory) juntamente com funcional B3LYP e conjunto de base 6-311G, difusos e polarizados à molécula de glicerol, como parte de aprimoramento na identificação do comportamento vibracional de compostos ácidos. Resultados em diferentes funcionais são correlacionados, e uma varredura da energia de conformação é obtida. Os resultados podem ser úteis na composição de estudos de natureza vibracional e conformacional de ácidos graxos.

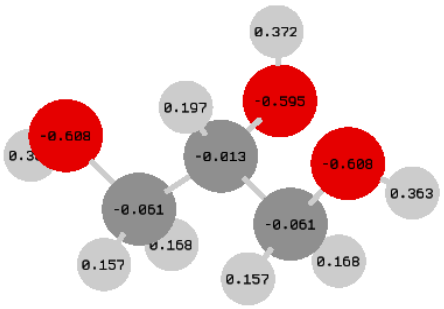

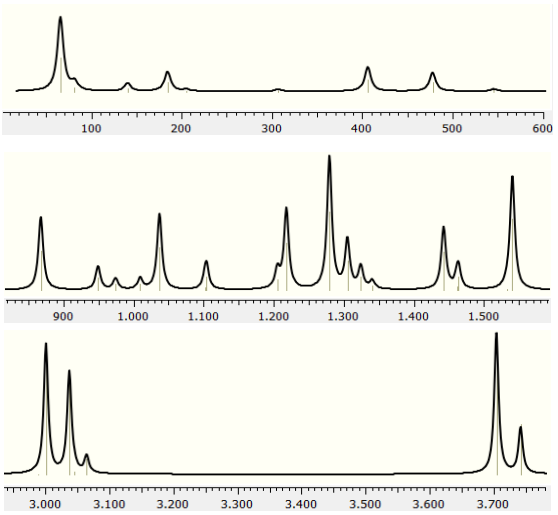

[01] Q.S. Martins, L.M.S. Santos, J.L.B. Faria, Vib Spectros, (2020)
https://doi.org/10.1016/j.vibspec.2019.102986
[02] P. Larkin (Peter J.), Infrared and Raman spectroscopy. Elsevier Inc. (2011)
[03] Heng Peng, Hua-Yi, Hou Xiang-Bai Chen, Quim. Nova, 44, (2021)
https://doi.org/10.21577/0100-4042.20170749

Agradecimentos/Acknowledgments

Agradecemos ao PIBIC 2022/2023. Ao grupo e laboratório de pesquisa Estrutura da Matéria e Física Computacional, DAF/JP - UNIR.

Espectroscopia Raman e Infravermelho aplicados a estudo de grupos carboxílicos de óleo vegetal

Asaf Ribas (IC),[1*] Roberta L. Cristina (IC),[1] Duíllio L.L. de Oliveira[1], Quesle S. Martins (PQ)[1]

asafribas@hotmail.com

[1] *Fundação Universidade Federal de Rondônia, UNIR.*

Palavras Chave: Espectroscopia Raman, Métodos DFT, Ácidos graxos e Grupos Carboxílicos.

Highlights

Raman and Infrared spectroscopy in the study of carboxylic groups in vegetable oil.
Raman and IR spectroscopy Vegetable oil (Brazil nuts oil - BNO); DFT calculations; Carboxylic groups vibrational modes.

Resumo/Abstract

Óleos de origem vegetal podem apresentar uma série de componentes chamados de ácidos graxos, dentre eles o ácido oleico, é componente majoritário no óleo de castanha-do-Brasil, que é objeto de estudo por espectroscopia Raman e no Infravermelho e por meio de DFT [1-3]. Dados experimentais Raman de BNO mostram ausência de banda de C=O, presentes em 1745 cm^{-1} e em 1721 cm^{-1} no espectro de ácido oleico (OA) 99% experimental e calculado. O método DFT se mostra uma ferramenta útil na identificação de grupos carboxílicos em óleos vegetais ao gerar modos Raman e IR que auxiliam na caracterização das bandas vibracionais presentes na amostra.

Figura 1: Espectros Raman e IR de molécula de ácido oleico calculado (B3LYP/6311G(d,p)).

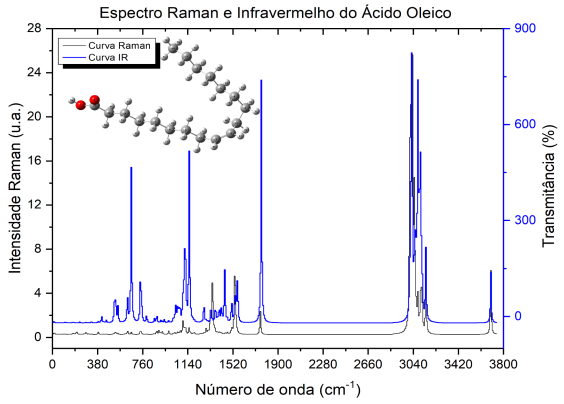

Tabela 1: Frequências Raman das amostras experimentais BNO e OA 99% e OA calculado.

BNO	OA 99%	OA/DFT	Assinaturas
-	1745	1721	*Str* C=O
1665	1656	1712	*Str* C=C
1439	1439	1527	*Sci* CH
1302	1302	1343	*Twi* CH
1262	1265	1328	*Twi* CC
1120	1123	1112	*Str* CC
1085	1085	1083	*Str* CC

Str=stretching; Sci=scissoring; Twi=Twisting

[01] Q.S. Martins, L.M.S. Santos, J.L.B. Faria, Vib Spectros, (2020) https://doi.org/10.1016/j.vibspec.2019.102986
[02] P. Larkin (Peter J.), Infrared and Raman spectroscopy. Elsevier Inc. (2011)
[03] Heng Peng, Hua-Yi, Hou Xiang-Bai Chen, Quim. Nova, 44, (2021) https://doi.org/10.21577/0100-4042.20170749

Agradecimentos/Acknowledgments

Agradecemos ao PIBIC-CNPQ nº 2021/Pibic/Dpesq/Propesq/2021). Ao Laboratório de Espalhamento de Luz - UFMT e Laboratório Estrutura da Matéria e Física Computacional DAF/JP - UNIR. À INOVAM BRASIL LTDA pela amostra cedida.

VII Encontro Brasileiro de Espectroscopia Raman
VII EnBraER
05 a 08/12/2022, São Pedro – SP

Raman spectroscopy applied to the study of Pterosaur bone from the Cretaceous of Bauru Basin, South – Brazil

Wemerson J. Alencar (PG) [1]*, João H. da Silva (PQ) [2], Renan A.M. Bantim (PQ) [3], Luiz C. Weinchultz (PQ) [4], Alexander W. A. Kellner (PQ) [5], João H. Z. Ricetti (PQ) [4] José A.S. da Silva (PG) [1], Anupama Ghosh (PQ) [1], Thiago A. de Moura (PG) [1], Paulo T.C. Freire (PQ) [1]

wemerson@fisica.ufc.br

[1]Departamento de Física, Universidade Federal do Ceará – UFC; [2] Universidade Federal do Cariri - UFCA, [3] Museu de Paleontologia Plácido Cidade Nuvens, Universidade Regional do Cariri – URCA; [4]Centro Paleontológico da Universidade do Contestado - CENPALEO, Mafra, SC, Brasil; [5]Laboratório de Sistemática e Tafonomia de Vertebrados Fósseis, Setor de Paleovertebrados, Departamento de Geologia e Paleontologia, Museu Nacional, Universidade Federal do Rio de Janeiro.

Highlights

- Brazilian *Pterosaur* bone was studied by analytical techniques;
- The main crystalline phases of the fossil were identified;
- The main fossilization process (silicification) could be inferred by the analytical measurements;
- Some carbon amount was found for Raman Spectroscopy.

Abstract

The purpose of the present work is to characterize the pterosaur bone (*Caiuajara dobruskii*) belonging to the Goiô-Erê Formation of the Bauru Basin, collected in the of Cruzeiro do Oeste city, Paraná. This study search to investigate the chemical composition of the fossil material and its matrix rock to make inferences about the fossilization processes and the paleoenvironment under study. Raman spectroscopy, X- ray diffraction (XRD) and energy dispersive spectroscopy (EDS) techniques were used. Through of Raman spectroscopy, it was possible to identify intense bands associated with the mineral quartz in the spectrum of matrix rock and of the fossil. In addition, it was possible to identify the D and G bands associated with amorphous carbon. In the X-ray diffractogram of the matrix rock, quartz was found as the majority phase and secondary phases involving the minerals hematite, calcite and feldspar. While in the fossils, it was found the presence in higher concentration of quartz and small amounts of hematite, feldspar, calcite and hydroxyapatite. In the EDS spectra, elements such as oxygen, silicon, calcium, aluminum, carbon, phosphorus and iron were identified, with greater emphasis on the amount of silicon in both samples. These results indicate that the dominant fossilization mechanism for the pterosaur bone was silicification. The silicates come from the Goiô-rê Formation, composed of quartz and sandstones deposited in a desert eolian environment. This work shows that the use of techniques such as Raman spectroscopy, XRD and EDS are of great relevance in the physical and chemical characterization of fossils, with emphasis on Raman spectroscopy that provided the identification of amorphous carbon in the samples, as well as to determine the different mechanisms responsible for their preservation over geological time.

Acknowledgments

Wemerson J. Alencar thanks FUNCAP for the financial support, Process number: BMD-0008-00128.01.26/21. The authors would like to thank the Physics Department of the Federal University of Ceará for making available the Vibrational Spectroscopy and Microscopy Laboratory (LEVM) and the Analytical Center. We acknowlegde University of Contestado paleontological research center – CENPALEO, in the city of Mafra, Santa Catarina State, for providing the fossil samples studied in this work.

VII Encontro Brasileiro de Espectroscopia Raman
VII EnBraER
05 a 08/12/2022, São Pedro – SP

Raman spectroscopy, XRF, SEM-EDS and powder X-ray diffraction characterization of Amazonian indigenous archaeological ceramics

Gerson A. C. Lopes (PG)[1,2]*, Javier A. Ellena (PQ)[1], Kléber O. Souza (PQ)[3], Daniel Atencio (PQ)[4], Marcelo B. Andrade (PQ)[1].

g.anderson@ifsc.usp.br

[1]Instituto de Física de São Carlos, USP; [2]Laboratório de Física, UEAP; [3]Centro de Estudos e Pesquisas Arqueológicas do Amapá, UNIFAP; [4]Instituto de Geociências, USP.

Palavras-chave: *Cultural heritage, Amapá ancient people, Crystallography, Mineral composition.*

Highlights

This study presents a vibrational, chemical and structural characterization of indigenous ceramics from Amapá, Amazon, Brazil and aims for further discussion on the technology used by ancient people from Brazil's North Region.

Abstract

Amazonian archaeological studies have grown in the last decades. However, most studies do not focus on vibrational, chemical and structural analyses. Raman spectroscopy, combined with other techniques such as XRF, SEM-EDS and powder X-ray diffraction, are important to provide composition data of these ceramics, specially on its mineral composition. These analyses allow further discussion on the process of fabrication of the ceramic pieces, the type of heating and temperature reached and the possible source for the raw materials.

Four ceramic pieces from Ilha Mirim archaeological site, Macapá-AP, were analyzed by several techniques (Fig. 1). XRF data indicated as main elements present Si, Al, Fe, Ti and K. Other presences were Mg, P, Ca, S, Zr, Ce, V and Ba. Powder X-ray diffraction indicates the main crystalline phases as quartz, ilite (mica group) and albite (feldspar group). SEM-EDS indicates the presence of Si, Al, Fe, Ti, Ca and K, and showed evidence on the presence of fibers.

Raman spectra of the samples were compared with RRUFF database using CrystalSleuth software, and the samples showed to be heterogeneous, presenting three different regions with main colours: black, white, and red. Black region showed to be hematite (Fig.2). White and Red regions, in turn, showed no direct correspondence, possibly due to heterogeneity or fluorescence, and are still being analyzed.

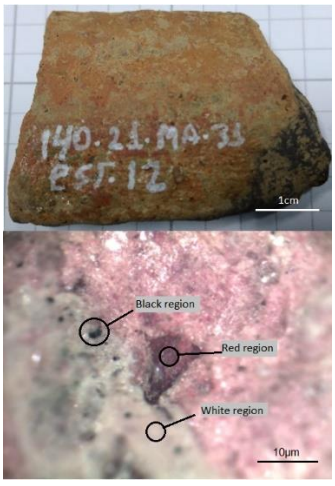

Figure 1: Different regions in ceramic sample

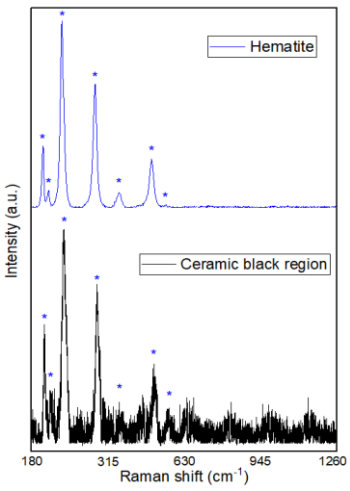

Figure 2: Raman spectra of the black region of ceramic.

Acknowledgments

FAPESP (19/23498-0, 13/03487-8). Universidade do Estado do Amapá.

VII Encontro Brasileiro de Espectroscopia Raman
VII EnBraER
05 a 08/12/2022, São Pedro – SP

Uso combinado de Microscopia Raman e SEM-EDS na análise de obras de arte: Independência ou morte!

Isabela F. S. dos Santos (PQ),[1,*] Yara L. M. M. Petrella (PQ),[1] Dalva L. A. de Faria (PQ)[2]

isafsodre@gmail.com

[1]Instituto de Química, Universidade de São Paulo; [2]Museu Paulista, Universidade de São Paulo.

Palavras Chave: *Obras de arte, Independência ou Morte!, Microscopia Raman; bens culturais; pigmentos.*

Highlights

Combined use of Raman microscopy and SEM-EDS in artwork analysis: Independência ou Morte! The iconic painting portraying the Cry of Ipiranga was analyzed by Raman microscopy and SEM-EDS aiming to add chemical information to the painting history and to help in the restoration procedure.

Resumo/Abstract

O Museu do Ipiranga abriga, desde 1895, a pintura Independência ou Morte! (óleo sobre tela, 760 cm x 415 cm,1888) de autoria de Pedro Américo de Figueiredo e Mello, obra icônica que apresenta uma versão idealizada do momento da independência do Brasil. As obras de revitalização do Museu, realizadas em preparação para o segundo bicentenário da Independência, incluíram a restauração de suas pinturas mais emblemáticas, dentre elas o Independência ou Morte!. Essa foi uma oportunidade ímpar para investigação detalhada da composição química dos materiais que a constituem através de métodos não destrutivos, objetivando ampliar o conhecimento técnico da obra, incluído sua moldura, bem como fornecer subsídios para sua restauração.

A partir da documentação fotográfica da pintura com luz visível e radiação UV, foram elaborados questionamentos a serem respondidos pelas análises químicas. Além da identificação dos pigmentos empregados e da caracterização de materiais e métodos usados no douramento da moldura, foi analisado o material usado no envernizamento da pintura e foram investigados os processos de degradação observados. Microamostras (tipicamente de 5 a 50 µm) foram coletadas de diversas áreas da pintura e da moldura, e analisadas por microscopia Raman e SEM-EDS; ATR-FTIR, microscopia FTIR e GC-MS foram usadas como técnicas complementares em alguns casos.

Foram identificados os pigmentos empregados nas áreas pintadas em vermelho (vermelhão (HgS) e hematita (α-Fe_2O_3)), rosa (vermelhão e branco de chumbo ($2PbCO_3{\cdot}Pb(OH)_2$)), branco (branco de chumbo), preto (carbono amorfo), amarelo (amarelo de zinco ($K_2O{\cdot}4ZnCrO_4{\cdot}3H_2O$), amarelo de crômio ($PbCrO_4$), goethita ($\alpha$-FeOOH) e massicote (PbO)), branco de chumbo e vermelhão), azul (azul da Prússia ($Fe_4[Fe(CN)_6]_3$) e azul de cobalto ($CoAl_2O_4$)), verde (azul da Prússia, amarelo de zinco, amarelo de crômio, branco de chumbo e branco de bário ($BaSO_4$) e marrom (hematita, vermelhão, carbono e branco de chumbo).

Os resultados de SEM-EDS (Au, com Al e Si em menor quantidade) de fragmentos dourados da moldura indicam o uso de ouro puro (Au) e sugeriram o uso de argilomineral, possivelmente, caulinita ($Al_2Si_2O_5(OH)_4$), usada para facilitar a aplicação da folha de metal. Como camada de preparação identificou-se gesso (sulfato de cálcio diidratado). Os resultados de FTIR indicam verniz baseado em resina triterpênica (dammar ou mastique); análise por GC-MS está em curso visando a discriminação entre elas.

A presença de orifícios na superfície da pintura foi investigada a partir da coleta de material em seus interiores e bordas. Os espectros FTIR obtidos para as amostras coletadas sugerem que se trate de vestígios de colonização anterior de micro-organismos (presença de bandas de material proteico), porém, a baixa quantidade de amostra e contribuições do verniz e do material pictórico nos espectros registrados ainda não permitiram conclusões definitivas.

A identificação dos materiais empregados na elaboração da moldura da pintura (base de gesso, argilomineral e folhas de ouro no douramento) e introduzido em intervenções prévias de restauro (verniz de resina triterpênica) foram importantes para as atividades de restauro, e a identificação dos pigmentos empregados pelo artista contribuíram para o conhecimento da técnica usada em sua elaboração. A possibilidade de colonização microbiológica anterior foi verificada, o que deverá ser confirmado a partir de análises mais detalhadas do material coletado.

Agradecimentos/Acknowledgments

Temático Fapesp 2016/21070-5.

VII Encontro Brasileiro de Espectroscopia Raman
VII EnBraER
05 a 08/12/2022, São Pedro – SP

From micro to nano Raman: new developments in the detection of micro and nanoplastics of marine origin from the Amazon basin to Santos

Niklaus Wetter (PQ)[1*], Anderson Z. Freitas (PQ)[1], Allan Bereczki (PG)[1], Diego R.C. Pascoal (PG)[1], Jessica Dipold (PG)[1], Duclerc Parra (PQ) [1], Wagner Rossi (PQ) [1], Fernanda V. Cabral (PG) [1], Martha S. Ribeiro (PQ) [1]

nuwetter@ipen.com

[1]*Instituto de Pesquisas Energéticas e Nucleares, IPEN-CNEN, 2242, A. Prof. Lineu Prestes, São Paulo, SP, Brazil*

Palavras Chave: *Nanoparticles, Raman spectroscopy, microplastics pollution*

Highlights

New analytical techniques are in place for determining nanoplastics pollution i.e., addressing chemical functionality and providing structural information with high spatial resolution.

Resumo/Abstract

The environmental accumulation of nanoplastics formed by material of anthropic origin has raised doubts about their safety, especially to the human body. While microplastics are accidentally consumed, nanoplastics (NPs) are even more concerning as they are much more likely to be absorbed by human body cells. It is known that plastics smaller than 200 nm can penetrate cell membranes and cross the blood-brain barrier. Studies have shown that polystyrene (PS) NPs from the environment carry a high load of toxins capable of compromising human brain cells. Very little is still known about what effects, cytotoxic or not, these plastics have on different organs. Understanding the property-function relationship of nanoparticles in various fields of application involves determining their physicochemical properties, which is still a formidable challenge to date. Our project focuses on the development of a methodology for the detection of micro- and NPs using micro-Raman, TERS (Tip Enhanced Raman Spectroscopy), collinear Raman and AFM, nuclear techniques, as well as a methodology for in vitro evaluation of the toxic effects of these materials through biochemical assays of cytotoxicity and genotoxicity. The project contemplates the determination of the adsorption capacity of metallic ions by NPs and the absorption of micro- and nanoplastics in cell cultures with radioactive tracers, the determination of microplastics in tissues from necropsies of marine animals and gamma spectroscopy of the cellular incorporation of NPs labeled with radioactive isotopes.

In figure 1 we show examples of (a) the detection of microplastics from the Santos basin and comparison to Raman reference database (KnowItAll®), (b) detection of NPs in mouse fibroblast cells and (c) detection of very small particles (50 nm) which can be achieved by co-localized techniques of AFM + Raman using special, narrow (50 μm), femtosecond laser written gratings on quartz.

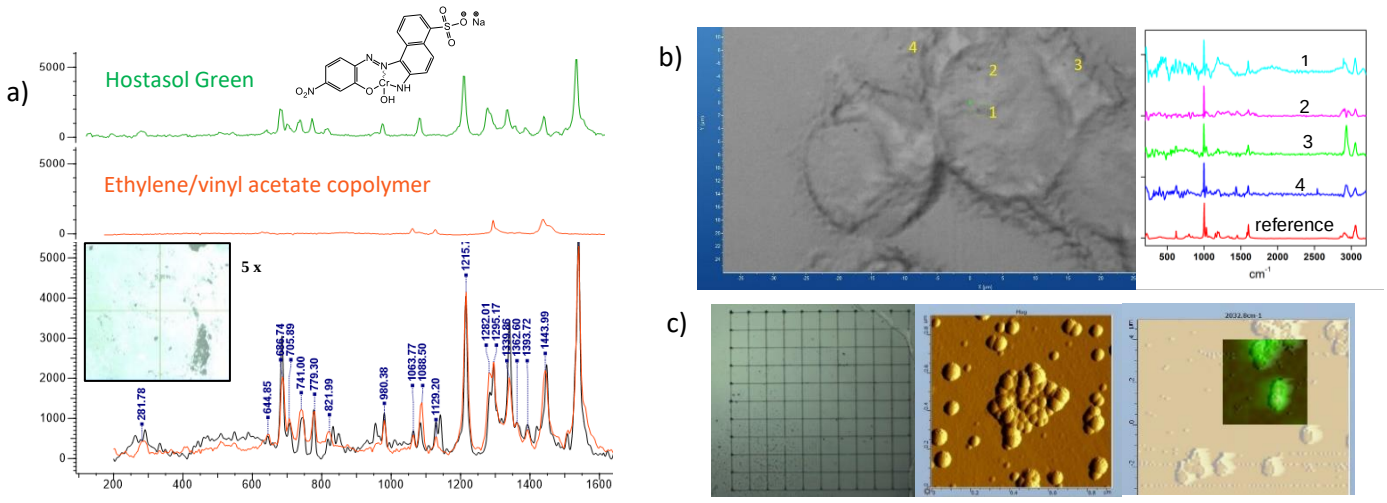

Figure 1: (a) Raman spectra of a micro-copolymer with pigment; (b) detection of 200 nm PS in cell culture; (c) detection of 50 nm nanoplastics

Agradecimentos/Acknowledgments

FAPESP grants 2016/02326-9, 2017/10765-5, EMU 2018/19240-5, 2019/06334-4, 2021/11316-5, 2022/07199-6

VII Encontro Brasileiro de Espectroscopia Raman
VII EnBraER
05 a 08/12/2022, São Pedro – SP

Determinação de sulfato em águas marinhas por espectroscopia Raman

Elisa M. B. Santos (PG)*, Nilvan A. da Silva (PG), Ivo M. Raimundo Jr. (PQ)

elisambsantos@gmail.com

Instituto de Química, UNICAMP, CP 6154, CEP 13085-563, Campinas, São Paulo

Palavras Chave: *Sulfato, Espectroscopia Raman, Incrustação.*

Highlights

Sulfate determination in marine water by Raman Spectroscopy

Pre-concentrated sulfate solutions using ion exchange resins were determined by Raman spectroscopy.

Resumo/Abstract

Os processos de incrustação ocorrem devido à precipitação de sais inorgânicos insolúveis em tubulações de diferentes processos industriais, sendo que o íon sulfato tem papel importante na precipitação de metais alcalino-terrosos. Considerando-se processos de extração de petróleo *offshore*, ocorre o encontro de diferentes tipos de águas ricas no íon em questão, dificultando o rendimento do processo e podendo ocasionar problemas como o aumento da pressão das tubulações. Devido a essa situação, a quantificação dos íons sulfato em águas marinhas é um fator importante para o monitoramento de incrustações. O sulfato apresenta uma banda característica na espectroscopia Raman, em aproximadamente 980 cm^{-1}, livre da interferência da banda de água e, portanto, sua determinação direta pode ser realizada empregando-se esta técnica.

As medidas de espalhamento Raman foram realizadas empregando-se um espectrofotômetro construído no laboratório, operando com um laser de diodo de 784,8 ± 0,5 nm, largura de banda de 40 pm e potência de 500 mW, um monocromador Andor/Oxford SR-500i-C-SIL (Czerny-Turner, distância focal de 50 cm e rede de difração de 600 linhas/mm) e uma câmera iCCD Andor/Oxford iDUS 416 (sensor matricial de 256 x 2000 pixels). A determinação de sulfato foi feita diretamente em solução aquosa, inicialmente na faixa de 500 a 3000 mg L^{-1}. A integração do sinal durante 180 s possibilitou uma resposta linear na faixa mencionada, com limites de detecção de 90 mg L^{-1} e de quantificação de 300 mg L^{-1}. Estes valores não são adequados para aplicação em águas marinhas, pois a concentração de sulfato nestas águas usualmente varia de 20 a 300 mg L^{-1}. Uma estratégia de pré-concentração em resina de troca iônica foi avaliada, usando-se resinas IRA 910 e IRA 402, ambas na forma de cloreto. Uma massa de 500 mg da resina foi colocada em 100 mL de uma solução de sulfato 1000 mg L^{-1}, mantida por agitação durante 1 h. Após secagem em estufa, a determinação foi feita diretamente na resina, que proporcionou resultados pouco promissores, em virtude da heterogeneidade do material. Foi empregada, então, uma coluna de 500 mg da resina Amberlite IRA 910, pela qual foram bombeadas 100 mL de soluções de sulfato com concentrações de 100 a 400 mg L^{-1}, por X minutos, a uma vazão de 1 mL min^{-1}. O sulfato retido foi eluído com 2 mL de uma solução de cloreto de sódio 1 mol L^{-1}, obtendo-se uma resposta linear e um limite de detecção e de quantificação de, respectivamente, 13 mg L^{-1} e 44 mg.L^{-1}.

A estratégia de pré-concentração de sulfato mostrou-se adequada e o método parece promissor para esta determinação. Embora o íon cloreto não interfira nas medidas Raman, a adição de 1,0 e 2,5 % de cloreto de sódio na solução de sulfato provocou efeitos significativos na etapa de pré-concentração e, portanto, estudos têm sido realizados no intuito de minimizar esta interferência.

Agradecimentos/Acknowledgments

Ao Instituto Nacional de Ciências e Tecnologias Analíticas Avançadas (INCTAA), FAPESP, CNPq e CAPES.

VII Encontro Brasileiro de Espectroscopia Raman
VII EnBraER
05 a 08/12/17, São Pedro – SP

Determinação de benzeno e tolueno em águas por espectroscopia Raman

Augusto F. S. de Oliveira (PG),* Jarbas J. R. Rohwedder (PQ), Ivo M. Raimundo Jr. (PQ)

augusto.fernando2011@gmail.com

Instituto de Química, UNICAMP, CP 6154, CEP 13085-563, Campinas, São Paulo

Palavras-Chave: *Benzeno, tolueno, xilenos, espectroscopia Raman,*

Highlights

Determination of benzene and toluene in water by Raman Spectroscopy

The use of PDMS monoliths allowed the extraction of benzene and toluene in saline waters and their quantification by Raman spectroscopy in low concentrations.

Resumo/Abstract

O aporte de compostos orgânicos voláteis (VOCs) nos ambientes aquáticos ocorre principalmente devido ao derramamento de produtos de petróleo, mas também devido ao tráfego rodoviário, produtos domésticos e agroindustriais. Dentre esses compostos, benzeno e tolueno constituem dois dos VOCs aromáticos mais produzidos no mundo e são considerados altamente tóxicos e de natureza cancerígena. Na água, esses compostos podem transportados por longas distâncias em condições redox favoráveis. Nesse contexto, é importante realizar o monitoramento da presença desses compostos em águas, bem como o emprego de técnicas analíticas rápidas e baratas. Este trabalho tem o objetivo de determinar benzeno e tolueno em água por meio de extração em fase sólida em monólitos de PDMS, com detecção por espectroscopia Raman.

A extração foi realizada colocando-se um monólito de PDMS de 2,0 mm de altura e 3,2 mm de diâmetro em solução de NaCl 2,0 mol L^{-1} contendo os hidrocarbonetos, sem espaço confinante (*headspace*) e mantida sob agitação por 60 min. Após a extração, os espectros dos monólitos foram obtidos utilizando um espectrômetro Raman construído no laboratório (fonte de laser de diodo de 784,8 ± 0,5 nm, potência de 500 mW; monocromador Andor/Oxford SR-500i-C-SIL e câmera iCCD Andor/Oxford iDUS 416).

A Figura 1 mostra que estas espécies podem ser determinadas simultaneamente, apresentando uma resposta linear na faixa de 10 a 100 mg L^{-1}. Limites de detecção (LOD) de 0,65 e 0,62 mg L^{-1} foram obtidos para benzeno e tolueno, respectivamente. A Tabela 1 mostra os resultados obtidos na análise de soluções aquosas contendo as duas espécies. A reprodutibilidade do método foi avaliada pela construção de três curvas de calibração em dias diferentes e com soluções estoque diferentes. Os resultados mostraram um desvio padrão relativo (RSD) de 1,4% referentes à inclinação das curvas obtidas para o tolueno.

Tabela 1: Resultados obtidos para as misturas de benzeno (Benz.) e tolueno (Tol.). CM = Concentração Medida; CR = Concentração Real

Misturas	CM Benz. ± SD (mg L^{-1})	CR Benz. (mg L^{-1})	Erro Relativo (%) Benz.
Mistura 1	22,5 ± 1,7	20,0	12,4
Mistura 2	49,2 ± 2,4	50,0	-1,5
Mistura 3	73,0 ± 9,3	80,0	-8,8
Misturas	**CM Tol. ± SD (mg L^{-1})**	**CR Tol. (mg L^{-1})**	**Erro Relativo (%) Tol.**
Mistura 1	76,2 ± 1,7	80,0	-4,8
Mistura 2	50,3 ± 3,4	50,0	0,5
Mistura 3	20,5 ± 2,4	20,0	2,4

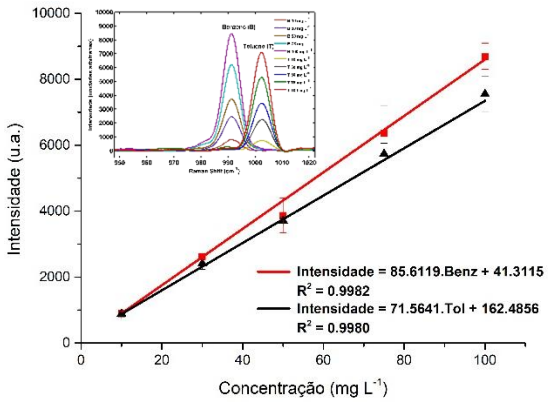

Figura 1: Curvas analíticas para benzeno (em vermelho) e tolueno (em preto).

Agradecimentos/Acknowledgments

Ao Instituto Nacional de Ciências e Tecnologias Analíticas Avançadas (INCTAA), Fapesp, CNPq e CAPES.

VII Encontro Brasileiro de Espectroscopia Raman
VII EnBraER
05 a 08/12/2022, São Pedro – SP

Raman spectroscopy and chemometrics to discriminate oxidative processes of biodiesel.

Maycom Cezar Valeriano[a]*, Antônio Carlos Ferreira Batista[b], Mónica Benicia Mamián-López[a]

***maycom.cezar@ufabc.edu.br**

[a]Federal University of ABC, Human and Natural Sciences Center. Santo André, São Paulo, Brazil, 09210-580. [b]Federal University of Uberlândia. Pontal Institute of Exact and Natural Sciences. Chemistry Department, Ituiutaba, Minas Gerais, Brazil, 38304-402
Palavras Chave: *(Biodiesel, Raman, Chemometrics, Machine Learning).*

Highlights

Use of Raman spectroscopy to discriminate biodiesel samples that have undergone oxidation processes. Through exploratory analysis it is possible to observe different oxidation routes.

Abstract

One of the most important biodiesel properties is oxidation stability. The biodiesel oxidation process generates contaminants that can compromise the engine's operation. The oxidation process of biodiesel occurs by the forming radicals close to unsaturations, where oxygen binds, causing the formation of acids that can lead to the formation of species such as aldehydes and even the formation of polymers. In this context, Raman spectroscopy can provide important structural information and, when associated with multivariate analysis, allows monitoring of these chemical changes over time and under different storage conditions. In this work, biodiesel samples were exposed to different storage conditions, and the oxidation process was studied through their Raman spectra and exploratory analysis. Two main patterns were observed through the scores plot (figure 1-a), firstly, for those samples stored without exposure to light, the oxidation process seemed slower, and over time, the unsaturations were being cleaved as the storage time increased (positive values of PC1). The samples that underwent a more pronounced oxidation condition are distributed along the PC2, and the corresponding loadings (figure 1-c) show an apparent influence of the peak close to 1650 cm-1, which may be related to the formation of polymeric species.

Figure 1: (a) Scores plot. (b) Modeled Raman spectra region. (c) PC1 and PC2 loadings. W1 to W4 stands for each sampling week .

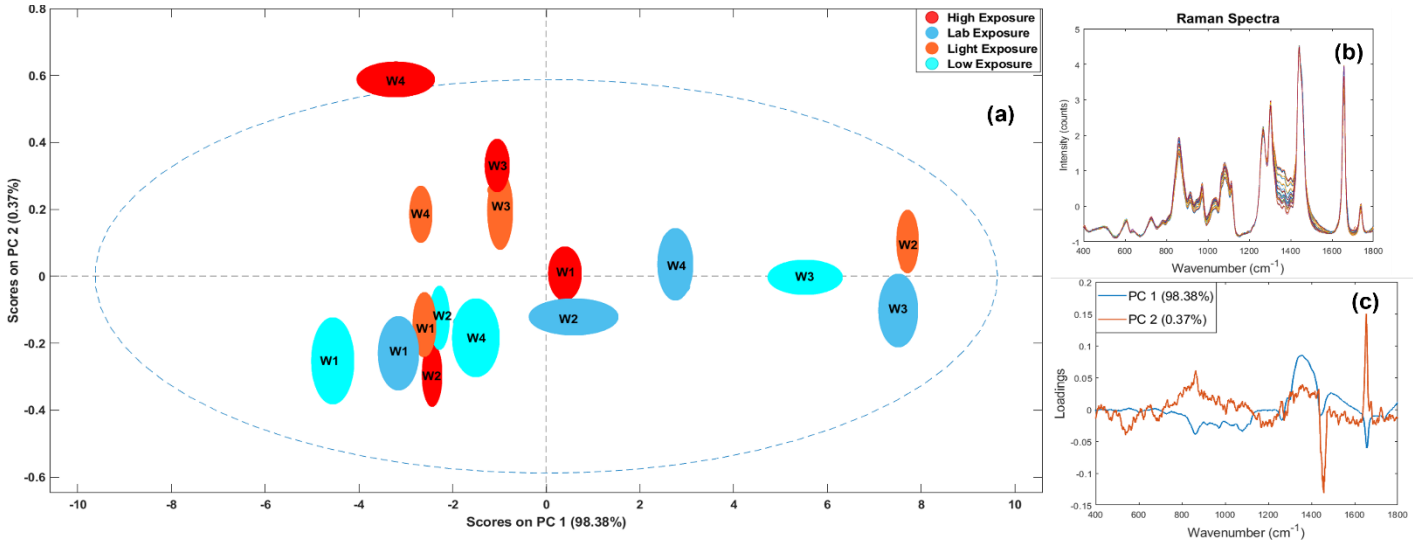

Acknowledgments

This work was supported by PRH-ANP (grant No. 045919). The authors are grateful to the Laboratory of Molecular Spectroscopy of the Institute of Chemistry of University of São Paulo (USP, Brazil), where part of the Raman spectra was measured (FAPESP, grant 2016/21070-5).

VII Encontro Brasileiro de Espectroscopia Raman
VII EnBraER
05 a 08/12/2022, São Pedro – SP

Is your transfusion free of Microplastics?: Identification of emerging contaminants in blood by Raman Spectroscopy

Bianca C. S. Miara Osatchuk (PG)[1], Gabriel Staichak (PG)[2], Augusto L. Ferreira Jr (PG)[3], Bruno R. Cruz (PQ)[4,5], Andressa Novatski (PQ)[1,6*], Susete W. Christo (PQ)[2,7], Giovani M. Favero (PQ)[1,7]**

***anovatski@uepg.br; ****gmfavero@yahoo.com.br**

[1]*Programa de Pós-graduação de Ciências da Saúde, Universidade Estadual de Ponta Grossa (UEPG), PR, Brasil;* [2]*Programa de Pós-Graduação em Biologia Evolutiva, UEPG, Ponta Grossa, PR, Brasil;* [3]*Programa de Pós-Graduação em Genética Evolutiva e Biologia Molecular, Universidade Federal de São Carlos, SP, Brasil;* [4]*Departamento de Análises Clínicas, UEPG, Ponta Grossa, PR, Brasil.;* [5]*Banco de Sangue do Hospital Universitário Regional dos Campos Gerais, UEPG, Ponta Grossa, PR, Brasil;* [6]*Departamento de Física, UEPG, Ponta Grossa, PR, Brasil;* [7]*Departamento de Biologia Geral, UEPG, Ponta Grossa, PR, Brasil*

Keywords: *Plastisphere, Pollutant, Microfibers, Platelet Concentrate, Human Health*

Highlights

- Microplastics (MP) are emerging contaminants increasingly detected in human health studies.
- Storage of blood transfusion contents are carried out in disposable materials, predominantly plastic.
- Does microplastic contamination occur for blood components in your storage?
- When making blood donations, can we be transferring microplastics?

Abstract

Plastic materials with a size between 0.1µ-5.0 mm are called microplastics. As plastics are present in the environment and in many products that are routine for humans, human exposure to MPs becomes inevitable. The objective of this work was to evaluate the presence of MPs in bags of platelet concentrates (n=15) and to relate it to their composition. The samples were analyzed by Optical microscopy, SEM-EDS RAMAN and FTIR spectroscopies. . SEM-EDS and RAMAN analysis of the pouch packaging showed it to be a kind of polyvinyl chloride (PVC), confirming the information described by the bag manufacturer (Figure 1). That is a alert to us to search for new materials for its production. According to SALIMI et al. (2022), PVC microplastic particles induce oxidative stress and organelle damage in human lymphocytes. Optical microscopy visualized 26 structures with physical and visual characteristics of MPs. MPs identified were all microfibers, with an average of 1.73±1.03 items/slide. These microfibers were blue-green (13.33%) and gray-black (86.67%), with 0% and 93.33% prevalence of microparticle (0 bags) and microfibers (14 bags), respectively (Figure 2).

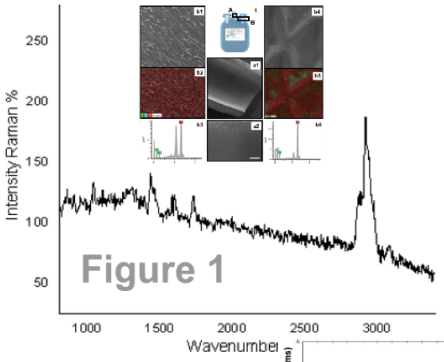

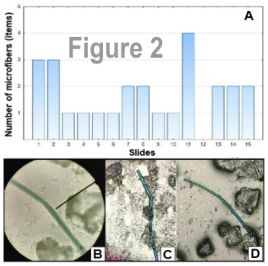

The frequent use of plastic material as one of humanity's main raw materials (NAPPER; THOMPSON, 2020) has increased human exposure to MPs (PRATA et al., 2020). The first observation of microfibers observed in our data in platelet concentrates indicates that the transfusion of blood components may be a new route of contamination of MPs. The confirmation that the material of the platelet concentrate bag is PVC and the identification of synthetic microfibers in the platelet concentrate alerts us to the need for a new methodology for this emerging contaminant.

REFERENCES

NAPPER, I. E.; THOMPSON, R. C. 2020. Plastic Debris in the Marine Environment: history and future challenges. ***Global Challenges***, http://dx.doi.org/10.1002/gch2.201900081.

SALIMI, A.; Alavehzadeh, A.; Ramezani, M.; Pourahmad, J. 2022. Differences in sensitivity of human lymphocytes and fish lymphocytes to polyvinyl chloride microplastic toxicity. ***Toxicology and Industrial Health***, https://doi.org/10.1177/07482337211065832

PRATA, J. C. *et al.* 2020. Environmental exposure to microplastics: an overview on possible human health effects. ***Science Of The Total Environment***, http://dx.doi.org/10.1016/j.scitotenv.2019.134455.

Acknowledgments

CAPES, CNPq, FINEP, Fundação Araucária, Hemepar, Propesp/UEPG, and LabMU/UEPG teams, in special Vanessa Parise Chagury and Silvio H. Gonsalves.

VII Encontro Brasileiro de Espectroscopia Raman
VII EnBraER
05 a 08/12/2022, São Pedro – SP

Micro-Raman spectroscopy for identification of microplastics in the São Vicente estuarine

Allan Bereczki (PG)[1*], Diego R.C. Pascoal (PG)[1], Jessica Dipold (PG), Giovana Teixeira Gimiliani (PG)[1], Duclerc Fernandes Parra (PQ)[1], Anderson Z. Freitas (PQ)[1], Niklaus Wetter (PQ)[1]

nuwetter@ipen.com

[1] *Instituto de Pesquisas Energéticas e Nucleares, IPEN-CNEN, 2242, A. Prof. Lineu Prestes, São Paulo, SP, Brazil*

Key words: *Microplastics, Raman, Environment*

Highlights

Micro-Raman was used to characterize polluting microplastics from the sea environment

Abstract

Microplastics (MPs) are a concern regarding our environment due to the risks posed by the interactions of the large amounts of anthropogenic MPs dumped in the environment with biological systems. MPs have been vastly found in the environment and are transferred to the food chain with MPs being detected in foods, beverages and even in human blood and breastmilk. Understanding the behavior and characteristics of MPs is critical to assessing potential health risks (human and environmental) related to MPs and taking steps to prevent them from entering the ecosystem. Micro Raman spectroscopy is a powerful tool for measuring and characterizing MPs particles, being considered the gold standard because it allows identification of both the polymer matrix and possible pigments and contaminants. Furthermore it offers the possibility of characterizing both the chemical structure as well as the morphological features of the MPs. We utilized a Raman system to characterize MPs from the environment. Results from a standard MP sample were successfully measured and identified to reference spectra and even small portions of the sample as small as a few µm are suitable for obtaining a high quality spectrum for identification of the material (Fig1). Samples collected from at the São Vicente estuarine are being studied and by means of comparison with the *Willey* database it was possible to identify MP, additives and contaminants, thus demonstrating the power of the technique.

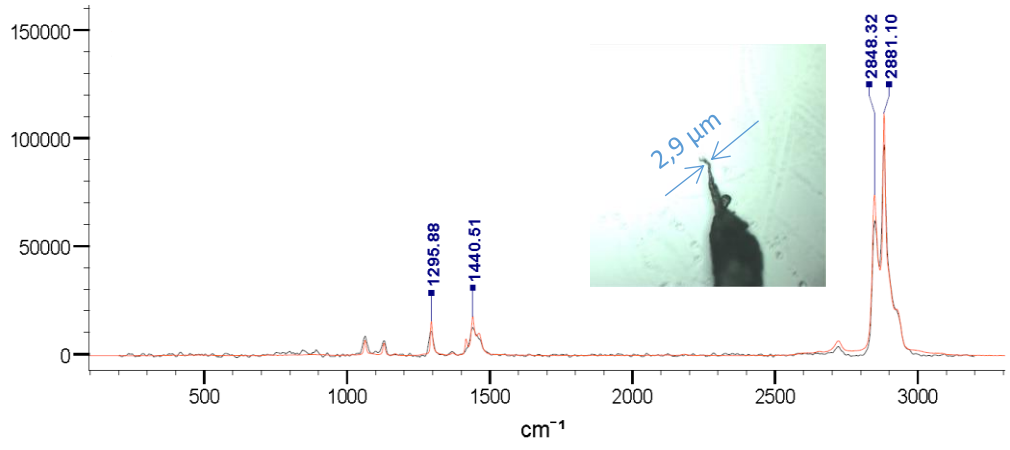

Figure 1: Raman spectra of a low density polyethylene microplastic compared to reference spectra. Measured spectrum (black line) and reference spectrum (orange line). Inset: sample picture indicating the measured region.

Acknowledgments

FAPESP grants 2016/02326-9, 2017/10765-5, EMU 2018/19240-5, 2019/06334-4, 2021/11316-5, 2022/07199-6.

Piperine-loaded polymeric microparticles by Eudragit RS30D and S100: Raman spectroscopy characterization.

Andressa Novatski (PQ)[1], Patricia Biscaia (PG)[2], Guilherme Camargo (PQ)[2], Jaqueline Gunha (PG)[1],Daniele Dias (PQ)[3] Jéssica Nadal (PQ)[2].

anovatski2@gmail.com

[1]Departamento de Física, UEPG; [2] Departamento de Ciências Farmacêuticas UEPG, [3] Departamento de Física UTFPR.

Palavras Chave: Piperin *(máximo 6, separadas por vírgula, primeiras letras em maiúscula, arial 9, itálico).*

Highlights

Colocar aqui o título em inglês e a seguir frases curtas também em inglês que devem resumir o conteúdo do trabalho de forma concisa e capturar rapidamente a atenção de um leitor em no máximo 200 caracteres com espaços (este número desconsidera os caracteres do título). No caso do título do trabalho já estar em inglês, omitir o título nesta parte e escrever apenas as frases. Fonte Arial 10, espaçamento simples.

Resumo/Abstract

Products derived from plants have been used in disease treatments for thousands of years. Phytochemicals are natural constituents that provide an alternative therapeutic approach, as they can act through multiple routes, but the low solubility and bioavailability of phytochemicals are limiting for their use, then, the nanotechnological approach is an alternative to bypassing this and other barriers, As possible adverse reactions, including gastric reactions that can be caused by pungent phytochemicals, such as piperin. Piperina (PIP) is an alcaloid found in the fruits and roots of pepper, in species of Piper nigrum and Piper longum and has been widely used because of its pharmacological activity, with anti-inflammatory effects, analgesic, antidepressant, cytoprotector, antioxidant and ability to increase bioavailability of drugs. Another important PIP activity is its thermogenic effect and fat reducer, however, its high pungency does not allow the population to use it at higher doses. In order to improve drug bioavailability and assessing their antiobesity activity, with a possible reduction of side effects, PIP-containing microparticles were developed using two different polymers, the Eudragit® RS30D and S100, by the spray drying method. The samples were characterized by Raman spectroscopy using a 785 nm laser excitation from a Horiba Xplora Plus spectrometer with a 50× microscope objective, with 15 s of integration time and five accumulations. For pure PIP, its C=C of the aromatic ring, CH of the phenyl group, CH2, and C-O-C produced scattering peaks at 1590, 1104, 1203, and 1256 cm−1, respectively [1,2]. Eudragit RS is a commercially available copolymer of methyl metracrylate, ethyl acrylate and trimethylammonum methacrylate chlorid. Compared to PIP, the spectrum of drug free Eudragit RS microparticles appeaed considerably weaker in intensity and less complex. Three major bands centered at 1718, 1438, and 960 cm-1 are characteristics of the polymer. The 1728 cm-1 arises from the carbonyl bond of the polymer ester function. The 1449 cm-1 bands is indexed for the deformation of the methylene groups and the 960 cm-1 for C-C stretching vibration[3,4]. For microparticles prepared with Eudragit® RS30D the Raman spectra did not present significant changes, on the other rand the microparticles prepared with Eudragit® S100 presented significant changes in broaden scattering peaks assigned for C=C of the aromatic ring, CH of the phenyl group, CH2, and C-O-C were recorded at 1582, 1090, 1205, and 1255 cm−1, respectively. These results indicate an amorphization of the compounds, suggesting that the microencapsulation using Eudragit® S100 to load piperine was more efficient than with Eudragit® RS30D.

[1] A. Hédoux A.H´edoux, L. Paccou,Y.Guinet, J.-F.Willart, andM.Descamps, Int, J. Med. Chem., 8723139, (2016).
[2] Dilip Sing, Shibu Narayan Jana, Subhadip Banerjee et al, Phytochem. Anal., 1-10, (2021).
[3] Peter Watts, Andrew Tudor, Stephen Church et al, Pharm. Research, 8, (1991)
[4] Garima Agrawal and Sangram K. Samal, ACS Biomater. Sci. Eng., 1285−1299 (2018)

Agradecimentos/Acknowledgments

The authors acknowledge the support from the Brazilian agencies CAPES, CNPq, Fundação Araucária, FINEP, C-LABMU and LabMult C²MMa.

VII Encontro Brasileiro de Espectroscopia Raman
VII EnBraER
05 a 08/12/2022, São Pedro – SP

Efeitos da radiação no mineral zircão via espectroscopia Raman.

Antonio S. W. Sales (PG)[1*], Luís R. Gentil (IC)[1], Thaís A. Janolla (PG)[1], Sandro G. Oliveira (PQ)[2], Airton N. C. Dias (PQ)[1].

antonio.sales@estudante.ufscar.br

[1]Departamento de Física, Química e Matemática, UFSCAR-So; [2]Departamento de Raios Cósmicos e Cronologia, UNICAMP.
Palavras Chave: *Espectroscopia micro-Raman, Zircão, Radiação, Rede cristalina, Termocronologia por Traços de Fissão.*

Highlights

Radiation effects on the mineral zircon via Raman spectroscopy. Thermochronology by fission tracks in zircon. Influence of radiation damage on TTF in zircon.

Resumo/Abstract

Minerais como apatita, zircão, epídoto e muscovita contêm Urânio e Tório em quantidades de ppm, portanto, esses minerais são adequados para aplicação em métodos de datação termocronológicos como Termocronologia por Traços de Fissão (TTF). Na rede cristalina destes minerais, esses átomos (Urânio e Tório) podem sofrer fissão espontânea ou decaimento. Isso gera modificação na rede cristalina do mineral que pode interferir nos mecanismos de datação como cinética de difusão, ataque químico, e annealing. Diante dessa premissa, este projeto pretende ampliar a discussão junto à comunidade científica de TTF e Ciências de Materiais investigando a influência da radiação na rede cristalina do zircão, especificamente. Para tal, quatro amostras do mineral zircão foram analisadas. Para obtenção de espectros comparativos dos danos causados à rede cristalina, uma amostra permaneceu em seu estado natural (ZST) e as demais sofreram tratamento térmico em temperatura e tempo suficiente para a restauração da rede cristalina. Após esse tratamento uma amostra permaneceu sem irradiação (ZAN) e duas delas foram irradiadas, da seguinte forma: *i)* irradiação somente com íons pesados (ZIR) e *ii)* íons pesados de alta energia e posterior irradiação com íons de baixa energia (ZIα). Tal sequência de irradiação visa simular o dano à rede cristalina mediante somente a fissão do ^{235}U em *i)* e o acúmulo de dano provocado pelo decaimento alfa, após a fissão do ^{235}U em *ii)*. Em seguida foram obtidos os espectros micro-Raman conforme Fig.1 e respectivos dados analíticos de cada modo Raman se encontram na Tab.1, dos doze modos Raman reportados, foram identificados oito, sendo dois de alongamento: 1008 cm^{-1} (B_{1g}, Si-O v_3), 976 cm^{-1} (A_{1g}, Si-O v_1); um de flexão: 440 cm^{-1} (A_{1g}, Si-O v_2) e cinco modos externos: 394, 357, 226, 215 e 202 cm^{-1}. Pelos dados apresentados na Tab.1 e espectro gerado (Fig.1), se pode inferir que a estrutura cristalina das amostras irradiadas sofreu um dano aparente pela redução observada da intensidade relativa e da ampliação da FWHM, em 1008 e 976 cm^{-1}, ainda nesses modos, o efeito restaurador do aquecimento para a rede cristalina é percebido pela amostra ZAN que apresenta em v_3 uma IR de 129% em relação à amostra ZST. Referente a v_2 as amostras irradiadas apresentam comportamento inverso entre si, havendo uma drástica redução de intensidade para a ZIR (i.e.; IR de 9%) enquanto que a Ziα permanece com IR próxima da ZST, mas ambas apresentam um visível abaulamento da FWHM. Os modos de 202 a 226 cm^{-1}, para as amostras irradiadas apresentam um comportamento inverso ao apresentado pelos modos v_3 e v_1.

Figura 1-Espectros micro-Raman.

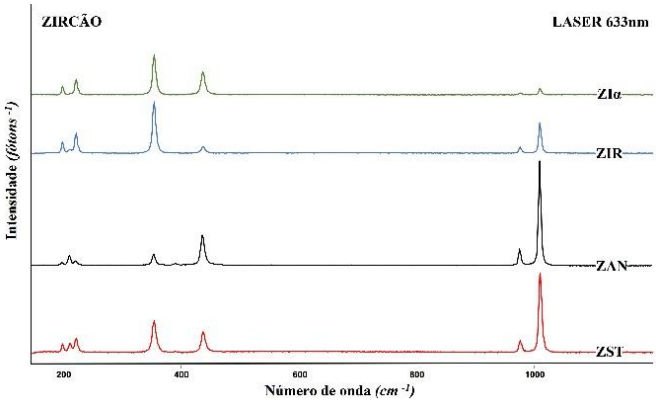

TABELA 1 – Dados espectroscopia micro Raman (número de onda, intensidade, FWHM) para grãos de zircão.

$\bar{\nu}$	Intensidade	[IR]	(FWHM)	$\bar{\nu}$	Intensidade	[IR]	(FWHM)	$\bar{\nu}$	Intensidade	[IR]	(FWHM)	$\bar{\nu}$	Intensidade	[IR]	(FWHM)
ZST				Ziα				ZIR				ZAN			
202,6	1907	11%	4,09	202,3	1687	10%	4,74	202,1	2383	14%	5,54	202,7	576	3%	6,16
215,7	2151	13%	5,33	216,1	252	2%	6,36	214,9	934	6%	6,52	214,4	1987	12%	6,16
225,3	3161	19%	7,54	225,3	3068	18%	5,43	225,3	4098	24%	4,82	226,1	988	6%	4,38
356,8	6634	39%	8,69	357,5	8045	48%	7,39	357,3	10490	62%	8,21	357,5	2291	14%	7,08
440,1	4448	26%	7,54	439,9	4669	28%	9,63	439,6	1502	9%	8,15	394,4	381	2%	8,85
976,4	2615	16%	6,11	975,5	370	2%	3,89	975,1	1383	8%	5,79	438,9	6241	37%	8,85
1008,5	16795	100%	5,94	1008,8	1253	7%	4.96	1008,2	6330	38%	5,33	975,2	3196	19%	5,76
												1009,3	21583	129%	5,06

ν (cm^{-1}) é o número de onda, IR é a intensidade relativa referente ao pico em 1008,5 cm^{-1}, FWHM é a largura total em meia amplitude do pico.

Agradecimentos/Acknowledgments

Ao Governo Federal pela CAPES e a FAPESP (processos 2014/13792-5, 2017/12208-6).

VII Encontro Brasileiro de Espectroscopia Raman

VII EnBraER

05 a 08/12/2022, São Pedro – SP

Micro-Raman spectroscopy characterization of dental pulp stem cells differentiation induced by calcium phosphate nanoparticles

Flavia R. O. Silva (PQ)[1], Diego R. C. Pascoal (PG)[1*], Allan Bereczki (PG)[1], Carla Renata Sipert (PQ)[2], Roberto Ruggiero Braga (PQ) [2], Maria Helena Bellini(PQ)[1], Luis Felipe Teixeira da Silva (PG)[1], Anderson Z. Freitas (PQ)[1], Niklaus U. Wetter (PQ)[1]

nuwetter@ipen.br

[1]*Instituto de Pesquisas Energéticas e Nucleares, IPEN-CNEN, 2242, A. Prof. Lineu Prestes, São Paulo, SP, Brazil.*
[2]*Faculdade de Odontologia da Universidade de São Paulo, São Paulo, SP, Brazil.*

Key words: *Nanoparticles, micro-Raman, Biostimulation*, cell differentiation, stem cell.

Highlights

Hydroxyapatite nanoparticles were successfully internalized by stem cells and calcium phosphate nodules and collagen biostimulation were observed.

Abstract

Calcium phosphates are chemical compounds used in medicine for tissue engineering. This work analyzes the process of cell differentiation by nanoparticles in dental pulp stem cells for tissues regeneration and the development of new therapeutic methods. The most widely used synthetic calcium phosphate based bioceramic is hydroxyapatite [HA, $Ca_{10}(PO_4)_6(OH)_2$]. Micro-Raman spectroscopy assays are a powerful tool for measuring and characterizing calcium phosphates nanoparticles internalized by cells because of its capability to detect the chemical bonds of nanoparticles and collagen simultaneously and evidencing their interaction within the cell-nanoparticle system. Microscope images (Fig.1a) and Raman spectra (Fig.1b) were obtained for HA-incorporated stem cells where it was possible to observe the formed nodules of calcium phosphate and the matrix in the incorporated samples. HA and collagen peaks were detected in the samples, showing that the nanoparticles induced osteogenic differentiation of the stem cells. The spectra of the nodules showed HA characteristic peaks, while matrix spectra displayed characteristic collagen peaks. Studies have been carried out for the development of new and modified calcium phosphate nanoparticles that should further improve biostimulation.

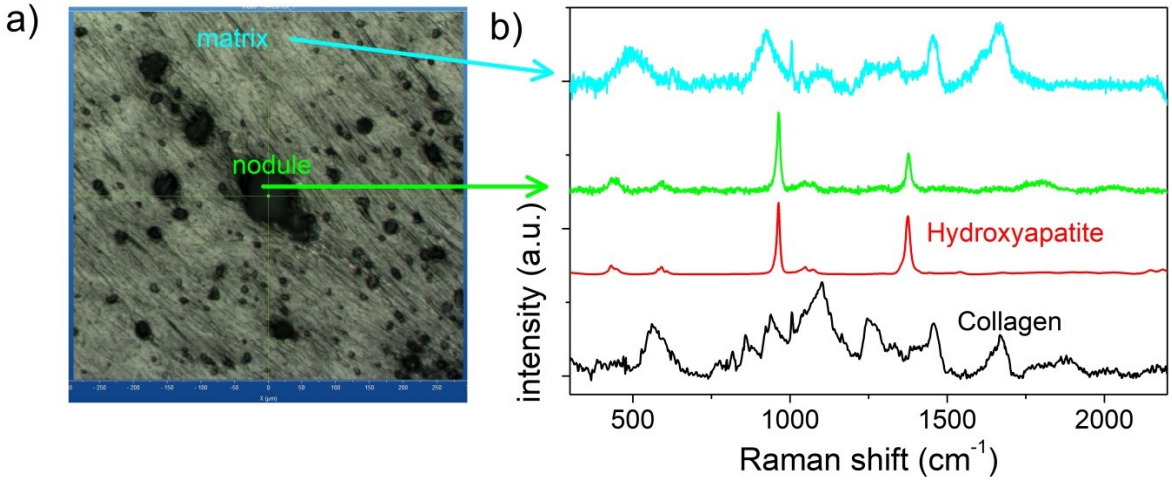

Fig.1. Nanoparticles-incorporated cells (a) showing HA nanoparticles nodules and Raman spectra (b) measured at nodules (green line), biostimulated cell matrix (cyan line) and reference spectra of hydroxyapatite (red line) and collagen (black line).

Acknowledgments

FAPESP grants 2016/02326-9, 2017/10765-5, EMU 2018/19240-5, 2019/06334-4, 2021/11316-5, 2022/07199-6.

Síntese e caracterização dos coacervatos de cálcio e seus produtos de decomposição térmica.

Thaís L. Oliveira (PG),[1*] Maurício A. P. Silva (PQ)[1], Patrick Carvalho (IC), Luiz Fernando C. Oliveira (PQ)[1]
thaislourenco@ice.ufjf.br

[1] Núcleo de Espectroscopia e Estrutura Molecular, Departamento de Química, UFJF;
Palavras Chave: *Coacervatos, Tratamento Térmico, Degradação, Caracterização, Raman, Ressonância Magnética Nuclear do Estado Sólido.*

Highlights

Synthesis and characterization of calcium coacervate and its thermal decomposition products. The relationships between the structure and the decomposition of polyphosphate coacervates were studied. Raman spectroscopy and ^{31}P NMR studies were used to evaluate the structural properties and their respective degradation products.

Resumo/Abstract

A coacervação é um processo de separação de fases, e ela acontece entre duas fases líquidas que diferenciam pela viscosidade e concentração em coloides[1]. A obtenção do coacervato se deu através da reação sol-gel[2], de soluções 4,0 mol L^{-1} de $(NaPO_3)_{n(aq)}$ e 2 mol L^{-1} de $CaCl_2.2H_2O$. Após a obtenção do coacervato de cálcio, foi feito seu tratamento térmico numa mufla à 200 ºC em tempos de 0,5, 1, 2 e 5h. São apresentados abaixo seus respectivos espectros Raman e RMNES ^{31}P. Foi feito também o tratamento térmico através de medidas Raman com variação de temperatura, de 30 a 180 ºC. Ao observar a figura 1, podemos propor que há uma formação de espécies cíclicas, uma vez que o desdobramento das bandas se encontra na região entre 680 e 750 cm^{-1} referentes ao modo vibracional do estiramento simétrico em ponte e com diferentes energias vibracionais nas diferentes espécies cíclicas. Os resultados do RMNES ^{31}P, corroboraram com os dados obtidos pela espectroscopia Raman. A partir da figura 2, podemos notar que com o aumento da temperatura há uma diminuição das intensidades relativas das bandas em torno de 1200 cm^{-1} referente ao modo vibracional do estiramento simétrico em ponte. Comparando os resultados da decomposição térmica em diferentes tempos com as diferentes temperaturas, observamos que quando mantemos a temperatura constante a banda em torno de 900 cm^{-1} desaparece, e o mesmo não aconteceu quando usamos o acessório de temperatura do Raman, onde a temperatura variou de 30 a 180 °C, essa banda não desapareceu nem quando atingimos a temperatura máxima. Isso pode ser explicado pela cinética da reação uma vez que na decomposição não-isotérmica, foi se aquecendo a amostra lentamente, porém na decomposição isotérmica as amostras já foram colocadas na mufla à 200 °C, onde a perda de água e as possíveis quebras de ligações aconteceram muito mais rapidamente, levando a diferentes processos de decomposição isotérmica e não-isotérmica.

Figura 1: Espectros Raman dos Coacervatos de Cálcio sem e com tratamento térmico (TT) nos tempos (a) sem TT, (b) 0,5, (c) 1, (d) 2 e (e) 5 h, λo = 1064 nm.

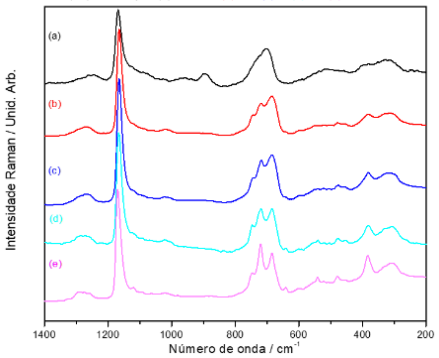

Figura 2: Espectros Raman da decomposição térmica do Coacervato de Cálcio em T = (a) 30, (b) 60, (c) 80, (d) 100, (e) 120, (f) 140, (g) 160 e (h) 180 °C, λo = 633 nm.

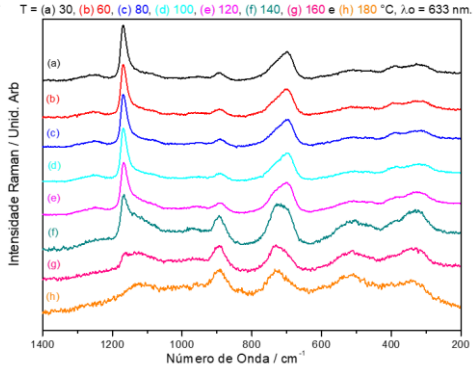

1-KOPP, W. et al. Calcium polyphosphate coacervates: Effects of thermal treatment. Journal of Sol-Gel Science and Technology, v. 63, n. 2, p. 219–223, 2012.

2-UMEGAKI, T.; NAKAYAMA, Y.; KANAZAWA, T., Bulletin of the Chemical Society of Japan, 1976.

Agradecimentos/Acknowledgments

Os autores agradecem à CAPES, CNPq e FAPEMIG e à Universidade Federal de Juiz de Fora pelo auxilio financeiro.

Síntese e caracterização de coacervatos com ácido telúrico.

Thaís L. Oliveira (PG),[1*] Patrick S. de Carvalho (IC), Maurício A. P. Silva (PQ)[1], Luiz Fernando C. de Oliveira (PQ)[1].

thaislourenco@ice.ufjf.br

[1] Núcleo de Espectroscopia e Estrutura Molecular, Departamento de Química, UFJF;

Palavras Chave: *Coacervatos, Tratamento Térmico, Degradação, Caracterização, Raman, Ácido Telúrico.*

Highlights

Synthesis and characterization of Telluric acid coacervates. The relationships between the structure and the decomposition of polyphosphate coacervates dopped with telluric acid [$Te(OH)_6$] were studied. Raman spectroscopy studies were carried out to evaluate the structural properties of the materials and their respective degradation products by the action of time and temperature.

Resumo/Abstract

A coacervação acontece através da interação entre soluções aquosas de polifosfato de sódio e sais de diferentes metais assim como Na^+, Ca^{2+}, Ni^{2+}, Co^{2+}, Mn^{2+} dentre outros, sendo um processo de separação de fases[1,3]. O ácido telúrico é um sólido bastante solúvel em água, constituído por moléculas octaédricas estáveis em solução aquosa por ser um ácido fraco. O material se decompõe em TeO_3/TeO_2 e devido à estabilidade das moléculas de $Te(OH)_6$ em solução, tornam o ácido telúrico um reagente de grande interesse na obtenção de novos materiais de polifosfatos contendo Te(VI) [2]. A obtenção do coacervato se deu através da reação sol-gel, de soluções $(NaPO_3)_{n(aq)}$ 4,0 mol L^{-1}, $CaCl_2.2H_2O$ 2 mol L^{-1} e ácido telúrico 4,0 mol L^{-1}. A figura 1, nos mostra a comparação dos espectros (a) ácido telúrico, (b) coacervato de cálcio e (c) coacervato com ácido telúrico. Podemos dizer então que, o ácido telúrico está incorporado à cadeia polifosfática, uma vez que há o deslocamento da banda que aparece no ácido telúrico em 664 cm^{-1} e no coacervato esta banda aparece em 652 cm^{-1}. Após a obtenção do coacervato com ácido telúrico, através de medidas Raman com variação de temperatura (figura 3), de 30 a 180 ºC (figura 2), onde as temperaturas variaram de 30 a 180 ºC. Observamos que com o aumento da temperatura há uma diminuição das intensidades relativas das bandas em torno de 1200 cm^{-1} referente ao modo vibracional do estiramento simétrico em ponte. Ao variar as temperaturas, a banda em torno de 650 cm^{-1}, relativa aos modos vibracionais das espécies TeO_6 coordenadas à cadeia polifosfática diminui de intensidade e desaparece em temperaturas acima de 140 °C e pode indicar que o ácido telúrico não se encontra mais coordenado à cadeia polifosfática.

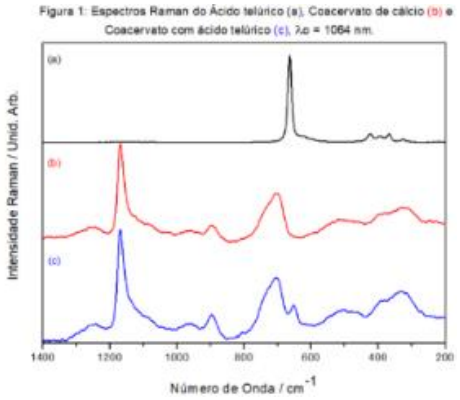

Figura 1: Espectros Raman do Ácido telúrico (a), Coacervato de cálcio (b) e Coacervato com ácido telúrico (c), λ_e = 1064 nm.

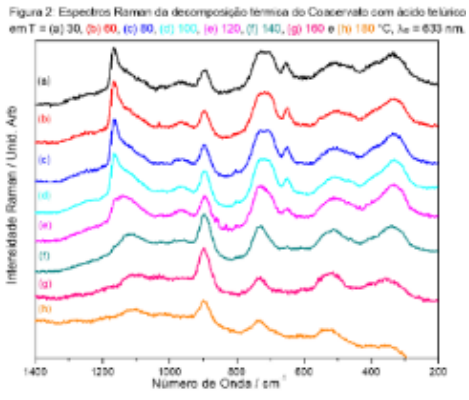

Figura 2: Espectros Raman da decomposição térmica do Coacervato com ácido telúrico em T = (a) 30, (b) 60, (c) 80, (d) 100, (e) 120, (f) 140, (g) 160 e (h) 180 °C, λ_e = 633 nm.

1- KOPP, W. et al. Calcium polyphosphate coacervates: Effects of thermal treatment. Journal of Sol-Gel Science and Technology, v. 63, n. 2, p. 219–223, 2012.

2- ROPP, R.C. Encyclopedia of the Alkaline Earth Compounds Chapter 3 - Group 16 (O, S, Se, Te) Alkaline Earth Compounds, p. 105–197, 2013.

3- UMEGAKI, et al. Bulletin of the Chemical Society of Japan, 1976.

Agradecimentos/Acknowledgments

Os autores agradecem à CAPES, CNPq e FAPEMIG e à Universidade Federal de Juiz de Fora.

VII Encontro Brasileiro de Espectroscopia Raman
VII EnBraER
05 a 08/12/2022, São Pedro – SP

Revisiting Raman Spectra of Some Mineral Carbonates

Julliana F. Alves (PG),[1]* Luiz F.C. de Oliveira. (PQ)

julliana@ice.ufjf.br

[1]*Núcleo de Espectroscopia e Estrutura Molecular, Universidade Federal de Juiz de Fora.*
Palavras-Chave: Minerais, Carbonatos, Espectroscopia Raman, Calcita, Aragonita.

Highlights

Discussion of vibrational modes of natural carbonate minerals. In many cases, small cations shift the Raman band to a higher wavenumber. The data shows two deviations of this trend and brings a comparison with synthetic samples.

Resumo/Abstract

Minerals in general are interesting object of study for their structures and optical properties. Carbonate minerals are an important target in Raman spectroscopy, for their peculiarities involving crystal structure, availability, and diversity. Therefore, this study has the purpose to revisit their spectra and to point the main differences between each other, discussing about how the vibrational modes of carbonate ion are affected by the different environments and conditions. Starting the discussion comparing two different systems, calcite, and aragonite, minerals with the same composition ($CaCO_3$), but with different crystal unit cells, differing in the low wavenumber region due to the crystal structures, since the amount and disposition of calcium atoms around carbonate ions is not the same.[1] Calcite and aragonite spectra show a Raman band at 1086 cm^{-1}, which corresponds to the symmetrical stretching mode of $CO3^{2-}$. For this vibration is not observed some variation between the two minerals. Possible shifts of this band are caused not by the quantitative presence of the calcium ion, but qualitatively. Then, this work compares, for the two systems, deviation in the Raman signals, when the calcium ion is replaced by a larger or smaller ion. Each mode is more strongly affected than the other, but in many of the cases small ions shift the signal to a higher wavenumber.[2] The collected data shows two deviations of this trend: the first one is rhodochrosite ($MnCO_3$) spectrum, that shows this increase in the wavenumber for signals in low region, but a decrease for high region, that is, looking the whole spectrum, and comparing with calcite, for rhodochrosite the signals appear to “come closer” to each other. The second one is the case of the partial substitution of Ca^{+2} for Mg^{2+}(dolomite); the spectrum of dolomite does not show more Raman signals than the rest of the group, that is, the mineral is not a mixture of crystals of calcite and magnesite, but a new carbonate of calcium and magnesium. In addition, given a partial replacement of calcium, the band shift to a higher wavenumber should be less than a total replacement (magnesite). This is observed for all Raman bands, except for the symmetric stretching of the carbonate ion. A possible explanation is that partial replacement leads to a loss of symmetry in the crystal lattice unit cell. In this case, for the structure remains crystalline, a possible shortening of the C-O bonds that influences with greater intensity the symmetrical stretching movement of these bonds, shifting it to a higher wavenumber. Finally, this work brings a comparation with synthetic carbonate samples to understand the degree of crystallinity for such natural samples as well the identification of the phonons for each one of the minerals.

References

[1] Z. Tomić, P. Makreski, B. Gajić, *Journal of Raman Spectroscopy* **2010**, *41*, 582.
[2] W. J. B. Dufresne, C. J. Rufledt, C. P. Marshall, *Journal of Raman Spectroscopy* **2018**, *49*, 1999.

Agradecimentos/Acknowledgments

Authors deeply grateful to Petrobras (Cooperation term Nº 0050.0121114.22.9), CNPq, FAPEMIG, FINEP and CAPES (all Brazilian agencies) for the financial support. Authors also thank Centro de Tecnologia Mineral (CETEM-RJ) for the help with some of the geological samples.

Eletrochemical SERS study of Thiram on gold nanoparticles

Ana Luiza Clivatti Yamanaka (IC),[1] Mari Ferreira Nicolas (PG),[1] Clara de Jesus Rangel (PG) ,[1] Rômulo Augusto Ando (PQ)[1]*
anayamanaka@usp.br
[1]Laboratório de Espectroscopia Molecular, Departamento de Química Fundamental, Instituto de Química, Universidade de São Paulo.
Palavras Chave: Eletrochemical *SERS, Thiram, Gold Nanoparticle, disulfide bond.*

Highlights

Electrochemical SERS spectrum of the pesticide Thiram and its dependence with potential; Monitoring the S-S band with applied potential variation; SERS differentiation of species on the electrode surface.

Resumo/Abstract

O Thiram é um fungicida amplamente utilizado no mundo inteiro e, devido ao seu potencial nocivo à saúde e ao meio ambiente, existem vários estudos acerca de seu comportamento. Dentre eles, análises do pesticida pela técnica SERS ganham destaque, pois dada a estrutura dessa molécula, a presença de átomos de enxofre na estrutura favorece a interação específica da molécula com superfícies de Au ou Ag, ocasionando em altos fatores de intensificação Raman[1]. Por outro lado, a forte interação dos átomos de enxofre com a superfície, também é responsável por causar a quebra de ligações do pesticida e, portanto, o que são detectados nos espectros são os seus fragmentos.

Neste trabalho é apresentado o estudo SERS eletroquímico do Thiram (Figura 1), através do acompanhamento das bandas em 394 e 1381 cm^{-1}, atribuídas ao ν(S-S) e ao δ(CH_3) + ν(CN)[1], respectivamente. A comparação com o espectro Raman do Thiram sólido sugere que a variação de potencial aplicado é responsável por mudanças como a adsorção e a dessorção do pesticida na superfície metálica. O acompanhamento da banda em 391 cm^{-1}, que diminui sua intensidade em potenciais menores, aponta que o Thiram está adsorvido na superfície metálica, já que a ausência desta indica a quebra da ligação entre os dois enxofres centrais. Simultaneamente, o acompanhamento das bandas em 559 e 1381 cm^{-1} atribuídas ao SERS do Thiram[1], corrobora com a hipótese de que a molécula está adsorvida na superfície nos potenciais 0 e 1 V[2]. Enquanto que para potenciais maiores, 1,3 V, as bandas características do SERS do Thiram diminuem bruscamente de intensidade e o aumento da intensidade relativa das bandas em 394 (S-S) e 442 cm^{-1} (S-C-S) [1] sugere dessorção promovida pela aplicação de potencial.

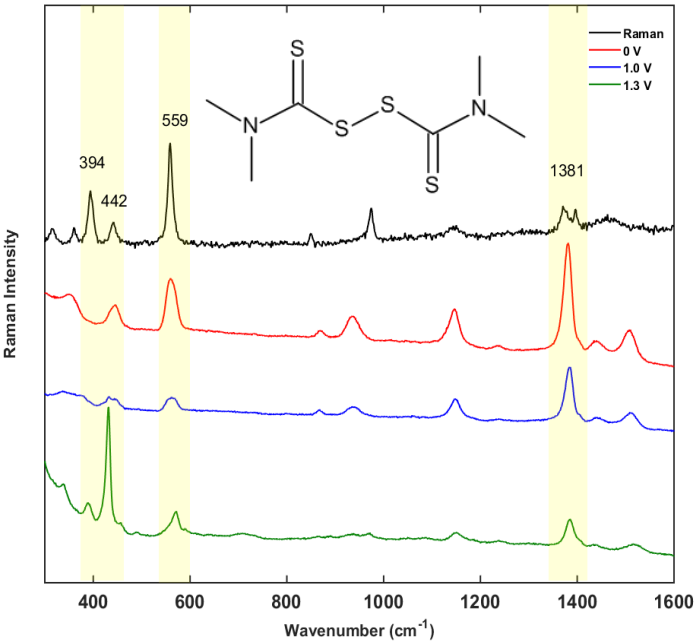

Figura 1. Espectros Raman sólido (preto) e SERS do Thiram em 0 V (vermelho), 1,0 V (azul) e 1,3 V (verde).

Deste modo o presente trabalho tem como objetivo desenvolver estratégias que promovam a elucidação dos mecanismos de adsorção e dessorção de moléculas em geral na superfície metálica, através da espectroscopia SERS para a análise desse tipo de sistema. A fim de comprovar as hipóteses, pretende-se realizar experimentos que alcancem maiores faixas de potencial aplicado e inúmeros ciclos para ver a reprodutibilidade do sistema.

[1] Oliveira, M. J. S.; Martin, C. S.; Rubira, R. J. G.; Batagin-Neto, A.; Constantino, C. J. L.; Aroca, R. F., Surface-Enhanced Raman Scattering of Thiram: Quantitative and Theoretical Analyses. *Journal of Raman Spectroscopy* **2021**.
[2] Juliana R. S.; Miriam H. K.; Artur J. M.; Mechanistic proposal for the electrochemical and sonoelectrochemical oxidation of thiram on a boron-doped diamond anode. *Elsevier Journals.* **2015.**

Agradecimentos/Acknowledgments

À Fundação de Amparo à Pesquisa do Estado de São Paulo (Fapesp 2016/21070-5 e 2022/06398-5) e ao Conselho Nacional de Desenvolvimento Científico e Tecnológico (CNPq 435805/2018-5).

VII Encontro Brasileiro de Espectroscopia Raman

VII EnBraER

05 a 08/12/2022, São Pedro – SP

Synthesis of Gold Nanoparticles in Ionic Liquids: SERS identification of the molecular species on the metallic surface

Mari Ferreira Nicolas (PG), Rômulo Augusto Ando (PQ)*

marifnicolas@usp.br

Laboratório de Espectroscopia Molecular, Departamento de Química Fundamental, Instituto de Química, Universidade de São Paulo.

Keywords: Synthesis of Gold Nanoparticles, Ionic Liquid, Tricyanomethanide, SERS, Stabilizer, Probe

Highlights

Successful synthesis of nanoparticles for SERS applications using Ionic Liquids; SERS spectra of EmimTCM as stabilizer is different from the SERS spectra of EmimTCM in Au colloid.

Resumo/Abstract

Different synthesis strategies have been used for obtention of gold nanoparticles as a substitution method for wet synthesis. Ionic liquids can be advantageous as a medium because of its high solvent structuring, creating a suitable environment to control the growth, nucleation and stability of nanoparticles (NPs).[1] Although many works show the synthesis of NPs using IL, the role of these ions in the morphology, size and stability of NPs is not yet fully elucidated. In this sense, the present study aims to use SERS spectroscopy to investigate the species on the metal surface for both the nanoparticles synthesized with the ILs and the conventional SERS of IL species in aqueous colloidal solution. Figure 1 A shows the comparison between the extinction spectra of the conventional AuNPs (AuCIT) and in the presence of IL (AuEmimTCM). It is noticed that in the case of IL there is a high degree of aggregation of the NPs during their synthesis, which results in desirable plasmonic properties to use them as SERS substrate (Figure 1B). The comparison between the SERS spectra in the region of 2200cm^{-1} suggests that the interaction of IL with NPs is through the TCM anion. The results suggest that the TCM species adsorbed on gold when it is used as stabilizer are distinct from the adsorbed species in the conventional SERS spectrum (Figure 1C). Probably, the main factor for these spectral changes are the different possible adsorption geometries of the anion with its CN groups on the metal surface.[2] In order to refine the conclusions and characterize the species present on the metal surface, it is intended to vary the concentrations of the reactants to identify their influence on the material properties, and to use the same methodology and analysis for other systems with different LI and investigate the correlation of the experimental and calculated vibrational spectra. Thus, this work may help in the understanding of which IL species are responsible for the controlled aggregation of NPs, bringing further elucidation in the role of ionic liquids in the synthesis and its interaction with gold nanoparticles.

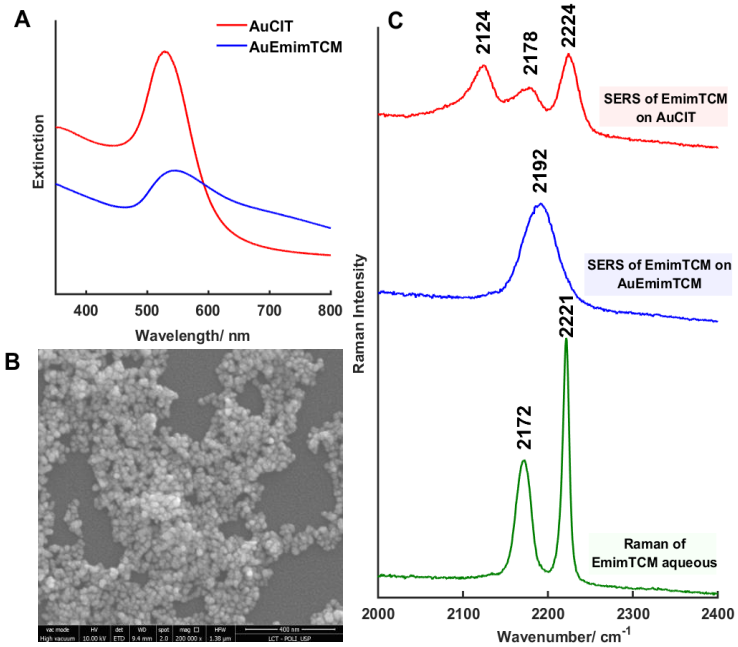

Figure 1. A) Extinction spectra of AuCIT and AuEMimTCM; B) SEM image of AuEmimTCM and C) Raman spectra of IL aqueous (green), SERS spectra of EmimTCM on AuEmimTCM (blue) and of EmimTCM on AuCIT (red).

[1] *He, Z. and P. Alexandridis. Nanoparticles in ionic liquids: interactions and organization.Physical Chemistry Chemical Physics 17(28): 18238-18261,* ***2015.***

[2] *Jacobs, M. B., P. W. Jagodzinski, et al. A Surfaced-Enhanced Raman Spectroscopy and Density Functional Theory Study of [Au(CN)2]−/[Au(CN)4]− Adsorbed on Gold Nanoparticles.The Journal of Physical Chemistry C, 115(49): 24115-24122,* ***2011.***

Agradecimentos/Acknowledgments

The autors thank the support of the Institute of Chemistry, University of São Paulo, FAPESP #2016/21070-5, CNPq #435805/2018-5 and CAPES #88887.639103/2021-00.

VII Encontro Brasileiro de Espectroscopia Raman
VII EnBraER
05 a 08/12/2022, São Pedro – SP

3D-printer microfluidic system for Gold Nanostructures deposition onto Si substrate used as SERS substrates for detecting of Triamterene molecule

Anerise de Barros (PQ),[1,*] Cleber S. Torres,[1] Igor Fier (PQ),[2] Maria L. Braunger (PQ),[3] Varlei Rodrigues (PQ),[4] Fernando A.Sigoli(PQ),[1] Italo O. Mazali (PQ)[1,*]

anerise@unicamp.com; mazali@unicamp.br

[1]Functional Materials Laboratory - Institute of Chemistry, University of Campinas – UNICAMP, Campinas, Brazil; [2]Quantum Design Latin America; [3]Universidade Estadual Paulista "Julio de Mesquita Filho", UNESP; [4]Institute of Physics Gleb Wataghin, UNICAMP

Palavras Chave: *Gold Nanorods, Microfluidic devices, SERS substrates, Triamterene, Sports doping molecule*

Highlights

Gold nanorods deposited on Si substrate by the 3D-printer microfluidic system. Surface-enhanced Raman scattering for detection of Triamterene doping molecule.

Abstract

The study of the interaction between light and metallic nanostructures is rapidly emerging as plasmonic devices, which are associated with analytical applications such as Surface-Enhanced Raman spectroscopy (SERS). This work shows ultrasensitive SERS detection of triamterene (TMT) drug, of high interest in illegal sport doping clinical analysis. The analysis is based on the molecule adsorption close to the electromagnetic localization field spot of plasmonic nanoparticles. We combine the flow injection self-assembled deposition in Si substrate functionalized with 3-mercaptopropyltrimethoxysilane (MPTMS) solution, followed by Gold Nanorods (AuNRs) deposition. A 1 cm^2 silicon substrate is embedded in a 3D-printed structure composed of two parts: a superior structure with inlet and outlet entries, a microchannel with 200µm width and 0.5 mm length; and the bottom part possessing a sample holder having exactly the Si substrate dimension. The effectiveness AuNRs synthesis is confirmed by UV-vis spectroscopy with plasmon bands at 514 and 703 nm, corroborated by TEM micrographs with a good homogeneity distribution. The SEM micrographs also reveal that the laminar flow injection favors the alignment of AuNRs, with a good, efficient hot spot coupling to detect trace levels of molecules. Detailed mapping was achieved to detect TMT in 10^{-5}mol $L^{-1}$to 10^{-12}mol L^{-1}range, with good reproducibility and sensitivity in the obtained analytical curves, as can be seen in Figure 1 (a-d).

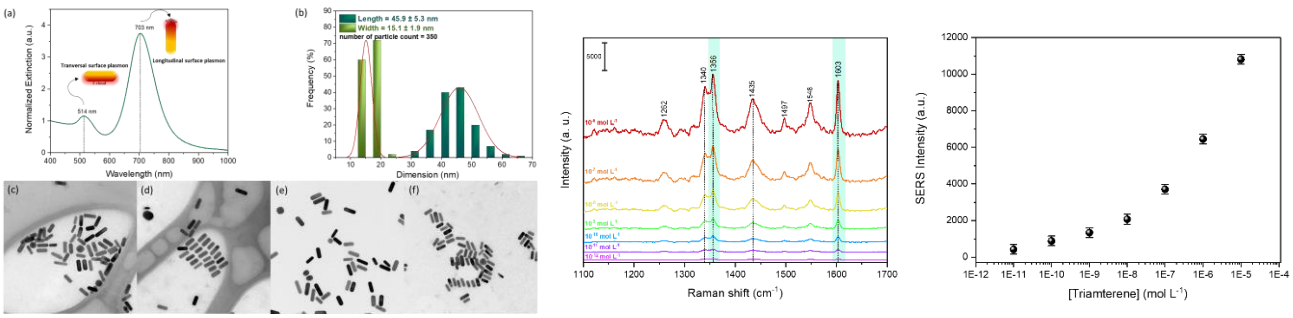

Figure 1. (a) Spectrum of extinction of AuNRs; (b) Histogram size distributium of AuNRs; (c) TEM micrographs of AuNRs; (d) Average SERS spectra for different Triamterene concentration, 10^{-5} mol L^{-1} to 10^{-12} mol L^{-1}; (e) Analytical curve for SERS intensity as function of TMT different concentration from 1603 cm^{-1} band as reference.

Agradecimentos/Acknowledgments

UNICAMP, Instituto de Química, Laboratório de Materiais Funcionais, LMMU Multi-User Laboratory for Advanced Optical Spectroscopy, FAPESP Ciência, Cultura e Desenvolvimento, CNPq, CAPES, LNNano, Inomat

VII Encontro Brasileiro de Espectroscopia Raman
VII EnBraER
05 a 08/12/2022, São Pedro – SP

Au nanostars as inkjet printing SERS substrate for the detection of molecules of biological and environmental interest

Edison H. Montoya (PG) *[1], Lucas F. Oliveira Fernando[1], A. Sigoli (PQ)[1], Italo O. Mazali (PQ)[1]

edisonqca@gmail.com*, mazali@unicamp.br[1]

[1]*Functional Materials Laboratory - Institute of Chemistry, University of Campinas – UNICAMP, Campinas, Brazil.*

Key Words: Gold Nanoparticles, Inkjet Printing, Surface Plasmon, SERS, Raman Spectroscopy.

Highlights

Au nanostars Ink for the design of functionalized paper-based SERS substrates, and study of the morphology effect in the SERS enhancement of organic molecules.

Abstract

Inkjet printing has emerged as a powerful tool for the design of low-cost high-performance SERS substrates that aim for real-practical applications. However, most of the reported studies focused on the fabrication of paper-based substrates are built around spherical nanoparticles. Thus, as discussed by Tian et al[1], for suspensions of equal nanoparticle and analyte concentration, the SERS effect increases as nanospheres < nanotriangles < nanostars (NSs), indicating that control over the number of local field “hot spots” can optimize the SERS efficiency. Thus, the aim of this research is the preparation and evaluation of Au NSs as inkjet printing paper-based SERS substrates. The morphology of the prepared Au NSs was confirmed by TEM, obtaining NPs with a tip-tip size between 50-100 nm and a broad absorption band around 690 nm. The viscosity of the ink was adjusted with a mixture of glycerol/ethanol to be similar to the commercial black ink EPSON 544. Then, chromatographic paper was chosen for the printing process since it presents a low fluorescence signal and background. The paper surface was modified from a hydrophilic to a hydrophobic surface to gather the analyte in the impressed region instead of spreading on the paper. The functionalization process was verified by contact angle (CA) measures, all the functionalized papers can be considered hydrophobic since all of them show CA values > 90°. The performance of the substrates was evaluated by measuring the SERS spectra of crystal violet (CV), varying the number of printing cycles (1,3 5, and 10). Results show a decrease in the spectra intensity and the CA value with the increase in the number of printing cycles, indicating a loss of hydrophobicity that allows water to spread out of the designed spot. Then, the substrate with 1 printing cycle showed the best performance in terms of SERS activity and repeatability among measures, which is an excellent result when compared with previous substrates developed at our lab[2], based on Au nanospheres, where the optimal performance was achieved for 5 printing cycles and a [Au] two times higher. [1] Tian, F et al. *Anal. Methods* **6**, 9116–9123 (2014). [2] Godoy, N. V. *et al. Sensors Actuators, B Chem.* **320**, (2020).

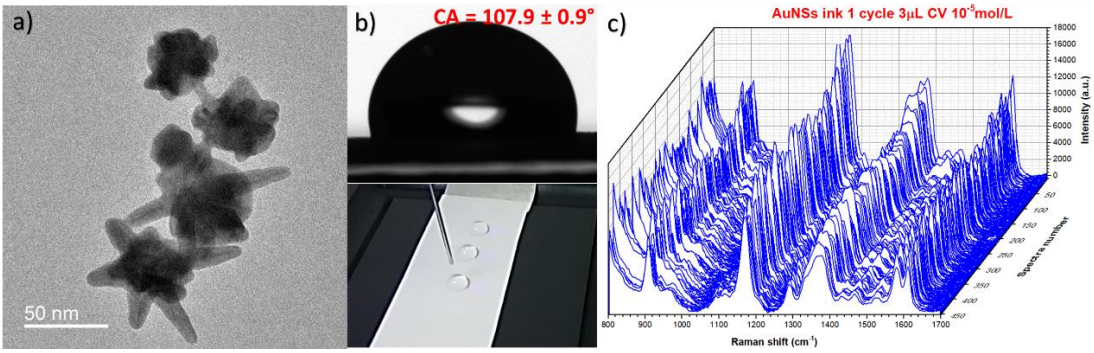

Figure 1. a) Au NSs TEM images. **b)** CA angle measures, and **c)** SERS spectra of CV on the Au NSs substrate.

Acknowledgments

UNICAMP, Instituto de Química, Laboratório de Materiais Funcionais, LMMU Multi-User Laboratory for Advanced Optical Spectroscopy, FAPESP, CNPq, CAPES, LNNano, Inomat

VII Encontro Brasileiro de Espectroscopia Raman
VII EnBraER
05 a 08/12/17, São Pedro – SP

Gold nanoparticles-conjugated magnetic nanoparticles for SERS analysis of dopamine

Celina M. Miyazaki (PQ),[1,*] Cibely S. Martin (PQ),[1] Aldo E. Job (PQ),[1] Carlos J.L. Constantino (PQ),[1]

celina.miyazaki@unesp.br

[1]*Departamento de Física, Faculdade de Ciências e Tecnologia, UNESP, Presidente Prudente.*

Palavras Chave: Gold nanoparticles, *Magnetic nanoparticles, SERS, magnetic separation, dopamine.*

Highlights

Magnetic-gold nanoparticles were applied for SERS detection of dopamine. The adsorption follows the Langmuir isotherm model. High reproducibility was found using magnetic separation before analysis.

Resumo/Abstract

Gold nanoparticles-conjugated magnetic nanoparticles (AuMNP) were synthesized via coprecipitation of magnetite followed by gold salt reduction method [1]. Inositol hexakisphosphate (IP6) was used as a soft template. The morphology investigation by SEM indicated most gold particles between 9 – 12 nm distributed on smaller magnetite nanoparticles agglomerates. The AuMNP suspension exhibited SERS for dopamine (DA) detection. After the addition of DA in 1.0 mL AuMNP colloidal suspension, a magnetic separation was performed per 2 min before measurement in a handheld Raman BRAVO BRUKER spectrometer (Fig. 1A). SERS spectra from 1.0×10^{-7} – 1.0×10^{-3} mol/L DA presented characteristic SERS bands. Following the non-planar ring vibration band at 634 cm^{-1} (Fig. 1B), the Raman intensity band versus DA concentration plot follows the Langmuir adsorption isotherm model (Fig. 1C). High reproducibility was achieved by the magnetic separation when compared to the direct suspension measurement. The signal standard deviation to 5.0×10^{-6} mol/L DA was 39.71 and 594.9 (a.u.) for magnetically separated and suspension measurements, respectively. AuMNP conjugates are promising candidates for high reproducible SERS measurements, which are usually limited by the Brownian motion of particles in the solution-phase SERS substrates.

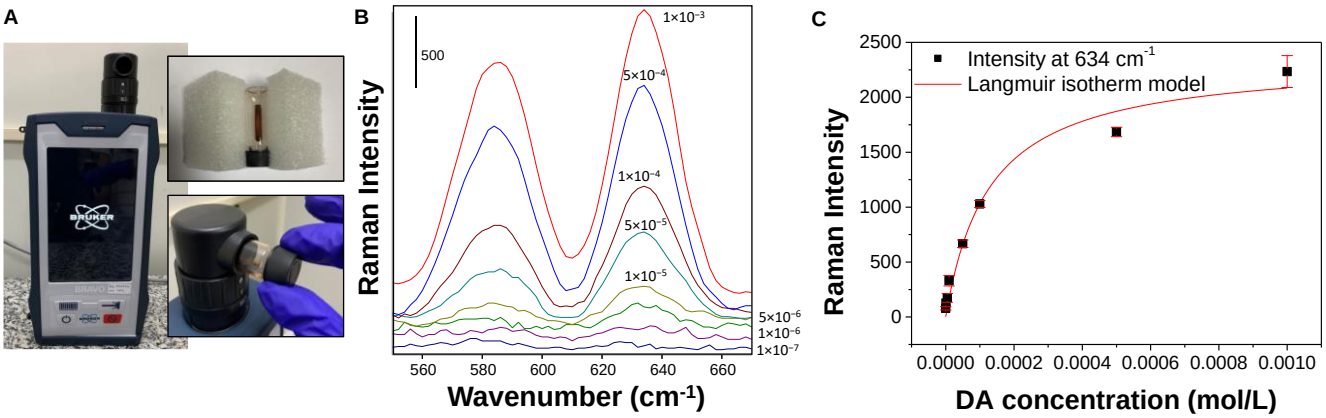

Figure 1. (A) Handheld Raman spectrometer and magnetic separation process before measurement. (B) 550 –670 cm^{-1} range SERS spectra of various DA concentrations-AuMNP suspensions. (C) Langmuir isotherm model plot on experimental data from (B) at 634 cm^{-1}.

Reference

[1] Yang et al. *Small* 10, 1325-1331, 2014.

Agradecimentos/Acknowledgments

FAPESP (2020/11803-0, 2018/22214-6, 2017/15019-0), CNPq, INCT/INEO, CAPES, Contrato de Repasse n° 0478373-12/2018 - MPF/MPSP/CESP-Programa de Compensação Ambiental.

VII Encontro Brasileiro de Espectroscopia Raman
VII EnBraER
05 a 08/12/2022, São Pedro – SP

Paraquat detection by SERS using the standard addition method

Cibely S. Martin (PQ)*, Marcelo J. Oliveira (PG), Carlos J.L. Constantino (PQ)

cibely.martin@unesp.br

Departamento de Física, Faculdade de Ciências e Tecnologia, UNESP, Presidente Prudente-SP.

Palavras Chave: *standard addition method, SERS, colloid, paraquat.*

Highlights

Standard addition method as an analytical tool for SERS;

SERS detection of paraquat using Ag colloid and their derivatives (coatings);

Paraquat quantification with a limit of detection of 0.4 µmol/L.

Resumo/Abstract

The surface-enhanced Raman scattering (SERS) is one of the most sensible and selective techniques, reaching the detection of the single-molecule [1]. However, in the colloid system, the analytical application as a quantitative tool decreases due to the low reproducibility and repeatability of the SERS signal. One of the reasons can be attributed to the aggregation of the nanoparticles, and the non-uniform formation of hot spots (the region with maximum Raman enhancement). Thus, sample preparation can play an important role in the quantitative application of SERS technique [2]. In this work, we evaluated de detection of paraquat (PQ, a non-selective contact herbicide) by SERS using the standard addition method. In this case, the AgNP as a colloid platform was used for the construction of the calibration curve. The detection was also evaluated using the AgNP@SiO_2, AgNP@SiO_2@AuNP (Ag nanoparticles with SiO_2 coating and AuNP adsorption, respectively) as a comparison. The SERS measurements were performed using a fixed volume (500 µL) of colloid following successive addition of a standard solution of PQ (stock concentration = 10^{-5} and 10^{-6} mol/L in ultrapure water). The aliquots from 1 to 55 µL of each stock solution were used to obtain a concentration range from $2.0x10^{-8}$ to $1.0x10^{-5}$ mol/L. The SERS spectra were collected using a micro-Raman Renishaw, model in-Via, at a laser line of 633 nm, 1800 l/mm, 10 seconds of acquisition, and 1 accumulation. The SERS spectra of PQ showed four intense bands at 843, 1201, 1302, and 1648 cm^{-1} ascribed to C-N stretching, C=N bending, chain distortion, and C=N stretching, respectively. These bands also showed high intensity in the PQ powder. However, using the AgNP@SiO_2 and AgNP@SiO_2@AuNP colloid, a significant enhancement was obtained only after the addition of 0.2 mol/L of NaCl, being twice higher than without salt addition. The calibration curve following the standard addition method in presence of salt showed a colloid instability for AgNP@SiO_2 and AgNP@SiO_2@AuNP. Thus, the successive addition of PQ promotes a faster aggregation with a decrease in SERS properties. The instability started at $5.3x10^{-6}$ mol/L of PQT, which corresponds to the eighth PQ addition, and an increase of signal deviation (c.a 40%) was observed. On the other hand, using the AgNP (without covering) an enhancement of the PQ band was observed between 10^{-8} to 10^{-5} mol/L PQ. The SERS intensity of the band at 1648 cm^{-1} (C=N stretching) showed two linear ranges, from $2.0x10^{-8}$ to $1.2x10^{-6}$ mol/L, and from $2.8x10^{-6}$ to $1.0x10^{-5}$ mol/L, with a limit of detection of $4.1x10^{-7}$ mol/L (LOD = 3xSD/slope = 0.4 µmol/L). Indeed, the limit of detection is in agreement with the ratio 3S/N (signal/noise), being the band at 1628 cm^{-1} from SERS spectra obtained at $4.8x10^{-7}$ mol/L with a S/N = 2.6. In conclusion, the standard addition method showed a promissory analytical method to improve the SERS as an analytical technique.

[1] C.J.L.Constantino, T. Lemma, P.A. Antunes, R. Aroca. Single-Molecule Detection Using Surface-Enhanced Resonance Raman Scattering and Langmuir-Blodgett Monolayers. Anal. Chem. **2001**, 73, 3674-3678.
[2] B.L.Darby, E.C. Le Ru. Competition between Molecular Adsorption and Diffusion: Dramatic Consequences for SERS in Colloidal Solutions. J. Am. Chem. Soc. **2014**, 136, 31, 10965–10973.

Agradecimentos/Acknowledgments

FAPESP 2017/15019-0 and 2018/22214-6, CNPq, INCT/INEO, CAPES.

VII Encontro Brasileiro de Espectroscopia Raman
VII EnBraER
05 a 08/12/17, São Pedro – SP

Drug delivery of fluconazole by AgNP for *in vitro* combat of *Candida spp.* investigated through SERS spectroscopy

Daphne Fonseca de Coppoli Lanferini (PG),[1,*] Antonio Carlos Sant'Ana (PQ),[1] Francis Moreira Borges (PQ)[2]

daphnecoppoli@ice.ufjf.br

[1]Departamento de Química, Instituto de Ciências Exatas, UFJF; [2]Departamento de Parasitologia, Microbiologia e Imunologia Instituto de Ciências Biológicas, UFJF.

Palavras-Chave: Silver nanoparticles; Candida spp.; Antifungal; Sinergy

Highlights

The AgNP and fluconazole association presented synergistic effect at *in vitro* tests against *Candida spp*.
The chemical affinity of fluconazole by Ag surface was monitored through SERS spectroscopy.

Resumo/Abstract

The minimum inhibitory concentration (MIC) and fractionary inhibitory concentration (FIC) index involving silver nanoparticles (AgNP) and fluconazole (FZL) association against C. albicans and C. tropicalis species was more effective than each one alone, indicating synergic effect. The FZL drug is consider a fungistatic agent, but the status changed to fungicide when in association with AgNP, with doses decreasing from 16 to 0,25 $\mu g.mL^{-1}$.

The mechanism of action of FZL depends on the formation of a covalent coordination bond between the N9 (Fig. 1) and the heme group in the CYP51 enzyme. However, the specificity of this binding depends on other interactions between the FZL molecule and amino acid residues at the target active site, such as the interaction between F2 and Phe152, also involved in decreasing toxicity to humans[1].

Fig. 1 – FZL conformational structure, in a vacum, and atom labeling Illustrated using DrawMol software.

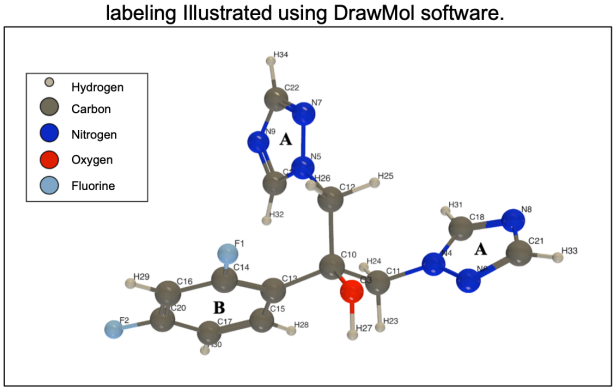

Note - A) Triazole rings; **B)** 2,4-difluorobenzyl
Developed by the author

In the SERS spectrum of FZL, presented in Figure 2-I, it is possible to observe the presence of intensified bands at 1014, 1078 e 1187 cm^{-1}, whose assignment allows to infer that the adsorption on Ag surface occurred through nitrogen atoms from A ring, F1 fluorine from B ring and O3-H27 hydroxyl. The presence, in the Raman spectrum of the solid (Fig. 2-II), of the bands at 588 cm^{-1} and 1253 cm^{-1}, assigned to vibrations involving F2 atom, was not intensified in the SERS spectrum, indicating this atom is not involved in the adsorption. The low intensity of the SERS band at 1137 cm^{-1}, assigned to normal modes involving N9 atom[2], allows to infer, if drug delivery system was internalized, such a molecular moiety was not precluded, by the adsorption, to interacts with enzyme target.

These results go along with those obtained by *in vitro* studies, proving that Raman and SERS spectroscopies can be a valuable tool in the biological test planning.

Fig. 2- FZL on AgNP surface SERS spectrum (λ_0= 633nm, 10 mW, 90s); **(I);** Solid state FZL Raman spectrum (λ_0= 1064 nm, 1000 mW, 512 scans) **(II).**

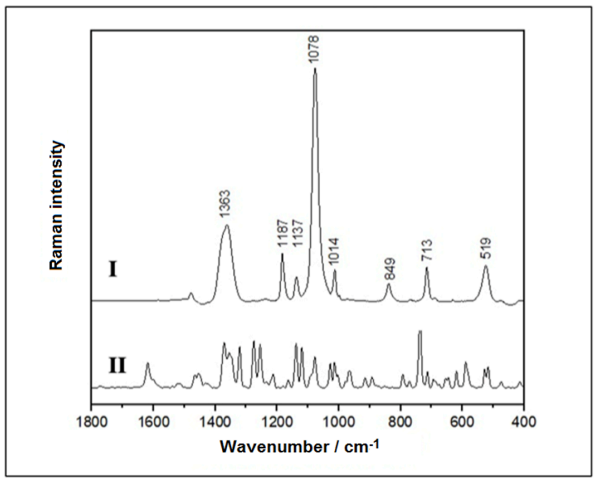

1 - (HONORATO-SIQUEIRA; MARTÍNEZ, 2020).

2- (CHANDRASEKARAN; THILAK-KUMAR, 2015).

Agradecimentos/Acknowledgments

The authors would like to thank UFJF and funding agencies CNPq, CAPES and FAPEMIG.

VII Encontro Brasileiro de Espectroscopia Raman
VII EnBraER
05 a 08/12/2022, São Pedro – SP

SERS monitoring of the photocatalytic degradation of the fungicide Tebuconazole by hybrid catalyst AgNP/TiO_2

Rafael de Oliveira (PG),[1]* Antonio Carlos Sant'Ana (PQ),[1]

antonio.sant@ufjf.br

[1]*Departamento de Química, Instituto de Ciências Exatas, Universidade Federal de Juiz de Fora*

Palavras Chave: *Nanopartículas de prata, Fotocatálise plasmônica, Tebuconazole, SERS*

Highlights

- The photodegradation of Tebuconazole by AgNP/TiO_2 hybrid catalyst was studied through the effect of reactional pH and changes in the incident radiation
- The best result was obtained using pH = 6.0 and UV-A radiation (λ_{max} = 368 nm), reaching efficiency around 80% after 100 minutes
- Surface-enhanced Raman scattering spectroscopy was used to monitor the photodegradation reaction
- Changes in spectral profiles were observed, confirming the applicability of SERS spectroscopy in monitoring chemical reactions and possible identification of products/intermediates

Resumo/Abstract

De suma importância na agricultura moderna, os pesticidas são extensamente utilizados em países com forte atividade agrícola, como o Brasil. No entanto, estas substâncias são consideradas parte significativa das contaminações ambientais por compostos orgânicas. No presente trabalho, a degradação do fungicida Tebuconazole (TEB; Figura 1A) foi avaliada empregando-se catalisador AgNP/TiO_2 e monitoramento SERS. Na Figura 1B é apresentado o monitoramento SERS da degradação do composto por catalisador AgNP/TiO_2 irradiado por luz UV. Durante monitoramento, diversas bandas do fungicida foram observadas, evidenciando a presença de moléculas inalteradas de TEB, mesmo após 18h. Maior mudança espectral é observada com a intensa e alargada banda entre 1610 e 1670 cm^{-1} no tempo de 410 minutos, possivelmente decorrente da formação de produtos contendo grupos como aldeídos e ácidos carboxílicos. Esta banda desaparece após 18h de reação, sugerindo a perda do carbono oxidado na forma de CO_2. Deslocamento de banda referente à respiração do anel foi observado (996 para 1002 cm^{-1}), sugerindo a modificação nos substituintes no grupo fenil. Banda em 1271 cm^{-1} (ωCH_2 de C2) deslocada para 1280 cm^{-1} e desaparecimento de banda em 1198 cm^{-1} referente a νCC (C1 e C2), sugerem que o grupo CH_2 da cadeia alifática possa ser um ponto de ataque radicalar. O surgimento da banda em 1069 cm^{-1}, atribuída ao 1,2,4-triazol livre (νCN), permite supor ser esse um produto da reação; a mesma banda pode ainda ser atribuída ao estiramento simétrico de íons CO_3^{2-}, um possível produto de oxidação. O deslocamento de banda em 964 para 971 cm^{-1} e o surgimento de banda intensa em 1355 cm^{-1} são observados no tempo de 410 min (ambas atribuídas a νCN), reiterando a presença do produto 1,2,4-triazol. Ao final do monitoramento SERS e análise dos resultados alguns produtos puderam ser propostos, como clorobenzeno, 4-clorofenol, e 1,2,4-triazol.

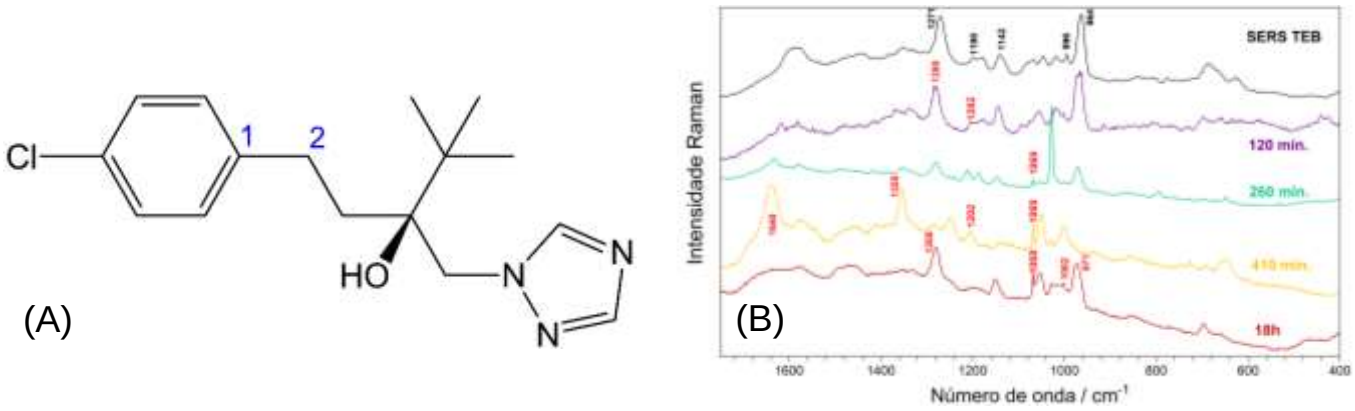

Figura 1. (A) Estrutura química de TEB. (B) Monitoramento SERS da degradação de TEB por AgNP/TiO_2/UV-A.

Agradecimentos/Acknowledgments

Os autores gostariam de agradecer à UFJF, e aos órgãos de fomento CNPq, CAPES e FAPEMIG.

VII Encontro Brasileiro de Espectroscopia Raman
VII EnBraER
05 a 08/12/2022, São Pedro – SP

Inclusion Complexes for the Detection of Pesticides by SERS Spectroscopy

Maelly A. Oliveira (IC), Clara J. Rangel (PG), Mari F. Nicolas (PG), Rômulo A. Ando (PQ)*

maellyoliveira@usp.br

Laboratório de Espectroscopia Molecular, Departamento de Química Fundamental, Instituto de Química, Universidade de São Paulo

Palavras-Chave: *Raman, SERS, cucurbiturils, pesticide, inclusion complex, detection*

Highlights

SERS was used to detect trace amounts of methyl parathion. Inclusion complexes with cucurbiturils allowed the selective detection of MP. The comparison of SERS spectra using Au and Ag was discussed.

Resumo/Abstract

Since the end of the last century, SERS has been a rising method for the detection and quantification of pesticides in environmental samples, mainly because of its high sensibility and possibility of a selective analysis, faster and less resource consuming than gas or liquid chromatography[1]. Better selectivity can be achieved employing cucurbiturils (CB) as hosts molecules capable to include pollutants. Therefore, CB7 was used in this work to form 5:1 (CB7:MP) inclusion complexes with MP to investigate a potential method for trace detection of this organophosphate insecticide in residual waters.

Figure 1 shows the Raman spectrum of solid MP, SERS spectra of MP in Au, Ag, and of its inclusion complex with cucurbituril CB7. The comparison of the SERS spectra in Au and Ag shows quite distinct profiles. While the SERS spectrum in MP-Au is very similar to the neat compound spectrum, the profile of MP-Ag spectrum presents a large band at 1267 cm^{-1} characteristic of well-known spectrum of nitrophenols[2], which suggested the degradation of the pesticide, according to the scheme in Figure 2. The hypothesis was supported by the SERS spectra of *p*-nitrophenol in Ag and Au and also by DFT calculations. Interestingly, the spectrum of the inclusion complex (MPcCB7) showed similarities with MP-Au spectra, being a clear evidence that most of MP degradation was inhibited.

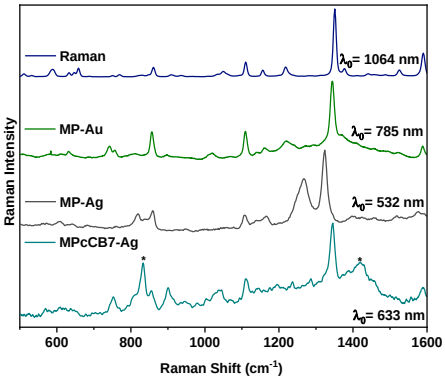

Figure 1 – Raman and SERS spectra of methyl parathion with Au, Ag, and inclusion complex. *CB7 modes.

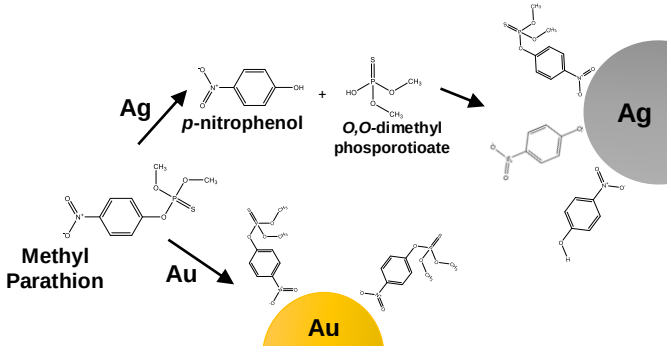

Figure 2 – Scheme of different interactions of MP with Ag and Au nanoparticles.

In conclusion, this work demonstrated that MP pesticide breaks when interacts with silver nanoparticles. The inclusion of MP in cyclic macromolecules apparently can prevent this event and aid to detect pesticides without the loss of its chemical identity.

Agradecimentos/Acknowledgments

We acknowledge the Conselho Nacional de Pesquisa e Desenvolvimento (CNPq 143622/2021-0 e 435805/2018-5) and Fundação de Amparo à Pesquisa do Estado de São Paulo (FAPESP 2017/21070-5).

[1]A. Bernat, M. Samiwala, J. Albo, X. Y. Jiang and Q. C. Rao, *J. Agric. Food Chem.*, 2019, **67**, 12341-12347.
[2]R. A. Ando, A. C. Borin and P. S. Santos, *The Journal of Physical Chemistry A*, 2007, **111**, 7194-7199.

VII Encontro Brasileiro de Espectroscopia Raman
VII EnBraER
05 a 08/12/2022, São Pedro – SP

Investigação SERS do inseticida fosmete em superfícies de Ag e Au

Larissa A. B. Ferreira (IC), Clara de Jesus Rangel (PG), Mari F. Nicolas (PG), Rômulo A. Ando (PQ)*

larissa.abf@usp.br

Laboratório de Espectroscopia Molecular, Departamento de Química Fundamental, Instituto de Química, Universidade de São Paulo;

Palavras-Chave: *Adsorption geometry, SERS, Pesticides, Nanoparticles.*

Highlights

SERS investigation of phosmet insecticide on Ag and Au surfaces

Study of insecticide phosmet shows distinct behavior in SERS spectra on Ag and Au surfaces. DFT calculations indicated different adsorption geometries of FM depending on the metal surface.

Resumo/Abstract

O uso deliberado de pesticidas no Brasil por várias décadas tem contaminado diferentes ambientes, e torna-se necessário o desenvolvimento de diferentes métodos de detecção e quantificação desses poluentes. A técnica SERS tem se destacado pela alta sensibilidade e identificação da espécie molecular. Neste trabalho foi investigada a detecção do inseticida organofosforado fosmete (FM) por espectroscopia SERS, em que foi observada uma interação diferente com a superfície, dependendo do metal utilizado para os substratos SERS Ag e Au. A Figura 1 mostra os espectros Raman, SERS em Ag e em Au obtidos para o FM. Nota-se o aparecimento de uma banda larga em 650 cm^{-1}, que pode ser atribuída ao estiramento ν(P=S) apenas no espectro SERS em Ag, o que sugere que a interação da espécie com a superfície é distinta dependendo da natureza do metal (Ag ou Au).

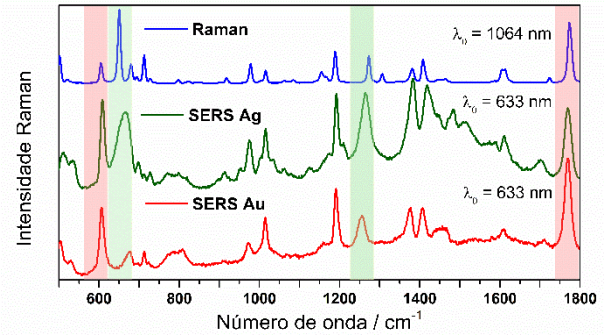

Figura 1. Espectros Raman, SERS Ag e SERS Au do fosmete.

Para dar suporte aos dados experimentais, foram realizados cálculos DFT com o FM interagindo por diferentes sítios de adsorção com clusters de Ag e Au (20 átomos). Os espectros calculados apresentados na Figura 2 indicam que as diferenças observadas são devido às diferentes geometrias de adsorção da molécula em Ag e Au.

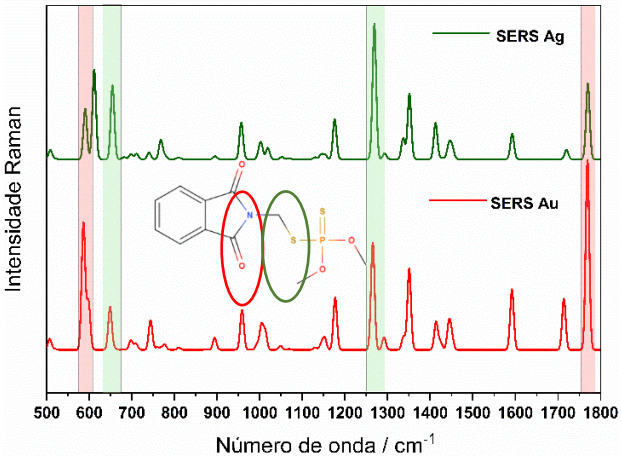

Figura 2. Espectros SERS Ag e Au teóricos, obtidos pelo cálculo DFT

Pode-se observar que quando é considerada a interação do FM do átomo de S com a Ag, são previstas bandas intensas de modos atribuídos ao sítio que contem a ligação P-S (círculo verde da Fig. 2). No caso em que a interação também considera o átomo de oxigênio (círculo vermelho da Fig. 2), as bandas mais proeminentes são observadas em 580 e 1760 cm^{-1}, que podem ser atribuídas a modos vibracionais envolvendo as carbonilas. Estudos SERS com sistemas moleculares semelhantes estão sendo realizados no momento para verificar a hipótese dos diferentes sítios de adsorção.

[1] FAN, Yuxia; LAI, Keqiang; RASCO, Barbara A.; HUANG, Yiqun. Analyses of phosmet residues in apples with surface-enhanced Raman spectroscopy. 2013. Disponível em: http://dx.doi.org/10.1016/j.foodcont.2013.09.01

Agradecimentos/Acknowledgments

À FAPESP (Processos 2016/21070-5 e 2022/06428-1) e ao CNPq (Processo 435805/2018-5).

VII Encontro Brasileiro de Espectroscopia Raman

VII EnBraER

05 a 08/12/17, São Pedro – SP

Silicon microchannel-driven Raman scattering enhancement to improved gold nanorod functions as a SERS substrate toward single molecule detection of R6G and Thiram

Jaciara Bär (PG), [1] Anerise de Barros (PQ),[1*] Davi H. S. de Camargo (PQ),[2] Mariane P. Pereira (PQ),[3] Leandro Merces (PQ),[3] Flavio M. Shimizu (PQ),[3] Fernando A. Sigoli(PQ),[1] Carlos C. B. Bufon (PQ),[2] Italo O. Mazali (PQ)[1,*]

mazali@unicamp.br; anerise@unicamp.com

[1]Functional Materials Laboratory - Institute of Chemistry, University of Campinas – UNICAMP, Campinas, Brazil.; [2]MackGraphe – Graphene and Nanomaterials Research Center, Mackenzie Presbyterian Institute; [3] Brazilian Nanotechnology National Laboratory (LNNano/CNPEM)

Palavras Chave: *SERS, SIERS, microchannel, three-dimensional hot spot, gold nanorods, single-molecule detection*

Highlights

SIERS, Shape-induced enhanced Raman scattering. Surface-enhanced Raman Scattering for R6G and Thiram detection.

Resumo/Abstract

Herein, we report an effect based on the shape-induced enhanced Raman scattering (SIERS) to improve the action of gold nanorods (AuNRs) as a SERS substrate. Scattered electric field simulations reveal that bare V-shaped Si substrates exhibit spatially distributed interference patterns from the incident radiation used in the Raman experiment, resulting in constructive interference for an enhanced Raman signal. Experimental data show a 4.29 increase in Raman signal intensity for bare V-shaped Si microchannels compared to flat Si substrates. The combination of V-shaped microchannels and uniform aggregates of AuNRs is the key feature to achieving detections in ultra-low concentrations, enabling reproducible SERS substrates having high performance and sensitivity. Besides SIERS effects, the geometric design of V-shaped microchannels also allows a “trap” to the molecule confinement and builds up an excellent electromagnetic field distribution by AuNRs aggregates. The statistical projection of SERS spectra combined with the SIERS effect displayed a silhouette coefficient of 0.83, indicating attomolar (10^{-18} mol L^{-1}) detection with the V-shaped Si microchannel. Additionally, we evaluated the V-shaped microchannels using the Thiram molecule until 10^{-10} mol L^{-1}. The analyses were collected in different regions of silicon microchannels to verify the SERS signal difference contributions as in the function of regions, i.e., on channel edge, channel deep, between channels, and flat Si to far of channels.

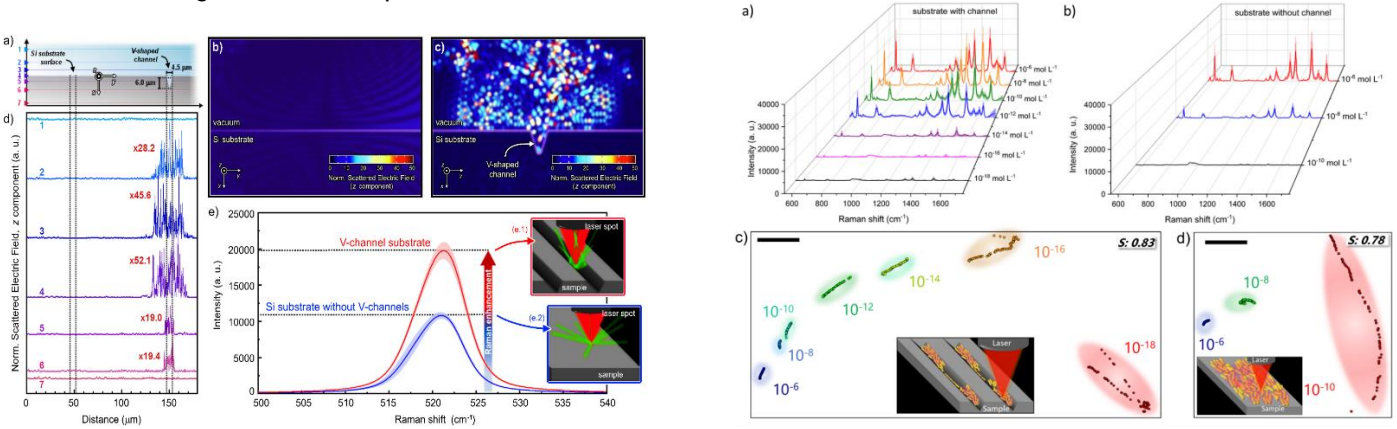

Figure 1. (a) Average SERS spectra for different

Agradecimentos/Acknowledgments

(Proc. 151153/2020-5)

VII Encontro Brasileiro de Espectroscopia Raman

VII EnBraER

05 a 08/12/2022, São Pedro – SP

Dynamic behavior of surface-enhanced Raman spectra for rhodamine 6G interacting with gold nanorods: implication for analysis under wet versus dry conditions

Anerise de Barros (PQ),[1,*] Flavio M. Shimizu (PQ),[2,3] Cristine S. de Oliveira (PQ),[1] Fernando A. Sigoli (PQ),[4] Diego Pereira dos Santos (PQ),[1] Italo O. Mazali (PQ)[1,*]

anerise@unicamp.com; mazali@unicamp.br

[1]Functional Materials Laboratory - Institute of Chemistry, University of Campinas – UNICAMP, Campinas, Brazil;; [2] Brazilian Nanotechnology National Laboratory – LNNano, Brazilian Center for Research in Energy and Materials – CNPEM; [3]Department of Applied Physics, Institute of Physics Gleb Wataghin, UNICAMP.

Keywords: *Gold Nanorods, SERS, dielectric effect, R6G dye, least square projection, BEM*

Highlights

SERS signals intensification from wet and dry effect.

Abstract

In this work, we report the dynamic behavior of surface-enhancement Raman scattering (SERS) spectra using Rhodamine 6G dye (R6G, 10^{-8} mol L^{-1}) adsorbed on gold nanorods (AuNRs). SERS spectra displayed a strong time-dependence intensity in wet to dry transition states. FEG-SEM images reveal a stacking of AuNRs organization that can lead to Raman signal improvements due to the formation of a 3D hot spot matrix that acts as a trap for target molecules. AuNRs nanostructured films were efficiently employed to form SERS substrates. The independent random AuNR organization in the SERS spectra exhibits a characteristic profile of intensities due to different dielectric environmental conditions. Despite the variations observed in the spectra array, a pattern was recognized by statistical analysis. Multidimensional analysis ensured the distinction of the study's requirements applied to the SERS response, exhibiting a silhouette coefficient of 0.92 with the least-squares projection technique. Changes in the SERS spectra profile from wet to dry state conditions of R6G dye solution can be interpreted as the dynamic behavior of R6G molecules correlated to distinct molecular adsorption and (or) surface distribution of the R6G molecules proving different plasmonic resonances. Simulations obtained from BEM calculation in experimental data corroborate that the SERS enhancement is strongly dependent on the nanoparticle coupling in nanoscale and the dielectric environment.

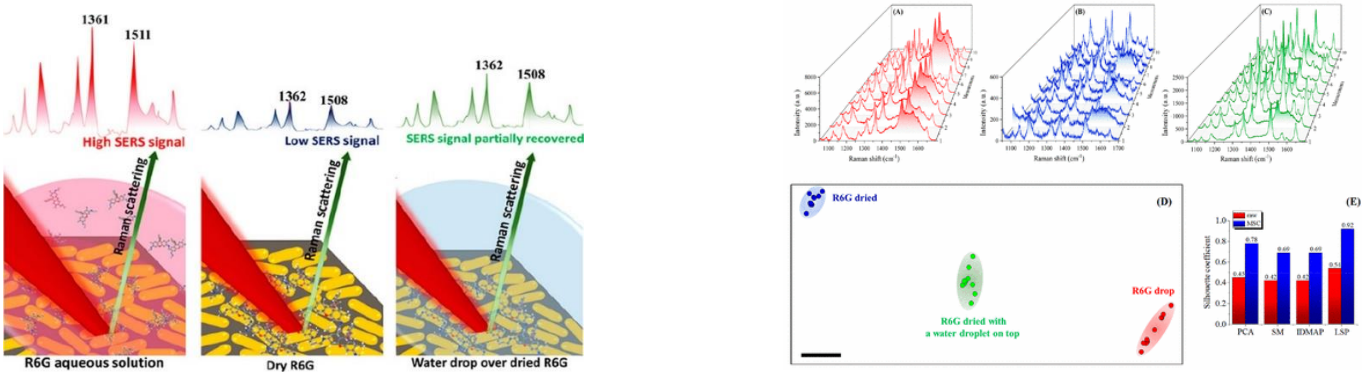

Figure 1. Schematic representation of SERS analysis in different dielectric conditions (A) SERS spectra with a 5 µL drop of R6G aqueous solution; (B) R6G dry on the SERS substrate; (C) 5 µL of a drop of water on the top of SERS substrate already with R6G. (D) LSP plot of the whole of the SERS spectra for R6G aqueous solution (red dots), R6G dried on the SERS substrate (blue dots), and a drop of water on the top of SERS substrate after R6G drying (green dots). The black bar is only a guide to measure distances between data points. The determined silhouette coefficient is 0.92. (E) Silhouette coefficient of each multivariate projection technique: PCA, SM, IDMAP, and LSP of whole Raman spectra before (red-colored) and after multiplicative scatter correction (blue-colored).

Agradecimentos/Acknowledgments

UNICAMP, Instituto de Química, Laboratório de Materiais Funcionais, EMMU Multi-User Laboratory for Advanced Optical Spectroscopy, FAPESP, CNPq, CAPES, LNNano, Inomat

VII Encontro Brasileiro de Espectroscopia Raman

VII EnBraER

05 a 08/12/2022, São Pedro – SP

SERS detection of acephate pesticide degradation product: methamidophos

Maíza S. Ozório* (PQ), Rafael J. G. Rubira (PQ), Cibely S. Martin (PQ), Luis F. C. Morato (PG) and Carlos J. L. Constantino (PQ)

e-mail: maiza.ozorio@unesp.br

São Paulo State University – UNESP, Faculty of Science and Technology (FCT), Physics Department, Presidente Prudente, SP, Brazil.

Keywords: *organophosphorus pesticides, acephate, methamidophos, degradation, SERS*

Highlights

Raman/SERS study of acephate pesticide degradation products.
One of the primary products of acephate degradation is methamidophos.
SERS spectra evidence the formation of methamidophos.

Abstract

Acephate (ACP) and methamidophos (MAP) are organophosphorus pesticides widely used in agriculture to control various plant pests and parasites. Both pesticides can cause damage to the ecosystem and to humans, however, ACP is the most used globally as it is less toxic (classified as moderately toxic - class II), compared to MAP (highly toxic - class IV) [1]. In Brazil, the use of ACP is authorized by government agency, but the MAP has been banned since 2012 due to suspected severe damage to fetal development and death of rural workers [2]. Some studies have shown that ACP can undergo degradation in three stages (primary, intermediate and final products) depending on the process (ultrasonic, ozonation, hydrolysis, microorganisms and photocatalytic processes) [3]. One of the primary products of ACP degradation is MAP. This fact makes questionable the authorization of government agencies, as the regulated pesticide degrades into a more toxic one. In this work, we present results from the ACP detection in aqueous media and evaluate its degradation process using the Surface-Enhanced Raman Scattering (SERS) technique. The analyzes were performed using a Renishaw micro-Raman spectrometer (model in-Via) coupled to a Leica optical microscope with a 50x objective lens and a 633 nm laser line. ACP ($1.0x10^{-4}$ mol/L) SERS spectra were obtained using spheric silver nanoparticles (AgNPs). Results showed a strong dependence of ACP degradation as a function of solution pH. At pH c.a. 5, there was no interaction of the pesticide with the AgNPs and thus, no bands associated with the molecule were observed. On the other hand, for colloid solution with pH 13, noticed well-defined spectra with bands at 680, 946, 1302, 1342, 1432 and 1618 cm^{-1}, attributed to the C–S vibration symmetry, P–N stretching, N–H bending, $–OCH_3$ bending deformation, and C=O stretching, respectively. It was possible to verify, that the spectrum of degraded ACP is similar to that reported by Xie et al., Fleming et al., and Zhang et al. [4-6] for MAP detection using SERS. SERS spectrum of degraded ACP, at pH 13, differs of the normal Raman spectrum of the molecule and this may be related to the loss of the carbonyl group in an aqueous medium resulting in MAP. In summary, the results show that the analysis of the potential for environmental contamination of the ACP must also take into account the by-products generated (MAP) from its degradation.

References

[1] Lin et al., Degradation of Acephate and Its Intermediate Methamidophos: Mechanisms and Biochemical Pathways. Front. Microbiol. 11:2045 (2020). doi: 10.3389/fmicb.2020.02045
[2] Oliveira et al., Controle sanitário de agrotóxicos no Brasil: o caso do metamidofós. Tempus – Actas De Saúde Coletiva, 7(1) 211-224 (2013). doi:10.18569/tempus.v7i1.1289
[3] Wang et al., Degradation of acephate using combined ultrasonic and ozonation method. Water Science and Engineering, 8(3), 233–238 (2015). doi:10.1016/j.wse.2015.03.002
[4] Xie et al., Establishment of rapid detection method of methamidophos in vegetables by surface enhanced Raman spectroscopy. European Food Research and Technology, 234(6), 1091–1098 (2012). doi:10.1007/s00217-012-1724-9
[5] Fleming et al., IR, Raman and SERS spectral analysis and DFT calculations on the Herbicide O,S-Dimethyl phosphoramidothioate, metamidophos. Spectrochimica Acta Part A: Molecular and Biomolecular Spectroscopy, 114, 120–128 (2013). doi:10.1016/j.saa.2013.05.012
[6] Zhang et al., Rapid simultaneous detection of multi-pesticide residues on apple using SERS technique. The Analyst, 139(20), 5148–5154 (2014). doi:10.1039/c4an00771a

Acknowledgments

The authors thank Fundação de Amparo à Pesquisa do Estado de São Paulo (FAPESP) (grants 2018/22214-6 and 2021/01161-4, 2020/05423-0 and 2017/15019-0), CNPq, INCT/INEO, and CAPES for technical and financial support.

VII Encontro Brasileiro de Espectroscopia Raman
VII EnBraER
05 a 08/12/2022, São Pedro – SP

Surface-enhanced Raman Scattering (SERS) Technique Applied in the Quantitative Analysis of Pesticide Detection

Marcelo J.S. Oliveira (PG)[1*], Rafael J.G. Rubira (PQ)[1], Leonardo N. Furini (PQ)[2], Augusto Batagin-Neto (PQ)[3], Carlos J.L. Constantino (PQ)[1]

carlos.constantino@unesp.br

[1]UNESP de Presidente Prudente; [2]Departmento de Física, Universidade Federal de Santa Catarina (UFSC); [3]UNESP de Itapeva.

Palavras Chave: *SERS, Ag colloid, Pesticide, Detection, Theoretical calculation.*

Highlights

Thiabendazole SERS analysis: $1.6x10^{-4}$ - $8.0x10^{-8}$ mol/L. Linear regimen for SERS intensity: $1.6x10^{-7}$ - $8.0x10^{-8}$ mol/L. Limit of detection: $7.0x10^{-8}$ mol/L. Thiabendazole adsorbs onto the Ag surface through S or N atoms.

Resumo/Abstract

The application of pesticides in large scale agriculture is a reality nowadays. Considering the possible risks for human health, monitoring the presence of those pesticides in the environment, beverages, and foods is necessary. The surface-enhanced Raman scattering (SERS) is a vibrational technique that presents selectivity and sensitivity [1], being a potential alternative for monitoring pesticides. However, its signal intensity depends strongly on experimental parameters such as size, shape and aggregation level of the metallic nanoparticles applied to achieve the SERS effect. Here we overtaken this issue using Ag colloid to detect the fungicide/parasiticide thiabendazole.

The thiabendazole purchased from Sigma-Aldrich was dissolved in a methanol stock solution, then diluted into an Ag colloid, which was synthesized following the method developed by Leopold and Lendl [2]. The SERS spectra from thiabendazole in the Ag colloid were recorded in triplicate using a Renishaw micro-Raman spectrograph, model in-Via. The UV-Vis absorption spectroscopy was applied as a complementary technique using a Varian spectrophotometer, model Cary 50, to monitor the aggregation level of the Ag colloid in the presence of thiabendazole. The adsorption mechanism of the thiabendazole onto de Ag nanoparticles was deeper evaluated through density functional theory (DFT) calculation.

The quantitative analysis was carried out varying the thiabendazole concentration from $1.6x10^{-4}$ to $8.0x10^{-8}$ mol/L. At this range of concentration, the SERS spectrum had its profile unchanged, indicating no thiabendazole reorientation or different interactions thiabendazole-Ag nanoparticle. A linear regimen for SERS intensity was found for thiabendazole concentration between $1.6x10^{-7}$ and $8.0x10^{-8}$ mol/L, leading to a limit of detection of ca. $7.0x10^{-8}$ mol/L, being comparable or lower than those reported in literature. For instance, the maximum limit allowed by the Brazilian regulatory agency ANVISA is 10 mg/kg (10 ppm) for citrus, with the acceptable daily intake being 0.1 mg/kg (0.1 ppm). Besides, the main enhanced bands of the thiabendazole SERS spectrum suggest the thiabendazole adsorption mechanism onto the Ag surface takes place by two possible sites: S or N atoms of the thiazole moiety, being the thiabendazole perpendicularly oriented in relation to the Ag surface. The theoretical calculations support the experimental data and indicate the interaction is preferentially stablished by the S atom.

In conclusion, the SERS technique was successfully applied as analytical tool to detect the pesticide thiabendazole diluted into Ag colloid. This goal was possible due to the detailed characterization of the analyte/metallic nanoparticle system. We have shown the dependence of both Ag colloid aggregation and thiabendazole adsorption mechanism onto Ag surfaces on thiabendazole concentration, which is crucial in SERS experiments. Therefore, we have paved the way to pursue the analytical application of SERS for real samples.

1. R. Aroca, Surface-Enhanced Vibrational Spectroscopy, John Wiley & Sons (2006).
2. N. Leopold and B. Lendl, J. Phys. Chem. B 107, 24, 5723–5727 (2003).

Agradecimentos/Acknowledgments

FAPESP (2013/14262-7 and 2018-22214-6), CNPq, CAPES, INCT/INEO, Center for Scientific Computing (NCC/Grid-UNESP) of the São Paulo State University (UNESP).

EnBraER

VII Encontro Brasileiro de Espectroscopia Raman

VII EnBraER

05 a 08/12/2022, São Pedro – SP

EnBraER

Gold/bohemite substrates for SERS detection of hepcidin in saliva for fast hyperinflammation screening

Carla Carolina Silva Bandeira (PG)[1,*], Julián M. Rayo Alape (PG)[1], Herculano da Silva Martinho (PQ)[1]

carla.bandeira@ufabc.edu.br

[1]UNIVERSIDADE FEDERAL DO ABC, Santo André - SP

Palavras Chave: Boehmite, Substrates, SERS, Hepcidin, Saliva, Hyperinglammation

Highlights

Substrates for SERS-based detection of the hepcidin metabolite in saliva for COVID-19 were developed for rapid screening and allowed to measure a SERS effect with 10X amplification.

Resumo/Abstract

In 2019, the pandemic caused by the new coronavirus of severe acute respiratory syndrome (SARS-CoV-2), resulted in the disease Covid-19, causing a global health crisis. Studies have proven that patients with severe Covid-19 have cytokine storm syndrome[1], being the inflammatory cytokine interleukin-6 (IL-6) a particularly prominent inducer of hepcidin, there may be the contribution of others, but it was seen that at high degrees of IL-6 is associated with Covid-19 grave. [2] Evidencing the excellent potential of hepcidin as a biomarker, can be detected in various biological fluids, such as blood, urine and saliva [3]. Some biological methods have been used for the diagnosis of Covid-19, as the enzyme-linked immunosorbent assay (ELISA) and Real-Time Polymerase Chain Reaction (RT-PCR), this is considered a gold method, for having several advantages [4], However, there has been a need for reliable and faster methods to meet the large-scale demand. Tiven these needs, spectroscopic techniques, in particular Surface-Enhanced Raman Spectroscopy (SERS), that inherits the rich chemical information from fingerprints in Raman spectroscopy and gains plasmon-enhanced excitation and scattering sensitivity. SERS combines the intrinsic advantages of Raman with high sensitivity that in some cases may even allow single molecule detection. [5] Indeed, SERS spectroscopy in serum and other biofluids for pathology diagnosis represents an emerging field, which showed promising preliminary results, for example, in various types of malignancies. Moisoiu et al. [6] Studies by Yamazoe et al. [7], related to the substrate based on gold deposition at a diagonal angle to the nanostructure obtained by oxidation of aluminum nano-layers (boehmite), observed that from this deposition, nanostructured arrays are created in the form of combs that generate "hot spots" where occurs the SERS, by favoring the identification of cancer cells through body fluid (stool). [8] Taking into account the need for new methods, in order to overcome the limitations of the RT-PCR and knowing that the SERS effect has great potential for diagnostics and screening of biofluids, as saliva in the detection of hepcidin. In this study we aimed to develop and test nanostructured substrates for SERS-based detection of the hepcidin metabolite in saliva for COVID-19 rapid screening applications. For the development of the substrates evaporative alumin images were taken in the Optical Microscope and Raman in order to analyze their quality. Boehmite films were prepared, followed by gold deposition and characterization by scanning and field emission electron microscopy and Atomic Force Microscopy. The substrates produced on the basis of bohemite and gold were tested with hepcidin biomarker, and showed promising results for SERS the effect with raman spectroscopy, and the parameters obtained allowed to measure a SERS effect with amplification of 10 X. We are currently working to optimize this amplification factor.

Agradecimentos/Acknowledgments

The authors would like to thank the Brazilian agencies Conselho Nacional de Desenvolvimento Científico e Tecnológico (CNPq – 311146/2015-5 and 307718/2019-0) and Coordenação de Aperfeiçoamento de Pessoal de Nível Superior (Projeto CAPES/Pandemias - 88881.504639/2020-01) for the financial support. The authors would also thank the experimental resources provided by Multiuser Central Facilities at UFABC (CEM/UFABC) and the financial support by UFABC (Projeto Enfrentamento à COVID19/reitoria).

VII Encontro Brasileiro de Espectroscopia Raman
VII EnBraER
05 a 08/12/2022, São Pedro – SP

Development of a biosensor based on AuNP/PS-b-P2VP thin film

Moyra F. Vieira (PG)[1,*], Bismark N. da Silva (PG)[1], Bruno G. da Fonseca (PG)[2], Alexandre G. Brolo (PQ)[2], Celly M. S. Izumi (PQ)[1]

moyra_freitas@yahoo.com.br

[1]*Departamento de Química – Universidade Federal de Juiz de Fora – Juiz de Fora – MG*
[2] *Department of Chemistry - University of Victoria – Victoria/BC – Canada*

Palavras Chave: *PS-b-P2VP, Copolymer, Gold nanoparticles, SERS, Biosensor*

Highlights

SERS substrates based on self-assemble Au nanoparticles in reconstructed PS-b-P2VP. Construction of a selective, sensitive, and reproducible biosensor based on LSPR.

Resumo/Abstract

In this work, the use of self-assemble Au nanoparticles in poly(styrene-block-2-vinylpyridine) (PS-b-P2VP) thin films as biosensors have been successfully demonstrated. The self-reconstruction of the polymeric matrix was obtained by direct immersion of the thin film in water, leading to the swelling and opening of the P2VP micelles and the formation of a porous morphology [1]. These reconstructed films were immersed in citrate-stabilized gold NPs solution for six hours. The immobilization of the negatively charged AuNPs occur by electrostatic interactions with the positively charged nitrogen in the P2VP domains [2]. Finally, a methodology was developed for the functionalization of the nanocomposites and direct detection of goat antigen (model bioanalyte) by SERS [3]. Fig 1a. show the UV-VIS spectrum of each step of the substrate functionalization. As the AuNPs surface is functionalized, a red-shifted of the LSPR band is observed, confirming the functionalization. Also, a shift to the red is induced by the antigen binding. The mean SERS spectra of each step of the substrate functionalization and detection of the interaction between anti-IgG/IgG are shown in Figure 1b. The modification of the substrate is indicated by changes in the relative intensities of several bands. Moreover, to obtain better discrimination between the anti-IgG and IgG spectra, a binary scatterplot of the PC1 × PC2 and PC6 × PC7 scores were obtained (Fig 1c). The resulting biosensor proved to be selective, sensitive and reproducible.

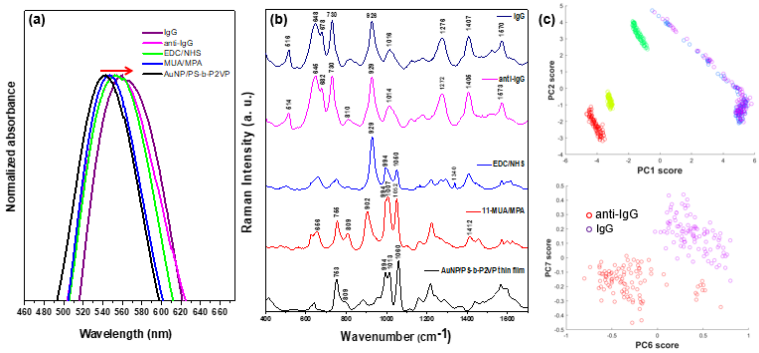

Fig. 1 - (a) UV-vis spectra of each step of the substrate functionalization, (b) Mean SERS spectra of each step of the substrate functionalization and (c) Binary scatterplot of the PC1 × PC2 scores of the substrate functionalization and PC6 × PC7 scores of anti-IgG and IgG spectra.

[1] M. Robertson, Q. Zhou, C. Ye and Z. Qiang. Macromol. Rapid Commun.2100300, 1–32(2021).
[2] Z. Liu, T. Chang, H. Huang and T. He, RSC Advances 3, 20464–20470 (2013).
[3] P. P. Austin Suthanthiraraj and A. K. Sen. Biosensors and Bioelectronics, 132, 38–46, (2019).

Agradecimentos/Acknowledgments

The authors thank the UFJF, University of Victoria – Canada, FAPEMIG and CNPq agencies. This study was financed in part by the Coordenação de Aperfeiçoamento de Pessoal de Nível Superior – Brasil (CAPES) – Finance Code 001.

VII Encontro Brasileiro de Espectroscopia Raman
VII EnBraER
05 a 08/12/2022, São Pedro – SP

Au nanoparticles prepared on PANI thin films for SERS application

Bismark N. da Silva (PG),[1*] Moyra F. Vieira (PG),[1] Rodrigo A. Dias (PQ)[2], Celly M. S. Izumi (PQ)[1].

bismarknogueirasilva@gmail.com.br

[1]Departemento de Química, Universidade Federal de Juiz de Fora, Juiz de Fora -MG; [1]Departemento de Física, Universidade Federal de Juiz de Fora, Juiz de Fora -MG

Palavras Chave: Polyaniline, Nanofibers, Dip-coater, Au nanoparticles, SERS substrate.

Highlights

PANI films were prepared using a homemade low-cost dip-coater. Globular Au nanoparticles were synthesized by PANI film. The PANI@Au composite was used as a SERS substrate.

Resumo/Abstract

Polyaniline (PANI) is a conductive polymer with the ability to reduce Au^{3+} ions for Au nanoparticles (AuNPs) synthesis [1]. The morphology of these nanostructures is influenced by the acid used as PANI dopant [2]. This composite PANI@Au can be used as *Surface-enhanced Raman spectroscopy* (SERS) substrate. In this work, PANI thin films were prepared using homemade low-cost dip coater equipment. PANI nanofibers (Figure 1a) were prepared by rapidly mixing acid solutions of aniline and ammonium persulfate. A glass slide was immersed in a suspension of PANI nanofibers doped with HCl for 15 minutes. Subsequently, the thin film was immersed in NH_4OH solution (10^{-1} mol L^{-1}) for 15 minutes for deprotonation, followed by immersion (24 h) in acetic acid solution (1 mol L^{-1}) for doping. Then, the film was immersed in $HAuCl_4$ solution (10^{-2} mol L^{-1}) for 24 h for AuNPs synthesis. PANI@Au film was used as a SERS substrate to detect rhodamine 6G (R6G) dye (10^{-4} mol L^{-1}). The Raman spectrum of the thin film of PANI doped with acetic acid (Figure 2b) shows the bands 1509, 1337/1322, and 1256 cm^{-1} assigned to the vibrations of the semiquinone segments present in the doped form. After AuNPs synthesis, the spectrum of the PANI@Au film shows the disappearance of these bands, indicating the occurrence of PANI oxidation. SEM images (Figure 1c) reveal the synthesis of globular AuNPs with an average size of 80 ± 2 nm and microstructures of Au. The R6G SERS spectrum (Figure 1d) shows the bands at 1644, 1601, 1502, 1355, 1314, 771, and 612 cm^{-1} assigned to the characteristic vibrations of this dye.

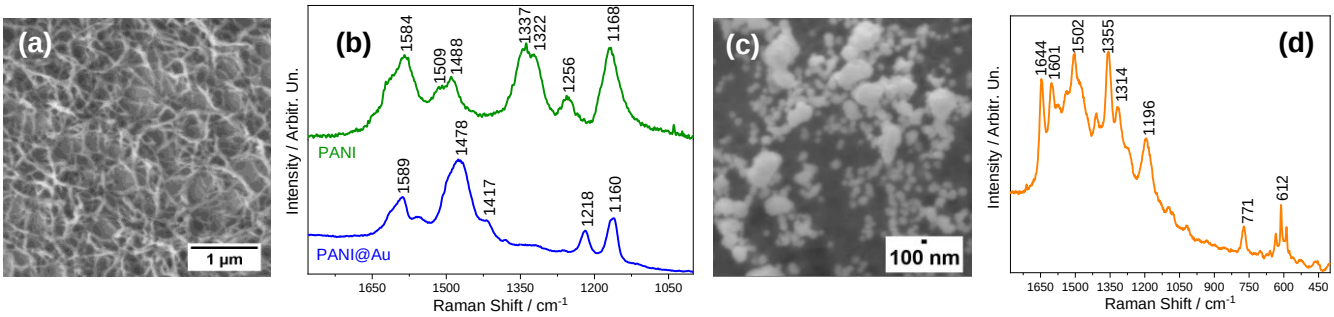

Figure 1. (a) PANI nanofibers MEV image, (b) Raman spectra of PANI and PANi@Au films, (c) PANI@Au MEV image, and (d) SERS spectra of R6G dye. (λ_0 = 632.8 nm)

[1]. P. Xu, X. Han, B. Zhang, Y. Du, H.-L. Wang, Chem. Soc. Rev. 43 (2014) 1349–1360. **[2]**. H.-L. Wang, W. Li, Q.X. Jia, E. Akhadov, Chem. Mater. 19 (2007) 520–525.

Agradecimentos/Acknowledgments

This study was financed in part by the Coordenação de Aperfeiçoamento de Pessoal de Nível Superior – Brasil (CAPES) – Finance Code 001. The authors thank the financial support of Fundação de Amparo à Pesquisa de Minas Gerais (FAPEMIG) and Conselho Nacional de Desenvolvimento Científico e Tecnológico (CNPq).

VII Encontro Brasileiro de Espectroscopia Raman
VII EnBraER
05 a 08/12/2022, São Pedro – SP

High-level Multiconfigurational Simulation of Resonant Raman and SERRS of a Tunable Thiadiazole Organic Dye

Adalberto V. S. de Araújo (PD)*, Clara J. Rangel (PG), Rômulo A. Ando (PQ)

adalberto.araujo@usp.br

Laboratório de Espectroscopia Molecular, Departamento de Química Fundamental, Instituto de Química, Universidade de São Paulo

Keywords: *Computational chemistry, Resonant Raman, SERS, SERRS, Organic dyes*

Highlights

RR and SERRS spectra of the thiadiazole DBTD were studied using multiconfigurational methods. The main features of the spectra were predicted. This methodology offers a robust approach to RR and SERRS.

Abstract

The theoretical study of Resonant Raman (RR) and Surface-Enhanced Resonant Raman Spectroscopy (SERRS) is a present challenge on computational chemistry, especially because of the difficulties related to the study of excited-states and large systems including metal atoms. A combined experimental and theoretical approach was carried employing DFT and the multiconfigurational CASPT2 and CASSCF methods to simulate the RR and SERRS spectra of the thiadiazole organic dye 4,7-Dibromobenzo[c]-1,2,5-thiadiazole (DBTD), a tunable donor-acceptor system applied in organic photovoltaics and solar-cells, in solution and absorbed in silver and gold nanoparticles (AgNP and AuNP). This kind of molecules presents an interesting challenge on the study of SERS/SERRS because of the competitive interacting sites of the molecule with the NP.

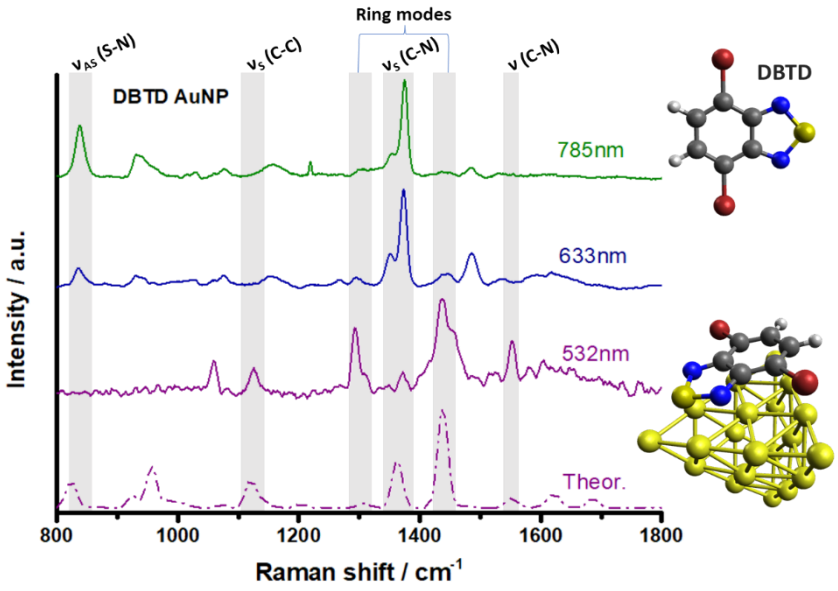

Figure 1 Experimental and theoretical SERS spectra of DBTD in AuNP in different excitation lines and multiconfigurational simulation of the 532nm spectrum.

The simulations considered a full optimization of the excited state geometries of model systems for RR and SERRS, which provided key insights into the interpretation of the convoluted spectra of the molecule. The results indicate that the DBTD presents a preference for interacting with the AuNP by the sulfur atom, while the nitrogen atoms are preferred with AgNP. Meanwhile the experimental DBTD-AuNP spectra show similar enhancements as the observed for the RR spectrum of the molecule, the DBTD-AgNP presents a different intensification pattern. The computational methodology was able to predict the main features of the SERRS spectra in good agreement, proving as a powerful tool in the study of RR and SERRS.

Acknowledgments

Adalberto V. S. Araújo acknowledges FAPESP (2021/07031-5), Rômulo. A. Ando acknowledges CNPQ (309513/2018-9) and FAPESP (2016/21070-5).

A Metal Based SERS Sensor for Nitric Oxide

Jayr H. Marin (PG), Leandro R. Marques (PG), Rômulo A. Ando (PQ)*

jayrhenrique@usp.br

Laboratório de Espectroscopia Molecular, Departamento de Química Fundamental, Instituto de Química, Universidade de São Paulo

Palavras Chave: *Nitric oxide, SERS, sensor*

Highlights

NO has high affinity for metal centers, which was exploited as a SERS sensor. SERS enhancement allows detection of low concentrations, in this case down to 0.02 mM of NO were able to be detected.

Resumo/Abstract

Due to the high affinity of NO to metals a SERS sensor based on an iron coordination complex, namely $[Fe(4Mpy)(CN)_5]^{3-}$ (4Mpy = 4-mercaptopyridine) was devised. This particular complex has a thiol moiety that is prone to interact strongly with gold nanoparticles (AuNP). NO reacts with this complex dislocating the axial cyanide anion (CN^-) forming a nitrosyl complex, which shows characteristic Fe-NO vibrations at 590 and 536 cm^{-1}, that were confirmed by theoretical calculations. Also, the results in the presence of NO show that the ring breathing mode vibration shifts from 1005 cm^{-1} to 1020 cm^{-1}, and a change in the relative intensity between the bands at ca. 1615 and 1590 cm^{-1}, that corresponds to 4Mpy asymmetric and symmetric ring stretching. The dislocated CN^- interacts with the AuNP surface, giving rise to an intense mode observed at 2133 cm^{-1} (Figure 1). The intensity of this later band correlates linearly with the NO concentration and a Limit of Detection (LOD) of 55 µM was calculated. This methodology proved to be simple and efficient as low amounts of solutions were necessary to perform the experiments, common contaminants didn't affect the obtained spectra and NO solutions of concentration down to 0.02 mM were able to be detected. This methodology is being evaluated as a potential sensor for organic NO sources, such as nitroso compounds.

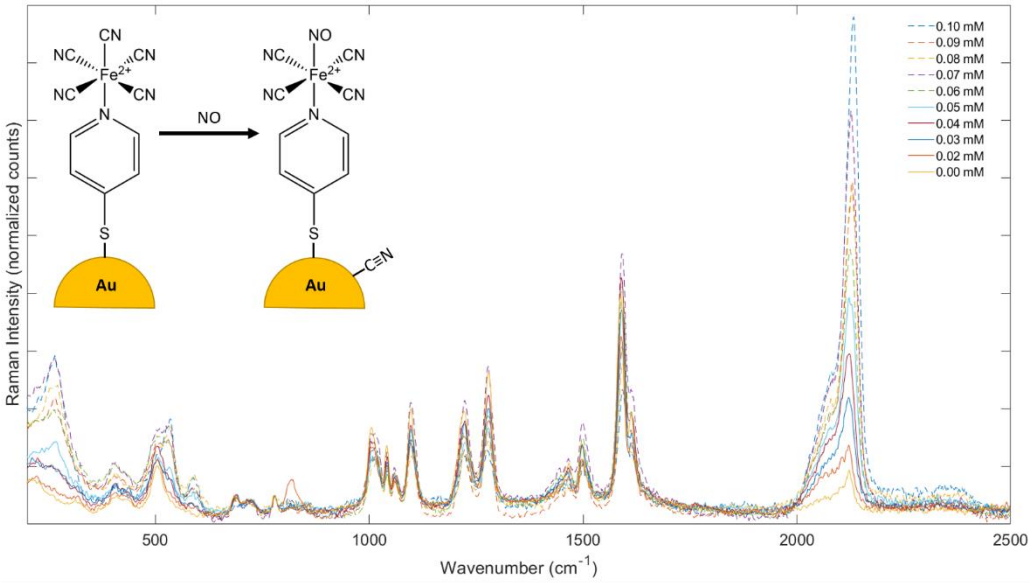

Figure 1 - SERS spectra of $[Fe(4Mpy)(CN)_5]^{3-}$ upon interaction with different concentrations of NO.

Agradecimentos/Acknowledgments

Jayr H. Marin acknowledges CNPq (142140/2019-8). Rômulo A. Ando acknowledges FAPESP (2016/21070-5). Leandro R. Marques acknowledges CAPES (88887.341021/2019-00).

VII Encontro Brasileiro de Espectroscopia Raman
VII EnBraER
05 a 08/12/17, São Pedro – SP

Detection of Atrazine herbicide through the SERS effect: evaluation of the influence of gold nanorods (AuNRs) on silicon substrate with V shaped microchannels in intensification of Raman peaks.

Matheus G. Ferreira (PG),[1,*] Anerise de Barros (PQ),[1] Davi H. S. Camargo (PQ),[2] Carlos C. B. Bufon (PQ),[2] Fernando A. Sigoli (PQ),[1] Italo O. Mazali (PQ)[1]

mazali@unicamp.br

[1]Functional Materials Laboratory - Institute of Chemistry, University of Campinas – UNICAMP, Campinas, Brazil. ; [2]MackGraphe – Graphene and Nanomaterials Research Center, Mackenzie Presbyterian Institute.

Palavras Chave: Atrazine detection; SIERS effect; SERS

Highlights

Detection of atrazine herbicide by the use of SERS sensing platform with V shaped microchannels.

Deposition of gold nanords (AuNRs) on a Si platform with V shaped microchannels for boost Raman peaks intensity,

Resumo/Abstract

The Surface Enhanced Raman Scattering (SERS) effect has been a significant rise in plasmonics area for different metallic nanoparticles, such as gold and silver, due to the high potential of achieving a limit detection on a single-molecule. This work presents the detection of Atrazine herbicide in concentrations beyond 10^{-10} M through a Si sensing platform with V-shaped microchannels. We show how de shape of the Si platform, called shaped-induced enhanced Raman scattering (SIERS) effect combined with plasmonic nanoparticles, such as Au nanorods (NRs), can influence the intensification of the Raman spectra of atrazine. The V-shaped microchannels were obtained via microfabrication etching process. The synthesis of the Au NRs were made by a well-established process in our research group and then confirmed by UV-Vis spectroscopy, and its size distribution were analyzed via transmission electron microscopy. An incubation mixed of AuNRs suspension and Atrazine solution was droped on the Si substrate and dried at environmental temperature. More specifically, the AuNRs and Atrazine incubation were prepared using 10 µL of Au NRs colloidal suspension, 10 µL of ultrapure H_2O, and 40 µL of atrazine solution; the incubation solution was kept undisturbed for 30 min before use. After deposition the sensing platform's efficiency was evaluated by the atrazine SERS signals intensification. Previous results presented a higher intensification of the Raman peaks inside the V-shaped microchannels at lower concentrations as 10^{-11} mol L^{-1}.

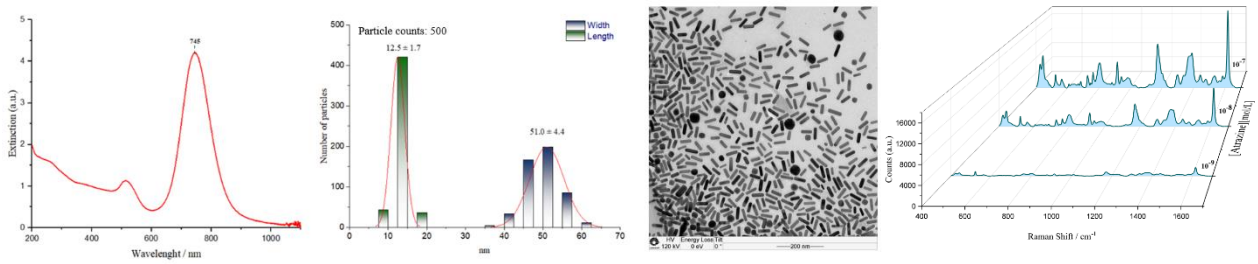

Figure 1. (a) AuNRs extinction spectra with its plasmon band maximum on 745 nm. (b) Width and length distribution of the AuNRs synthesized. (c) TEM micrography of the AuNRs. (d) Average SERS spectra of atrazine for different concentrations(10^{-7} to 10^{-9} mol L^{-1}).

Agradecimentos/Acknowledgments

UNICAMP, Instituto de Química, Laboratório de Materiais Funcionais, EMMU Multi-User Laboratory for Advanced Optical Spectroscopy, FAPESP Ciência, Cultura e Desenvolvimento, CNPq, CAPES, LNNano, Inomat

VII Encontro Brasileiro de Espectroscopia Raman
VII EnBraER
05 a 08/12/17, São Pedro – SP

Desenvolvimento de sensor SERS indireto para detecção de Hg atmosférico

Deysiane A. L. dos Santos (PG),[1*] Anerise de Barros (PQ),[1] Fernando A. Sigoli (PQ),[1] Italo O. Mazali (PQ)[1*]

deyseals@gmail.com; mazali@unicamp.br

[1]*Functional Materials Laboratory - Institute of Chemistry, University of Campinas – UNICAMP, Campinas, Brazil.*

Palavras Chave: *Nanobastões de ouro, Sensor SERS indireto, Detecção de mercúrio atmosférico, Amalgamação.*

Highlights

Development of Indirect SERS Sensor for Atmospheric Hg Detection. Indirect SERS sensor for $Hg^0_{(g)}$ detection, exploiting the suppression of the plasmonic effect of gold nanoparticles caused by $Hg^0_{(g)}$ amalgamation.

Resumo/Abstract

O mercúrio é considerado um 'poluente global' devido as suas propriedades que lhe conferem um tempo de residência na atmosfera na ordem de um ano, facilitando seu transporte por longas distâncias e deposição numa escala global. O $Hg^0_{(g)}$ é extremamente tóxico, podendo causar efeitos devastadores nos tecidos celebrais. Este trabalho apresenta o desenvolvimento de um sensor de espalhamento Raman aprimorado por superfície (SERS) indireto para a detecção de $Hg^0_{(g)}$ baseado em nanobastões de ouro (AuNRs). A detecção é baseada no efeito de degradação das características plasmônicas dos AuNRs durante o processo de formação da amalgama Au-Hg. O sensor é constituído de AuNRs depositados sobre a superfície de um substrato de Si de 4 mm^2 previamente funcionalizado com as moléculas de 3-mercaptopropiltrimetoxissilano (MPTMS), seguido da deposição da molécula-sonda Rodamina 6G. O espectro UV-Vis para a suspensão de AuNRs constata a eficiência do método de crescimento dos AuNRs mediante ao aparecimento das bandas plasmons transversal e longitudinal em 515 e 673 nm, respectivamente. A partir do histograma obtido a partir das micrografias de TEM verifica-se uma distribuição estreita de tamanho para os AuNRs, indicando uma excelente homogeneidade. A quantificação do teor de ouro realizada por ICP MS demonstra uma concentração total de 522,5 mg L^{-1} que corrobora com o resultado teórico esperado para esta síntese. A Figura 1 apresenta o mapeamento Raman realizado para a detecção do $Hg^0_{(g)}$ na faixa de 180 a 4592 ng por meio do monitoramento da redução da intensidade SERS da banda 1509,7 cm^{-1} da rodamina 6G. Os resultados preliminares indicam que os substratos SERS propostos são bastante promissores para detecção indireta do $Hg^0_{(g)}$ com boa reprodutibilidade e sensibilidade, na ordem de nanogramas. Sendo esta estratégia pouco explorada na literatura como sensores SERS e inovadora quanto a detecção de $Hg^0_{(g)}$., uma vez que, não há relato na literatura para a detecção do mesmo na sua forma gasosa.

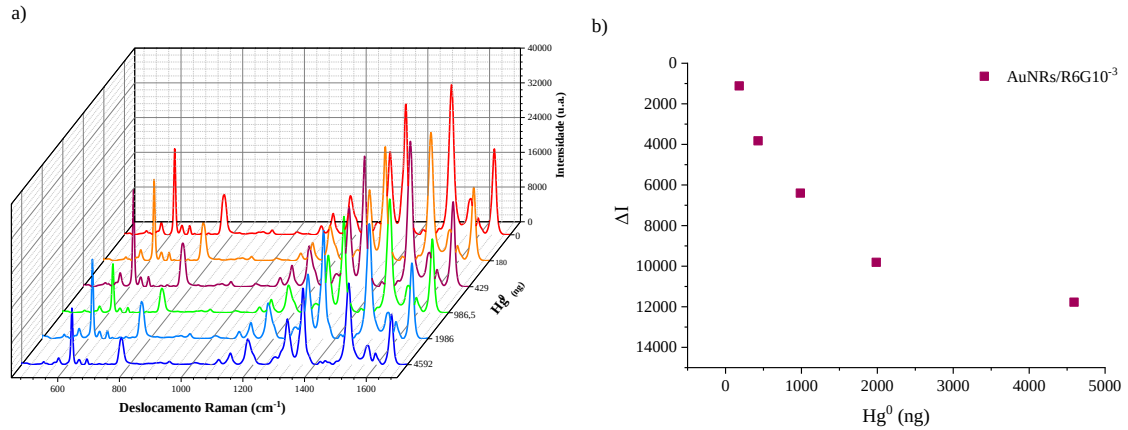

Figura 1. a) Redução da intensidade SERS da Rodamina 6G em função da concentração de $Hg^0_{(g)}$ de 180 a 4952 ng; (b) Curva analítica para a variação da intensidade SERS da banda 1509,74 cm^{-1} da Rodamina 6G em função do aumento da concentração de $Hg^0_{(g)}$.

Agradecimentos/Acknowledgments

UNICAMP, Instituto de Química, Laboratório de Materiais Funcionais, EMMU Multi-User Laboratory for Advanced Optical Spectroscopy, FAPESP, CNPq, CAPES, LNNano, Inomat

VII Encontro Brasileiro de Espectroscopia Raman
VII EnBraER
05 a 08/12/2022, São Pedro – SP

Paper-based SERS substrate applied to the detection of acephate pesticide

Grazielle O. Setti (PQ)*, Maíza da S. Ozório (PQ), Rafael J. G. Rubira (PQ), Carlos J.L. Constantino (PQ).

grazielle.setti@unesp.br

Departamento de Física, Faculdade de Ciências e Tecnologia, UNESP, Presidente Prudente.

Key words: *SERS substrate, paper substrate, acephate, pesticide, AgNPs.*

Highlights

Hydrophobic barrier production using wax transfer mask was successfully applied for SERS substrate fabrication.

Using paper-based SERS substrate for acephate detection is reported for the first time.

SERS spectra obtained suggest acephate degradation.

Resumo/Abstract

Surface enhanced Raman scattering (SERS) effect has been broadly applied to detect and quantify analytes at very low concentration. Since portable Raman spectrometers are commercially available at a relatively low cost, SERS spectroscopy is proving to be a potential alternative to labor intensive and expensive techniques, such as chromatography. The development of SERS substrates using fast, simple and low-cost materials and techniques are desirable. The paper's properties such as ease of using, high portability, and flexibility, combined with the capability of production on large scale and low-cost make it attractive for using on SERS substrates.[1] In this work a filter paper was used as support for Ag nanoparticles (AgNPs). A circular area of the paper (d = 4mm) was surrounded by wax in order to limit a hydrophilic area. Wax barrier was applied as follows: a cutting printer was used to cut the circular area onto a sheet of parchment paper. A 35 x 15 mm piece containing 3 circular holes (d = 4mm) was dipped in molten wax for 2 seconds and removed. Excess wax was allowed to drain and the wax was dried at room temperature. The waxed paper acted as a wax transfer mask. Two pieces of filter paper were placed, one on each side of the waxed paper and wrapped with aluminum foil. It was pressed and heated at 150 ºC for 3 seconds. Then the pieces of filter paper were immediately removed from de aluminum foil. The wax passed to the filter paper, penetrating its fibers, forming the hydrophobic barrier when drying. Colloidal AgNP was added to the paper, dispersing homogeneously over the unwaxed area. After drying, the SERS substrate was immersed in aqueous acephate pesticide solution (0,1 mol L^{-1}) for 8 min, removed and allowed to dry. SERS measurements were performed using a spectrograph micro-Raman (Renishaw, In-Via), laser line at 633 nm. A 50 x magnification lens was used and the sample was exposed to the laser for 10 s. Two SERS substrates were prepared and it was obtained 6 spectra in aleatory points in the SERS substrate. Characteristic peaks were observed at 686 cm^{-1} (C–S stretching), 1302 cm^{-1} (N–H bending), 1450 cm^{-1} (–OCH3 bending) and 1618 cm^{-1} (N–H, scissoring).[2] These results suggest the occurrence of acephate degradation in methamidophos. To the best of our knowledge, it is the first time that acephate has been detected using a paper-based SERS substrate. For further work, spectra of different concentration of pesticide will be obtained, as well as analytical parameters.

[1]Oliveira, T.R. *Talanta*, 195 (2019) 480.
[2]Xie, Y. *et al*., *European Food Research and Technology*, 234 (2012) 1091.

Agradecimentos/Acknowledgments

We thank FAPESP (processes 2018/22214-6, 2020/16269-2, 2020/05423-0, 2021/01161-4), CNPq, INCT/INEO and CAPES for the financial supporting.

Detection of carbendazim by SERS using Ag colloid: a comparison of portable and benchtop Raman equipment

Tatiana A. Oliveira (PG), Isabela B. Carvalho (IC), Grazielle O. Setti (PQ), Carlos J.L. Constantino (PQ).

Tatiana.oliveira@unesp.br

Department of Physics, Faculty of Science and Technology, FCT-UNESP, Presidente Prudente.

Palavras Chave: *(SERS, pesticide, carbendazin).*

Highlights

Comparing portable and benchtop Raman equipment performance in the sensitivity and reproducibility of the SERS signal for different concentrations of carbendazim in Ag colloid.

Resumo/Abstract

The fungicide methyl benzimidazol-2-ylcarbamate (MBC), commonly called carbendazim, is used in Brazil in food plantations such as cotton, rice, beans, corn and soybeans[1]. The MBC is classified as "a product dangerous to the environment" (Class III) by the *Agência Nacional de Vigilância Sanitária* (ANVISA)[2]. Using surface-enhanced Raman scattering (SERS) it is possible to detect MBC at different concentrations. The SERS technique can provide not only the fingerprint of the target molecule through its vibrational spectrum (selectivity), but also allow the detection of target molecules at low concentrations (sensitivity)[3]. The objective of this work was to detect the fungicide MBC via SERS, comparing the performance of portable and benchtop Raman spectrometers. For SERS measurements, silver nanoparticles (AgNPs) colloid was used in the presence of MBC with final concentration of the mixture from $1.0x10^{-5}$ to $1.0x10^{-9}$ mol L^{-1} (line laser 785 nm). The samples were prepared by mixing 960 µL of AgNPs + 40 µL of KNO_3 (0.5 mol L^{-1}). Then 10 µL of this dispersion were removed and soon after 10 µL of MBC were added to obtain a mixture with final volume of 1000 µL. Two samples were prepared for each concentration of the MBC stock solution ($1.0x10^{-3}$ to $1.0x10^{-7}$ mol L^{-1}), since the same final concentrations were used for both equipment, one to be used in each equipment. In measurements with the benchtop Raman (Renishaw, in-Via model) 350 uL of each mixture was added to a sample port to perform the measurements. In measurements with the portable Raman (Bruker, Bravo model) 1000 µL of each mixture were added to a specific sample equipment port. The most intensity observed bands at 628, 1228 and 1523 cm^{-1} are attributed to vibrational modes of the benzimidazole group, which suggest its adsorption on the surface of the AgNPs. The results show that both equipment allowed the detection of MBC in the concentration range studied. Furthermore, no significant differences were observed in the relative intensity of the band nor in the spectral profile for, the results obtained with both equipment. Concluding, both equipment showed efficiency in detecting the SERS signal of the MBC pesticide at concentrations investigated here. In addition, the results show similar SERS spectrum profiles for both equipment regardless of concentrations.

References
1- Carbendazim CROP BR. *Ministério da Agricultura, Pecuária e Abastecimento* – MAPA
2- *Agência Nacional de Vigilância Sanitária* (ANVISA). *Regularização dos Agrotóxicos*
3- Rubira *et al*. Detection of trace levels of atrazine using surface-enhanced Raman scattering and information visualization. Colloid and Polymer Science. 292, 2014, 2811-28.

Agradecimentos/Acknowledgments

FAPESP (2018/22214-6, 2020/16269-2 and 2022/04020-5), CAPES, CNPq and INCT/INEO.

VII Encontro Brasileiro de Espectroscopia Raman
VII EnBraER
05 a 08/12/2022, São Pedro – SP

Direct detection of SARS-CoV-2 antigen based on surface-enhanced Raman scattering (SERS) using machine learning

Wallance M. Pazin (PQ) [1], Leonardo N. Furini (PQ) [2], Daniel C. Braz (PQ) [3,4], Mário P. Neto (PQ) [5,6], José D. Fernandes (PQ)[7], Carlos J.L. Constantino (PQ) [7], Osvaldo N. Oliveira Jr (PQ) [3]

wallance.pazin@unesp.br

[1]Department of Physics, School of Science, UNESP, Bauru; [2]Department of Physics, Federal University of Santa Catarina, Florianópolis; [3]São Carlos Institute of Physics, USP, São Carlos; [4]Mato Grosso do Sul State University (UEMS), Dourados; [5]Federal Institute of São Paulo (IFSP), Araraquara; [6]Institute of Mathematics and Computer Sciences (ICMC), University of São Paulo (USP); [7]Department of Physics, School of Sciences and Technology, São Paulo State University (UNESP), Presidente Prudente;

Palavras Chave: *COVID-19, Nanobiosensor, SERS, Machine Learning*.

Highlights

Direct detection of SARS-CoV-2 antigen based on surface-enhanced Raman scattering (SERS) using machine learning;

Detection of SARS-CoV-2 was done by using a less complex SERS platform developed by means PVD of gold; Artificial intelligence as machine learning (ML) can be applied to improve biosensor sensibility;

Resumo/Abstract

To date, the coronavirus disease 19 (COVID-19) is still registered as a pandemic due to the significative number of cases worldwide and deaths, although the later has been drastically reduced after almost 70% of world population have been fully vaccinated, according to World Health Organization (WHO). Unfortunately, the socioeconomic inequities of African countries reflect in a lack of vaccination access of their population, leading the severe acute respiratory syndrome coronavirus 2 (SARS-CoV-2) still to be a pandemic cause with oscillations in the disease peaks. The search for rapid COVID-19 tests has been intensely increased as a consequence of the high COVID-19 transmissibility, even for those who are either in contact with confirmed cases or are asymptomatic. In this study we have explored the detection of SARS-CoV-2 spike S1 antigen by using a less complex SERS platform developed by means of physical vapor deposition (PVD) of gold, forming gold nanoislands into a simple glass substrate, conjugated with 4-ATP used as the reporter for the SERS signal and the antibody for antigen detection. It is known that this platform is less sensitive when compared to the so-called sandwich structure and, aiming to solve this problem, methodologies based on artificial intelligence as machine learning (ML) can be applied to reduce limitation and enhance accuracy by the improvement of the biosensor. A good distinction between the devices in the absence and presence of the antigen could be obtained with supervised learning algorithms, taking into account the mean value of the SERS spectra intensities. The results indicate that the method can be used for diagnosis in spite of the simplicity and limited sensitivity of the biosensor, reflecting the importance and necessity of computational decision for the analysis.

Agradecimentos/Acknowledgments

FAPESP (2020/12129-1 and 2018/22214-6); CNPq; CAPES; INEO.

Ultrasensitive SERS immunoassay for stress biomarker monitoring in biological fluids

Javier E.L. Villa (PQ),[1,*] Maria D.P.T. Sotomayor (PQ),[2] Luis M. Liz-Marzán (PQ)[3]

jelv@unicamp.br

[1]Instituto de Química, UNICAMP, Campinas-SP; [2]Instituto de Química, UNESP, Araraquara-SP; [3]CIC BiomaGUNE, Donostia-País Vasco, Espanha

Palavras Chave: *Stress biomarker, Gold nanostars, Magnetic separation, Raman spectroscopy, Addison disease, Plasmonics*

Highlights

High sensitivity and specificity are combined. Nanostars, nanospheres and nanorods were synthesized and tested. Important advantages over the conventional methods for diagnosis are presented.

Resumo/Abstract

Globalization, living style, work competition, and pandemic, are some the main reasons of the alarming increased levels of human stress worldwide. Accordingly, reliable methods capable to routinely monitor stress are necessary to improve the global life quality. Cortisol is a steroid hormone that plays an important role to trigger the human stress response in challenging, threatening, or startling situations. Thus, cortisol is considered the main stress biomarker and is called the 'stress-hormone'. Even though the cortisol response to stressful situations is essential for survival, abnormal cortisol concentrations in biological fluids are associated with serious health risks. For example, Cushing's and Addison's disease for higher and lower cortisol concentrations, respectively. Cortisol concentrations in biological fluids can therefore serve as an excellent biomarker for stress and various diseases, and its determination represents a crucial task for human health care. In this work, we have developed a novel cortisol biosensor by combining a highly sensitive analytical technique (surface-enhanced Raman spectroscopy, SERS) and a highly specific assay (competitive immunoassay). To fabricate the gold nanotags, three types of nanoparticle shapes were tested (spheres, rods, and stars) and compared in terms of sensitivity using three different lasers (532, 633 and 785 nm). The Raman reporter used was 4-mercaptobenzoic acid combined with SH-PEG-COOH (M_V=5000) to modify the nanosurface and to obtain stable nanoparticles for further surface modification. BSA bound to cortisol was covalently bound onto the nanoparticles via EDC/NHS reaction. Since stars shaped nanotags showed the greatest sensitivity, they were used in all the immunoassay experiments. Regarding the capture agent, magnetic beads (MBs) of ~800 nm diameter and glass slides coated with a 200 nm gold film were evaluated as the capture substrates. Cortisol monoclonal antibody was covalently bound to the MBs beads via EDC/NHS reaction, thereby promoting well-oriented linkage of the antibodies. The experimental conditions to carry out the immunoassay were optimized to maximize the sensitivity and the reproducibility. Under such optimized conditions, the magnetically assisted immunoassay was selected as the proposed method and was applied to quantify cortisol in biological fluids, particularly urine and serum. The percent of cortisol recoveries in these samples were ranged between 85 and 94% and there was no significant difference with the cortisol concentration reported in a serum certified reference material, thus demonstrating an excellent accuracy. Additionally, there were no significant differences between these recovery values and those obtained using the well-developed analytical technique high performance liquid chromatography coupled to mass spectrometry (HPLC-MS). ELISA was also used as a reference method for comparison. Nevertheless, the proposed SERS immunoassay exhibited some key advantages: (1) lower limit of detection (down to 4 ng/mL), (2) minimal sample preparation, (3) portability, and (4) rapid sample analysis. Therefore, the proposed SERS immunoassay is suitable for monitoring human stress levels by means of cortisol measurements and presents a great potential for a wide variety of point of care applications.

Agradecimentos/Acknowledgments

The authors would like to thank FAPESP (process 2018/24202-5), the European Research Council and the Spanish State Research Agengy (MDM-2017-0720) for the financial support.

VII Encontro Brasileiro de Espectroscopia Raman
VII EnBraER
05 a 08/12/2022, São Pedro – SP

KNO_3 mediated aggregation of silver nanoparticles for SERS detection of the fungicide carbendazim

Isabela B. Carvalho* **(IC), Cibely S. Martin (PQ), Tatiana A. de Oliveira (PG), Marcelo J.S. Oliveira (PG), Carlos J.L. Constantino (PQ).**

isabela.bianchi-carvalho@unesp.br

Faculdade de Ciências e Tecnologia, UNESP, Presidente Prudente.

Keywords: *Carbendazim, SERS, detection, aggregation, salt addition.*

Highlights

Successive CBZ additions induce AgNPs aggregation. Aggregation is favored by the addition of salt, allowing the detection of CBZ at lower concentrations.

Resumo/Abstract

Faced with the impossibility of finding a safe dose for human consumption, in august of this year, the use of the fungicide carbendazim (CBZ) was prohibited by Anvisa [1]. In that regard, the detection and monitoring of CBZ is of utmost importance. Among the existing techniques, the SERS technique (Surface-Enhanced Raman Spectroscopy) has often been used for the detection of pesticides [2]. The aggregation levels of nanoparticles used as amplifiers of Raman signal, however, play an important role in the enhancement [3]. In this work, a study of the aggregation of silver nanoparticles (AgNPs) in colloid induced by the addition of CBZ and its effect on the SERS signal in the absence and presence of salt was carried out. The samples were characterized by extinction spectroscopy, dynamic light scattering (DLS) and zeta potential. Four stock solutions were used (10^{-6}, 10^{-5}, 10^{-4} e 10^{-3} mol/L), the most concentrated being in ethanol. Successive aliquots (1, 6, 7, 8 and 9 µL) of each CBZ stock solution were added to a fixed volume of Ag colloid (500 µL for the characterization techniques and 2500 µL for the SERS technique). The characterization measures were carried out by diluting this colloidal dispersion in ultrapure water. For measurements in the presence of salt, 100 µL of KNO_3 0,5 mol/L were added in two orders: before adding water to the Ag colloid (Order 1) and after adding water to the colloid (Order 2). Increasing concentration of CBZ from $4x10^{-10}$ to $1.3x10^{-6}$ mol/L, no variation was observed in the plasmon band in the UV-Vis extinction measurements without salt. However, after aliquots of the ethanol stock solution (10^{-3} mol/L) were added, with CBZ concentration ranging between $1.7x10^{-6}$ mol/L and $2.4x10^{-5}$ mol/L, there was a decrease in the 400 nm band and a gradual increase in a band at longer wavelengths, indicating the aggregation of AgNPs promoted by CBZ. In the samples with added salt, the formation of the characteristic band of aggregates was not observed. For Order 1, when CBZ was added, there was a decrease in the intensity of the 400 nm band as its concentration increased. As for Order 2, when CBZ was added, the same behavior of the 400 nm plasmon band was also observed. However, at the concentration of $6.7x10^{-8}$ mol/L there was a considerable decrease in the intensity of this band compared to the others, reaching stability afterwards. In the study of size distribution in the absence of salt, it was observed that the population of greater intensity suffered an increase in size with successive additions of CBZ (as well as in the presence of salt), which occurs more sharply from concentration $1.7x10^{-6}$ mol/L onwards. Ag colloid in the absence of CBZ has a zeta potential of -43±1 mV. When CBZ aliquots were added, the zeta potential values became less negative, indicating the adsorption of CBZ on AgNPs. The zeta potential values obtained for measurements with salt indicate loss of dispersion stability, since colloids are stable at zeta potential values lower than -20 mV or higher than +20 mV [4]. This may be related to the fact that the formation of bubbles on the electrodes (electrolysis) was observed [5]. In the absence of salt, the lowest concentration at which it was possible to obtain the SERS signal from CBZ was $4x10^{-6}$ mol/L. On the other hand, in the presence of salt, the SERS signal was obtained at $4x10^{-7}$ mol/L of CBZ. That is, with the salt it was possible to detect CBZ at a concentration 10 times lower than in the absence of salt. It is worth mentioning that the concentration at which CBZ was detected for the first time in the absence of salt ($4x10^{-6}$ mol/L) is the same that first showed the formation of the band at longer wavelengths in the extinction measurements, corroborating the aggregation hypothesis in a high degree of aggregation from this concentration. Therefore, the aggregation is favored by the addition of salt, allowing the detection of CBZ at lower concentrations.

[1]https://agenciabrasil.ebc.com.br/saude/noticia/2022-08/anvisa-proibe-uso-do-fungicida-carbendazim-em-produtos-agrotoxicos. [2]Rubira, R.J.G. et al. S. *Vib.Spectrosc*. **2021**, 114, 103245. [3]R. Aroca; *Surface-Enhanced Vibrational Spectroscopy*; John Wiley & Sons: Toronto, **2006**. [4]Badawy, A.M.E. et al. *Environ. Sci*. Technol. **2010**, 44, 1260–1266. [5]Particle Characterization. Flow Pressurization Eliminates Bubbles for More Accuracy.

Agradecimentos/Acknowledgments

FAPESP (2021/02746-6 and 2018/22214-6), CNPq, INCT/INEO, CAPES.

VII Encontro Brasileiro de Espectroscopia Raman
VII EnBraER
05 a 08/12/2022, São Pedro – SP

Detection of thiabendazole pesticide in matrix of food by surface-enhanced Raman scattering (SERS)

Marcelo J.S. Oliveira (PG)[1], Rafael J.G. Rubira (PQ)[1], Augusto Batagin-Neto (PQ)[2], Carlos E.M. de Campos (PQ)[3], Carlos J.L. Constantino (PQ)[1], Leonardo N. Furini (PQ)[3]

leonardo.furini@ufsc.br

[1]São Paulo State University (Unesp), School of Technology and Sciences, Presidente Prudente, SP, Brazil, [2]São Paulo State University (Unesp), Campus of Itapeva, Itapeva, SP, Brazil, [3]Federal University of Santa Catarina (UFSC), Departament of Phisics, Florianópolis, SC, Brazil.

Palavras Chave: Thiabendazole, pesticides, nanoparticles, SERS, food.

Highlights

Surface-enhanced Raman scattering (SERS) applied to detection of thiabendazole pesticide in matrix food.
Optimizing the conditions to detect thiabendazole pesticide.
Digital protocol using SERS to determine the thiabendazole concentration.

Resumo/Abstract

Surface-enhanced Raman scattering (SERS) provide a large signal enhancement being a promising tool of detection of molecules attached to nanometer-sized metallic structures. One of limitations of technique is the signal fluctuations on the SERS intensity when the substrate is a solid and the spectra are collected point-by-point. Such behavior remains a challenge to obtain a linear regimen and build a calibration curve. Here, we propose apply SERS as tool of detection but instead to take the SERS intensity, take the number of SERS events to quantify thiabendazole (TBZ) pesticide. For this purpose, the detection was optimized using three syntheses of nanoparticles: silver reduced by hydroxylamine (AgH) or citrate (AgCT) and gold nanoparticles reduced by citrate (AuCT). These nanoparticles were deposited onto apple peel and applied as SERS substrates to detect TBZ pesticide using Raman mapping under 785 nm laser excitation. Previously, theoretical calculations were performed studying the torsion barrier of thiazol ring in relation to benzimidazole ring to investigate the conformer which presents lower energy for TBZ molecules. The *trans* conformer was the most stable, in agreement with XRD patterns. The extinction spectra present a maximum at 416, 435 and 521 nm for AgH, AgCT and AuCT, respectively. In presence of pesticide the maximum was red-shifted for three nanoparticles and for AgH and AuCT arise a new band at longer wavelength, reveling the strong interaction between TBZ and AgH and AuCT. TBZ SERS spectra using AgH, AgCT and AuCT are similar each other with lightly differences among them which can be related to the different interaction between TBZ and nanoparticle surface. In terms of intensity, AgH showed the higher SERS signal to TBZ and it was chosen for the next experiments. The dependence of TBZ SERS spectra in different pH medium was investigated from pH 2 up to pH 12. While SERS signal was absent at pH 10 and 12, at lower pHs (2-8) the changes in SERS spectra are related to difference of states of protonation of TBZ molecules. Finally, the TBZ detection was performed at the range 1.0×10^{-3} – 1.0×10^{-8} mol/L using streamline mapping. The TBZ SERS signal was also evaluated in the presence of interferents such as carbendazim and thiram pesticides.

Agradecimentos/Acknowledgments

CNPq (405087/2021-7, 304100/2018-8, 304756/2019-9, 311601/2020-0), PIBIC/CNPq/UFSC, FAPESP (2018/22214-6).

VII Encontro Brasileiro de Espectroscopia Raman
VII EnBraER
05 a 08/12/2022, São Pedro – SP

Silver nanocubes SERS substrate: a possibility of plasmon-mediated reactions using SERS

Adriana Santinom (PG),[1] Italo Odone Mazali (PQ),[1] Alexandre Guimarães Brolo (PQ),[2] Diego Pereira dos Santos (PQ)[1,*]

santosdp@g.unicamp.br

[1]Instituto de Química, UNICAMP; [2]Chemistry Department, University of Victoria.

Palavras Chave: *SERS, silver nanocubes, plasmon-mediated reactions,*

Highlights

Surface-enhanced Raman spectroscopy can be used as a tool to mediate reactions through surface plasmon enhancement, this work aims to bring some evidence of these possibilities.

Resumo/Abstract

The interaction between nanoparticles and light gives rise to particular effects that can be studied through optical techniques such as Raman Spectroscopy, Dark Field Microscopy and computer simulations. One of these effects can generate reactions mediated by surface plasmons. In this work, we are trying to understand what happens in a system when we have couple particles interacting in different ways to enhance the analyte signal.

Using cubic silver nanoparticles deposited on a vitreous substrate, it was possible to generate experimental data with several different deposition concentrations. It is possible to interpret the data using PCA (Principal Component Analysis) and MRC-ALS (Multivariate Curve Resolution Alternating Least Square) in sets according to the study system setup, and finally the simulations allow the comparison with the data obtained experimentally.

Studies were carried out to identify spectral profiles that could alter the analyte response, the probe molecule 4-ABT (4-aminobenzothiol). Already described in the literature as a molecule capable of undergoing dimerization, the search for the work focuses on identifying changes in the band patterns expected for the probe molecule. As there is the possibility of plasmon-mediated reactions on surfaces, we sought to find profiles of 4-ABT, dimers and possible profiles of 4-ABT reaction products, either its own degradation or other byproducts.

Agradecimentos/Acknowledgments

Conselho Nacional de Desenvolvimento Científico e Tecnológico (CNPq) for the scholarship provided.

Coordenação de Aperfeiçoamento de Pessoal de Nível Superior - Brasil (CAPES) for the internacional scholarship provided.

VII Encontro Brasileiro de Espectroscopia Raman
VII EnBraER
05 a 08/12/2022, São Pedro – SP

SM-SERS spectra of 4-mercaptobenzoic on H-bonds induced hot spots in acidic medium.

Flávia C. Marques (PG) [1], Raisa S. Alves (PG)[2], Diego P. dos Santos (PQ)[2], Gustavo F. S. Andrade (PQ)[1,*]

[1]Departamento de Química, Instituto de Ciências Exatas, Universidade Federal de Juiz de Fora, Juiz de Fora, MG, [2]Instituto de Química, Departamento de Físico-Química, Universidade Estadual de Campinas, Campinas, SP.

Palavras-Chave: *4-mercaptobenzoic acid, SERS, hot spots*.

Highlights

This abstract reports a direct approach to generating efficient Ag nanoparticles (AgNP) hot spots using the 4-mercaptobenzoic acid (4-MBA) molecule. 4-MBA linked to the Ag surface by a thiolate-Ag bond triggered an AgNP self-assembly process at pH=4 caused by H bonds between the carboxylic groups located in different AgNP. The SM-SERS of 4-MBA was demonstrated experimentally, and the experimental results were associated with a large number of hot spots formed.

Resumo/Abstract

The surface-enhanced Raman scattering (SERS) results in increased Raman intensities of molecules attached to plasmonic nanoparticles (NP) [1]. The SERS enhancements can reach up to 8 orders of magnitude or even higher values in regions of strongly confined electromagnetic fields, known as “hot spots”. The presence of “hot spots” increases the SERS efficiencies, which allows the detection of a single molecule (SM) [2]. To improve the understanding of the dynamics of hot spots, we proposed in the present study a direct approach with 4-mercaptobenzoic acid (4-MBA) that presents strong adsorption of the thiol group on AgNP. The generation of hot spots was triggered by H-bonds between the COOH group of 4-MBA molecules on different AgNP. In this way, the adsorbate is centered in the region of the greatest electric field increase, enhancing the plasmonic substrate SERS performance. Figure 1(a) exhibits the time evolution of the UV-Vis spectra of the AgNP/4-MBA (5.0×10^{-7} mol L^{-1}) suspension in pH=4 (below pK_a(4-MBA)=4.79). The most intense LSPR band decreases with time, followed by the appearance of a new band at 521 nm, which reaches its maximum intensity around 60 min. The new 521 nm band in UV-Vis spectra indicates that the change in acidity induced the self-assembly of AgNP by H-bonding of 4-MBA carboxylic groups in different AgNP.

The sensitivity of SERS for 4-MBA at pH=4 was verified in two concentrations, 5.0×10^{-8} mol L^{-1} and 3.0×10^{-9} mol L^{-1} (Figure 1(b) and(c)), which are equivalent to 32 and 2 molecules in the probed confocal volume, respectively. Two low intensities bands of 4-MBA at 1590 and 1078 cm^{-1} were observed in the SM regimen (Figure 1 (c)), but both bands were less intense than the water band at 1638 cm^{-1}. The above experimental results were confronted with generalized Mie Theory calculations, which reinforced that the SM-SERS sensitivity was possible due to the large number of hot spots triggered by 4-MBA protonation and H-bond formation.

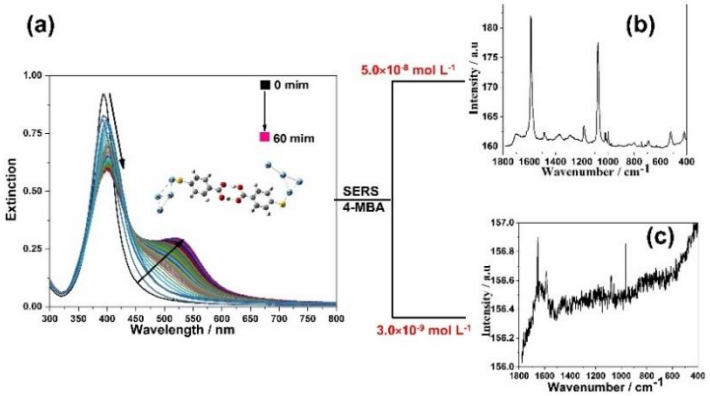

Figura 1. (a) Evolution of UV-Vis spectra of AgNP/4-MBA (5.0×10^{-7} mol L^{-1}) in pH=4 as a function of time and averaged SERS spectra of concentrations: (b) 5.0×10^{-8} mol L^{-1} and (c) 3.0×10^{-9} mol L^{-1}. λ_0= 633 nm.

[1] M. Fan, G.F.S. Andrade, A.G. Brolo, **Anal. Chim. Acta**. 1097, 1–29, 2020.
[2] D.P. Dos Santos, M.L.A. Temperini, A.G. Brolo, , **Acc. Chem. Res**. 52, 456–464, 2019.

Agradecimentos/Acknowledgments

FAPEMIG, CNPq, CAPES, UFJF.

VII Encontro Brasileiro de Espectroscopia Raman
VII EnBraER
05 a 08/12/2022, São Pedro – SP

In-situ Raman photocatalysis mediated by NIR radiation: coupling $NaREF_4$ upconversion nanoparticles with plasmonic Au nanoparticles

Gesiane P. de Sousa (PG)[1,*], Anerise de Barros (PQ)[1], Flávio M. Shimizu (PQ)[2,3], Fernando A. Sigoli (PQ) [1], Italo O. Mazali (PQ)[1]

mazali@unicamp.br

[1]Functional Materials Laboratory - Institute of Chemistry, University of Campinas – UNICAMP, Campinas, Brazil. [2]Brazilian Nanotechnology National Laboratory (LNNano), Brazilian Center for Research in Energy and Materials (CNPEM), Campinas, Brazil; [3]"Gleb Wataghin" Institute of Physics, University of Campinas - UNICAMP, Campinas, Brazil

Keywords: *Upconversion, rare-earth, plasmon, photocatalysis, Au, 4ATP.*

Highlights

In-situ Raman photocatalytic dimerization of 4ATP to DMAB, mediated by indirect localized plasmon resonance excitation. LSPR band excitation promoted by emissions in the visible region by upconversion nanoparticles excited under NIR radiation.

Resumo/Abstract

Upconversion is a phenomenon in which the sequential absorption of lower energy photons leads to the emission of higher energy photons. The most common host lattice used for upconversion applications is the sodium yttrium fluoride in the hexagonal crystalline phase (β-$NaYF_4$), due to its low phonon energy, which decreases the possibility of nonradiative relaxation. Additionally, the matrix β-$NaYF_4$ is usually doped with Yb^{3+} and Er^{3+} ions, which act as sensitizers and activators, respectively. In this case, the Yb^{3+} ions are responsible for the near-infrared (NIR) absorption (when excited at 980 nm) and the Er^{3+} ions emit radiation in the green (510 - 540 nm) and red regions (630 - 675 nm). The Nd^{3+} ions also can be incorporated in such matrixes as sensitizers (λ_{exc} = 808 nm). In this case, the Yb^{3+} ions act as a 'bridge', in the sense, that the radiative NIR energy absorbed by the Nd^{3+} ions is transferred to Er^{3+}, by the Yb^{3+} ions. UCNPs present many applications, such as in bioimaging, photodynamic therapy and fluorescence intensity ratio thermometry. Furthermore, its use in plasmonic photocatalysis have been emerging, since coupling UCNPs with plasmonic nanoparticles leads to harvesting of UV-VIS-NIR light. Moreover, the UV-VIS photons emitted by the UCNPs during the NIR excitation can be radiatively transferred to semiconductors and plasmonic nanoparticles, and therefore, used to improve the efficiency of the photocatalyst. In this work, UCNPs composed by β-$NaYF_4$:Er,Yb@3$NaYF_4$:Nd@2$NaYF_4$@SiO_2-NH_2 were coupled with Au NPs to promote the plasmonic driven model reaction of dimerization of 4-aminothiophenol to 4,4'-dimercaptobeneze (DMAB). The reaction was monitored in-situ through Surface-enhanced Raman Spectroscopy (SERS). Optimal conditions were achieved in order to promote the photocatalytic dimerization mainly through the indirect excitation of the localized surface plasmon resonance (LSPR) band of the Au NPs by the upconversion emissions of the UCNPs. Hexagonal crystalline UCNPs (22 ± 3 nm), composed by β-$NaYF_4$:Er,Yb@3$NaYF_4$:Nd@2$NaYF_4$ were synthesized by the thermal decomposition of trifluoroacetates. The UCNPs were encapsulated with a silica shell, through the microemulsion method (shell width: 22.6 ± 3 nm). The UCNPs and the UCNPs@SiO_2 samples showed similar upconversion luminescence intensity under both 980 nm and 808 nm excitation, indicating that the thick SiO_2 shell did not interfere in the luminescent properties. Colloidal spherical Au NPs (ca. 15 nm) were obtained through the Turkevich method, and exhibited LSPR band at 518 nm. The silica shell was modified with amino groups, in order to promote the chemical affinity among the UCNPs@SiO_2 and the Au NPs. Before and after the amino functionalization, the silica-capped UCNPs exhibited zeta-potential of -36.3 ± 5.91 and + 45.6 ± 5.64, respectively. Surface-enhanced Raman Spectroscopy (SERS) substrates containing either SiO_2-NH_2/Au NPs or UCNPs@SiO_2-NH_2/Au were prepared by the drop cast method in a Si wafer (4x4 mm^2). Both substrates were illuminated for 5 s, and 30 s, with a 980 nm laser, at 25.7 mW, and 60 spectra were collected randomly throughout each substrate. The intensity ratio between characteristic Raman bands related to the product and reagent DMAB:4ATP ($I_{DMAB,1140\ cm-1}/I_{4ATP,1078\ cm-1}$) was 1.0 and 0.1, respectively, for the SiO_2-NH_2/Au NPs and UCNPs@SiO_2-NH_2/Au substrates, which confirms the energy transfer process between the UCNPs and plasmonic Au nanoparticles.

Acknowledgments

VII Encontro Brasileiro de Espectroscopia Raman
VII EnBraER
05 a 08/12/2022, São Pedro – SP

Investigação Raman Ressonante de uma sonda de ligação de hidrogênio em líquidos iônicos

Beatriz R. de Moraes (PG), Leandro R. Marques (PG), Rômulo A. Ando (PQ)*

bearmoraes@usp.br

Laboratório de Espectroscopia Molecular, Departamento de Química Fundamental, Instituto de Química, Universidade de São Paulo;

Palavras Chave: Raman Ressonante, Líquidos iônicos, Disperse Orange 3, Ligação de hidrogênio

Highlights

Resonant Raman investigation of hydrogen bond probe in ionic liquids. Modification of the enhancement pattern of azo group vibrational modes of Disperse Orange 3 (DO3) between the ionic liquids (IL) systems. DO3 can be used as probe of hydrogen bond in IL.

Resumo/Abstract

As ligações de hidrogênio têm um papel fundamental na estrutura e propriedades dos líquidos iônicos (LIs), pois ela é responsável por perturbar o arranjo de cargas induzidos pelas interações de Coulomb, ocasionando maior fluidez no LI. Entretanto, a comprovação experimental da presença dessas ligações no sistema é sutil, já que geralmente são ligações de hidrogênio não usuais. Uma das abordagens possíveis para a identificação de tais ligações em LIs é a inserção de moléculas sonda sensíveis a essas interações. Neste trabalho foi utilizado como sonda o corante Disperse Orange 3, um azocomposto que possui em sua estrutura um grupo aceptor (-NO_2) e um grupo doador (-NH_2) de elétrons na posição *para* do anel benzênico. A estrutura eletrônica desse composto é modificada pela interação entre o corante e o meio, o que deve se manifestar nos espectros Raman ressonante. O DO3 foi solubilizado em dois diferentes LIs, EMIMNTf_2 e EDMIMNTf_2, ambos apróticos, sendo que o EMIMNTF_2 apresenta um hidrogênio relativamente ácido na posição C2 que altera significativamente suas propriedades físico-químicas. Os espectros eletrônicos foram comparados com o DO3 solubilizado em etanol (EtOH) e diclorometano (DCM). Em relação ao DCM, os espectros nos LIs apresentam um deslocamento para maiores comprimentos de onda devido à estabilização do estado excitado do DO3, porém uma menor estabilização em relação ao EtOH. Através dos espectros UV-VIS não é possível estabelecer uma correlação direta entre ligações de H dos LIs e o DO3 pois não há deslocamento do máximo de absorção. Contudo, o Raman Ressonante (RR) se mostra uma técnica sensível às mudanças na estrutura eletrônica do DO3, dependendo do meio. No espectro RR do DO3 e os LIs nas radiações incidente de 514 nm e 457 nm, no caso em que é mais provável a interação por ligação de hidrogênio, ou seja, entre o EMIMNTf_2 e o DO3, pode ser observada uma intensificação preferencial dos modos relativos à ligação azo νNN (1458, 1428 e 1397 cm^{-1}). Tal intensificação seletiva pode estar associada ao fato de que é a ligação azo que interage via ligação de hidrogênio na posição C2, o que não ocorre no caso do EDMIMNTf_2. Estudos em diferentes solventes e em outras classes de líquidos iônicos estão sendo realizados no momento para uma melhor compreensão das interações presentes nesses sistemas e do uso do DO3 como molécula sonda para ligações de hidrogênio.

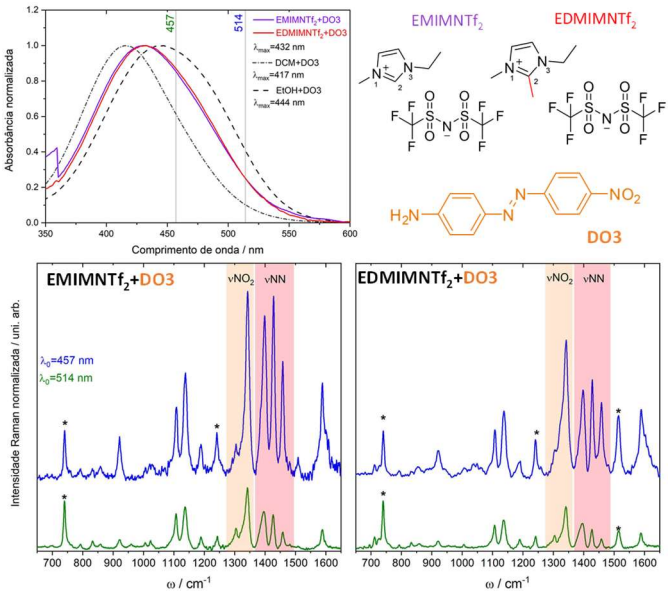

Agradecimentos/Acknowledgments

Rômulo A. Ando e Beatriz R. de Moraes agradecem à Fundação de Amparo à Pesquisa do Estado de São Paulo (FAPESP 2016/21070-5 e 2020/09250-3). Leandro R. Marques agradece à Coordenação de Aperfeiçoamento de Pessoal de Nível Superior (CAPES 88887.341021/2019-00).

VII Encontro Brasileiro de Espectroscopia Raman
VII EnBraER
05 a 08/12/2022, São Pedro – SP

Solventes eutéticos profundos baseados em alcanolaminas para captura de CO_2

Pedro H. P. Sabanay (IC), Giovanni R. Morselli (PG), Rômulo A. Ando (PQ)*

pedrosabanay@usp.br

Laboratório de Espectroscopia Molecular, Departamento de Química Fundamental, Instituto de Química, Universidade de São Paulo.
Palavras-Chave: DES, CO_2, alcanolaminas, Raman.

Highlights

Alkanolamines Based Deep Eutectic Solvents for CO_2 Capture. CO_2 capture through DES consisting of alkanolamines and chloride salts. Spectroscopic study to characterize the products of the mixture and intermolecular interactions.

Resumo/Abstract

Metodologias viáveis para a captura de CO_2 tem sido cada vez mais requeridas. Neste sentido a utilização dos solventes eutéticos profundos (DES) tem se destacado devido ao baixo custo e facilidade de preparação. Neste trabalho é apresentado um estudo sistemático da capacidade de absorção de CO_2 por soluções de alcanolaminas para a formação de DES à base de cloreto de colina: 2-(Metilamino)etanol (MAE) (1:6) e cloreto de colina: 2-(Etilamino)etanol (EAE) (1:6) (Figura 1), utilizando de medidas espectroscópicas (Raman) e capacidade de absorção procurou-se entender a natureza da captura do gás pelos compostos.

Figura 1. Estrutura DES de alcanolamina / ChCl

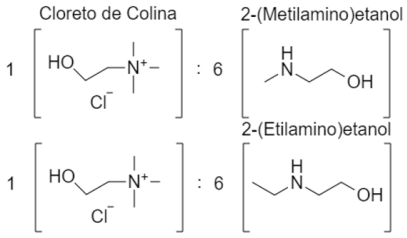

O grupo álcool nas alcanolaminas age como doador de ligações de hidrogênio (HBD) no DES[1], enquanto a presença do grupo amino possibilita absorção do CO_2 que se pela formação de carbamatos[2], isso pode indicar um futuro método utilizando de DES's a base de aminas como meios para a captura e conversão de CO_2 em produtos de valor agregado, como carbamatos, carbonatos e afins, assim verificando-se a viabilidade de reciclagem do material de partida. A Figura 2 mostra os espectros Raman dos DES antes e após a absorção de CO_2. Foi possível confirmar a formação do carbamato como produto da reação devido ao surgimento de uma banda em 606 cm^{-1} , que pode ser atribuída ao modo de deformação angular do grupo $(N)CO_2^-$.[2]

Tabela 1. *Absorção de CO_2 pelas misturas.*

Amostra	g CO_2 / g Solução
MAE/H_2O	0,0833
EAE/H_2O	0,0878
MAE/ChCl	0,0898
EAE/ChCl	0,1108

Figura 2. *Espectros Raman, alcanolaminas na presença e na ausência de CO_2.*

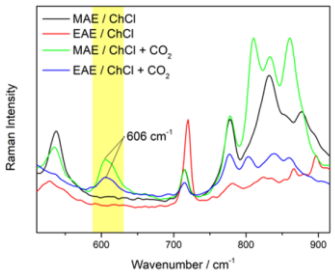

De acordo com a Tabela 1 observou-se que a o DES formado de EAE é capaz de absorver maior quantidade de gás. Isso pode indicar que a captura de CO_2 via DES à base de alcanolaminas e sais de cloreto podem se tornar alternativas viáveis. No momento estão sendo investigados diferentes alcanolaminas e sais para otimizar o processo de captura.

[1] Nowosielski, B.; Jamrógiewicz, M.; Łuczak, J.; Warmińska, D. Novel Binary Mixtures of Alkanolamine Based Deep Eutectic Solvents with Water—Thermodynamic Calculation and Correlation of Crucial Physicochemical Properties. *Molecules* **2022**, *27*, 788. https://doi.org/10.3390/molecules27030788

[2] Ohno, K.; Inoue, Y.; Yoshida, H.; Matsuura, H. *The Journal of Physical Chemistry A* **1999** *103* (21), 4283-4292. https://pubs.acs.org/doi/10.1021/jp984821q

Agradecimentos/Acknowledgments

À Fundação de Amparo à Pesquisa do Estado de São Paulo (Fapesp 2016/21070-5 e 2022/06710-9).

VII Encontro Brasileiro de Espectroscopia Raman
VII EnBraER
05 a 08/12/2022, São Pedro – SP

Kinetic study of the devitrification process of an ionic liquid using MCR-ALS hard-modeling and low-frequency Raman spectroscopy.

Mónica Benicia Mamián-López (PQ),[1] Vitor H. Paschoal (PQ),[2,*] Mauro Carlos Costa Ribeiro (PQ)[2]

monica.lopez@ufabc.edu.br

1Universidade Federal do ABC, Av. dos Estados, 5001, 09210-580, Santo André, (SP), Brasil; 2 Laboratório de Espectroscopia Molecular, Instituto de Química, Universidade de São Paulo. C.P. 26077, 05513-970, São Paulo (SP), Brasil.

Palavras Chave: *Crystallization kinetics, Ionic Liquids, Hard-modelling, Multivariate Curve Resolution-Alternating Least Squares).*

Highlights

Low-frequency Raman demonstrates amorphous-crystal phase transition. MCR-ALS hard-modeling reveals a two-step mechanism of devitrification. Crystal polymorph is dependent on the rate-determining step.

Resumo/Abstract

Room temperature ionic liquids (RTILs) are systems formed by molecular-like cations and anions that, despite being charged, are liquid at temperatures far below their inorganic counterparts. These systems are usually regarded as good glass formers yielding amorphous phases in experiments done at typical cooling rates, with either a glass or a supercooled liquid (i.e., a liquid sample below its melting point) being obtained. Although crystallization can occur, it is a slow process relying either on long annealing times (on cooling or heating) or related to the cold-crystallization process, where an amorphous to crystal conversion is observed upon heating. The ionic liquid 1-butyl-3-methylimidazolium hexafluorophosphate ([C4C1Im][PF6], Figure 1a) is one typical example of an RTILs that is easily supercooled and exhibits a cold-crystallization (or devitrification) at ca. 225 K, where these different phases can be easily picked-apart using low-frequency Raman spectroscopy, as shown in Fig.1b. Furthermore, this system shows polymorphism where its α or β phase can be obtained, being marked by different conformations of the C4 group (Fig. 1a) showing characteristic bands (shown in Fig. 1b). In this work, we will analyze the devitrification of this liquid using time-dependent low-frequency Raman spectroscopy and Multivariate Curve Resolution with Alternating Least Squares (MCR-ALS) hard-modeling to unveil the kinetics of this process. Multivariate decomposition done by this method shows that the devitrification occurs following a two-step mechanism with either the α or β phases associated with different rate-determining steps, as shown by the corresponding optimized profiles (Fig. 1c).

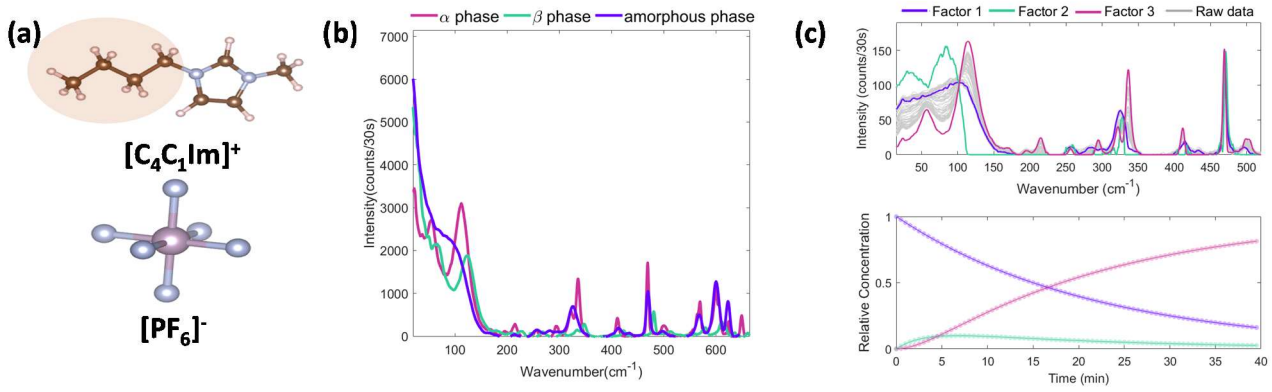

Figure 1: (a) Structure of the $[C_4C_1Im]^+$ and $[PF_6]^-$. C_4 group is shown in red. (b) Examples of low-frequency Raman spectra of amorphous (lilac), α (magenta) and β (green) phases at 225 K. (c) Optimized profiles of the intermediates from the MCR-ALS hard-modelling (upper panel) and relative concentrations as a function of time (lower panel).

Agradecimentos/Acknowledgments

The authors thank FAPESP (grants 2016/21070-5 and 2019/00207-0), and CNPq (grants 301553/2017-3 and 405087/2021-7).

VII Encontro Brasileiro de Espectroscopia Raman
VII EnBraER
05 a 08/12/2022, São Pedro – SP

Espectroscopia vibracional e reologia de solventes eutéticos profundos baseados em ureia e sais de colina

Ícaro F. T. de Souza (PG)[1]*, Mauro C. C. Ribeiro (PQ)[1]

1. Instituto de Química, Universidade de São Paulo, São Paulo 05508-000, Brasil
**icaro.francescato.souza@usp.br*

Palavras Chave: Solventes eutéticos profundos, colina, reologia, espectroscopia vibracional.

Highlights

Vibrational spectroscopy and rheology study of deep eutectic solventes based on urea and choline salts.

- [Chol][DHP]:U presents a Maxwellian behavior of the elastic (G') and viscous (G") modules as a function of the frequency of mechanical oscillation.
- Spectral analysis shows that hydrogen bonds are stronger in the DES containing [DHP], due to the anion-anion interaction itself.
- The [Ac] anion's presence leads to the highest deformation of urea in the DES structure.

Resumo/Abstract

Solventes eutéticos profundos (DES) são frequentemente definidos como uma mistura binária ou ternária de compostos capazes de se associariam através de ligações de hidrogênio, interações de van der Waals e/ou ligações de caráter iônico. Para esse trabalho, foram escolhidos o cloreto de colina ([Chol]Cl), acetato de colina ([Chol][Ac]) e dihidrogenofosfato de colina ([Chol][DHP]) como aceptores de ligações de hidrogênio (HBAs) e a ureia (U) como doadora de ligações de hidrogênio (HBD).

A dependência dos módulos G' e G", para os DESs que possuem [Ac] e [DHP], em função da frequência de oscilação é similar à vista nos líquidos viscoelásticos, porém o [Chol][DHP]:U segue o comportamento Maxwelliano, característico de sistemas formados por longas cadeias mantidas por ligações intermoleculares. Os espectros de infravermelho na região de baixas frequências indicam que essas cadeias são mantidas ligações de hidrogênio entre os ânions [DHP], mais fortes que as vistas na presença do [Ac] ou do cloreto. O mesmo é observado na região do infravermelho médio através do padrão de bandas "ABC".

A estrutura e dinâmica das interações intermoleculares entre os componentes do DES foi analisada através dos espectros Raman em função da temperatura, como a distorção da planaridade da ureia causada pela presença dos diferentes ânions. (Figura 1). O deslocamento das bandas do [Ac] em função da temperatura indicam que fortes ligações de hidrogênio ocorrem entre o carboxilato do ânion e os grupos NH_2 da ureia no DES [Chol][Ac]:U, o que gera uma estrutura tridimensional característica de um fluido viscoelástico, diferente do que ocorre na presença do [DHP].

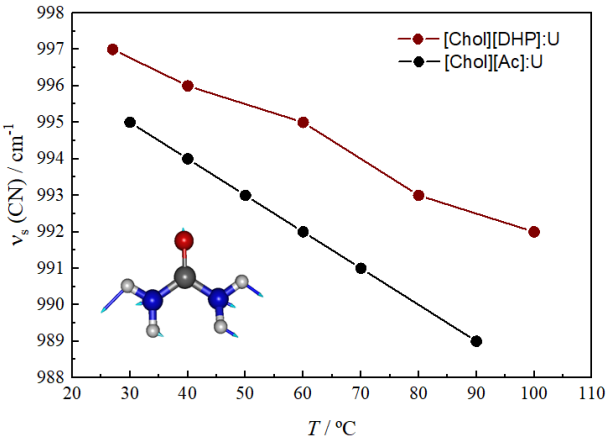

Figura 1. Deslocamento da banda de estiramento simétrico CN da ureia em função da temperatura durante o aquecimento dos DESs [Chol][Ac]:U e [Chol][DHP]:U.

Como o [Ac] é o menos coordenante da série de ânions e não forma estruturas extensas ânion-ânion como o [DHP], é o que causa a maior distorção na ureia entre os DESs analisados.

Agradecimentos/Acknowledgments

Ao CNPq e a FAPESP pelas bolsas e financiamento no Laboratório de Espectroscopia Molecular do IQ-USP.

Porous liquids of ZIF-67 with gemini ionic liquids based on benzylammonium acetate for CO_2 adsorption.

Ahmed D. Páez (PG),[1] Nicolas Keppeler (PG),[2] Omar A. El Seoud (PQ),[2] Rômulo A. Ando (PQ)[1,*].

ahmedlem44@usp.br

[1]Laboratório de Espectroscopia Molecular, Departamento de Química Fundamental, Instituto de Química, Universidade de São Paulo.
[2]Grupo de Polímeros e Surfactantes, Departamento de Química Fundamental, Instituto de Química, Universidade de São Paulo

Keywords: Vibrational Spectroscopy, CO_2 Adsorption, Gemini Ionic Liquids.

Highlights

Gemini ionic liquids (GILs) are adequate to form porous liquids (PL) due to their large size. The adsorption of CO_2 was followed by ATR-IR spectroscopy.

Resumo/Abstract

The search for sustainable materials to mitigate CO_2 emissions through fixation (carbon capture and storage, CCS) is a priority within the scientific community. Porous liquids (PL) as nonvolatile and versatile materials, has been highlighted, as a way to improve gas adsorption capacity and allow a greater diffusion within the material.[1] The use of GILs can facilitate the synthesis of PL due to the large size of the ions, that precludes their penetration in the pores of the solid matrix. Herein, two novel (GILs) based on trimethylene-1,3- and pentamethylene-1,5-bis(dimethylbenzylammonium acetate) salts were synthesized, named as C3-Gem and C5-Gem, respectively. Then, two new porous liquids were prepared by mixing rational quantity of a metal organic framework, ZIF-67, with each GIL, doubling the maximum CO_2 adsorption capacity in porous liquids compared to pure GILs (Figure 1).

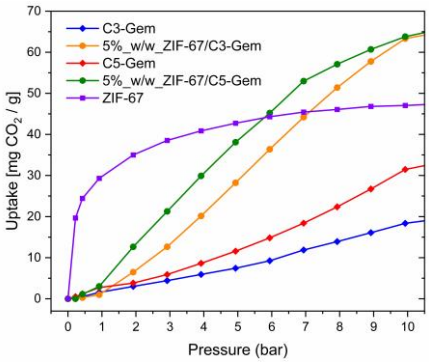

Figure 1. CO_2 sorption isotherms at 35 ºC for materials studied. Blue line, C3-Gem; orange line, ZIF-67/C3-Gem, red line, C5-Gem; green line, ZIF-67/C5-Gem, and purple line, ZIF-67.

In this work, one of the main objectives is to characterize the materials before and after CO_2 adsorption by vibrational spectroscopy. Figure 2 shows ATR-IR spectra of ZIF-67/C5-Gem porous liquid before and after CO_2 adsorption. Significant differences were observed after CO_2 absorption. Two new bands appear at 2335 cm^{-1} and 649 cm^{-1}, that can be attributed to the $\nu_{as}(CO_2)$ and the $\delta(CO_2)$ of the CO_2, respectively. At 1638 cm^{-1}, it is observed the δ(OH), resulting probably from the absorption of water during the sample extraction and storage process, which in contact with CO_2 produces the formation of bicarbonate ions, resulting in the appearance of a band at 838 cm^{-1}. In the spectrum of PL + CO_2, other differences are observed that must be better characterized, such as the broadening of the band at 992 cm^{-1} and the appearance of the band at 1260 cm^{-1}. Our aim in this study is to characterize such differences to understand the interactions between the species, and contribute to the development of more efficient methodologies for capturing gases.

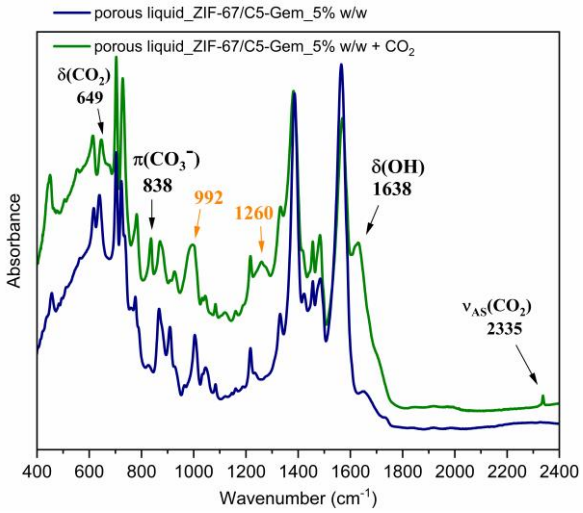

Figure 2. ATR-IR spectra in the region from 400 – 2400 cm^{-1} for ZIF-67/C5-Gem porous liquid before and after CO_2 adsorption.

1. Gomes, M.C., et al., Porous Ionic Liquids or Liquid Metal-Organic Frameworks? Angewandte Chemie-International Edition, 2018. 57(37): p. 11909-11912.

Agradecimentos/Acknowledgments

Financial support by FAPESP (2018/25737-0), (2016/21070-5) is acknowledged.

VII Encontro Brasileiro de Espectroscopia Raman
VII EnBraER
05 a 08/12/2022, São Pedro – SP

Tetraalkylammonium Chlorides Based Deep Eutectic Solvents for SO_2 Capture

Giovanni R. Morselli (PG) [1,2], Pedro H. P. Sabanay (IC),[1] Rômulo A. Ando (PQ)[1,2*]

giovanni.morselli@usp.br

[1]Laboratório de Espectroscopia Molecular, Departamento de Química Fundamental, Instituto de Química, Universidade de São Paulo; [2]RCGI – Research Centre for Greenhouse Gas Innovation

Palavras Chave: SO_2 capture, Deep Eutectic Solvents, Charge Transfer Interactions.

Highlights

The interactions of SO_2 within Deep Eutectic Solvents of some tetraalkylammonium chlorides and glycerol are characterized through Raman spectroscopy.

Resumo/Abstract

Deep Eutectic Solvents (DES) has been highlighted as the evolution of Ionic Liquids due to having many of their advantages as extreme-low vapor pressure, while exhibiting simplified preparation, lower cost and higher biodegradability. They are formed by the mixture of a hydrogen bond acceptor (HBA), which is often a quaternary ammonium salt, with a hydrogen bond donor (HBD). Tetraalkylammonium chlorides are widely available HBAs employed to prepare DES.

Among different applications, DES are being studied to capture sulfur dioxide (SO_2), which is a pollutant gas that still has high anthropogenic emissions. Shed light on interactions of SO_2 within the DES is an important step to optimize the capture and conversion process. Hence, this work aims to study interactions of SO_2 with the pure HBAs tetraalkylammonium chlorides of ethyl (TEAC), propyl (TPAC) and butyl (TBAC), and its DES containing the HBD glycerol through Raman spectroscopy.

It is worth noticing that a colorless liquid is formed by the contact of gaseous SO_2 with the pure salts (precursors of DES). The molar sorption capacity reached values around 2,8 mol of SO_2/ mol of salt for all of them. This result will be compared with the corresponding DES, containing glycerol as HBD, in terms of spectroscopic variations. For all samples, the $\nu_s(SO_2)$ exhibited a typical Raman shift of charge transfer specific interactions between the chloride anion and SO_2, as well-characterized in the literature.[1] In the mixtures of SO_2 with the pure salts at a same molar ratio, the influence of the cation alkyl chain size in the interaction is observed through the analysis of the shoulder of $\nu_s(SO_2)$ that appears at lower wavenumbers, as shown in Figure 1. The longer the cation alkyl chain, the broader the shoulder and less relatively intense. This behavior will be discussed based on specific charge transfer interactions and different solvation states of SO_2 within the mixture, which will be further analyzed with the variation of SO_2 molar ratio (X_{SO2}). It will be also shown that the analysis of $\nu_s(SO_2)$ in mixtures of the gas with the corresponding DES, along with the aforementioned results, may give insights into the structure of these solvents.

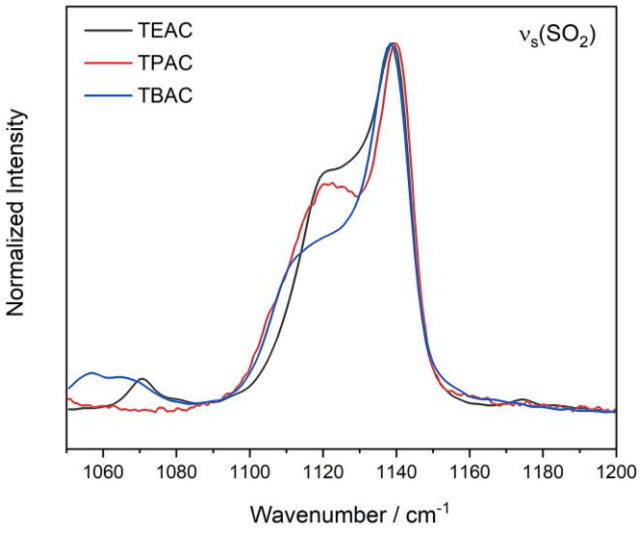

Figure 1. Spectral region of $\nu_s(SO_2)$ in Raman spectra of mixtures of TEAC, TPAC and TBAC at X_{SO2} = 1.4, registered with λ_0 = 1064 nm.

References

1. G.R. Morselli, R.A. Ando, Chemical Physics Letters 784 (2021) 139106.

Agradecimentos/Acknowledgments

The authors are indebted to FAPESP (2016/21070-5; 2022/06710-9 and 2020/15230-5) and FUSP/RCGI (68 - GHG - D.3.Project_5) for the financial support.

VII Encontro Brasileiro de Espectroscopia Raman
VII EnBraER
05 a 08/12/2022, São Pedro – SP

Investigação *in situ* por espectroscopia Raman da formação de vacâncias de oxigênio na estrutura do óxido de cério (IV) durante reduções catalíticas em fase gasosa

Gustavo D. L. de Andrade (IC)[1]*, Fernando A. Sigoli[1], Italo O. Mazali (PQ)[1]

g171282@dac.unicamp.br, mazali@unicamp.br

[1]*Functional Materials Laboratory - Institute of Chemistry, University of Campinas – UNICAMP, Campinas, Brazil.*

Palavras Chave: *Espectroscopia Raman, Vacâncias de Oxigênio, Catálise Heterogênea, Nanomateriais, Óxido de Cério.*

Highlights

In situ investigation of the oxygen vacancies formation in the structure of cerium (IV) oxide during gas phase catalytic reductions. Raman spectroscopy was used to monitor oxygen vacancies in ceria nanorods used in catalysis. The results suggests that oxygen vacancies have an important role in the catalysis mechanism.

Resumo/Abstract

O óxido de cério desponta como um catalisador heterogêneo eficiente e versátil, possuindo diversas aplicações, tais como celas de exaustão de veículos e formulação de catalisadores para redução de SO_x.[1] Recentemente, nanobastões de ceria foram reportados como catalisadores seletivos para a hidrogenação da carbonila do crotonaldeído.[2] Esta seletividade é impressionante, uma vez que a hidrogenação da dupla ligação presente neste aldeído é favorecida, pois possui menor energia de ativação. As vacâncias de oxigênio que se formam na estrutura dos nanobastões de CeO_2 são apontadas como essenciais para a seletividade desta reação. Portanto, o monitoramento da formação destas vacâncias no material é fundamental para uma melhor compreensão do mecanismo que descreve a atividade catalítica do óxido de cério nanoestruturado. A espectroscopia Raman é uma técnica que permite monitorar a variação na concentração de vacâncias de oxigênio na estrutura da ceria, em especial em nanobastões. A posição da banda t_{2g} do CeO_2 foi demonstrada estar diretamente ligada à formação e consumo de vacâncias de oxigênio.[3] Com isto, este projeto promoveu um estudo, utilizando espectroscopia Raman, do comportamento das vacâncias de oxigênio em nanobastões de óxido de cério usados na hidrogenação catalítica do crotonaldeído. Os resultados obtidos demonstram que a catálise em estudo possui um efeito pronunciado e detectável sobre a banda t_{2g} dos nanobastões de ceria, indicando que as vacâncias de oxigênio possuem, de fato, um papel essencial no mecanismo de hidrogenação do crotonaldeído.

Referências:

1. A. Trovarelli, *Catal. Rev.*, 1996, 38, 439–520.

2. Z. Zhang, Z.-Q. Wang, Z. Li, W.-B. Zheng, L. Fan, J. Zhang, Y.-M. Hu, M.-F. Luo, X.-P. Wu, X.-Q. Gong, W. Huang and J.-Q. Lu, *ACS Catal.*, 2020, 10, 14560–14566.

3. I. C. Silva, F. A. Sigoli, I. O. Mazali, *J. Phys. Chem. C*, 2017, 121, 12928–12935.

Agradecimentos/Acknowledgments

VII Encontro Brasileiro de Espectroscopia Raman
VII EnBraER
05 a 08/12/2022, São Pedro – SP

In-situ monitoring of crystalline transformation of $NaREF_4$ from cubic to hexagonal using Raman Spectroscopy

Gesiane P. de Sousa (PG)[1], Anerise de Barros (PQ)[1], Claudia M. S. Calado (PQ)[1], William M. Oliva (PG)[1,*], Nagyla A. de Oliveira(PG)[1], Sérgio F. N. Coelho(PG)[1], Fernando A. Sigoli (PQ) [1], Italo O. Mazali (PQ)[1].

mazali@unicamp.br

[1]*Functional Materials Laboratory - Institute of Chemistry, University of Campinas – UNICAMP, Campinas, Brazil.*

Keywords: *$NaREF_4$, Sodium rare-earth fluoride, cubic, hexagonal, Raman Spectroscopy.*

Highlights

Raman spectroscopy can be used to monitor the crystalline phase of as-synthesized $NaREF_4$ nanoparticles.

Abstract

Sodium rare-earth fluoride matrixes ($NaREF_4$) exhibit optical transparency in the UV-VIS-NIR region, low toxicity, high thermal stability and low phonon energy. Due to these features, such matrix is an excellent host lattice for luminescent applications. Therefore, in the literature, its use in bioimaging, photodynamic therapy, temperature sensing, fingerprint recognition, among others, has been widely studied. $NaREF_4$ nanoparticles may crystallize in two polymorphs: cubic (α) and hexagonal (β) crystalline phases. In the α-$NaREF_4$, the rare earth ions occupy a cubic site with high symmetry (O_h), whereas in the β-$NaREF_4$ the luminescent RE ions occupy sites with lower symmetry (C_{3h}). The distortion of the crystalline field around the RE ions leads to mixing between wavefunctions with different parity (5d with 4f). Therefore, RE ions in lower symmetry sites leads to higher luminescence emission intensities, due to the relaxation of the Laporte (parity) selection rule. Therefore, the β-$NaREF_4$ crystal phase is very commonly studied for luminescent applications. The α-$NaREF_4$ crystal phase is more widely studied for magnetic applications.

$NaREF_4$ can be obtained through different experimental procedures, such as: hydrothermal method, solvothermal method, co-precipitation, reverse micelle and thermal decomposition of sodium and rare-earth trifluoroacetates. The latter is nowadays known to yield high-monocrystalline nanocrystals, hence, they exhibit excellent luminescent properties. Since, the α- crystal phase is metastable, and the β-$NaREF_4$ crystal phase is thermodynamically stable, the parameters of the synthesis must be very well controlled to obtain the desirable crystal phase for each application. For instance, in the thermal decomposition of sodium and rare-earth trifluoroacetates method, vital parameters for the obtention of the desired crystal phase and morphology are: temperature; Na:RE ratio; solvents composition and molar ratio and reaction time.

In this work, we synthesized $NaREF_4$ (RE: Gd^{3+}, Y^{3+}, Yb^{3+}, Er^{3+}, Nd^{3+}, Tb^{3+} and Eu^{3+}) nanoparticles with different crystal phases (α or β) and compositions through the thermal decomposition method. The samples were characterized by XRD, transmission electron microscopy (TEM) and Raman Spectroscopy. Despite the different sizes and composition, all the cubic samples showed the same Raman spectra profile. The same observation can be stated for the hexagonal samples. Therefore, herein, we report that Raman Spectroscopy can be used to infer about the crystal structure of the $NaREF_4$ samples. In fact, considering that the Raman spectra acquisition process is fast and practical, the use of Raman spectroscopy can be very helpful to differentiate between the cubic and hexagonal crystal phases of the as-synthesized $NaREF_4$ nanoparticles.

Acknowledgments

VII Encontro Brasileiro de Espectroscopia Raman
VII EnBraER
05 a 08/12/2022, São Pedro – SP

Influence of Ag nanoparticles in waveguides on doped germanate glasses

Camila D. S. Bordon (PG)[1], Jessica Dipold (PG)[2*], , Wagner de Rossi (PQ)[2], Anderson Z. Freitas (PQ)[2], Luciana R. P. Kassab (PQ)[3], Niklaus U. Wetter (PQ)[2]

jessica.dipold@gmail.com

[1]Departamento de Engenharia de Sistemas Eletrônicos, Escola Politécnica da USP, São Paulo, Brazil; [2]Instituto de Pesquisas Energéticas e Nucleares, IPEN-CNEN, 2242, A. Prof. Lineu Prestes, São Paulo, SP, Brazil; [3]Faculdade de Tecnologia de São Paulo, CEETEPS, São Paulo, SP, Brazil

Palavras Chave: *Nanoparticles, Raman, Doped glasses*

Highlights

Femtossecond laser writing causes structural changes inside GeO_2-PbO glasses for waveguiding and Ag nanoparticle clustering for improved emission. Changes are characterized by Raman Spectroscopy.

Resumo/Abstract

Writing by using femtossecond (fs) laser enables fast prototyping and has low complexity compared to other fabrication methods. For materials that do not allow light confinement and propagation, waveguiding by double-line technology is necessary. Previously, we demonstrated waveguiding in double-lines for undoped germanate and tellurite glasses, as well as GeO_2-PbO doped with Er^{3+}/Yb^{3+} and Nd^{3+}. The results for the Nd^{3+} glass were promising for the fabrication of integrated amplifiers, lossless components and lasers. This motivated the present investigation, where silver (Ag) nanoparticles (NPs) were added to the Nd^{3+} doped GeO_2-PbO bulk in order to enhance its guiding capabilities.

Raman measurements were made with a LabRam HR Evolution – HORIBA, using a 532 nm laser with 100 mW power and a 10 x objective lens with 0.25 NA. An integration time of 1 second and 15 accumulations was used to reduce noise and make the observed peaks clearer.

First, the Raman spectrum was measured for the bulk (*b*) glass (Fig. 1a) and between the written lines (Fig. 1a). There are no substantial changes between these, indicating, as expected, that there are no relevant structural changes in the guiding region between the two lines. However, comparing the bulk region (Fig. 1a) with the inside of the written line with 4 superimposed lines (Fig. 1b), there are major changes in some of the peaks. The peak at 411.2 cm^{-1} (*b*) shifted to 433.9 cm^{-1}, indicating modification in the symmetric stretching vibrations of the Ge-O-Ge bonds. The peak at 517.5 cm^{-1} (*b*) to 508.1 cm^{-1} shows changes in the symmetric stretching vibrations along the Ge-O-Ge chain, demonstrating lower density of these bonds in the irradiated region. A slight change of the 782.3 cm^{-1} and 867.4 cm^{-1} (*b*) are also verified, and are related to the Ge-O^- and Ge-O-Ge symmetric stretching vibrations in the GeO_4 tetrahedral units and asymmetric stretching vibrations of the Ge-O-Ge bonds, respectively. These changes are larger than the ones previously shown for the same material without the Ag NPs, which shows the influence of the nanoparticles during the writing process.

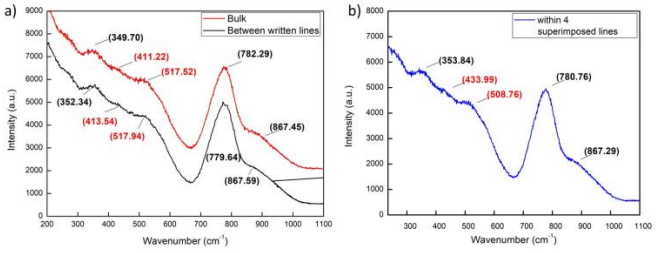

Figure 1: Raman spectrum of the (a) glass bulk and the region between the double waveguide; and (b) inside the four overlapping written lines region.

Agradecimentos/Acknowledgments

We'd like to thank FAPESP (2019/06334-4, 2016/02326-9, 2017/10765-5 and 2013/26113-6, EMU 2018/19240-5, 2017/50332-0) and from INCT/CNPq 465.763/2014 (INCT de Fotônica), Grant: 302532/2019-6, IPEN/CNEN 2020.06.IPEN.33.PD and Grant: SISFÓTON-MCTI 440228/2021-2 (Sistema Nacional de Laboratórios de Fotônica).

VII Encontro Brasileiro de Espectroscopia Raman
VII EnBraER
05 a 08/12/2022, São Pedro – SP

Raman gain coefficient of Sm^{3+} ions doped tellurite glasses

Jaqueline V. Gunha (PG)[1,*], Robson F, Muniz (PQ)[2], Aloisi Somer (PQ)[1], Daniele T. Dias (PQ)[3], Raouf El-Mallawany (PQ)[4], Carlos Jacinto (PQ)[5], Nelson G. C. Astrath (PQ)[6], Andressa Novatski (PQ)[1]

jaquegunha@gmail.com

[1]Department Physics, State University of Ponta Grossa; [2]Department of Science, State University of Maringá, Goioerê; [3]Departament Physics, Federal University of Technology – Parana, Ponta Grossa; [4]Physics Department, Faculty of Science, Menoufia University, Shibin Al Kawm, Egypt; [5]Group of Nano-Photonics and Imaging, Federal University of Alagoas Maceió, Alagoas; [6] Department Physics, State University of Maringá, Maringá.

Keywords: *Raman gain, Raman gain coefficient, spectroscopy, rare earth*

Highlights

- It is possible to observe two bands centered at 500 to 1500 cm^{-1} and 1700 to 2600 cm^{-1}, greatly differentiating the emission;
- The intensity of the bands is concentration and doping dependent;
- And finally, the Raman gain coefficient was obtained from the bands for each of the bands, these being: $^6H_{5/2}$ and $^6H_{7/2}$.

Abstract

Recently, investigation of new materials for high-speed optical communications are of special interest. Tellurite glasses are good candidates for these applications; since they have broad transmission range from 0.3 to 5.0 μm and hence they have highest Raman cross section as compared to other glasses systems [1]. In addition, these glasses present Raman gain of 58 times higher than fused silica [2] making these glasses interesting to be applied in Raman amplifiers, fiber Raman lasers, microsphere Raman lasers, etc. [2]. In this work, tellurite glasses were prepared with $65TeO_2$-$15Li_2O$-20ZnO composition doped with different concentrations of Sm_2O_3 (0.1; 0.15; 0.2; 0.35; 0.5; and 1.0 mol%) by melting quenching technique. The Raman gain coefficients of these glasses were obtained from Raman scattering experiments using 532 nm excitation from a Horiba Xplora Plus spectrometer with a 50× microscope objective, with 15 s of integration time and five accumulations. Raman spectra show two broad bands, the first at 500 to 1500 cm^{-1} and the second at 1700 to 2600 cm^{-1}, which become broader with Sm^{3+} concentration. From the Raman measurements we can observe stark split for the emissions of the levels $^6H_{5/2}$ and $^6H_{7/2}$ that correspond to the two broad bands found. The Raman gain was determined following the methodology presented in the reference [1]: the observed Raman intensity was corrected for Fresnel reflection at the surface of the glass. The spontaneous Raman intensity was normalized to the Raman intensity of silica at a peak in 440 cm^{-1}. We observed that the Raman gain coefficient increased with Sm^{3+} concentration and these values were larger than other silicate, tellurite glasses reported in the literature [1,3]. The gain Raman spectra showed a quenching effect for concentrations higher than 0.2 mol % Sm_2O_3, for both bands. Following the same behavior as the lifetime for the emissions corresponding to these bands. Therefore, the analyses showed the potential of the studied materials as new gain media for band Raman amplifiers.

[1] El S. Yousef et al., Chalc. Glasses 12, 653 (2015).
[2] M El-Okr, M. Ibrahem, M. Farouk, J. Phys. Chem. Solids 69, 2564 (2008).
[3] El S. Yousef et al., Opt. Las. Tech. 74, 138 (2015).

Acknowledgments

The authors acknowledge the support from the Brazilian agencies CAPES, CNPq, Fundação Araucária, FINEP, C-LABMU and LabMult C²MMa.

VII Encontro Brasileiro de Espectroscopia Raman
VII EnBraER
05 a 08/12/2022, São Pedro – SP

$PbO.SiO_2$ glass under high pressure: ex-situ and in-situ Raman analysis

Rafaella B. Pena[1*], Veronic Laurent[2] (PG) Elodie Rameo[2] (PG),Thierry Deschamps[2] (PQ), Christine Martinet[2] (PQ), Adalberto Picinin[1] (PQ), Paulo S. Pizani[1] (PQ),[1]

pizani@df.ufscar.br

[1]*Universidade Federal de São Carlos, Departamento de Física, Centro de Ciências Exatas e Tecnologia, São Carlos, SP*
Institute Matière Lumière, Université Jean Claude Bernard, Lyon, France.
Palavras Chave: *Raman, metasilicate glass, high-pressure, plastic deformation.*

Highlights

$PbO.SiO_2$ glass under high pressure: ex-situ and in-situ Raman analysis

Permanent densification of glasses

In-situ and ex-situ under high-pressure Raman analysis

Resumo/Abstract

Lead metasilicate glasses ($PbO.SiO_2$) were densified at different maximum pressures in a diamond anvil cell (DAC) at room temperature. The glass samples were investigated ex-situ and in-situ by Raman spectroscopy to probe their pressure-induced transformations and permanent structural modifications on the Q(n) distribution (Fig.1). With a high Pb content (50% mol), this glass exhibits a low elastic limit at about 5 GPa, and a saturation limit at ~ 20 GP, behavior denounced by the barycenter shift, Fig.2. On the other hand, the in-situ Raman spectra acquired during compression and decompression the barycenter displays expressive changes under pressure, presenting higher values for the compression than for the decompression path. The stepwise increase upon compression suggests the occurrence of important structural modifications, which cannot be fully attributed to anharmonic effects. Spectral curve fitting of the high-frequency region of the Raman spectra, consisting of symmetric Si-O stretching modes, exhibit subtle Q(n) population modifications with maximum pressure. This can be attributed to silica network depolymerization where the proportion of non-bridging oxygens (NBO) increases at the expense of bridging oxygens (BO). Possible densification mechanisms are discussed in contrast to those known in other silicate glasses.

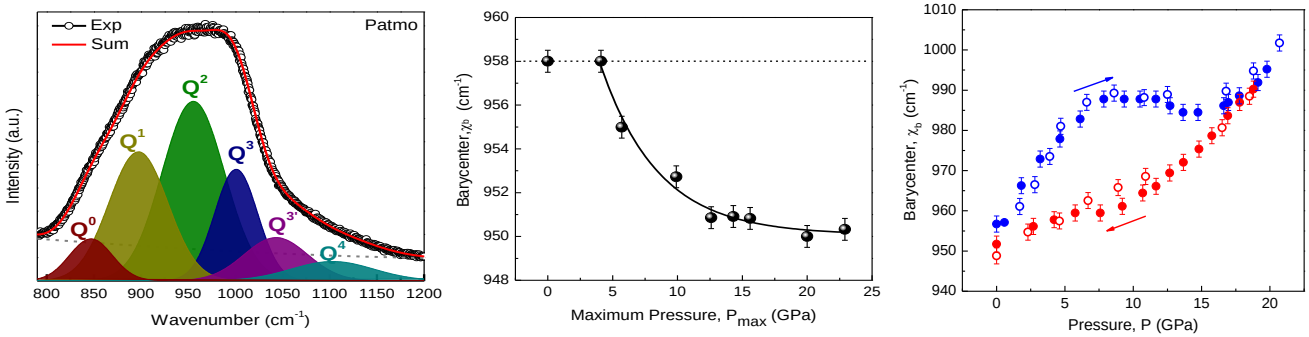

Agradecimentos/Acknowledgments

Fundação de Amparo a Pesquisa do Estado de São Paulo, FAPESP, proc. 2013/07793-6, 2017/118968-2 and 2019/11446-6.

Conselho Nacional de Desenvolvimento Científico e Tecnológico, CNPq proc. 303020/2021-0.

VII Encontro Brasileiro de Espectroscopia Raman
VII EnBraER
05 a 08/12/2022, São Pedro – SP

SYNTHESIS AND CHARACTERIZATION OF MoO_2 NANOPARTICLES

Hilton B. da Silva (IC),[1,*] Gilberto D. Saraiva (PQ),[1] Aline Alves de Freitas (IC),[1] Raí F. Jucá (IC),[1] Joel R. de Castro (PQ),[2] Alessandra Alexandrino Aquino[1].

hilton.beserra@gmail.com* , gilberto.saraiva@uece.br

[1] Faculdade de Educação, Ciências e Letras do Sertão Central, UECE, CEP: 63.902-;098; [2] Universidade Federal do Ceará - Campus de Quixadá, Cedro – Quixadá – Ceará 63902-580; [3] Universidade Federal do Ceará - Rede Nordeste de Ensino (RENOEN); [4] Departamento de Física, Universidade do Estado do Rio Grande do Norte, Mossoró-RN, CEP: 59610-210, Brazil.

Palavras Chave: *Molybdenum Dioxide, Nanoparticles, Hydrothermal Method, Raman Spectroscopy.*

Highlights

Synthesis and characterization of MoO_2 nanoparticles.
Process of synthesis of nanoparticles of molybdenum dioxide (MoO_2) by means of the hydrothermal method; Raman Spectroscopy analysis of and classification of vibrational modes.

Resumo/Abstract

This work aims to describe the process of synthesis of the molybdenum dioxide (MoO_2) nanoparticles using the hydrothermal method, as well as its structural, morphological and vibrational characterization. The characterization techniques used were X-ray diffraction (XRD), scanning electron microscopy (SEM) and Raman spectroscopy. During the synthesis process, molybdic acid was used as precursor agent for MoO_2 nanoparticles. To reduce this acid (oxidation-reduction process) the compound dodecanethiol was used as solvent, which also had the purpose of forming MoO_2 micelles, leading to the formation of molybdenum dioxide nanoparticles. The XRD measurements indicated that the structure of the system is monoclinic with space group P21/c and with a high level of purity, greater than 95%. As per the refinement of XRD measurements, the lattice parameters are: a = 5.61020 Å, b = 4.85730 Å, c = 5.62650 Å, α = 90,000 Å, β = 120.9150 Å, and γ = 90,000 Å. The obtained molybdenum dioxide nanoparticles have an average diameter of 42.92 nm, observed by SEM. Corroborating the XRD analysis, the Raman spectra of the molybdenum dioxide nanoparticles also indicated a monoclinic structure. In addition, the observed Raman modes were classified using the actual literature. Therefore, the synthesis method was effective in the preparation of MoO_2 nanoparticles that were characterized structurally, morphologically and in terms of their vibrational modes.

Agradecimentos/Acknowledgments

UECE - Faculdade de Educação, Ciências e Letras do Sertão Central, CAPES - Coordenação de Aperfeiçoamento de Pessoal de Nível Superior, CNPq - Conselho Nacional de Desenvolvimento Científico e Tecnológico.

VII Encontro Brasileiro de Espectroscopia Raman
VII EnBraER
05 a 08/12/2022, São Pedro – SP

Transition of ferroelastic nature observed in double perovskite $Cs_2AgBiBr_6$ through Raman Spectroscopy

Fabio E. O. Medeiros* **(PG)[1], Laura M. T. Vidal (PG)[2], Alejandro P. Ayala (PQ)[1]**

fabio@fisica.ufc.br

[1] Department of Physics, Federal University of Ceará, PO Box 6030, Campus of Pici, Fortaleza|CE; [2] Department of Pharmacy, Federal University of Ceará, Campus of Porangabuçu, Fortaleza|CE.

Key Words: *Raman, Spectroscopy, Perovskite, Ferroelastic, Transition.*

Highlights

Raman Spectroscopy, Double Perovskite, Cs2AgBiBr6, Ferroelastic Transition.

Abstract

Lead-free, non-toxic perovskites have attracted the attention of the scientific community in recent years around the world. Its optoelectronic physical properties have been widely used in the production of various technological devices. One of the most explored is the photovoltaic property, capable of transforming solar energy into electrical energy. Such a property is at the forefront of studies and being improved day after day in order to achieve the ability to produce clean energy on a large scale and surpass the current market leaders, which are silicon photovoltaic panels. In this scenario, one of the most promising materials is the $Cs_2AgBiBr_6$ double perovskite, due to its ease of production, energy conversion efficiency, low cost and stability to atmospheric exposure. However, in addition to all its usability in the industry, it can still present a basic physical property, which is the partially ferroelastic phase transition. The present work shows an anomalous phonon exhibiting soft mode re-normalization behavior after a critical temperature of approximately 122 K (Fig1(c)), where a structural phase transition also occurs. Such behavior has already been used to characterize transitions of this nature[1-4]. The objective of this work was to determine the existence of a ferroelastic transition in this compound, so, in view of the evidence presented and the similarities existing in previous works, such as the re-normalization of the soft mode, after the structural phase transition from cubic ($Fm\bar{3}m$) to tetragonal ($I4/m$) and the analysis of possible ferroelastic species demonstrated in the works of Aizu[5], we have strong indications that the tetragonal phase of the double perovskite $Cs_2AgBiBr_6$ is ferroelastic (or more precisely, partially ferroelastic) belonging to the *m3m*F*4/m* species. Therefore, we believe it is possible to call such a transition as a *Partially ferroelastic phase transition*.

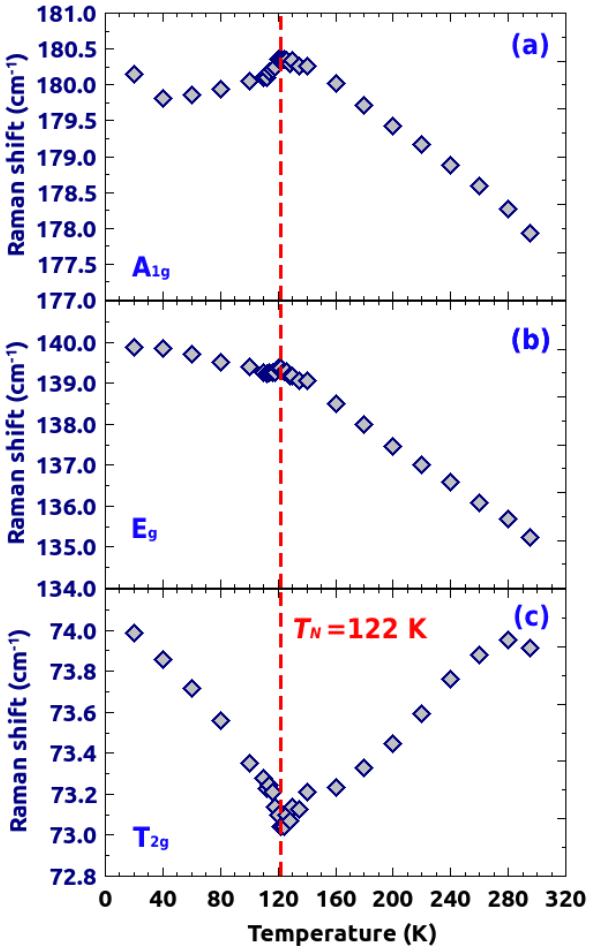

Fig1: $Cs_2AgBiBr_6$ perovskite Raman modes centers as a function of temperature

[1]**H G Unruh** *Condensed Matter* (1992), [2]**A Pinczuk** *Sol. State. Comm.* (1977), [3]**G Errandonea** *Phys. Rev. B* (1981), [4]**J Haines** *Phys. Rev. B* (1998), [5]**K Aizu** *J. Phys. Soc of Japan* (1969)

Acknowledgments

The authors thank the CAPES and CNPq funding institutions for this research.

VII Encontro Brasileiro de Espectroscopia Raman
VII EnBraER
05 a 08/12/2022, São Pedro – SP

Investigação no Espectro Vibracional de Compostos $SrTiO_{3-\delta}$

Natália Pincelli Westin* (IC),[1] Eduardo Granado Monteiro da Silva (PQ)[1], Rodolfo Tartaglia Souza (PG)[1], Felipe Souza Oliveira (PG)[2] e Carlos Alberto Moreira dos Santos (PQ)[2]

n204000@dac.unicamp.br

[1]Instituto de Física "Gleb Wataghin", UNICAMP; [2]Escola de Engenharia de Lorena, USP

Palavras Chave: *Titanatos, Materiais Avançados, Espectroscopia Raman*

Highlights

Investigation on the Vibracional Spectrum of the $SrTiO_{3-\delta}$ Compunds. The influence of oxygen vacancies in STO monocristals has been studied by means of Raman spectroscopy. Unexpected modes for the space group symmetries were observed on the more doped samples.

Resumo/Abstract

A perovskita $SrTiO_3$ e compostos similares são alvo de pesquisas desde longa data. Apesar do cristal puro se apresentar isolante à temperatura ambiente, é possível induzir novas caracteristicas notáveis por diferentes formas. Supercondutividade à baixas temperaturas no *bulk* ou na interface deste com outros materiais [1], além de ferroeletricidade induzida por dopagem [2], são alguns exemplos que podem ser inicialmente citados.

Outra característica de interesse no STO é a alta permissividade elétrica. Esta grandeza aumenta com o resfriamento do material a partir da temperatura ambiente, conjuntamente à diminuição na frequência de um fônon em particular, conhecido como *soft-mode* ferroelétrico. Esta resposta da polarização na matéria sugere a possibilidade de um reordenamento atômico que deve originar uma transição ferroelétrica. Todavia, esta transição não ocorre, assim como o a frequência do *soft-mode* não vai a zero, devido efeitos de flutuações quânticas [3].

Neste estudo, foram caracterizadas amostras cristalinas de STO dopadas com oxigênio. Esta dopagem foi obtida através de tratamentos térmicos de 5 horas a temperaturas distintas, em vácuo dinâmico de 10^{-5} mbar, dentro de um tubo de quartzo selado. Para análise, medidas de espectroscopia Raman foram realizadas entra 15 e 320 K, em vácuo da ordem de 10^{-6} mbar.

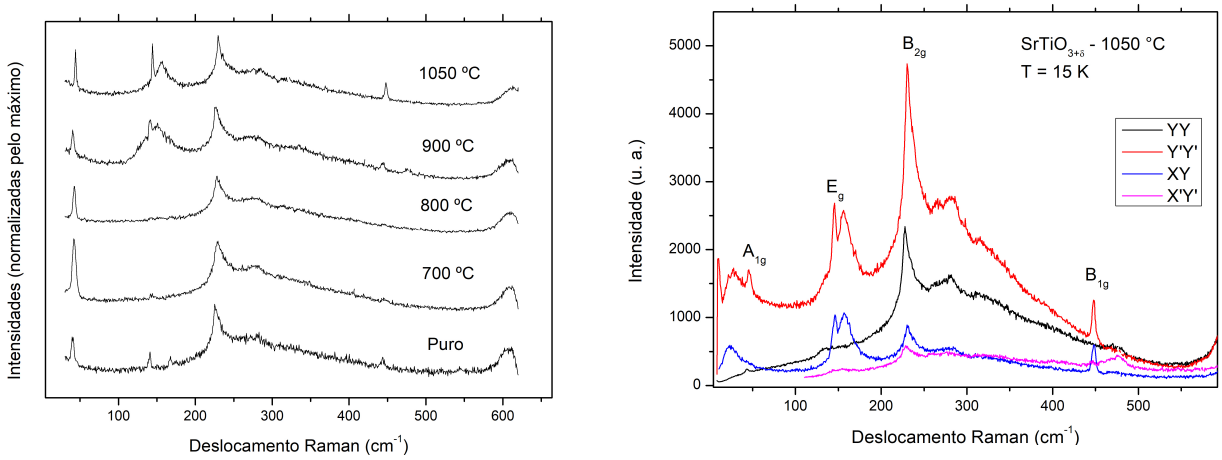

Acima, esquerda, espectros comparativos para diferentes amostras em T=15 K. Nitidamente, um pico no entorno de 150 cm^{-1} ocorre apenas nas amostras de maior dopagem. Seu comportamento com a polarização pode ser observado na figura da direita, à mesma temperatura, medida na amostra tratada a 1050 ºC.

As vacâncias de oxigênio inseridas no material induziram modificações nos espectros. A mais nítida, conforme pode ser observado nas Figuras, é um pico largo de frequência próxima a 150 cm^{-1}. Este pico também aparece em espectros adquiridos sobre uma superfície recém cortada de uma das amostras, indicando que a dopagem não fora

apenas superficial. Aumentando a temperatura, observamos o desaparecimento deste modo próximo a 60 K, o que não coincide com a transição antiferrodistorsiva do material em 105 K. Isso indica, claramente, que se trata de um fenômeno físico diferente. De fato, já fora predito que anomalias poderiam ocorrer no entorno de 70 K, com temperatura de transição diminuída pelo acréscimo na quantidade de vacâncias de oxigênio [4]. Um segundo acontecimento interessante é a aparição de picos ativos da fase cúbica do STO apenas em IV, a saber, em 173 e 473 cm^{-1}. Este é um indicativo de quebras locais de simetria de inversão, causadas pela inserção das vacâncias de oxigênio. Além disso, sugere a existência de pequenas regiões ferroelétricas. Esta ideia é apoiada por estudos anteriores, que também propuseram a existência destas regiões [4], e que as observaram em amostras dopadas com cálcio [2].

Referências

[1] Chi-Sheng Li *et al,* Oxide-based Materials and Devices VIII, 101051T (2017)

[2] Ouillon *et al* J. Phys.: Condens. Matter 14 2079 (2002)

[3] Oliveira, Felipe S., Tese de dout., USP (2021)

[4] J. F. Scott, Ferroelectrics Letters Section, 20:3-4, 89-95 (1995)

[5] H. Uwe , H. Yamaguchi e T. Sakudo, Ferroelectrics, 96:1, 123-126 (1989)

Agradecimentos/Acknowledgments

Este projeto teve o apoio da Fundação de Amparo à Pesquisa do Estado de São Paulo (FAPESP), processo 2020/06701-4.

VII Encontro Brasileiro de Espectroscopia Raman
VII EnBraER
05 a 08/12/2022, São Pedro – SP

Raman spectroscopic study towards the growth of $CuO/CuWO_4$ heterostructure

Laura C. Fonseca (PG)[1], Carlos A. Parra (PQ)[1], Paulo T. Cavalcante (PQ)[2], Miryam Rincón (PQ)[3], Angela M. Raba (PQ)[4,*]

angelamercedesrp@ufps.edu.co

[1]Grupo de Física de Materiales GFM, Universidad Pedagógica y Tecnológica de Colombia UPTC; [2]Departamento de Física, Universidade Federal do Ceará; [3]Departamento de Física, Universidad Nacional de Colombia; [4]Grupo de Investigación en Materiales Poliméricos GIMAPOL, Universidad Francisco de Paula Santander UFPS.

Key words: *CuO, $CuWO_4$, Heterostructure, Characterization, Crystalline phase.*

Highlights

$CuO/CuWO_4$ heterostructured system was obtained via one-step wet process.

Raman modes verified the presence of the monoclinic and triclinic phases in the heterostructured system.

Indirect band gap of samples was between 1.79 to 2.15 eV for the $CuWO_4$ and around 1.37 eV for the CuO.

Abstract

This work describes the preparation of $CuO/CuWO_4$ heterostructured system by facile one-step wet process. Raman spectroscopy analysis confirmed the growth of $CuO/CuWO_4$ heterostructure for different concentrations of the CuO and the $CuWO_4$ crystalline phases. Raman vibrational modes indicated the presence of the monoclinic and triclinic phases in the heterostructured system; the short-range structural ordering in the lattice of the heterostructured materials also was analyzed. Additionally, XRD, FE-SEM and DRS characterization techniques confirmed the formation of type-II heterojunction on as function of crystalline phase concentrations of CuO and $CuWO_4$ oxides. XRD results allowed to quantify the percentages of crystalline phases and to calculate the lattice parameters. Morphological analysis showed the presence of two different morphologies in the obtained samples. The heterostructures exhibited indirect gap band energies from 1.79 to 2.15 eV for the $CuWO_4$ and around 1.37 eV for the CuO, which are smaller than early reported value (~1.78 eV and 1.2 – 1.5 eV, respectively).

Agradecimentos/Acknowledgments

This work was supported by Universidad Francisco de Paula Santander, Universidad Pedagógica y Tecnológica de Colombia, and Universidad Nacional de Colombia.

VII Encontro Brasileiro de Espectroscopia Raman
VII EnBraER
05 a 08/12/2022, São Pedro – SP

Structural and vibrational properties of tricobalt tetroxide obtained by anodizing

Miryam R. Joya (PQ)[1], Leydi J. Cárdenas F.(PG)[2], José A. S. Silva(PG)[3], Paulo Tarso C. Freire(PQ)[3]

[1]Departamento de Física, Facultad de Ciencias, Universidad Nacional de Colombia-Bogotá, Carrera 30 Calle 45-03, Bogotá 111321, Colombia
[2] Facultad de Ingeniería-Departamento de Ingeniería Mecánica y Mecatrónica, Universidad Nacional de Colombia-sede Bogotá
[2] Departamento de Ingeniería Mecánica y mecatrónica, Fundación Universidad de América, Bogotá, Colombia
[3]Departamento de Física, Universidade Federal do Ceará, Caixa Postal 6030, Campus do Pici, 60455-970 Fortaleza, Ceará, Brazil.
mrinconj@unal.edu.co

Palavras Chave: *(Co_3O_4, anodizing, Raman, TEM, XPS).*

Highlights

*With the optimization of the anodizing conditions, the spinel phase is obtained.

*It is possible to observe different morphologies in the material by varying small variables in the anodizing.

*Raman vibrational modes show a typical spectrum of the Co3O4 phase.

*Through TEM measurements, the size of the nanoparticles in the samples and the crystallographic planes of the spinel phase are observed.

Resumo/Abstract

In the present work, the best anodizing conditions in a cobalt sheet were investigated to obtain the Co_3O_4 phase in the final samples. The samples were characterized by x-ray, FESEM, TEM and Raman spectroscopy. With the x-ray results, the spinel phase was obtained, through the FESEM measurements, the different morphologies of the samples were observed depending on the anodizing conditions. With the TEM measurements, the crystallographic planes of the Co_3O_4 samples were verified. From the Raman spectroscopy measurements, the vibrational modes of the spinel phase were observed.

Agradecimentos/Acknowledgments

The authors thank Universidad Nacional de Colombia – Campus Bogotá in Colombia, Universidade Federal do Ceará Fortaleza Brazil, Professor Jorge Bautista UFPS Cúcuta Colombia.

VII Encontro Brasileiro de Espectroscopia Raman
VII EnBraER
05 a 08/12/2022, São Pedro – SP

Espectroscopia Raman aplicada no estudo da transformação de fase em cerâmicas odontológicas de zircônia

Monique de Souza (PG)[1], Fernanda M. Tsuzuki (PG)[2,*], Evaldo P. Beserra Neto (PG)[2], Américo B. Correr (PQ)[2], Ana R. Costa (PQ)[2], Lourenço Correr-Sobrinho (PQ)[2],Mauro L. Baesso (PQ)[1]

monikedsouza@gmail.com

[1]Departamento de Física, Universidade Estadual de Maringá, UEM, Maringá-PR, Brasil; [2]Departamento de Materiais Dentários, Faculdade de Odontologia de Piracicaba/Universidade Estadual de Campinas, FOP/UNICAMP, Piracicaba-SP, Brasil.

Palavras Chave: *Espectroscopia Raman, Zircônia, Transformação de Fase.*

Highlights

Raman spectroscopy applied to the study of phase transformation in zirconia dental ceramics

Sandblasting was carried out with Al_2O_3 particles in different sintering stages with varying pressure on the zirconia.

Raman spectroscopy analyzed the bands of the tetragonal and monoclinic phases.

Resumo/Abstract

A zircônia estabilizada por ítria apresenta dificuldade na adesão de sua estrutura ao cimento odontológico devido à sua natureza rígida e cristalina[1]. O protocolo de tratamento de superfície mais utilizado é o jateamento com partículas de óxido de alumínio (Al_2O_3), esse tratamento gera uma rugosidade na superfície da zircônia que melhora a ligação com o cimento odontológico. No entanto, ao sofrer o impacto em sua estrutura, a zircônia pode sofrer transformação de fase, deixando-a mais suscetível a degradação a longo prazo[2]. Nesse aspecto, o objetivo desse estudo foi avaliar por meio da espectroscopia Raman a transformação de fase em cerâmicas de zircônia após o tratamento de superfície com jateamento de Al_2O_3 variando a pressão e em diferentes estágios de sinterização.

Os espectros Raman obtidos permitiram detectar a transformação de fase na superfície das cerâmicas de zircônia. Na Figura 1 pode-se observar a presença das bandas características da fase tetragonal e monoclínica. Na condição pré sinterizada apenas as bandas referentes à fase tetragonal estavam presentes nos espectros, independente da pressão de jateamento utilizada. Para as amostras expostas a condição pós sinterizada, uma mistura das fases tetragonal e monoclínica existia nos espectros, para todas as pressões de jateamento utilizadas, indicando que ocorreu a transformação de fase nessa condição de sinterização. O cálculo da quantidade de fase monoclínica foi realizado de acordo com o método proposto por Clarke e Adar[3]. O resultado mostrou que não houve variação significativa da quantidade de volume monoclínico com alteração da pressão de jateamento.

Figura 1: Espectros Raman da zircônia em diferentes condições de sinterização (pré e pós) e pressões de jateamento (2, 3 e 4 bar). As letras t e m identificam as bandas das fases tetragonal e monoclínica, respectivamente.

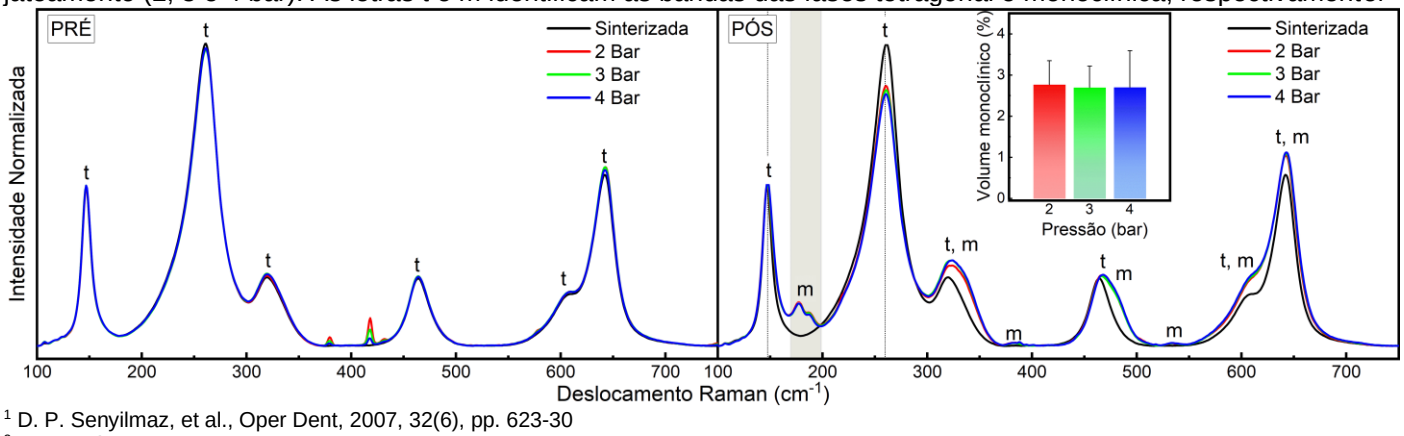

[1] D. P. Senyilmaz, et al., Oper Dent, 2007, 32(6), pp. 623-30
[2] I. L. Aurélio, et al., Dent Mater, 2016, 32(6), pp. 827-45
[3] D.R. Clarke, F. Adar, J Am Ceram Soc, 1982, 65(6), pp. 284-88

Agradecimentos/Acknowledgments

Os autores agradecem à CAPES, CNPq, Fundação Araucária, Finep, UNICAMP e a UEM pelo suporte financeiro.

VII Encontro Brasileiro de Espectroscopia Raman
VII EnBraER
05 a 08/12/17, São Pedro – SP

Effect of storage solutions on the mineral and organic content of dentin and enamel: a Raman spectroscopy study

Mariana S. Gibin (PG)[1]*, Lidiane V. de Castro-Hoshino (PQ)[1], Henrique dos Santos (PG)[1], Raquel S. Palácios (PG)[1], Renata C. Pascotto (PQ)[2], Hugo M. S. Deróide (PG)[1], Antonio Medina Neto (PQ) [1], Francielle Sato (PQ) [1].

marigibin32@gmail.com

[1]Physics Departament, Universidade Estadual de Maringá, UEM, Maringá – PR.
[2]Odontology Departament, Universidade Estadual de Maringá, UEM, Maringá – PR.

Keywords: Dentin, Enamel, Storage, Mineral Content, Organic Content.

Highlights

Study indicates conservation in enamel mineral content when stored in fixative solutions. In contrast, dentin exhibits significant molecular changes in mineral and organic content.

Abstract

Teeth for research purposes, after being extracted from the oral cavity, must be handled in order to prevent contamination, as they are composed of organic and mineral portions. For this, storage is necessary, requiring solutions capable of avoiding teeth dehydration, physical and chemical changes, as well as possible cross-contamination between extracted teeth and the growth of microorganisms [1]. In this sense, the objective of this work was to evaluate the action of fixing solutions compared to a standard solution (positive control) on the mineral and organic content of dentin and enamel.

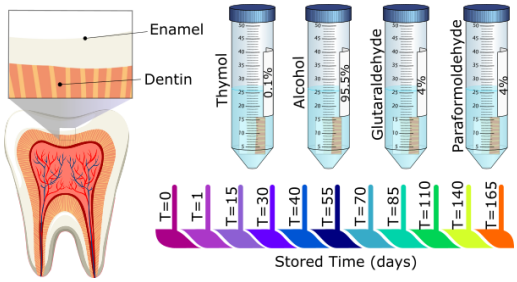

Figure 1: Experimental methodology.

The FT-Raman spectrometer (λ=1064 nm, Bruker Optik GmbH, Ettilingen, DEU) was used to analyze sound human teeth, dentin and enamel (n=5) at different storage periods. Spectra from before the immersion process (T=0) were acquired and used as a control group.

The results showed significant molecular variations for both amide and dentin phosphate. For enamel, there was no significant variation during the storage period in the fixing solutions. Since, fixing solutions are also known as crosslinking agents, which bond to the free amino acid residues of collagen and change the structural stability [2]. As dentin has a greater contribution of organic matter than inorganic, compared to enamel, tissue changes are expected to be more pronounced in dentin when compared to enamel.

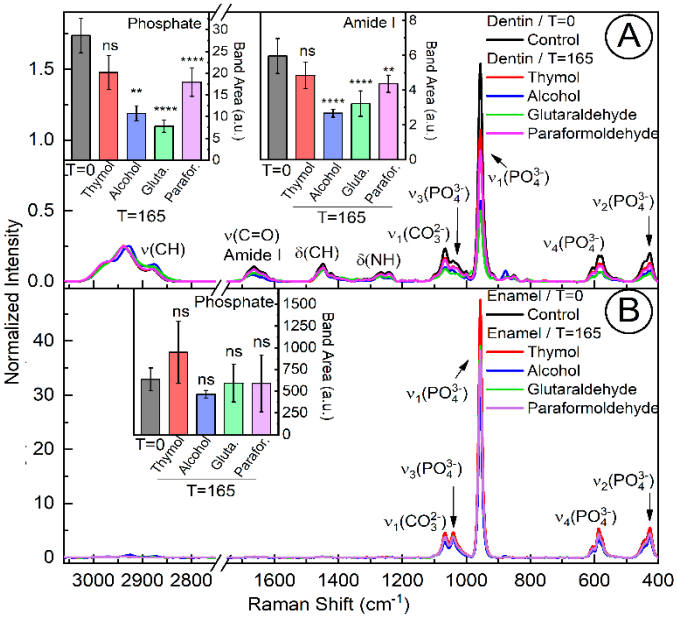

Figure 2: Dentin (A) and enamel (B) spectra for control and final storage time in different solutions. The Inset refers to bands areas of mineral and organic content to dentin and mineral content to enamel.

[1] T. Buchwald et al. **Vib. Spectrosc.** (96), 2018;
[2] L. Mengyao, et al. Int. **J. Food Prop.** (21), 2018.

Acknowledgments

The authors are grateful to the Brazilian agencies, CAPES, CNPq, Finep and Fundação Araucária for their financial support in this work and Universidade Estadual de Maringá.

VII Encontro Brasileiro de Espectroscopia Raman
VII EnBraER
05 a 08/12/2022, São Pedro – SP

Estudo da pele humana *in vivo* avaliada por espectroscopia Raman

Julia M. A. Abdala (PG),[1*] Lázaro P. M. Neto (PQ),[1] Gustavo C. Silva (PG)[1], Priscila P. Fávero (PQ)[1], Airton A. Martin (PQ)[1,2].

juabdala@yahoo.com.br

[1]Universidade Brasil, Rua Carolina Fonseca, 584, Itaquera, São Paulo; [2]DermoProbes: Skin and hair efficacy test, Av. Cassiano Ricardo, 601, Jd. Aquarius, São José dos Campos, São Paulo.

Palavras Chave:Espectroscopia Raman, diagrama de cluster, camadas da pele, análise de componentes principais.

Highlights

Study *in vivo* of human skin evaluated by Raman spectroscopy:

- Band intensities were correlated with dermal collagen in 940 cm^{-1} and 1650 cm^{-1}, and with hydrophobic structure of the outermost layer of the epidermis, in 1310/1450 cm^{-1}.
- In the statistical analyzes dermis and epidermis showed separation.
- *In vivo* confocal Raman spectroscopy is a promising non-invasive tool for skin assessment.

Resumo

Introdução: A técnica de espectroscopia Raman permite a pesquisa da composição bioquímica de amostras biológicas *in vivo*, de forma seletiva e não destrutiva (Harris, 2009). O estudo da árvore hierárquica pela análise de cluster, HCA, permite a classificação dos dados espectrais médios para cada camada de pele, epiderme e derme, e a análise de componentes principais, PCA, permite uma combinação linear de todas as variáveis originais gerando os índices de agrupamento de indivíduos de acordo com suas características (Varella, 2008). **Objetivo:** O objetivo deste estudo é avaliar a pele humana pela técnica de espectroscopia Raman confocal associada a HCA e PCA. **Metodologia:** As análises foram realizadas na empresa Dermo Probes – Pesquisa, Inovação e Desenvolvimento, o antebraço volar de dez voluntários, entre 34 e 45 anos, Vol_A, Vol_B, Vol_C, Vol_D, Vol_E, Vol_F, Vol_G, Vol_H, Vol_I, Vol_J, foi demarcado, selecionados a partir de critérios de inclusão. As avaliações *in vivo* da pele foram realizadas usando o um sistema Raman confocal (River Diagnosis, Modelo 3510) associado a um laser 785 nm. Dados Raman foram adquiridos por meio do software RiverIcon® 2.5.2 e analisados com o software Skin Tools® v 2.0 (River Diagnostics). Os espectros foram analisados no software OriginPro®, HCA e PCA no software Minitab® com dados previamente normalizados**.** **Resultados e Discussão:** Na figura (a), houve formação de dois grupamentos: (Vol_A,Vol_B, Vol_H, Vol_D) e (Vol_C, Vol_F, Vol_J, Vol_E, Vol_I, Vol_G), dentro desses grupos derme e epiderme apresentaram separação entre si, devido influência do colágeno só observado na DER (Tfayli *et al,* 2008; Lademann *et al,* 2009). Na figura (b) picos em 1130 cm^{-1}, 1310 cm^{-1} e 1450 cm^{-1}, referentes às estruturas lipídicas lamelares da parte mais externa da epiderme, o estrato córneo. Na região de derme picos em 852 cm^{-1} e 940 cm^{-1} referente à prolina, 1250/1296 cm^{-1} referente à amida I e III, e 1650/1654 cm^{-1}, referente ao colágeno e precursores. Na figura (c), foram obtidos (PC1, PC2, PC3, PC4, PC5, PC6), houve separação dos dados de derme e epiderme em todas as comparações em relação ao PC2 o mais discriminante.

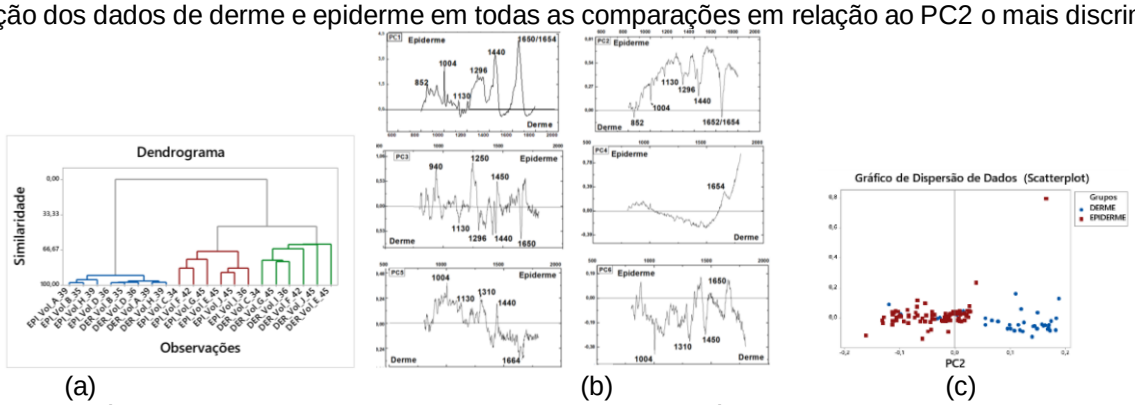

(a) (b) (c)

Conclusões: Foi possível associar os resultados dos componentes bioquímicos de cada camada avaliada e verificar a separação das camadas, confirmada nos dados do gráfico de dispersão e análises de HCA.

Agradecimentos

PROBES CAPES UB UNIVERSIDADE BRASIL

VII Encontro Brasileiro de Espectroscopia Raman
VII EnBraER
05 a 08/12/2022, São Pedro – SP

Hyaluronic acid detection in human skin by *in vivo* confocal Raman spectroscopy

Lázaro P. Medeiros Neto (PQ)[1*], Gustavo C. da Silva (PG)[2], Ritiane M. Almeida (IC)[1], Claudio A. Tellez Soto (PQ)[2], Sidney B. Cartaxo (PQ)[3], Airton A. Martin (PQ)[1,2]

lpmn_777@yahoo.com.br

[1]DermoPROBES - Skin and Hair Technology, São José dos Campos, SP, Brazil; [2]Science and Technology Institute, University of Brazil, São Paulo, SP, Brazil; [3]Surgery Department, Federal University of São Paulo, São Paulo, SP, Brazil.

Keywords: *Hyaluronic acid; confocal Raman spectroscopy; in vivo analysis; immunohistochemistry.*

Highlights

Rapid identification of hyaluronic acid concentration in the skin.
Decreased hyaluronic acid with advancing age.
Knowing the presence of hyaluronic acid in the skin promotes more effective products.

Abstract

Hyaluronic acid (HA) is a natural polysaccharide in the body whose main function is to bind water molecules, promoting skin hydration and reducing the effects of aging. Currently, its evaluation on the skin is carried out by invasive techniques, making it difficult to obtain information about its disposition on human skin. Thus, this study aimed to analyze in human skin the endogenous HA by *in vivo* confocal Raman spectroscopy (CRS) associated with immunohistochemistry (IHC) in groups of different ages. A River Diagnostics® CRS (Model 3510 Skin Composition Analyzer) with a 785 nm laser was used for the study. The analysis took place in the spectral range from 400 to 1800 cm^{-1}, with a maximum depth of 110 µm. In the IHC technique, the detection of CD44 protein was performed in formalin-fixed paraffin-embedded (FFPE) human skin tissue. Thus, different Raman peaks markers for HA were identified in the dermis region. The peak at 1104 cm^{-1} was the one that best showed the statistically significant differences ($p > 0.001$) in the concentration between the age groups 31-40 years (4,086 a.u.) and 51-65 years (2,412 a.u.) (Figure 1). This decrease in HA concentration was also noted in the IHC assessment. It should be considered that the CRS technique was able to identify endogenous HA in an *in vivo* and non-invasive way, expanding the knowledge of the disposition of HA in human skin, contributing to the understanding of aging processes and support for the development of new dermocosmetics and claims.

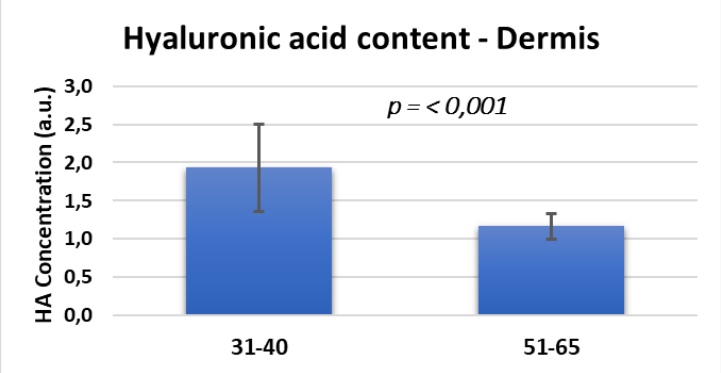

Figure 1: Bar graph of HA concentration in the dermis of 31-40 and 51-65 years group. Values obtained by the intensity of the peak 1104 cm^{-1} in the second derivative spectra. HA: Hyaluronic acid.

Acknowledgments

Lázaro Pinto Medeiros Neto thanks the São Paulo Research Foundation (FAPESP) – Grant: 2020/00928-7 / 2021/14696-3. A.A.M thanks to CNPq – Grant number 30996/2021-3

Kidney Injury biomarkers using FT Raman

Gabrielle Luana Jimenez Teodoro Nepomuceno (PG),[1] Herculano da Silva Martinho(PQ).

[1] *Universidade Federal do ABC, UFABC*

Keywords: Biomarkers, FT Raman, CKD, Raman Spectroscopy.

Highlights

Discovering the molecular compositions and changes arising from Renocardial Syndrome (CKD) for the discovery of biomarkers was the distinguishing feature of this work.

Resumo/Abstract

The application of spectroscopic techniques allows advances in precision medicine. For example, researchers have been studying the application of this technique in studies on renocardial syndrome (CKD). In the present work, we investigate the spectral characteristics by Fourier-Transform Raman spectroscopy (FT-Raman) due to physiological changes induced by renal ischemia-reperfusion, aiming at the discovery of biomarkers related to the progression from acute to chronic renal injury and predictors of mortality. C57BL/6J mice were subjected to unilateral occlusion of the left renal pedicle for 60 min and reperfusion for 5, 8, and 15 days. Cardiac and renal tissue biopsies were analyzed. Our findings indicated that cysteine/cystine, fatty acids, collagen methyl groups, α-form of proteins, tyrosine, and tryptophan were modulated during the process of renal ischemia and reperfusion. These changes are consistent with fibroblast growth factors and changes in collagen III content. Interestingly, Tyrosine and Tryptophan, precursor molecules for the formation of uremic toxins such as indoxyl sulfate and p-cresyl sulfate were also modulated and are considered a marker of renal injury, and their increase is strongly correlated with cardiovascular mortality. Furthermore, we noticed that the Tyrosine and Tryptophan bands (1558, 1616, and 1625 cm^{-1}) are consistent with fibroblast growth factors and changes in collagen III. content, and are also precursor molecules for uremic toxin formation.

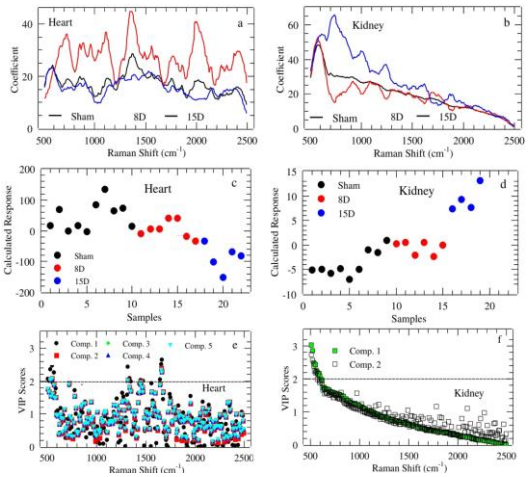

Figure 1. Regression coefficient in PLS-DA for Heart (**a**) and Kidney (**b**). Calculated response for heart (**c**) and kidney (**d**) using up to 5th and 2th component, respectively.Average PLS-DA Variable Importance in Projection (VIP) for those components with best classification performance for Heart (**e**) and Kidney (**f**).

Agradecimentos/Acknowledgments

The authors would like to thank the Brazilian agencies Conselho Nacional de Desenvolvimento Científico e Tecnológico (CNPq – 311146/2015-5 and 307718/2019-0). The authors would also thank the experimental resources provided by Multiuser Central Facilities at UFABC (CEM/UFABC).

VII Encontro Brasileiro de Espectroscopia Raman
VII EnBraER
05 a 08/12/2022, São Pedro – SP

Evaporation dynamics of water droplets used in the assembly of L, L-Diphenylalanine nanostructures.

Letícia Foiani (IC)[1*],Carla Bandeira (PG)[1] ,and Herculano Martinho (PQ)[1]

***leticia.foiani@aluno.ufabc.edu.br**

[1]Center for Natural an Human Ciences (CCNH), UFABC

Palavras Chave: *Water Evaporation, Kinetic Accompaniment, L, L- Diphenylalanine, Nanostructures, Nanotubes, Peptides.*

Highlights

This study aims to explain how the evaporation of water droplets used in the preparation of L, L - diphenyalanine nanotubes impacts their formation kinetics.

Resumo/Abstract

Depending on the preparation method, L, L - Diphenialanine nanotubes can have biological characteristics compatible with a lot of biomedical needs, such as: biocompatibility, biodegradability, extreme stability (in terms of body clearance) and optimal drug release into the plasma membrane (due to the low reactivity with their active ingredients). For the production of these structures, both water or aqueous solutions can be used as solvents. In this study, we aim to demonstrate how water droplets, used in the synthesis of nanotubes, behaves in terms of evaporation and how this phenomenon can directly influence the formation of peptide bonds, and therefore, their structures. The samples were analyzed by three methods: Fourier transform infrared spectroscopic analysis (FTIR), which enabled the monitoring of evaporation from the change of the spectra within time, the quantification of water mass within time during the evaporation process and, finally, the analysis with the optical microscope in order to make the visual monitoring of evaporation and show the possible anomalies that water would present. Throughout the research, it was noted that the evaporation of water droplets happens in a non-linear way and depends directly on conditions beyond the ambient temperature and pressure. FTIR monitoring reveals important water characteristics for this study, showing in detail what happens to the molecules during the evaporation process, while the other forms of analysis help to explain more concisely what is seen in the spectra and understand what happens in different ways inside the droplet.

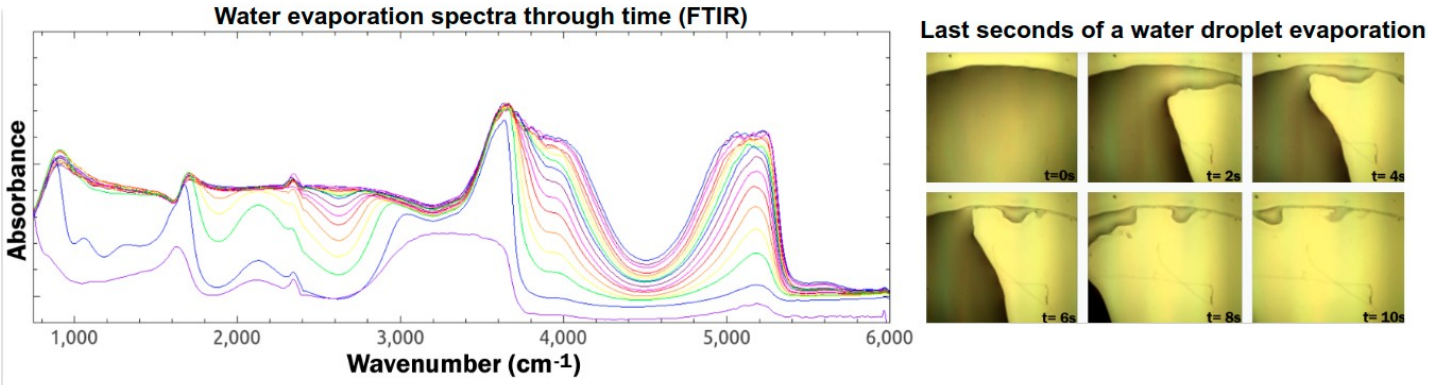

Agradecimentos/Acknowledgments

The authors would like to thank both the Biotechnoscience and Biophotonics Research Group and the experimental resources provided by Multiuser Central Facilities at UFABC (CEM/UFABC). This research was funded by the National Council of Technological and Scientific Development (CNPq).

VII Encontro Brasileiro de Espectroscopia Raman
VII EnBraER
05 a 08/12/2022, São Pedro – SP

Structural, QTAIM topological and spectroscopic analysis, and ADMET study of Methyl-2-(4-isobutylphenyl) propanoate

Maria R. Xavier (PG),[1] Leonardo P. da Silva (PG),[2] Kevin K.A. de Castro (PQ),[3] Amanda P. de Sousa (IC),[3] João P. da Hora (PQ),[3] Larissa S. Oliveira (IC),[3] Matheus N. da Rocha (IC),[4] Antônio C.H. Barreto (PQ),[2] Márcia M. Marinho (PQ),[3] Emmanuel S. Marinho (PQ),[4] Murilo S.S. Julião (PQ),[3] Paulo N. Bandeira (PQ),[3] Hélcio S. dos Santos (PQ),[1,3] Alexandre M.R. Teixeira (PQ) [1,4]

alexandre.teixeira@uece.br

[1]Instituto [1]Regional University of Cariri, Crato, CE, Brazil; [2]Federal University of Ceará, Fortaleza, CE, Brazil; [3]State University Vale do Acaraú, Sobral, CE, Brazil; [4]State University of Ceará, Campus FAFIDAM, Limoeiro do Norte, CE, Brazil

Keywords: *Ibuprofen derivative, NMR, ATR-FTIR; FT-Raman, UV-Vis spectroscopy*

Highlights

A liquid compound of methyl ibuprofen ester was synthesized; A full structural, topological and spectroscopic analysis was carried out; Pharmacokinetic proprieties of this compound was evaluated.

Abstract

In this work, the methyl ibuprofen ester, named methyl-2-(4-isobutylphenyl) propanoate ($C_{14}H_{20}O_2$, hereinafter MET-IBU) was synthesized and characterized by NMR, ATR-FTIR, FT-Raman, and UV-Vis spectroscopy, while their structural, QTAIM topological and spectroscopic properties were investigated using DFT calculations. Through the analysis of the topological properties of the electron density computed at bonding critical points (BCP's) for the MET-IBU molecule were determined the electron density, the Laplacian of electron density, the eigenvalues of Hessian matrix, the ellipticity of electron density, the potential energy density, the kinetic energy density in the Lagrangian and Hamiltonian forms, the total energy density, the Lagrangian density, and the electron delocalization index. Density Functional Theory (DFT) calculations were also used to determine the vibrational normal modes, the frontier molecular orbitals (FMOs), the dipole moment, and the molecular electrostatic potential (MEP) of MET-IBU. The interatomic surfaces of some atoms of the MET-IBU molecule were also given providing information where the charge density is maximum. The ATR-FTIR and FT-Raman spectra of this compound were obtained, and the assignment of the normal modes was done by means of potential energy distribution. In particular, it was observed that the stretching mode of the carbonyl group of MET-IBU appears at 1767 cm^{-1} in the ATR-FTIR spectrum with very strong intensity. Comparing the values of the global reactivity descriptors, it was observed that the MET-IBU compound has greater susceptibility to accept electronic density and, consequently, a better electrophilic character than ibuprofen compound. Theoretical UV absorption spectrum was also evaluated from time-dependent density functional theory (TD-DFT) providing the electronic transitions, which are expected for this compound. The experimental and theoretical UV spectra were compared, and the electronic transitions corresponding to the six singlet states were identified. The maximum absorption was experimentally observed at the wavelength of 227 nm (5.46 eV), which corresponds the energy transition of the HOMO to LUMO. The molecular descriptors of the properties of absorption, distribution, metabolism and excretion, and toxicity (ADMET) were obtained. ADMET study showed that the MET-IBU has a distribution volume that allows permeability and activity in the central system nervous (CNS), with structural contributions from the side chain of isobutyl and methoxy that favor liver metabolism and excretion with a low toxic response. Furthermore, the MET-IBU does not have ionizable centers compared to its analog ibuprofen constituting a more lipophilic chemical product.

Acknowledgments

We acknowledge the financial support from CNPq, FUNCAP, and CAPES. Computational support from CENAPAD/UFC for the use of the Gaussian09 software package is also acknowledged.

VII Encontro Brasileiro de Espectroscopia Raman
VII EnBraER
05 a 08/12/2022, São Pedro – SP

MULTI-WAVELENGTH RAMAN SPECTROSCOPY OF POLY(FURFURYL ALCOHOL)

Durval Bertoldo Menezes[3], Maurizio E. Musso[1], Francesco D'Amico[2], Raphael J.F. Berger[1], Andreas Reyer[1], Letizia Scarabattoli[1,4], Nicola Cefarin[2], Thomas Sepperer[5,6], Gianluca Tondi[7], Thomas Schnabel[5], Lisa Vaccari[2]

durval@iftm.edu.br

1 University of Salzburg, Department of Chemistry and Physics of Materials, Jakob-Haringer-Strasse 2a, 5020 Salzburg, Austria

2 Elettra-Sincrotrone Trieste S.C.p.A., Strada Statale 14 km 163,5 in AREA Science Park, 34149 Basovizza (TS), Italy

3 Federal Institute of Triângulo Mineiro, Uberlândia, Minas Gerais, Brazil

4 Università degli Studi di Perugia, Department of Chemistry, Perugia, Italy

5 Salzburg University of Applied Sciences, Forest Products Technology & Timber Construction Department, Marktstrasse 136a, 5431 Kuchl, Austria

6 Salzburg Center for Smart Materials, Jakob-Haringer-Strasse 2a, 5020 Salzburg, Austria

7 University of Padova, Land, Environment, Agriculture and Forestry D 16, 35020 Legnaro (PD), Italy

Palavras Chave: *Poly(furfuryl alcohol), Raman Spectroscopy.*

Highlights

Poly(furfuryl alcohol) (PFA) is a thermo-setting, and an intriguing polymer, his molecular structure is not obvious, and the cross-linking in cured PFA is still not clear. The thermal property, glass transition, is also an important characteristic of this polymer.

Abstract

Poly(furfuryl alcohol) (PFA), produced through polymerization of furfuryl alcohol, is a thermo-setting polymer and basis of thermoset resin systems, and it has been investigated in several studies (IR, 13C-NMR, Raman, DSC), new aspects being considered each time. Nevertheless, PFA still remains an intriguing polymer, since curing, apart from being promoted by the presence of an acid catalyst, can be also induced by heat or suitable radiation, the resulting molecular structure of PFA consequently not being that obvious. Despite the scientific literature already available concerning the Raman spectra of PFA, at present an unambiguous assignation of the Raman bands recorded in cured, cross-linked, and consequently irreversibly hardened PFA is still missing. The purpose of the present study was to investigate the presence and the grade of cross-linking and of conjugation in cured, hardened (thermosetted) PFA in comparison to the pristine, viscous PFA by means of multi-wavelength Raman spectroscopy in the visible and in the ultraviolet spectral range, using excitation wavelengths from several laser sources and from a synchrotron light source. Additionally, by taking advantage from previous findings and foreseen possible molecular structures of PFA, Raman spectra were simulated by first-principles and semi-empiric methods for exploiting them to evaluate their matching with experimental ones. Comparison of published PFA Raman spectra with those obtained in our study evidences important differences for the pristine, viscous PFA and the cured, irreversibly hardened and cross-linked PFA, due to a different molecular structure of the polymer as consequence of the curing process. Furthermore, with excitation wavelengths in the UV range, resonance Raman enhancements can be observed, being also the case in the simulated spectra. Furthermore, Raman measurements of a cured, irreversibly hardened PFA sample in a temperature range between -160°C and 300°C showed some remarkable changes of the spectral profile across this temperature range, being associable with the glass transition. This Raman spectroscopic study of viscous and cured PFA enables us to get a deeper understanding of the spectral features observable in the Raman spectra, possibly improving knowledge for the various applications of PFA.

Acknowledgments

The authors acknowledge financial support provided by the European Regional Development Fund and Interreg V-A Italy Austria 2014 2020 through the Interreg Italy Austria project ITAT1023 InCIMa "Smat Characterization of Intelligent Materials" and ITAT1059 InCIMa4 "InCIMa for Science and SMEs".

VII Encontro Brasileiro de Espectroscopia Raman
VII EnBraER
05 a 08/12/2022, São Pedro – SP

Effect of the pressure on Raman spectra and lattice dynamic calculations of $Bi_2(MoO_4)_3$ crystal

G. D. Saraiva[1*], A. J. Ramiro de Castro[2], A. M. R. Teixeira[3], V. O. Sousa Neto[1], J. A. Lima Jr[4], R. F. Juca[5], J. Maria[5], P.T.C. Freire[4], F. F. de Sousa[6] and W. Paraguassu[6].

gilberto.saraiva@uece.br

[1]Faculdade de Educação Ciências e Letras do Sertão Central, Universidade Estadual do Ceará, CEP 63.902–098, Quixadá, CE, Brazil; [2]Universidade Federal do Ceará - Campus Quixadá. – Cedro – Quixadá – Ceará 63902-580; [3]Faculdade de Filosofia Dom Aureliano Matos, Universidade Estadual do Ceará, CEP 62.930–000, Limoeiro do Norte, CE, Brazil; [4]Departamento de Física, Universidade Federal do Ceará, P. O. Box 6030, CEP 60.455–970, Fortaleza , CE, Brazil; [5]Departamento de Física, Universidade do Estado do Rio Grande do Norte, Mossoró-RN, CEP 59610-210, Brazil; [6]Instituto de Ciências Exatas e Naturais, Universidade Federal do Pará, CEP 66075-110, Belém, PA, Brazil.

Palavras Chave: Raman spectroscopy, $Bi_2Mo_3O_{12}$, Pressure-dependence, Lattice dynamic

Highlights

Pressure-dependent Raman spectra of $Bi_2(MoO_4)_3$ crystal;
Lattice dynamic calculations and vibrational properties of $Bi_2(MoO_4)_3$ based on a rigid ion model;
The principal component analysis (PCA) and hierarchical cluster analysis (HCA).

Resumo/Abstract

This work reports a pressure-dependent Raman spectroscopy study and a theoretical lattice dynamic calculation (LDC) of $Bi_2(MoO_4)_3$ crystal. The LDC was performed, based on a rigid ion model, in order to understanding the vibrational properties of the $Bi_2(MoO_4)_3$ system and in order to assign the experimental Raman modes under ambient conditions. The calculated vibrational properties were helpful to support the pressure-dependent Raman results such as structural changes induced by pressure changes. The Raman spectra were measured in the spectral region between 20 to 1000 cm^{-1} and the pressures values evolution were recorded in the interval of 0.1–14.7 GPa. The pressure-dependent Raman spectra showed changes observed at 2.6, 4.9 and 9.2 GPa, being these changes associated with structural phase transformations. Finally, principal component analysis (PCA) and hierarchical cluster analysis (HCA) were performed to infer the critical pressure of phase transformations undergone by $Bi_2(MoO_4)_3$ crystal.

Agradecimentos/Acknowledgments

The authors, acknowledges the support from the FUNCAP/CAPES/CNPq.

Structural and vibrational properties under low temperatures of the tin-based organohalide (NH4)2SnCl6

Vasco Stascxak Neto (PG) [*1], **Mayra A. P. Gomez (PG)**[1], **Alejandro P. Ayala (PQ)**[1]

vasconeto@fisica.ufc.br

[1] *Departamento de Física, Universidade Federal do Ceará*

Perovskite, Low temperatures, X-rays diffraction.

Highlights

In this work we synthesized and studied the temperature dependency of the Raman spectra of the organohalide (NH4)2SnCl6 and compared with X-Ray diffraction measurements under low temperatures.

Abstract

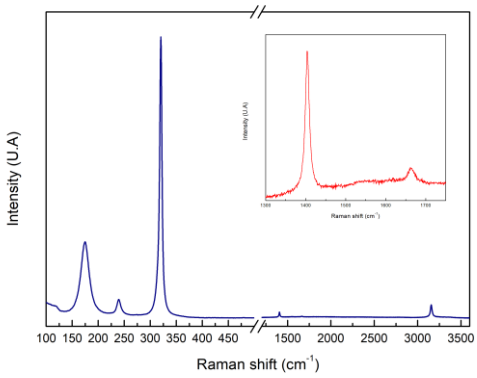

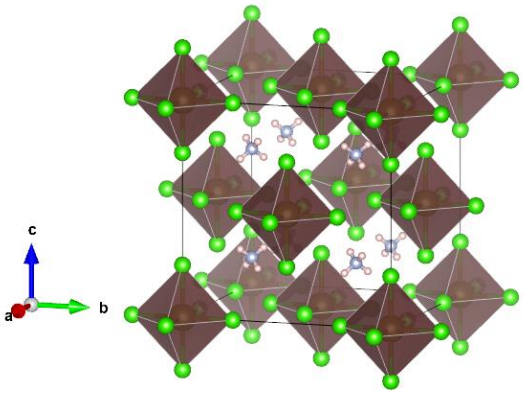

Since the discovery of photovoltaic properties of lead organohalides in 2009 (Kojima et al., 2009), hybrid perovskite-like materials have revolutionized the photovoltaic and photoelectronic industries. However, it is necessary to find alternatives to replace the lead in the metal site of such materials due to its toxicity and one of the possible substitutes is the tin. In this work we synthesized the perovskite-like organohalide (NH4)2SnCl6 by using the slow evaporation method. We were able to determine its structure at various points between 300 K and 90 K by using monocrystal X-rays diffraction. By using temperature dependent Raman spectroscopy, we investigated the vibrational properties of the inorganic and organic ions present in this compound. Through the analysis of the linewidth of the peaks related to organic vibrations we identified that thermal orientation is the main cause of band broadening of these modes, while the anharmonicity contribution was negligible.

Kojima, A., Teshima, K., Shirai, Y., & Miyasaka, T. (2009). Organometal Halide Perovskites as Visible-Light Sensitizers for Photovoltaic Cells. *Journal of the American Chemical Society*, *131*(17), 6050–6051. https://doi.org/10.1021/ja809598r

Acknowledgments

This work was possible thanks to the financial contribution of CAPES and CNPq, as well as the infrastructure provided by Universidade Federal do Ceará.

VII Encontro Brasileiro de Espectroscopia Raman
VII EnBraER
05 a 08/12/17, São Pedro – SP

The Pressure-Induced structural phase transition of $CsCuCl_3$ like-perovskite compound

Juan S. Rodríguez H. (PG),[1,*] Mayra A. Padron G. (PG),[1] Leonardo O. Kutelak (PG),[2] Gustavo A. Lombardi (PG),[2] Ricardo D. Reis (PQ),[2] Alejandro P. Ayala (PQ),[1] and Carlos W. A. Paschoal (PQ).[1]

juan.hernandez@fisica.ufc.br

[1] *Departamento de Física, UFC, Campus do Pici, Bloco 928, Fortaleza, Ceará, Brasil. CEP 65455-900;*
[2] *EMA beamline, Laboratório Nacional de Luz Sincrotron, LNLS, Campinas, São Paulo, Brasil. CEP 13083-100.*

Keywords: *(High-pressure measurements, Synchrotron Radiation, Raman Spectroscopy, structural phase transition, Perovskites).*

Highlights

We deepen further on the high-pressure measurements with the SXRPD (Synchrotron X-ray Powder Diffraction) and Raman spectroscopy on the $CsCuCl_3$ compound in order to quantify the $CuCl_6$ distortion.

Abstract

Halide perovskites are widely studied for several physical properties. In fact, have been described as widespread interest research for revealing astonishing stability in extreme conditions. The like-perovskite halide $CsCuCl_3$ belongs to the ABX_3 materials described as (A=Rb, Cs; B=Mn, Fe, Co, Ni, Cu; X= Cl, Br). It is composed of $CuCl_6$ octahedra chains along the *c*-axis and separated by the isolated Cs^+ ions [1] (***Figure 1a***). The compound below T_N = 10.7 K displayed an antiferromagnetic phase [2], in which it was found that the pressure-induced generates quantum magnetic phases that could be quantified by the $CuCl_6$ distortion [3,4]. In this context, we carried out the high-pressure measurements of the sample, we noticed an abrupt SXRPD pattern (**Figure 1b**) changes consistent with the Raman spectroscopy measurements (**Figure 1c**). Over the Raman experiment, three phases could be extrapolated: a) ***I-Phase*****:** (0 - 2.51) GPa, which is related to the room-temperature crystal structure; b) ***I-II Phase***: (2.79 - 3.57) GPa, a mixture of both low- and high-pressure phases; and c) ***II-Phase****:* (4.01 - 6.94) GPa, the new crystal structure phase determined with the synchrotron radiation. The observed phonons correspond to the internal vibrations of the $CuCl_6$ (**Figure 1d**). The pressure-induced shifts of the vibrational mode frequencies increase linearly with the pressure of all peaks until the ***I-II Phase***, where the number of Raman bands increases, describing a re-orientation of the crystal. The analysis indicated a structural phase transition under pressure at 2.51 GPa from the hexagonal ($P6_522$) to a monoclinic P2 determinate with the Le Bail refinement method.

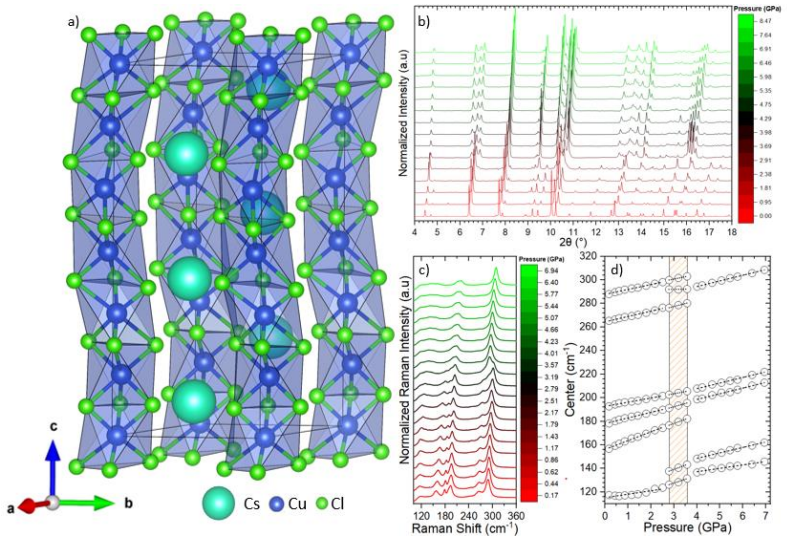

Figure 1: *a) Room-temperature crystal structure of the $CsCuCl_3$ ($P6_522$), b) x-ray synchrotron diffractograms, c) the Raman spectrum and d) Raman modes evolution under high-pressure.*

[1] *Eur. J. Inorg. Chem.* **22**, 2165-2169 (**2020**), [2] *Phys. Rev. B* **105**, 144408 (**2022**), [3] *Nat. Comms.* **12**, 4263 (**2021**), [4] *Phys. Rev. B* **96**, 014419 (**2017**)

Acknowledgments

This investigation was financed in part by the Fundação Cearense de Apoio ao Desenvolvimento Científico e Tecnológico (FUNCAP/PRONEX PR2-0101-00006.01.00/15) and the Conselho Nacional de Pesquisa e Desenvolvimento do Brasil (CNPq – Projeto 140390/2019-7). We also acknowledge the support and facilities from the EMA beamline team at the Laboratório Nacional de Luz Síncrotron SIRIUS.

VII Encontro Brasileiro de Espectroscopia Raman
VII EnBraER
05 a 08/12/2022, São Pedro – SP

Analyzing of Ti-Nb_2O_5 catalysts phase changes after pressure-assisted heat treatment

Daniele T. Dias (PQ),[1*] Pietra B. Pires (IC),[1] Andressa O. Rodrigues (PG),[1] Betina C. Semianko (IC),[1] Maria E. K. Fuziki (PG)[2], Giane G. Lenzi (PQ)[1], Sergio M. Tebcherani (PQ)[1], Simone do R. F. Sabino (PG)[3], Andressa Novatski (PQ)[3]

danieletdias@utfpr.edu.br

[1]Universidade Tecnológica Federal do Paraná - PG; [2]Universidade Estadual de Maringá; [3]Universidade Estadual de Ponta Grossa.

Palavras Chave: *(sol-gel, anatase, rutile, orthorhombic, monoclinic, titanium niobium oxide).*

Highlights

Ti, Nb and Ti:Nb by sol-gel method were characterized. The calcination caused crystalline phase change. Less flexible crystal structures were affected by PAHT. Rutile-TNO 800°C aP showed lowest gap.

Abstract

The improvement in the properties of TiO_2 and the development of new photocatalysts with properties close to or superior to those of titania is one of the points of interest and study in research on photocatalysis and the synthesis of nanomaterials. In this context, the present work aimed to develop TiO_2, Nb_2O_5 and mixed oxides of TiO_2:Nb_2O_5 with characteristics and properties suitable for use as a photocatalyst. In an original synthesis via the sol-gel method [1], the mass of $NbCl_5$ and the volume of isopropoxide of titanium used were varied to obtain photocatalysts with different molar ratios Ti:Nb (100:0; 50:50; 0:100), being finished in a mixture of molar ratio NH_4OH:M=2:1 (where M is the sum of Ti^{4+} and Nb^{5+} ions) and in two temperature levels of calcination (400°C: 800°C). Subsequently, the six synthesized Ti:Nb catalysts were subjected to pressure-assisted heat treatment (PAHT) performed under an air pressure of 2.1 MPa at 110°C for 36 h. Raman spectroscopy provided clear peaks indicating the high crystallinity of the samples. In general, the Raman study showed that an increase in the synthesis temperature of the oxides Ti, Nb and the mixed Ti:Nb caused a change in the crystalline phase from [2; 3]: anatase (Fig.1a) to anatase-rutile (Fig. 1b); T- Nb_2O_5 ($Nb_{16.8}O_{42}$) (Fig. 1c) to H-Nb_2O_5 ($Nb_{12}O_{29}$) (Fig.1d); and anatase-rutile_T-Nb_2O_5 (Fig. 2a) to rutile- titanium niobium oxide ($Ti_2Nb_{10}O_{29}$, TNO) (Fig. 2b), respectively. Fig.1a shows that PAHT did not affect the anatase crystalline phase. On the other hand, PAHT caused a decrease in intensity of several peaks of the oxides at 800°C (Fig.1b and 1.d) and of the mixed oxide at 400°C (Fig. 2a), suggesting that more stable but less elongated and therefore less flexible crystal structures (such as rutile and H-Nb_2O_5) were the most affected by PAHT. In this context, an increase in the ordering of the rutile network and consequent decrease in crystallinity after PAHT can be perceived by the reduction in the band's intensity around 235 cm^{-1} (Fig.1b) supposedly induced by a second-order scattering process or latent disharmony [2]. As in this case, it is possible to discard the way in which the TiO_2 powders were oxidized to their formation (when comparing without - wP and after PAHT - aP); the variation of the bands referring to the phonons of the rutile structure 600 ($A1_g$) and 418 cm^{-1} (E_g) are conditioned to the regular occurrence of defects planar oxygen-deficient rutile [2]. For the well-developed crystal structure of T-Nb_2O_5 at 400°C (in Fig.1c) the bands in the region of 400 – 800 cm^{-1} are attributed to the symmetrical and antisymmetrical elongation mode of the Nb-O-Nb bond. While the Raman band at 235 cm^{-1} becomes the Nb-O-Nb bending mode. The Raman spectrum of sample Nb_2O_5 at 800°C in Fig.1d matched that of H-Nb_2O_5 (monoclinic). A sharp peak is seen at about 1000 cm^{-1}, probably arising from the significant amount of edge-sharing NbO_6 with many short Nb=O bonds in a compact structure. For the samples at 400°C, there is a shoulder at 755 cm^{-1}, but much larger than the one in the region centered at 1000 cm^{-1}, suggesting longer bond lengths and less structural stiffness than for H-Nb_2O_5. Practically all peaks decrease for the anatase-rutile crystal structure and T-Nb_2O_5 (orthorhombic) of the Ti:Nb oxide at 400°C, suggesting oxygen-deficient and an increased flexibility. Using the Shuster-Kubelka-Munk function to obtain the band gap energy from diffuse reflectance measurements, the monoclinic oxide [3] and rutile-TNO oxide (at 800°C) showed the lowest band gap, both with reduction of this optical property after PAHT, the values being 3.01 and 3.00 eV.

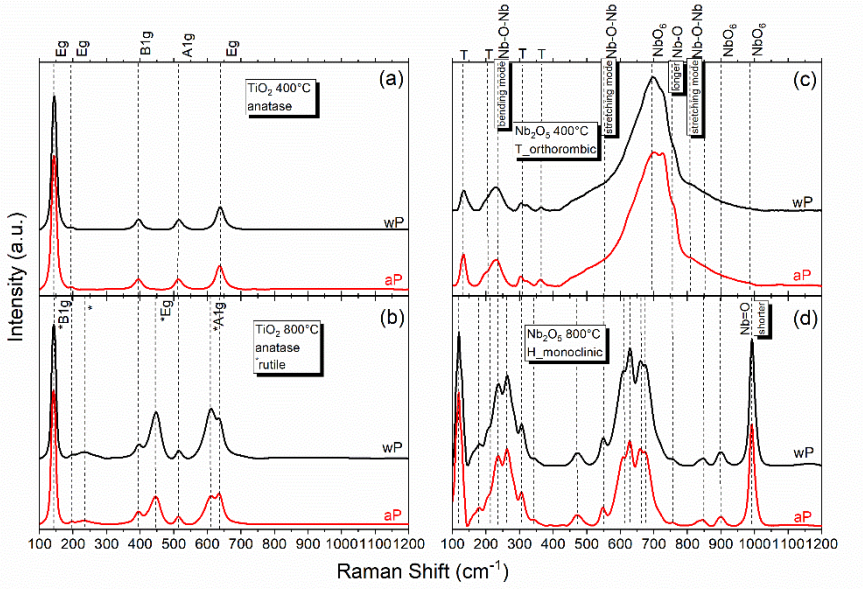

***Fig. 1**: Raman Spectra of TiO_2 and Nb_2O_5 at; (a) and (c) 400°C; (b) and (d) 800°C, respectively. wp=without PAHT; aP=after PAHT*

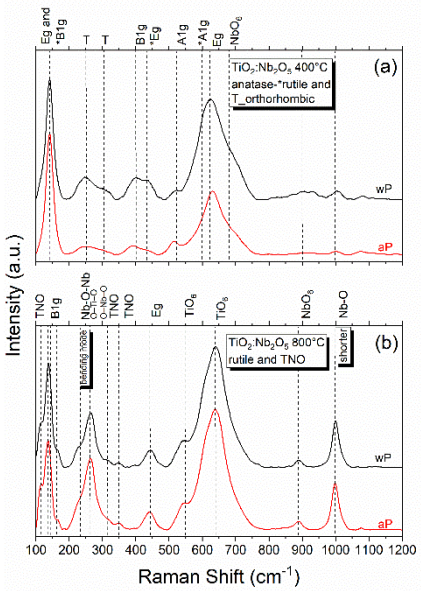

***Fig. 2**: Raman Spectra of Ti:Nb at: (a) 400°C; and (b) 800°C. wp=without and aP=after PAHT*

[1] Fuziki, M. E. K. et al. **Journal of Water Process Engineering**, v. 42, p. 102163, 2021.
[2] Melendres, C. A. et al. **Journal of Materials Research**, v. (5), p. 1246, 1989.
[3] Graça, M. P. F. et al**. Journal of Alloys and Compounds**, v. 553, p. 177, 2013.

Acknowledgments

The authors thank FUNTEF and Fundação Araucária for their financial support and C-LABMU_UEPG and C²MMa_UTFPR for the analyzes carried out.

VII Encontro Brasileiro de Espectroscopia Raman
VII EnBraER
05 a 08/12/17, São Pedro – SP

In-situ pressure measurements in microfluidic devices by micro-Raman spectroscopy

André M. Batista* **(PG)[1], Herculano Martinho (PQ)[1].**

a.batista@ufabc.edu.br

[1]*Programa de Pós-graduação em Nanociências e Materiais Avançados - Universidade Federal do ABC - Av. dos Estados 5001, Santo André/SP.*

Keywords*: Raman, Spectroscopy, Microfluidic Devices*

Highlights

Due to the high use of microfluidic devices to simulate biological assays and in view of the numerous open questions for various pathologies. The objective of this work is to show that Raman spectroscopy can provide a non-invasive and label-free way to evaluate local pressure in microfluidic systems, based on polymers, that simulate biological behavior.

Resumo/Abstract

The microfluidic platform has opened new horizons in the fabrication of biomaterials for the generation of nanomaterials of various structures. Even more interesting is the making of microfluidic organs on chips, which provide a new biological tool in disease modeling, drug discovery, and toxicology research. One of the main causes of death is linked to cardiovascular diseases (CVDs), mainly ischemic heart diseases, hypertension, and cerebrovascular diseases, and its diagnostics has always been considered the most challenging part of cardiac pathology. CVDs, also including coronary heart disease and stroke, is the most common noncommunicable diseases worldwide. Therefore, many studies to miniaturize and simulate these systems are being done, characterizing through Raman spectroscopy which has been showing good results on this subject for some time.

Knowing this, we sought to simulate an artery using a microfluidic device based on a polymer, polydimethylsiloxane (PDMS), which, with our synthesis route, has a Young's modulus very close to that of a human artery (870KPa). We used ethanol and liquid isopropanol to flow in the microchannel (725 µm in diameter) of the microfluidic device to study its behavior under different pressures (Fig. 1). As shown in an example in Fig. 2, we were able to evaluate the pressure variation (ΔP) for a specific band of alcohol, and follow the kinetics of the reaction that takes place in the fluidic medium. Values from 0.1 to 0.5 mL indicate the variation of pressure exerted in mL of the syringe used in the experiments.

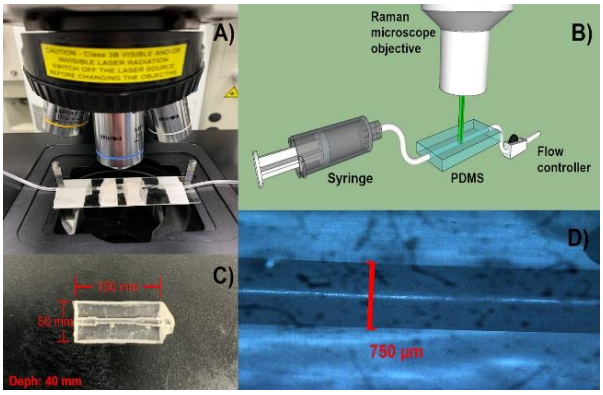

Fig.1

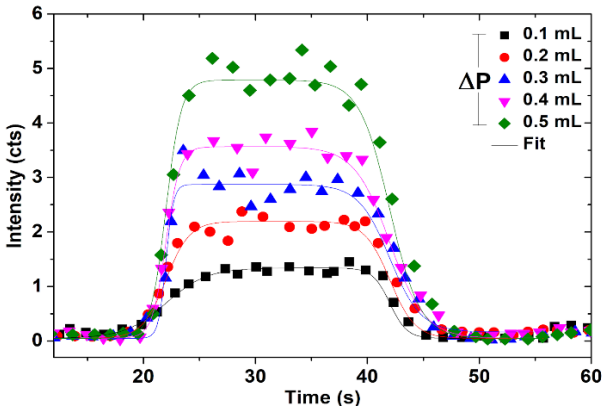

Fig.2

Therefore, the study in question shows a specific profile for each concentration of the two alcohols separately, showing the potential of Raman spectroscopy in an innovative way.

Agradecimentos/Acknowledgments

I would like to thank the Multiuser Experimental Center for making its equipment available for carrying out the experiments. To Professor Herculano for the shared knowledge. We would also like to thank CAPES for the financial support, and the Graduate Program in Nanosciences and Advanced Materials at UFABC.

VII Encontro Brasileiro de Espectroscopia Raman
VII EnBraER
05 a 08/12/2022, São Pedro – SP

Defect Engineering Control on Lanthanum-Doped Ceria Nanoparticles for the Oxidative Coupling of Methane

Fabiane J. Trindade (PQ), Bria Cisi (IC),[1] Daniele C. Ferreira (PQ),[1] Andre S. Ferlauto,[1]

fabianejtrindade@gmail.com

[1]*Centro de Engenharia Modelagem e Ciências Socais Aplicadas, Universidade Federal do ABC, Santo André-SP, Brazil*

Palavras Chave: *cerium oxide, catalyst, doping, defect engineering, oxygen vacancy, disorder*

Highlights

- Defect control on La-doped ceria nanoparticles are critical for applications such as high-temperature oxide catalysts;
- Higher concentrations of La^{3+} doping induces selectivity for OCM reactions;

Resumo/Abstract

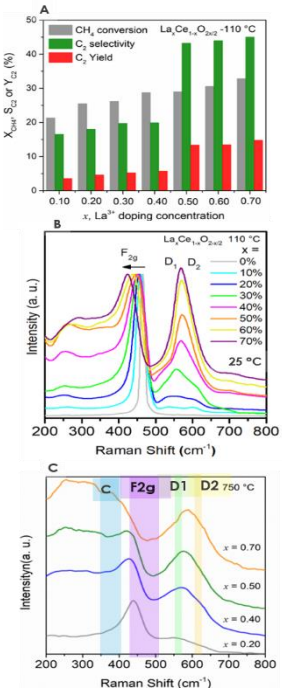

The instability of petroleum prices and the advancements in extraction technologies of natural gas has increased the interest in the direct conversion of methane to C2 products via oxidative coupling of methane (OCM) reactions. The design of catalysts by tailoring the structural defects and disorder has a significant impact on their performance. Within this context, in this work, the fine-tuning of structural defects in rod-like NPs was performed via La^{3+} doping ($La_xCe_{1-x}O_{2-1/2}$), x, in the 10-70 mol% range. The NPs characterization was performed by SEM, HRTEM, XRD, BET and μ-Raman spectroscopy, and the OCM catalytic performance was evaluated at 750 °C (Fig 1a). The relative concentration of reagents (CH_4 and O_2) and products H_2, CO, CO_2, C_2H_4, and C_2H_6 was measured by an online mass spectrometer. XRD and Raman analysis revealed that the CeO_2 fluorite crystalline structure is essentially maintained in the doped nanorods, even for x = 0.7 (Fig1B). The Raman spectra analysis indicates that La doping results in the formation of extrinsic and intrinsic oxygen defects, which increase proportionally to La concentration (Fig.1B). While in-situ μ-Raman reveal at higher La^{3+} content a (F + C) biphasic region was observed, with C being the cubic atomic arrangement typical of sesquioxides of the heaviest rare earths (Fig1c). The catalysts showed good performance for OCM with methane conversion up to 32% and C_2 selectivity up to 44% for x=0.5. In addition, all catalysts showed high stability within 20h time on stream. The demonstrated structural defect control on La-doped CeO_2 NPs can provide important insights to improve the performance of OCM reactions.

Agradecimentos/Acknowledgments

The authors acknowledge the Multiuser Central Facilities (Universidade Federal do ABC), The authors gratefully acknowledge support from the Center for Innovation on New Energies Shell (ANP)/FAPESP(2017/11937-4) and the FAPESP SPRINT project (2019/00776-5) and PRH49-ANP/UFABC.

VII Encontro Brasileiro de Espectroscopia Raman
VII EnBraER
05 a 08/12/2022, São Pedro – SP

In situ Raman spectroscopy of CeO_2:Gd nanoparticles and CeO_2:La nanoplates

Daniele C. Ferreira (PQ), [1,2,*] **Andre S. Ferlauto (PQ)** [1,2]

ferreira.daniele@ufabc.edu.br

[1]*Centro de Engenharia, Modelagem e Ciências Sociais Aplicadas, UFABC;* [2]*Center for Innovation on New Energies – CINE M2P*

Palavras Chave: C*eria, Raman, In situ, Defects.*

Highlights

F_{2g} red shift is observed due to thermal expansion; Increase of I_D/I_{F2g} during heating.

Resumo/Abstract

Ceria (CeO_2) is a material used in catalytic reactions at high temperatures, as heterogeneous catalyst for automotive and oil refineries emissions, due to its oxidation/reduction properties based on Ce^{3+}/Ce^{4+} ratio, good capacity to store oxygen and thermal and chemical stability during catalysis[1,2]. These properties can be enhanced by the incorporation of dopants in the structure, leading to the formation of oxygen vacancies (V_O), produced by a charge compensation mechanism and structural changes such as lattice expansion/contraction and disorder[1,3]. Lanthanum doped ceria nanoplates (10 mol%), named LaC-NP, were synthesized using a co-precipitation method at room temperature, using $NaHCO_3$ as a precipitation agent[4]. Lanthanum was found to enhance the oxygen vacancy formation and enhance catalytic oxidation of CO over other rare-earth dopants[5]. Additionally, the partial substitution of Ce^{4+} for M^{3+} can decrease the reduction temperature of ceria (1400-1500ºC)[6]. Oxygen vacancies can be introduced by doping or thermal treatments in reducing atmospheres[7]. In order to understand the activity of these catalysts at high temperature processes, *in situ* Raman spectroscopy can provide information about the intermediate species formed during a reaction. Raman spectrum of ceria presents one active-mode triply degenerate, F_{2g}, located at 465 cm^{-1}, characteristic of the fluorite structure. According to Nakajima *et al.*[8], the modes at 550 cm^{-1} and 600 cm^{-1} are associated with defect space containing an oxygen vacancy caused by the replacement of Ce^{4+} for Ce^{3+} or a M^{3+} dopant, and the vibration of a MO_8 complex including the dopant, respectively. Raman spectra of LaC-NP were measured at various temperatures using a Linkam CCR1000 stage connected to a temperature controller. With this stage it is also possible to measure Raman spectra under gas flow. With increasing temperature, a red shift is observed due to thermal expansion and there is a reduction in F_{2g} area (I_{F2g}), while the areas of the defect bands (I_D) are almost unchanged until 500ºC. After that, there is a small increase in peak area of defect bands, suggesting an enhancement of oxygen vacancies. Since the doping can decrease the reduction temperature of ceria, release of oxygen from its lattice is possible. A more detailed analysis is still necessary, since some authors report a different behavior of Raman modes as a function of temperature, indicating that is not accurate to compare the ratios between the areas of the peaks to determine if defects are increasing or not [9,10]. For comparison, the same measurements were carried out in a commercial sample of Gd doped ceria nanoparticles.

1. Trovarelli, A., **Catalysis Reviews-Science and Engineering,** 38 (4), 439-520, 1996.
2. Ricken, M.; Nolting, J.; Riess, I., **Journal of Solid State Chemistry,** 54 (1), 89-99, 1984.
3. Hu, Z. P.; Metiu, H., **Journal of Physical Chemistry C,** 115 (36), 17898-17909, 2011.
4. Su, F., Li, P., Huang, J. et al. **Sci Rep** 11, 85, 2021.
5. Singhania, A. **Ind. Eng. Chem. Res.**, 56, 13594-13601, 2017.
6. Sediva, E., et al. **ACS Appl. Energy Mater.**, 4, 2, 1474–1483, 2021.
7. Schimmit, R. et al.. **Chem. Soc. Rev**., 49, 554, 2020.
8. Nakajima, A.; Yoshihara, A.; Ishigame, M. **Physical Review B**, v. 50, n. 18, p. 13297, 1994.
9. Piumetti, M. et al. **Catalysts 7**, 174, 2017.
10. Sartoretti, Enrico et al. **Scientific reports**, v. 9, n. 1, p. 1-14, 2019.

Agradecimentos/Acknowledgments

SHELL, CEM-UFABC, FAPESP, CNPq, CAPES e IPEN

VII Encontro Brasileiro de Espectroscopia Raman
VII EnBraER
05 a 08/12/2022, São Pedro – SP

Structural and Magnetic Properties of $Yb_2Zr_xTi_{2-x}O_7$

Francisco Lieberich (PG)[1], Pedro L. O. Silva (IC)[1], Dimy Nanclares (PQ)[2,3], André S. Ferlauto (PQ)[2], Rafael S. Freitas (PQ)[1] *

dimy.nanclares@ufabc.edu.br

[1]Instituto de Física, USP; [2]Centro de Engenharia, Modelagem e Ciências Sociais Aplicadas, UFABC; [3]Laboratório Nacional de Luz Síncrotron, LNLS.

Palavras Chave: Pyrochlore, Defect fluorite, Disorder, Magnetic Frustration, Spin Liquid.

Highlights

$Yb_2Ti_2O_7$ undergoes a transition from pyrochlore to defect fluorite as Ti is substituted by Zr.

Magnetic ordering is suppressed by increasing structural disorder, suggesting a spin liquid ground state.

Abstract

The pyrochlore family of materials, consisting of over 200 compounds with the structural formula $A_2B_2O_7$, has been explored for many scientific and technological applications and is regarded as one of the most promising experimental models of frustrated magnetism. The extensively studied $Yb_2Ti_2O_7$ pyrochlore is a prominent example of magnetic frustration, displaying a rich magnetic phenomenology, including a puzzling almost-gapless excitation spectrum. Our current understanding of $Yb_2Ti_2O_7$ is that it lives at the very edge of competing ferromagnetic and antiferromagnetic phases, a conclusion already anticipated by the sensitivity to non-stoichiometry at a < 1% level on bulk magnetic and calorimetric properties. There are no previous studies on magnetic properties of $Yb_2Zr_2O_7$ or of the intermediary compounds $Yb_2Zr_xTi_{2-x}O_7$. Pyrochlore family compounds are usually synthesized by the solid-state (SS) reaction. As an alternative, in the sol-gel (SG) method precursor chemicals are mixed in liquid form and the resulting gel is dried out to obtain the desired product. Our group synthesized samples of $Yb_2Zr_xTi_{2-x}O_7$ (x = 0.0, 0.15, 0.3, 0.5, 1.0, 1.5, 2.0) using both methods, to compare their properties and understand the relative advantages of each synthetic route. Structural properties were determined by x-ray diffraction and Raman spectroscopy, indicating that SS samples with x > 0 contain impurities due to unreacted oxide precursors, even after sintering at 1500°C for 120h with three intermediate grindings. SG samples are chemically homogeneous but display significant local structural disorder. When Ti is substituted by Zr (increasing x in $Yb_2Zr_xTi_{2-x}O_7$) the material undergoes a structural transition from an ordered pyrochlore to a disordered defect fluorite for x = 1.0, culminating in the even less symmetric δ-phase for x = 2.0 ($Yb_2Zr_2O_7$). Raman scattering (fig.1) confirms the presence of disorder in SG samples, through broadening of the vibrational modes and appearance of IR modes that are Raman-inactive in the pyrochlore structure. Magnetic susceptibility measurements (fig.2) show that with increasing Zr content the transition temperature to the magnetic ground state decreases (fig.3), consistent with the expectation that structural disorder suppresses magnetic ordering. The ground state of $Yb_2Zr_2O_7$ could be a spin liquid, given the effects of disorder on an already frustrated lattice.

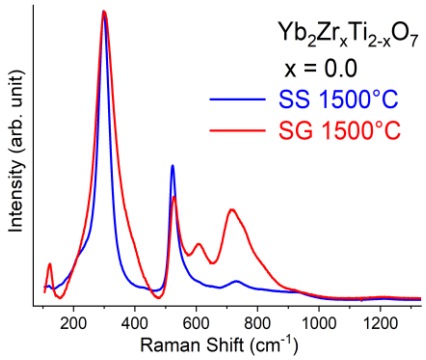

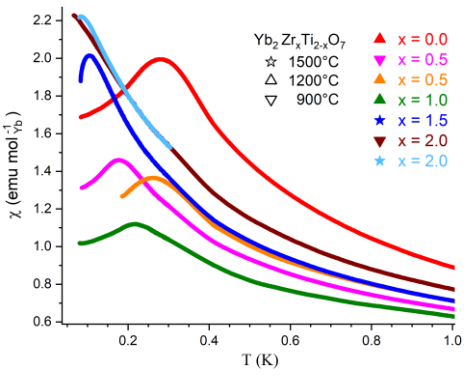

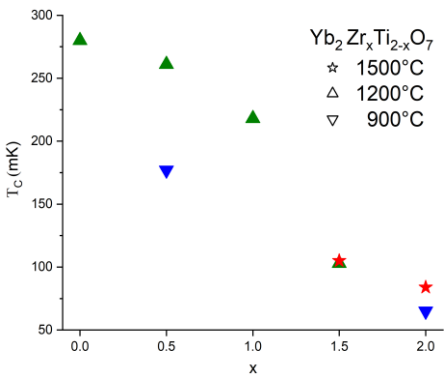

Acknowledgments

We would like to thank CEM-UFABC, FAPESP (2017/11937-4, 2019/00776-5, 2022/08128-5) and CAPES.

VII Encontro Brasileiro de Espectroscopia Raman
VII EnBraER
05 a 08/12/2022, São Pedro – SP

Espectroscopia Raman no estudo de ordem-desordem em catalisadores óxidos mistos para conversão do metano

Dimy Nanclares (PQ),[1,2*] Fabiane J. Trindade (PQ),[1] André S. Ferlauto (PQ)[1].

dimy.nanclares@ufabc.edu.br

[1]Centro de Engenharia, Modelagem e Ciências Sociais Aplicadas, UFABC; [2]Laboratório Nacional de Luz Síncrotron, LNLS.

Palavras Chave: *Desordem, Defeitos, Catálise, Óxidos, Fluorita, Pirocloro.*

Highlights

Raman spectroscopy study on the structural order-disorder in mixed oxides catalysts for methane conversion.

Methane to ethylene direct conversion enhancing by order-disorder control in fluorite-like catalysts.

Resumo

A aplicação bem sucedida de óxidos como catalisadores é profundamente afetada pelos mecanismos de formação de defeitos e propriedades como a condutividade iônica desses materiais. Tais características são intimamente relacionadas ao ordenamento na distribuição dos cátions e vacâncias na rede cristalina. Em particular, para a aplicação de óxidos com a estrutura fluorita no acoplamento oxidativo do metano, nossos estudos sugerem que o ordenamento local de vacâncias melhora a seletividade da reação para a conversão direta do metano em produtos C_2, evitando a oxidação completa do reagente. Este trabalho tem como objetivo controlar a desordem estrutural em óxidos mistos de cério e lantânio, de modo a maximizar o rendimento da reação, encontrando um equilíbrio entre a conversão do metano e sua seletividade para a produção de etileno. Utilizando o modelo de confinamento de fônons, caracterizamos as amostras quanto a sua desordem e tamanhos de partículas a partir dos comprimentos de correlação dos fônons, determinados via ajuste do espectro Raman. Demonstramos que a inclusão gradual de zircônio na rede cristalina ($La_2Ce_{2-x}Zr_xO_7$) induz uma transição da fase controlada da fluorita desordenada para o pirocloro, uma superestrutura ordenada da fluorita, abrindo caminhos para uma engenharia de defeitos aplicada ao sistema de interesse.

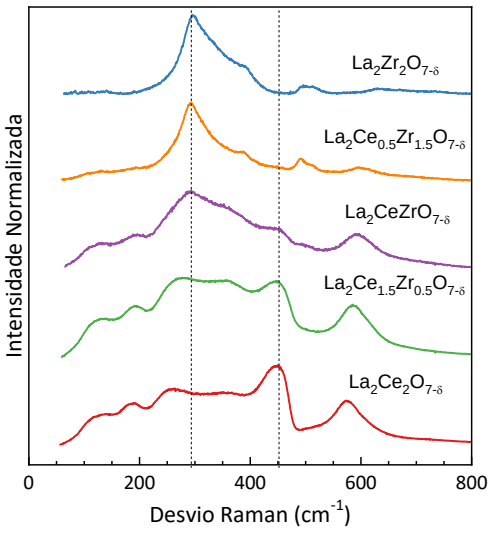

Figura: Espectro Raman das amostras $La_2Ce_{2-x}Zr_xO_7$.

Agradecimentos

Agradecemos à Central Experimental Multiusuário da UFABC, onde foram realizadas as medidas de espectroscopia Raman, e à FAPESP (2017/11937-4, 2019/00776-5, 2022/08128-5) pelo financiamento da pesquisa.

VII Encontro Brasileiro de Espectroscopia Raman
VII EnBraER
05 a 08/12/2022, São Pedro – SP

Vibrational, electronic, electrical, and magnetic properties of double perovskite Sr_2FeMoO_6 prepared by co-precipitation.

Raí F. Jucá (PG),*[1] João M. Soares (PQ),[2] Francisco F. Sousa (PQ),[3] Luiz. F. Lobato (PQ),[3] Antônio J. R. de Castro (PQ),[4] Alexandre M. R. Teixeira (PQ),[5] Marcelo A. Macedo (PQ),[1] Pablo R. T. Ribeiro (PQ),[6] Fernando L. A. Machado (PQ)[6] and Gilberto D. Saraiva (PQ),[7].

[1]Deparatamento de Física, Universidade Federal de Sergipe, São Cristovão-SE; [2]Departamento de Física, Universidade do Estado do Rio Grande do Norte, Mossoró-RN; [3]Instituto de Ciências Exatas e Naturais, Universidade Federal do Pará, Belem-PA; [4]Universidade Federal do Ceará, Quixadá-CE; [5]Faculdade de Filosofia Dom Aureliano Matos – Limoeiro do Norte - Ce; [6]Departamento de Física, Universidade Federal de Pernambuco, Recife-PE. [7]Faculdade de Educação Ciências e Letras do Sertão Central, FECLESC, Quixadá-CE;

Palavras Chave: *Sr_2FeMoO_6, Double perovskite, magnetic properties, EPR, Raman and IR spectroscopy.*

Highlights

Synthesis of the double perovskite Sr_2FeMoO_6 (SFMO) and analysis by X-Ray diffraction (XRD);
Electronic and electrical properties of Sr_2FeMoO_6 semiconductor material;
The magnetization versus applied field (MxH) curve and the electron paramagnetic resonance (EPR) spectroscopy;
Lattice dynamic calculations (LDC) and density-functional theory (DFT).

Resumo/Abstract

In this research study, we report the synthesis of the double perovskite Sr_2FeMoO_6 (SFMO) and analysis by X-Ray diffraction (XRD), Raman and Fourier transform infrared (FT-IR) spectroscopy, scanning electron microscopy (SEM), electronic properties (EP), vibrating sample magnetometer (VSM), magnetoresistance (MR), electron paramagnetic resonance (EPR), electrical transport properties (ET) and lattice dynamics calculation (LDC). At room temperature, the crystalline structure of Sr_2FeMoO_6 was identified as with a tetragonal symmetry structure and I4/mmm (D_{4h}^{17}) space group, with two formulas per unit cell (Z = 2). The scanning electron microscopy (SEM) micrographs of Sr_2FeMoO_6 show that the microparticles form the sample. The microparticles size distribution was evaluated statistically by measuring an average diameter of 1.58 μm, with a second average diameter of the nanoparticles dispersed on the bulk surface of D_{SFMO} = 47.6 nm. In addition, the magnetization versus applied field (MxH) curve and the electron paramagnetic resonance (EPR) spectroscopy were discussed. The magnitude of negative MR with the magnetic field of 5 kOe at 5 and 300 K is as large as 5.8 and 1.7%, respectively. Moreover, vibrational properties were performed using a rigid ion model to assign the experimental Raman and infrared bands.

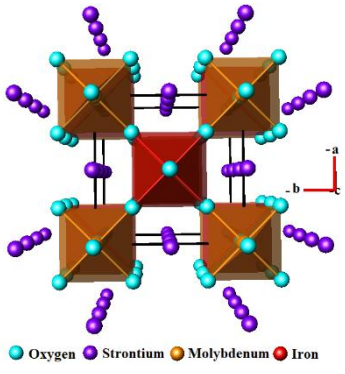

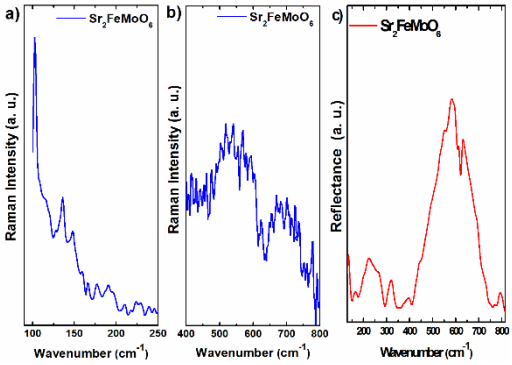

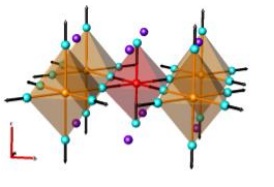
R [770.2 cm^{-1} (υ_1) - A_{1g}]

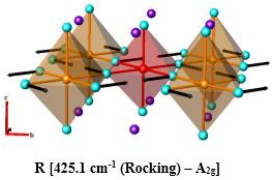
R [425.1 cm^{-1} (Rocking) – A_{2g}]

Agradecimentos/Acknowledgments

The authors, acknowledges the support from the FUNCAP/CAPES/CNPq.

VII Encontro Brasileiro de Espectroscopia Raman
VII EnBraER
05 a 08/12/2022, São Pedro – SP

Investigating the distinct thermal conductivity of AD_2O_6 (*A* = Ni, Co, Zn; *D* = Sb, Ta) using Raman Spectroscopy

Rodolfo Tartaglia (PG),[1] Narayan Prasai (PQ),[2] Aaron. B. Christian (PQ),[3] John J. Neumeier (PQ),[3] Joshua L. Cohn (PQ),[2] and Eduardo Granado (PQ)[1,*].

rtartaglia@if.unicamp.br; egranado@if.unicamp.br

[1]"Gleb Wataghin" Institute of Physics, UNICAMP; [2]Department of Physics, University of Miami; [3]Department of Physics, Montana State University.

Palavras Chave: Thermal Conductivity, Trirutiles, Raman Spectroscopy, Anharmonicity.

Highlights

Substituting Sb by Ta in trirutiles suppresses thermal conductivity by up to one order of magnitude. Raman spectroscopy revealed large lattice anharmonicity as a possible explanation.

Resumo/Abstract

The AD_2O_6 (*A* = Ni, Co, Zn; *D* = Sb, Ta) has attracted recent attention due to the presence of near degenerate magnetic ground states with distinct dimensionality.[1,2] Another intriguing feature of this family is the suppression of the thermal conduction in Ta-based compounds compared with Sb-based ones, regardless of the transition metal ion. A possible scenario of this suppression is the presence of a resonant phonon scattering displayed only by compounds with Sb.[3] Here we explore the origins of the distinct thermal conduction in these samples by measuring the temperature dependence of optical phonons using Raman Spectroscopy. Indeed, our previous work has revealed a strong interaction between e_g orbital excitations and phonons in the $CuSb_2O_6$.[4,5] Measurements were performed between room temperature and 15 K in $NiTa_2O_6$, $NiSb_2O_6$, $CoTa_2O_6$, and $ZnSb_2O_6$. For compounds with Ta, a rich spectrum is observed at low frequencies ($\omega < 180$ cm^{-1}) with phonons that are strongly temperature-dependent, softening upon cooling in the whole temperature range. The low-frequency portion of the spectra is featureless for Sb-based samples, supporting the hypothesis of a coupling between low-energy optical phonons with acoustic ones in the Ta-based compounds. Interestingly, the overall phonon Raman spectra of the Sb-based samples are similar to each other but entirely different to the spectra of the Ta-based compounds despite their similar crystal structure. These discrepancies between the phonon Raman spectra of Ta and Sb-based compounds may be key to understanding their largely different thermal conductivity behavior.

[1] A. B. Christian, S. H. Masunaga, A. T. Schye, A. Rebello, J. J. Neumeier, and Yu-Kuo Yu, Phys. Rev. B **90**, 224423 (2014)
[2] A. B. Christian, C. D. Hunt, and J. J. Neumeier, Phys. Rev. B **96**, 024433 (2017).
[3] N. Prasai, A. Rebello, A. B. Christian, J. J. Neumeier and J. L. Cohn, Phys. Rev. B **98**, 134449 (2018).
[4] D. T. Maimone, A. B. Christian, J. J. Neumeier and E. Granado, Phys. Rev. B **97**, 104304 (2018).
[5] D. T. Maimone, A. B. Christian, J. J. Neumeier and E. Granado, Phys. Rev. B **97**, 174415 (2018).

Agradecimentos/Acknowledgments

The authors would like to thank funding agencies FAPESP (Grants No. 2019/10401-9) and CNPq.

VII Encontro Brasileiro de Espectroscopia Raman
VII EnBraER
05 a 08/12/2022, São Pedro – SP

Polarized Raman spectroscopy of monoclinic $(In,Sc)_2Ge_2O_7$ ceramics

Jéssica I. Viegas (PG),[1*] Anderson Dias (PQ)[1]

jessicaviegas88@gmail.com

[1]*Departamento de Química, ICEx, UFMG*

Keywords: *Pyrogermanates, Ceramic Materials, Rare Earth, Polarized Raman Scattering, Group Theory*

Highlights

$In_2Ge_2O_7$ and $Sc_2Ge_2O_7$ pyrogermanates were studied regarding their optical-vibration properties. Polarized Raman spectroscopy was applied to determine and assign all their phonon modes in sintered ceramics.

Abstract

Ceramic materials with the general formula $A_2B_2O_7$ have attracted much attention in recent decades, mainly due to their versatile chemical compositions, resulting in a big variety of crystal structures, and technological properties. Among the many chemical possibilities, the monoclinic $In_2Ge_2O_7$ and $Sc_2Ge_2O_7$ ceramics exhibit a real opportunity to investigate the effects of cationic changes on their optical-vibration properties. In this work, the materials were obtained by the solid-state reaction route, and their features were analyzed by X-ray diffraction, transmission electron microscopy, and Raman spectroscopy. Furthermore, the ceramic materials were investigated using polarized Raman spectroscopy, in order to assign all the fifteen phonon modes predicted by group theory for the monoclinic phase, *C2/m* space group, as shown in Fig.1. Fitting procedures were applied to the unpolarized spectra to determine the band positions for both materials, and to compare the values based on the rare earth ion present in the structure.

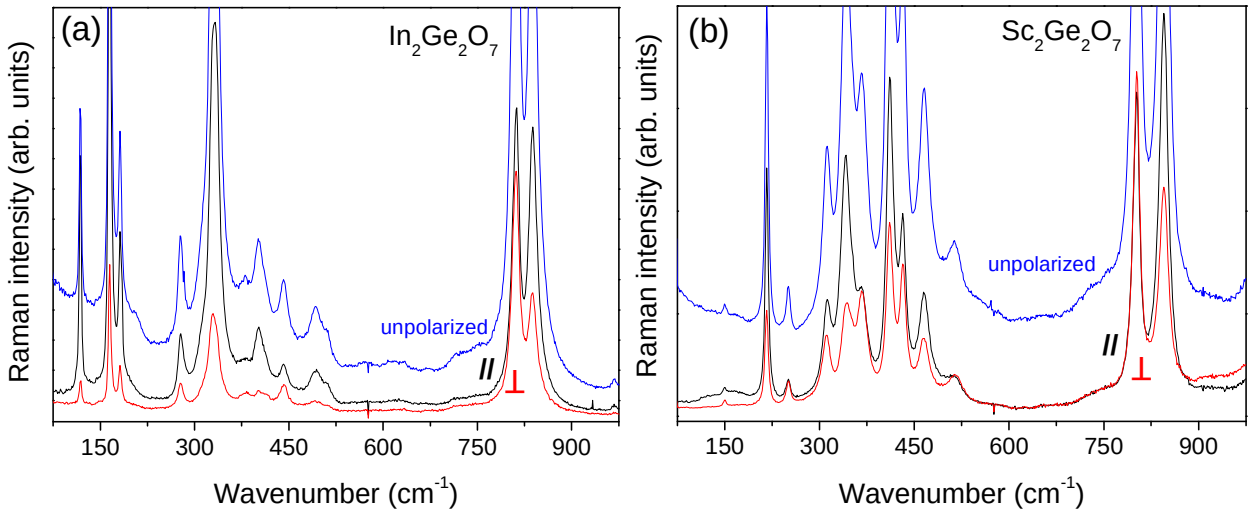

Fig.1: Polarized Raman spectra of (a) $In_2Ge_2O_7$ and (b) $Sc_2Ge_2O_7$ sintered ceramics. A_g modes are favored in parallel configuration (black curves), while B_g modes are enhanced in perpendicular light (red curves). The unpolarized spectra are shown in blue.

Acknowledgments

The authors acknowledge the financial support from Conselho Nacional de Desenvolvimento Científico e Tecnológico (CNPq) and Fundação de Amparo à Pesquisa do Estado de Minas Gerais (FAPEMIG).

VII Encontro Brasileiro de Espectroscopia Raman
VII EnBraER
05 a 08/12/2022, São Pedro – SP

Vibrational and magnetic properties of iron tungstate (Fe_2WO_6) at low temperature

Raí F. Jucá (PG),[1,*], Antônio J. R. de Castro (PQ),[2] João M. Soares (PQ),[3] José A. S. da Silva (PG),[4] Francisco G. S. Oliveira (PQ),[5] Igor F. Vasconcelos (PQ),[5] and Gilberto D. Saraiva (PQ),[1].

[1]Faculdade de Educação Ciências e Letras do Sertão Central, FECLESC, Quixadá-CE; [2]Universidade Federal do Ceará, Quixadá-CE; [3]Departamento de Física, Universidade do Estado do Rio Grande do Norte, Mossoró-RN; [4]Departamento de Física, Universidade Federal do Ceará, Fortaleza-CE; Pós-graduação em Engenharia e Ciências de Materiais, Centro de Tecnologia, Universidade Federal do Ceara, Fortaleza-CE,

Palavras Chave: Fe_2WO_6, *Raman* spectroscopy*, FTIR, magnetic properties, tungstate and Mossbauer.*

Highlights

Synthesis of the iron tungstate Fe_2WO_6 and analysis by X-Ray diffraction (XRD);
Investigation of the magnetic properties of iron tungstate Fe_2WO_6 at low temperatures;
The magnetization versus applied field (MxH) curve and the electron paramagnetic resonance (EPR) spectroscopy.

Resumo/Abstract

In this research study, we report the synthesis of iron tungstate (Fe_2WO_6) through the solid-state reaction method. The characterizations of Fe_2WO_6 was made using X-ray diffraction techniques; Raman and Fourier transform infrared spectroscopy (FT-IR), vibrating sample magnetometer (VSM) and Mossbauer spectroscopy. The temperature dependence Raman spectroscopy and vibrating sample magnetometer were measurements in a temperature range of 300-10K. At room temperature, the crystal structure of Fe_2WO_6 was identified as having orthorhombic symmetry structure and Pbcn space group (D_{2h}^{14}), with one formula per unit cell (Z = 1). The magnetization versus applied field (MxH) and the Mossbauer spectrum of Fe_2WO_6 at room temperature was discussed. The slight Raman spectral changes occurring in the vibrations of the lattice modes and in the region of the internal modes. In addition, it was also possible to observe changes in the (MxH) curve at low temperature.

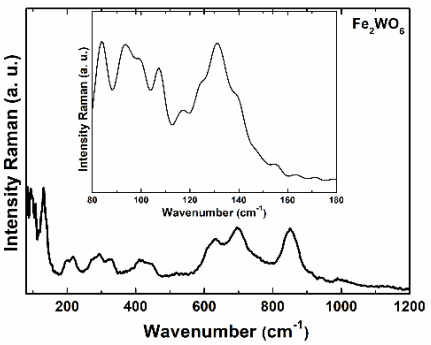

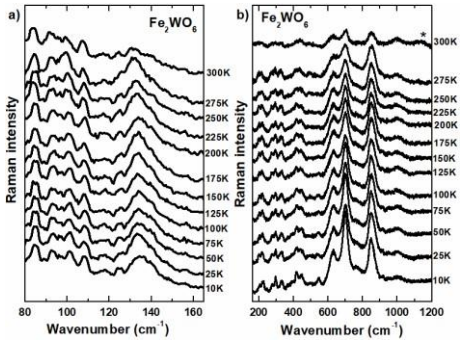

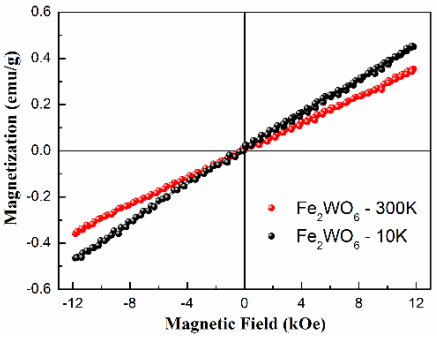

Agradecimentos/Acknowledgments

The authors, acknowledges the support from the FUNCAP/CAPES/CNPq.

VII Encontro Brasileiro de Espectroscopia Raman
VII EnBraER
05 a 08/12/2022, São Pedro – SP

Observation of coupled orbital-lattice dynamics in $CuSb_2O_6$

Carlos W. Galdino (PG) [1], Tulio C R Rocha (PQ)[1,2], Eduardo Granado (PQ) [1]

tulio.rocha@lnls.br

[1]Instituto de Física Gleb Wataghin (IFGW), Universidade Estadual de Campinas (UNICAMP); [2] Laboratório Nacional de Luz Síncrotron (LNLS), Centro Nacional de Pesquisa em Energia e Materiais (CNPEM)

Palavras Chave: Orbital, Electronic Raman, Cuprate, X-ray, RIXS, Strongly correlated

Highlights

Quantum spin chain Mott insulator $CuSb_2O_6$ with trirutile structure
Raman indicates phonon anomalies assigned to orbital dynamics
RIXS shows orbital ordering and coupled orbital-lattice excitations

Resumo/Abstract

Emerging collective excitations are ubiquitous in solids and play a central role in understanding materials whose macroscopic properties are governed by quantum behavior. Well known exemples are phonons, the collective excitations corresponding to lattice vibrations in a crystal, and magnons, the corresponding spin waves in a magnetically ordered states. Similarly, modulations in the shape of the electronic clouds in an orbitally ordered state can give rise to orbital waves, or 'orbitons'. One of the best studied orbitally ordered systems is the perovskite $LaMnO_3$, in which the dispersive orbiton has been theoretically predicted. Raman scattering reported the orbitons in $LaMnO_3$ [1], however, its existence has not been verified by other experiments. Another prototypical orbital ordered perovskite is $KCuF_3$ for which experimental efforts to observe dispersive orbital waves have been unsuccessful for many years [2]. Here, we investigate the Mott insulator $CuSb_2O_6$ with trirutile structure, for which an unconventional $3z^2-r^2$ orbital ordered ground state was theoretically proposed to explain its intriguing one-dimensional Heisenberg antiferromagnetism. In previous work, Granado and co-workers observed notable anomalies in the Raman scattering $CuSb_2O_6$ [3]. An electronic excitation at 550 cm^{-1}, ascribed to an orbital wave, which softens on warming and strongly interferes phonons, causing an asymmetric broadening of the latter and a possible formation of a vibronic state above 300 K. In this work we employ high energy-resolution Resonant Inelastic X-ray (RIXS) to elucidate the orbital order of $CuSb_2O_6$ and the nature of the electronic excitations observed by Raman. RIXS at the L-edge resonance is a well-established method for directly probing local and collective excitations in transition metal oxides [4]. We observe inelastic features at 1.2-1.5 eV corresponding to local crystal field excitations with t_{2g} symmetry. At 0.45 eV, we observe a broad feature assigned to the e_g excitation. Single ion cluster multiplet calculations confirm these assignments. Both e_g and t_{2g} excitations are nondispersive in the reciprocal space, but have asymmetric lineshapes considerably broader than instrumental resolution, suggesting strong coupling to phonon modes. The elastic scattering at zero energy loss shows strong intensity enhancement at (±¼, ±¼, l) in reciprocal space, clearly indicating electronic correlations assigned to dynamical orbital order. Moreover, the low energy quasi-elastic region shows a feature around 40-80 meV (~323-645 cm^{-1}) compatible with the peak in Raman scattering assigned to an orbiton, with significant momentum dispersion indicative of a collective nature. Polarization resolved experiments are still needed to confirm the orbital character of this excitation. Nevertheless, the combination of RIXS and Raman have already provided clear indications of orbital dynamics coupled to phonons in $CuSb_2O_6$ not observed in the canonical orbital ordering perovskite systems.

[1] E. Saitoh et al. *Nature*. **410**, 180–183 (2001).
[2] J. Li et al. *Phys. Rev. Lett.* **126**, 106401 (2021).
[3] D. T. Maimone et al. *Phys. Rev. B*. **97**, 1–5 (2018).
[4] L. J. P. Ament et al. *Rev. Mod. Phys.* **83**, 67 (2010).

Agradecimentos/Acknowledgments

We thank the Swiss Light Source, Diamond Light Source and BessyII for the use of RIXS beamlines.

VII Encontro Brasileiro de Espectroscopia Raman
VII EnBraER
05 a 08/12/2022, São Pedro – SP

Synthesis, structural, vibrational and optical properties of the $SrCuSi_4O_{10}$ ceramic.

Raí F. Jucá (PG),[1,*], José S. Sarmento (PG),[2] Pierre B. A. Fechinea (PQ),[2] João M. Soares (PQ),[3] W. Paraguassu (PQ),[4] Francisco F. de Sousa (PQ),[4] Luiz. F. Lobato (PQ),[4] Antônio J. R. de Castro (PQ),[5] and Gilberto D. Saraiva (PQ),[1].

[1]Deparatamento de Física, Universidade Federal de Sergipe, São Cristovão-SE; [2]Grupo de Química de Materiais Avançados (GQMat), Departamento de Química Analítica e Físico-Química, Universidade Federal do Ceará, Fortaleza-CE; [3]Departamento de Física, Universidade do Estado do Rio Grande do Norte, Mossoró-RN; [4]Instituto de Ciências Exatas e Naturais, Universidade Federal do Pará, Belém-PA; [5]Universidade Federal do Ceará, Quixadá-CE; [6]Faculdade de Educação Ciências e Letras do Sertão Central, FECLESC, Quixadá-CE;

Palavras Chave: *$SrCuSi_4O_{10}$; Dielectric ceramic; electronic properties; SEM; Raman and IR spectroscopy.*

Highlights

Synthesis of the $SrCuSi_4O_{10}$ ceramic and analysis by X-Ray diffraction (XRD);
Electronic and electrical properties of $SrCuSi_4O_{10}$ ceramic dieletric;
Electron paramagnetic resonance (EPR) of the $SrCuSi_4O_{10}$;
Lattice dynamic calculations (LDC) and density-functional theory (DFT).

Resumo/Abstract

This research reports the synthesis and characterization of the ceramic $SrCuSi_4O_{10}$. To obtain the $SrCuSi_4O_{10}$ ceramic powder, the solid-state synthetic route was applied. The $SrCuSi_4O_{10}$ ceramic characterization were made by using X-ray diffraction, Raman and Fourier transform infrared (FT-IR) spectroscopy, scanning electron microscopy (SEM), reflectance (R), electron paramagnetic resonance spectrum (EPR), lattice dynamic calculations and the electronic properties calculations were performed on the basis of Density Functional Theory (DFT). The ceramic $SrCuSi_4O_{10}$ belongs to a tetragonal system with the P_4/ncc space group, containing two formula units per unit cell (Z = 2). SEM micrographs of the $SrCuSi_4O_{10}$ presents a morphology layered microplates with some irregularity in their size and shapes. The UV-vis diffuse reflectance spectra shown three intense reflection regions. Regarding vibrational properties, the calculation was performed using a rigid ion model in order to assign the experimental Raman and infrared bands and the electronic properties calculations were performed based on Density Functional Theory (DFT).

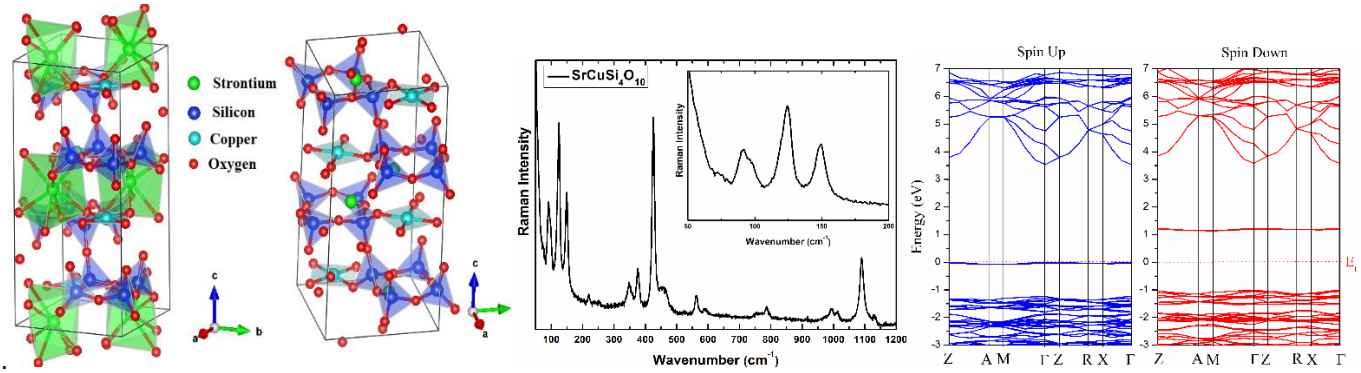

Agradecimentos/Acknowledgments

The authors, acknowledges the support from the FUNCAP/CAPES/CNPq.

VII Encontro Brasileiro de Espectroscopia Raman
VII EnBraER
05 a 08/12/2022, São Pedro – SP

O espalhamento Raman correlacionado Stokes-anti-Stokes: um estudo da influência da largura temporal do pulso de excitação.

Lucas V. Carvalho (PG),[1] Tiago A. Freitas (PG),[2] Paula D. Machado (PG),[1] Raul Corrêa (PG),[1] Carlos H. Monken (PQ),[1] Marcelo F. Santos (PQ),[3] Ado Jorio (PQ)[1,*]

l.carvalente@gmail.com

[1]Departamento de Física, UFMG; [2]Departamento de Engenharia Elétrica, UFMG; [3]Instituto de Física, UFMG.

Highlights

The Stokes-anti-Stokes (SaS) correlated Raman scattering: a study of the influence of the temporal width of the excitation pulse. In this work, we studied the influence of the excitation pulse temporal width on the production efficiency of Stokes-anti-Stokes correlated pairs and measured the spectrum of formation of these pairs.

Resumo/Abstract

Nesse trabalho estudamos o espalhamento Raman correlacionado Stokes-anti-Stokes (SaS) em uma amostra de diamante e a influência que a largura temporal do pulso de excitação possui na intensidade de formação dos pares correlacionados produzidos no processo. Para esse estudo foram utilizados dois sistemas de excitação com diferentes larguras temporais de pulso, um com largura temporal de femtossegundos e um com largura temporal de picossegundos. Com esses lasers de excitação foram realizados dois experimentos com diferentes modos de filtragem do sinal: No primeiro experimento essa filtragem é realizada com filtros passa-banda, e nessa configuração temos uma eficiência maior de detecção que nos permite comparar melhor a eficiência de produção de pares entre as diferentes excitações; no segundo experimento, utilizamos um monocromador para realizar a filtragem do sinal, essa configuração nos possibilita uma varredura no comprimento de onda da detecção e, assim, conseguimos medir o espectro de formação desses pares correlacionados.

Os resultados apresentados nesse trabalho nos mostraram que a eficiência na formação de pares correlacionados é maior com o uso do laser de excitação de pulso de femtossegundos, o que é esperado para um processo óptico não-linear. Na região de frequência ressonante Raman, observamos uma intensidade aproximadamente 1,5 vezes maior com o laser de femtossegundos, e nas regiões fora de ressônancia a intensidade de formação foi aproximadamente 5 vezes mais intensa na região de frequência menor e 9 vezes mais intensa na região de frequência maior que a frequência de ressonância.

Nas medidas do espectro de formação desses pares no entorno da região de frequência ressonante do pico de espalhamento Raman de primeira ordem, nossos resultados confirmaram a existência de uma assimetria na formação dos pares entre as regiões de dessintonização positiva e negativa. Essa assimetria ainda permanece sem uma explanação teórica satisfatória.

Agradecimentos/Acknowledgments

Agradeçemos às agências de fomento CAPES e CNPq pelo apoio financeiro para a realização do projeto.

VII Encontro Brasileiro de Espectroscopia Raman
VII EnBraER
05 a 08/12/2022, São Pedro – SP

Estudo das polarizações dos fótons Stokes e anti-Stokes no espalhamento inelástico de luz correlacionado no diamante

Tiago Abreu Freitas (PG),[1*] Paula D'Avila Machado (PQ),[2] Raul Corrêa(PQ),[1] Lucas V. de Carvalho(PG),[1] Carlos H. Monken (PQ),[2] Marcelo F. Santos (PQ)[3], Ado Jorio (PQ),[1,2]

tiago.tiagofreitas@gmail.com

[1]Programa de Pós-Graduação em Engenharia Elétrica, UFMG; [2]Departamento de Física, UFMG; [3]Departamento de Física, UFRJ

Palavras Chave: *Informação Quântica, Espalhamento Raman, Correlação Stokes e anti-Stokes, tomografia de estados.*

Highlights

Study of the properties of Stokes and anti-Stokes in the inelastic scattering of light by matter for application in quantum information

Stokes–anti-Stokes correlated photons.
Photonic transport of information.
Quantum state tomography of two photons.
Two-photons polarization entanglement.
Quantum Transport of Information.

Resumo/Abstract

As últimas décadas foram marcadas por intensas pesquisas voltadas para a evolução dos sistemas computacionais e de comunicação. Dentro desse contexto, a computação quântica tem sido uma das áreas que mais despertam interesse e esforços por parte dos pesquisadores, devido ao imenso potencial oferecido. Pesquisas de informação quântica tem passado por inúmeros estágios de evolução, sendo que o transporte fotônico apresenta-se como um dos mais promissores para o processamento de informações. Pesquisas relacionadas à geração de estados quânticos em grande escala são motivadas devido ao seu potencial para revolucionar a computação e as comunicações por meio de tecnologias quânticas otimizadas. Os canais de comunicação ótica redefiniram o escopo e as aplicações da computação clássica; semelhantemente, a transferência fotônica de informações quânticas promete abrir novos cenários para a computação quântica, sendo uma das fronteiras mais promissoras para o processamento de informações. Dentro do contexto da utilização de fótons para o transporte de informação, a espectroscopia Raman, que consiste em uma técnica de espectroscopia ótica baseada no espalhamento inelástico da luz, onde os fótons espalhados carregam informação referente à energia de vibração do meio, apresenta-se como uma via interessante para a codificação e transporte quântico de informação. Neste trabalho exploramos o fenômeno do espalhamento Raman correlacionado, analisando a caráter quântico do fenômeno. Foi implementado um aparato experimental para a medida do caráter de correlação dos fótons gerados nos espalhamentos Stokes e anti-Stokes em diamante, confirmando seu caráter quântico e otimizando o fenômeno para seu uso na codificação e transmissão de informações. Mais especificamente, foram realizadas medidas de tomografia de estado gerado sob esta configuração, com o objetivo de caracterizar o estado do fenômeno SaS de forma a validar o emaranhamento em polarização do respectivo fenômeno, com objetivo de utilizá-lo como base para implementação de um protocolo para codificação e transmissão de informações.

Agradecimentos/Acknowledgments

Os autores agradecem à Fapemig, Capes, Finep.

VII Encontro Brasileiro de Espectroscopia Raman
VII EnBraER
05 a 08/12/2022, São Pedro – SP

Synthesis and characterization of hydrochar obtained from nanocellusose and cellulose.

Alessandra A. Aquino (PG)[1], Antonio J. R. Castro (PQ)[2,*], Gilberto D. Saraiva (PQ)[3], Raí F. Jucá (PG)[4], Vicente O. Sousa Neto (PQ)[3], Antonio G. Souza Filho (PQ)[5], Adley Forti Rubira[6] e Odair P. Ferreira (PQ)[7*]

[1]Universidade Federal do Ceará - Rede Nordeste de Ensino (RENOEN); [2]Universidade Federal do Ceará (UFC) - Campus Quixadá; [3]Faculdade de Educação, Ciências e Letras do Sertão Central; [4]Universidade Federal de Sergipe; [5]Universidade Federal do Ceará – Departamento de Física. [6]Universidade Estadual de Maringá – Departamento de Química, [7]Universidade Estadual de Londrina – Departamento de Química. E-mail: joelcastro@fisica.ufc.br

Palavras Chave: Biomass Hydrochar, Biochar, FTIR, Carbonaceous materials,

Highlights

- A systematic study on the influence of the reaction parameters to obtaining hydrochars was carried out;
- The hydrochars were characterized by their structural, vibrational, compositional, textural, and morphological properties.

Resumo/Abstract

The hydrochars (HC) were prepared from hydrothermal carbonization (HTC) of nanocellulose and cellulose. The reaction parameters (time, temperature, pH and initial mass) were varied to understand the influence of each in the final products. The Van Krevelen diagram of these HC showed that the carbonization degree is directly proportional to the initial mass, temperature and reaction time. The compositional analysis CHNS revealed that the reaction medium acts as a catalyst (acidic pH) or retarding (basic pH) of the carbonization reactions. Furthermore, it was observed that increasing reactional temperature the carbon contents in the hydrochars were also increased and, consequently, increasing the heating energy value (HHV). The FTIR spectrum of hydrochar, prepared at 230°C, differs drastically from the precursor. This distinction can be observed by the spectral profile of the precursor and HC, such as relative intensity of the bands, width at half height, and disappearance or appearance of several bands. In this context, the hydrochars have functional groups distinct from the precursor, such as hydroxyls, carboxylic acid, alcohol, and other chemical groups. In addition, the presence of the C = C bond around 1580 cm^{-1} attributed to the aromatic domains was identified. It was also revealed that the increase in initial mass, temperature and reaction time intensifies the bands between 700 and 900 cm^{-1} attributed to C-H and C=C bonds of aromatic rings. The diffraction pattern of hydrochars is typical of amorphous carbon. The morphology of the particles is irregular, but it was possible to observe some microsized spherical particles embedded in the carbonaceous matrix. The nitrogen adsorption- desorption isotherms of the hydrochars were of type II and III with type III hysteresis, reveling that these products are non-porous materials and they have relatively low specific surface areas (between 19 and 35 m^2g^{-1}). The set of results discussed in this work showed that the HTC process is promising in the generation of carbonaceous or composite materials, making it possible to add value to biomass and increase its potential for applications.

Agradecimentos/Acknowledgments

The authors acknowledges the support from the FUNCAP/CAPES/CNPq.

VII Encontro Brasileiro de Espectroscopia Raman
VII EnBraER
05 a 08/12/2022, São Pedro – SP

Synthesis and characterization of hydrochar and biochar from chitosan

Antonio J. R. Castro (PQ)[1,*], Alessandra A. Aquino (PG)[2], Gilberto D. Saraiva (PQ)[3], Vicente O. Sousa Neto (PQ)[3], Raí F. Jucá (PG)[4], Antonio G. Souza Filho (PQ)[5], Alcineia C. Oliveria (PQ)[6], Odair P. Ferreira (PQ)[7*]

[1]Universidade Federal do Ceará (UFC) - Campus Quixadá; [2]Universidade Federal do Ceará - Rede Nordeste de Ensino (RENOEN); [3]Faculdade de Educação, Ciências e Letras do Sertão Central; [4]Universidade Federal de Sergipe; [5]Universidade Federal do Ceará – Departamento de Física; [6]Universidade federal do Ceará – Departamento de Química, [7]Universidade Estadual de Londrina – Departamento de Química. E-mail: joelcastro@fisica.ufc.br

Palavras Chave: Hydrochar, Biochar, FTIR, Carbonaceous materials, Chitosan.

Highlights

- This work presents a systematic study on the preparation of hydrochar and biochar obtained from the HTC and pyrolysis of chitosan.
- Materials were characterized to understand structural, vibrational, compositional, textural, and morphological properties.

Resumo/Abstract

The recent scientific and technological developments from biomass produced with inputs from sustainability using renewable sources are generating new materials with different properties such as, morphological, porosity and structural. In this sense, it was used the hydrothermal carbonization (HTC) and pyrolysis from chitosan to produce carbonaceous materials. The emphasis on the structural and textural properties were given. Furthermore, the influence of time (6, 12, 24, 48 and 120 h) and temperature (160/180 °C) parameters on the physicochemical characteristics of hydrothermal carbon was evaluated. The pyrolysis of chitosan was carried out under nitrogen flow, with a heating rate of 10 °C/min, at temperatures from 200 to 800 °C and remained for 1 h at the desired temperature, with 500 mg of the initial mass. The structural, textural, compositional, and morphological analyzes were performed using the following techniques: XRD, EDS, FTIR, Raman, CHN, TGA, SEM, TEM and BET. Typical low structural ordering of amorphous carbon was observed for the hydrothermal products. Compositional results have shown that the carbon contents increased with increasing of the time and temperature of HTC. Nitrogen contents varied from 5 to 6 %, independently of the reaction parameters. Additionally, hydroxyl, amine, and amide groups remained or were produced on solid surfaces, as show in FTIR. Besides, the biochar (pyrolyzed chitosan) obtained from the pyrolysis carried out at 300 °C reveals that the chitosan structure was lost, indicating the formation of a non-ordered carbonaceous material, characteristic of amorphous carbon, but increasing the reaction temperature causes the graphitization process. When the pyrolysis was carried out at 300 °C, the surface area of the solids was 82 m^2/g and the values of the textural properties decreased with increasing reaction temperature (>500 °C) to values close to zero, indicating a non-porous solid. The functional groups of biochar decrease with the increasing temperature of pyrolysis, where the precursor source undergoes drastic dehydration. The features of the nanomaterials produced in this work enable them to act as catalyst supports, and new adsorbents, showing promise in agriculture fields as well.

Agradecimentos/Acknowledgments

The authors, acknowledges the support from the FUNCAP/CAPES/CNPq.

VII Encontro Brasileiro de Espectroscopia Raman
VII EnBraER
05 a 08/12/2022, São Pedro – SP

Number of layers and defect density characterization in graphene. From nano optics to industrial application

Vítor Monken* (PG)[1,2], João Luiz E. Campos* (PQ)[1], Rafael Nadas (PG)[1], Thiago L. Vasconcelos (PQ)[3], Cassiano Rabelo (PQ)[1], Hudson Miranda (PQ)[1], Ado Jorio (PQ)[1,2], Luiz Gustavo Cancado (PQ)[1,2]

vitor.pena.monken@gmail.com

[1]Departamento de Física , Universidade Federal de Minas Gerais, Belo Horizonte.
[2]Programa de pós graduação em inovação tecnológica, Universidade Federal de Minas Gerais, Belo Horizonte.
[3]Divisão de Metrologia de Materiais, Instituto Nacional de Metrologia, Qualidade e Tecnologia, Duque de Caxias.

Palavras Chave: *(Espectroscopia Raman, Grafeno, Nano metrologia, Densidade de Defeitos, TERS, Nano óptica.*

Highlights

-Tip enchanced Raman Spectroscopy of graphene nanoflakes.
-Defect density caracterization and determination of number of layers of industrially produced graphene.
-Nano caracterization to support in-line quality control protocol of a Graphene production industrial plant.
-Nanometrically resolved non destructive optical caracterization

Resumo/Abstract

The growing interest in the study and application of nanomaterials generated the need to develop specific metrological tools and methods for the area. This movement gave rise to Nanometrology, a multidisciplinary field addressing the most diverse knowledge areas. In this work, we discuss the results of Raman spectroscopy experiments conducted in the nanometric resolution, with the application of tip-enhanced Raman spectroscopy of graphene nanoflakes produced by liquid phase exfoliation at an industrial scale. With these experiments, we were able to measure individual nanoflakes in great detail and thus, verify the validity of previous works conducted by the MG graphene project, where a well-defined relationship between defect density and number of layers was established. With this relationship validated, we show its applicability in the macro metric monitoring of the industrial production of graphene, via in-line Raman spectroscopy monitoring of the processing plant. With this development, we trace a parallel between nano, micro and macro scale raman spectroscopy of Graphene, and apply our findings to improve industrial production of this material.

Agradecimentos/Acknowledgments

The authors acknowledge Fapemig, Capes ad Codemge.

VII Encontro Brasileiro de Espectroscopia Raman
VII EnBraER
05 a 08/12/2022, São Pedro – SP

Tip-enhanced Raman Spectroscopy: a historical perspective based on event chronology analysis

Márcia Dias Diniz Costa (PQ),[1,2] Luiz Gustavo de O. L. Cançado (PQ),[2] Ado Jorio (PQ)[2,*]

marciaddc@ufmg.br

[1]Instituto Nacional de Metrologia, Qualidade e Tecnologia, INMETRO; [2]Departamento de Física, Instituto de Ciências Exatas, UFMG

Palavras Chave: *Tip-enhanced Raman Spectroscopy, History Review, Scientific Instrumentation Development, Retrospective Technology Roadmapping, Event Frame*

Highlights

Tip-enhanced Raman spectroscopy is in the verge of raising the community of users by its diffusion to other application areas. Academic institutions have been the leading actors in this endeavor.

Resumo/Abstract

The development of tip-enhanced Raman spectroscopy (TERS) is studied from the perspective of scientific instrumentation development [1]. The research is based on the analysis of qualified events in the history of electron microscopy, scanning probe microscopy and TERS, aimed to capture the influencing factors in the development of a scientific instrument for nanotechnology. In the case of TERS history, events are qualified papers categorized by experts as dominated by science (S), technology (T), application (A) and market emphasis (Figure 1). Our results indicate that although, in total, more papers have focused on technological development, application-oriented works become the most important type of publication in the last years, mainly by the academic community, alone or in association with national laboratories [2]. As part of the analysis, we invited TERS VII International Conference participants to answer an e-mail survey about TERS trajectory. We conclude that to be more diffused, TERS needs to raise the community of users by being applicable to other areas, which will be possible by turning the instrument in a "one-hour photo lab" type [3].

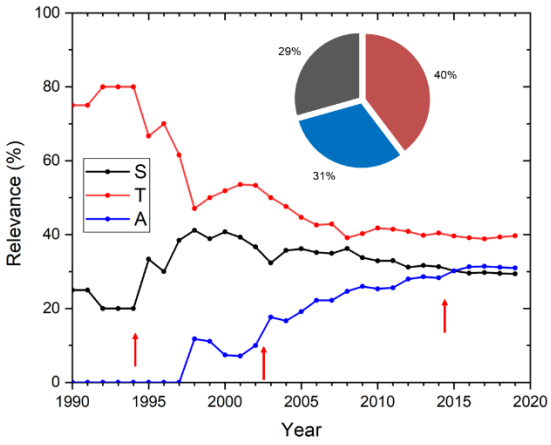

Figure 1 – Evolution of relevance (in %) of documents according to the science (S), technology (T), application (A), or market approach. The inset shows the total accumulated % distribution. The red arrows point on the years of changes in behavior.

[1] A. Van Helden. The Uses of Science in the Age of Newton. Berkeley: University of California Press, p. 49-84 (1993).
[2] M.D.D. Costa, A. Jorio, L.G. Cançado. Journal of Raman Spectroscopy 52:587-599 (2021).
[3] D. Baird, A. Shew. Discovering the Nanoscale. Amsterdam: IOS Press, p. 145-156 (2004).

Agradecimentos/Acknowledgments

Programa de Pós-Graduação em Inovação Tecnológica e Propriedade Intelectual da UFMG, Inmetro.

VII Encontro Brasileiro de Espectroscopia Raman
VII EnBraER
05 a 08/12/2022, São Pedro – SP

Tip-Enhanced Raman spectroscopy (TERS) of TiO_2@Al_2O_3 core-shell nanoparticles

Victor H. F. Sales (PG)[1], Thiago A. de Moura (PG)[1], Gabriel A. P. Rocha (IC)[1], Davino M. A. Neto (PG)[1], Pierre B. A. Fechine (PQ)[1], Alexandre R. Paschoal (PQ)[1].

contato@enbraer.org

[1]*Departamento de Física, Universidade Federal do Ceará.*

Palavras Chave: *TiO_2, Functionalized Nanoparticles, Raman, TERS.*

Highlights

On this work, we characterize nanoparticles (NPs) of TiO_2 coated with Al_2O_3 by means of the sub-nano resolution technique TERS. Results show remarkable differences between the spectra from the isolated nanoparticles in comparison to the bulk material, suggesting that a strong TERS effect was obtained.

Resumo/Abstract

TiO_2 is an inorganic filter commonly used in industry in suncreens due to its protective effect against UV radiation on the skin. However, its inherent photocatalytic activity limits its use. The process of coating TiO_2 can decrease this activity, and one such common coating agent is Al_2O_3. Hence, on this work, the spectroscopic properties of the surface functionalization of TiO_2 with Al_2O_3 are studied. Analyzing the Raman spectrum of the bulk material (powder form), we observed four proeminent bands (Fig. 1 a)): at 134 cm^{-1}, 225 cm^{-1}, 436 cm^{-1} and 597 cm^{-1}. For the spectrum of the isolated NPs (Fig. 2 b)), we also observed four peaks: at 144 cm^{-1}, 223 cm^{-1}, 436 cm^{-1} and 595 cm^{-1}. By comparing the Raman spectra of the bulk and dispersed material, there's a clear change in the relative intensities and widths of the bands. While the spectrum of the bulk sample, the most intense peaks are at 436 cm^{-1} and 597 cm^{-1}. For the TERS spectrum of a single nanoparticle, the peak at 144 cm^{-1} seems far away dominant over the other two bands observed in the bulk material. This suggests that the 436 cm^{-1} and 597 cm^{-1} bands are related to bulk properties. Another remarkable difference between the spectra is the change in the half-width at half-maximum (HWHM) of the first band of each sample. In the bulk material, the 134 cm^{-1} band has HWHM of 8.03 cm^{-1}, for the isolated NP, the 144 cm^{-1} peak has HWHM of 4.82 cm^{-1}. Raman peaks assignments and data treatment of the TERS images are under analysis for today's date.

Figure 1 – Raman spectra of the a) bulk material and b) isolated nanoparticle.

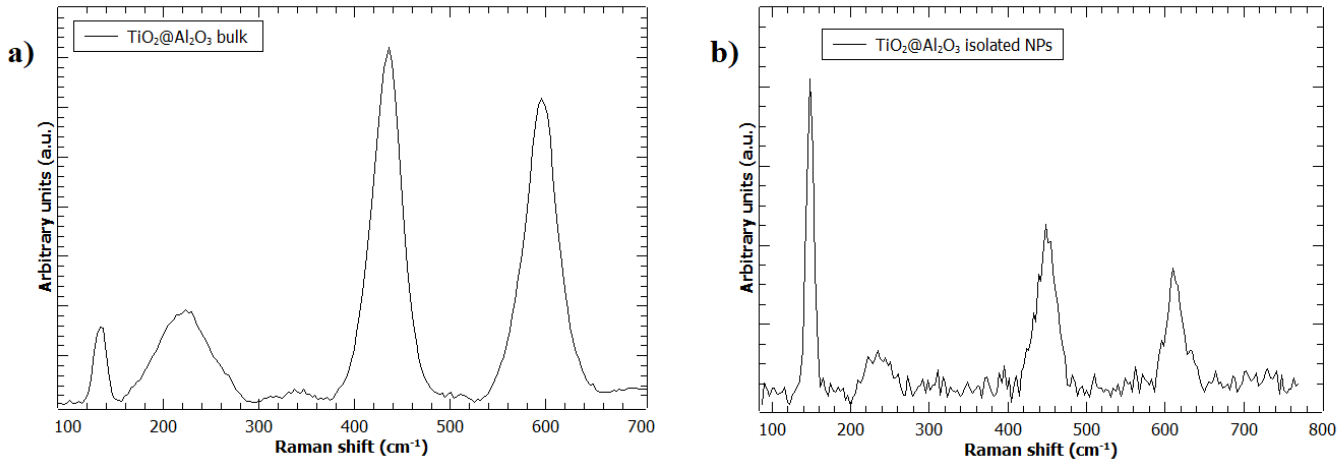

Agradecimentos/Acknowledgments

The authors wish to acknowledge the financial support of the Brazilian National Research Council (CNPq).

VII Encontro Brasileiro de Espectroscopia Raman
VII EnBraER
05 a 08/12/17, São Pedro – SP

Characterization of phosphorous dopped Carbon Quantum Dots by Tip-Enhanced Raman Spectroscopy

Thiago A. Moura* (PG),[1,2] Ludwing Marenco (PG),[1] Antônio A. Cruz (PG),[3] Samuel V. Carneiro (PG),[3] Manoel L. A. Neto (IC),[1] Rafael M. Freire (PQ),[3] Pierre B. A. Fechine (PQ),[3] Carlos L. César (PQ),[1] Alexandre R. Paschoal (PQ),[1].

thiagomoura@fisica.ufc.br

[1]Departamento de Física, UFC; [2]Instituto Federal de Educação, Ciência e Tecnologoa do Ceará, IFCE; [3]Departamento de Química Analítica e Físico-Química, UFC.

Palavras Chave: *Carbon Quantum Dots, Tip-Enhanced Raman Spectroscopy, Principal Component Analyses.*

Highlights

The isolated doped Carbon Quantum Dot's (CQD's) sample was investigated through Tip-Enhanced Raman Spectroscopy (TERS) and Principal Componente Analyses (PCA) in order to characterize its structural and surface defects.

Resumo/Abstract

Carbon quantum dots have found several applications in recent years, some of them based in dispersed nanoparticles, but the complete characterization of its vibrational properties remained unclear, as the Raman spectra of isolated carbon dots have too low intensity. We have investigated bottom-up synthetized carbon quantum dots (CQDs) prepared using citric acid and doped with phosphorous in order to characterize its chemical structure in isolated or almost isolated samples, revealing characteristics that are not evident in bulk samples and that may be relevant for several applications. The analyses with Tip-Enhanced Raman Spectroscopy (TERS) allowed the characterization in nanoscopic scale of the doped CQD sample. It was observed that the Raman spectra varies significantly over different carbon dots, indicating that each one may possess different configurations of terminal groups and defects. The spectra of Figure 1 show that the vibrational properties of the sample varies quickly from isolated building blocks (Figure 1a) to small aggregates (Figure 1b), and consequently to bulk sample (Figure 1c). Such a fact can be explained by considering that the study of isolated CQDs allows a clear analysis of the individual vibrational contributions to the Raman spectrum; another contribution to this might come from the variation of surface area at each case. Despite most of the bands present in the bulk sample Raman spectrum are also observed in the TERS spectra of isolated particles, they vary significantly in intensity position over the isolated or almost isolated sample. In order to surpass this difficulty and to provide a detailed analysis of the Raman peaks, Principal Component Analysis (PCA) tools were employed to process the TERS data. Finally, part of the results obtained through TERS are in agreement with SERS experiments in purified graphene quantum dots in reference (Wu et al., 2018).

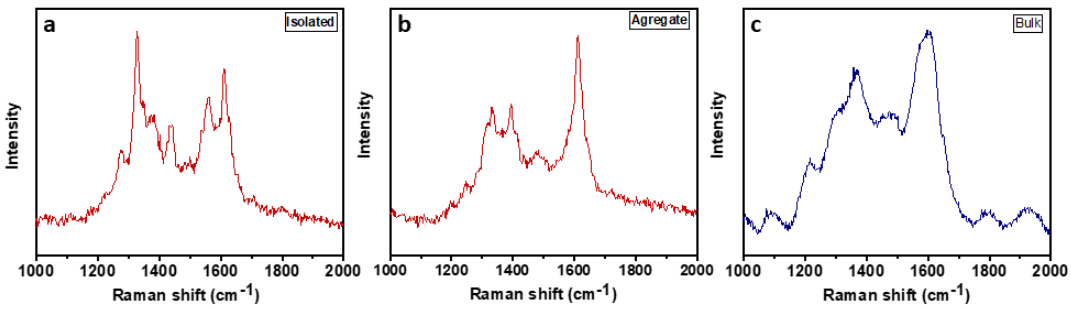

Figure 1. (a) TERS spectrum of an isolated CQD. (b) TERS spectrum of a small agregate of CQDs. (c) Confocal Raman spectrum of the CQD's bulk sample.

Agradecimentos/Acknowledgments

This investigation was financed in part by the Conselho Nacional de Pesquisa e Desenvolvimento do Brasil (CNPq).

VII Encontro Brasileiro de Espectroscopia Raman
VII EnBraER
05 a 08/12/2022, São Pedro – SP

The electron-phonon coupling to produce photoluminescence excitonic states in the 2D $CsPb_2Br_5$ related-perovskite

Mayra A. P. Gómez (PG),[1,*] Juan S. R. Hernández (PG),[1,] Wellington C. Ferreira (PQ),[1] Bruno S. Araújo (PQ),[1] Carlos W.A. Paschoal (PQ),[1] Alejandro P. Ayala (PQ)[1]

mayra@fisica.ufc.br

[1]*Departamento de Física, Universidade Federal do Ceará, UFC.*

Keywords: **(***2D Perovskite, Electron-Phonon Coupling, Raman Spectroscopy, Self-Trapped Excitons).*

Highlights

The $CsPb_2Br_5$ as indirect bandgap material is more susceptible to strong electron-phonon coupling. In L-T Raman and PL spectroscopy experiments were possible to attribute the origin of the narrow PL.

Abstract

The 2D $CsPb_2Br_5$ is one of the perovskites-related inorganic derivates from the $CsPbBr_3$ compound, which is an ideal candidate for photodetectors and solar cell due to their low-cost raw-element constitution and their high-quality optoelectronic properties. We discuss the modification in the materials with the Single Crystal X-Ray Diffraction (SCXRD), Raman spectroscopy, and Photoluminescence (PL) techniques. Also, the $CsPb_2Br_5$ as indirect bandgap material is more susceptible to strong electron-phonon coupling, allowing excitons states. Hence, with the low temperatures, Raman **(Figure 1a)** and PL spectroscopy **(Figure 1b)** experiments were possible to attribute the origin of the narrow PL in the material to a free-excitons (FE) mechanism emission. The low-dimensional sample energy distribution of emissive states excitons allows a self-trapped exciton (STE) broadband at temperatures lower than 60 K displaying an exciton-exciton recombination process, where the PL emission increase the intensity. The Raman modes evolution at low temperatures described the dynamics in the crystal lattice and is dominated by anharmonic effects.

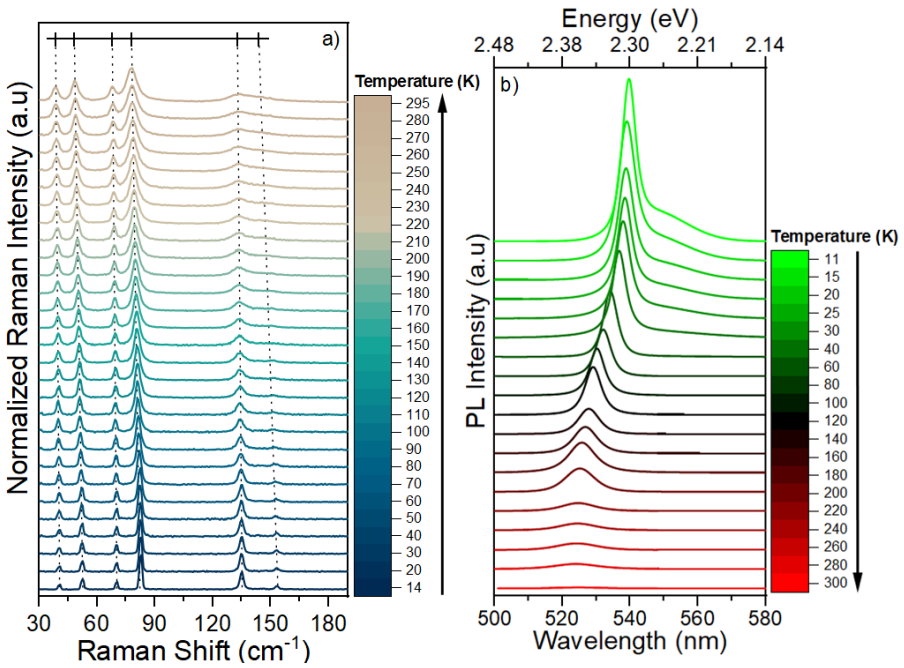

Figure 1: *Low-temperature a) Raman Spectroscopy and b) Photoluminescence experiments in the 2D $CsPb_2Br_5$ perovskite-related.*

Acknowledgments

This study was partially financed by the Brazilian Agencies CAPES (Finance Code 001), FUNCAP (PRONEX PR2 0101- 00006.01.00/15), FINEP (CTINFRA 2013), and CNPq (grant no. 427478/2016-2).

VII Encontro Brasileiro de Espectroscopia Raman
VII EnBraER
05 a 08/12/2022, São Pedro – SP

Effect of preheating a composite resin on physicochemical properties and degree of conversion

Lidiane V. Castro-Hoshino (PQ)*[1], Mariana S. Gibin (PG)[1], Antonio Medina Neto (PQ)[1], Mauro Luciano Baesso (PQ)[1], Francielle Sato (PQ)[1].

lidiane.hoshino@gmail.com

[1]*Physics Departament, Universidade Estadual de Maringá, UEM, Maringá-PR.*

Keywords: *composite resin, preheating, physicochemical, degree of conversion.*

Highlights

Study indicates the heating of the composite resin showed spectral differences between the initial (20 ºC) and final (70 ºC) temperature, however, the preheating did not improve the DC.

Abstract

Preheating dental resins improves material flow dynamics, mechanical properties and degree of conversion (DC), contributing to the restorations longevity [1]. In this sense, the objective of this work was to evaluate the physicochemical changes caused during heating and the DC of the composite resin (Filtek Universal A2, 3M), using Raman spectroscopy. A confocal Raman spectrometer (λ=785 nm, Senterra, Bruker Optik GmbH) was used in the analysis. The heating of the sample (n=5) was performed using a temperature control system (T95, Linkam Scientific) in the range of 20 to 70 ºC, for 60 minutes. The degree of conversion (DC) was evaluated by selecting 10 points along the length of the sample (n=5). The analysis as a function of heating show spectral differences when compared to the group at the initial temperature (20 ºC), indicating physicochemical changes. Principal Component Analysis (PCA) was applied to the spectra to distinguish the different temperatures. In PC1 loading, it was observed that the bands 1639, 1026 and 996 cm^{-1} present a great contribution to differentiate the spectra. To quantify the bands, the area under the curve of each region was calculated. The results showed a statistically significant difference between the initial (20 ºC) and final (70 ºC) temperatures. The monitoring of the samples temperature for the evaluation of the DC showed that after preheating the resin was at 59.90 ºC, after being inserted into the matrix and before photoactivation it was at 26.10 ºC. The DC analysis were performed by evaluating the area ratio of the bands centered at 1639 and 1600 cm^{-1}, referring to the aliphatic C=C and aromatic C=C bands, respectively. The results showed the same decreasing behavior between the group at initial temperature (20 ºC) and preheated to (70 ºC). The heating of the samples showed spectral differences between the initial (20 ºC) and final (70 ºC) temperature, however, the preheating did not improve the DC.

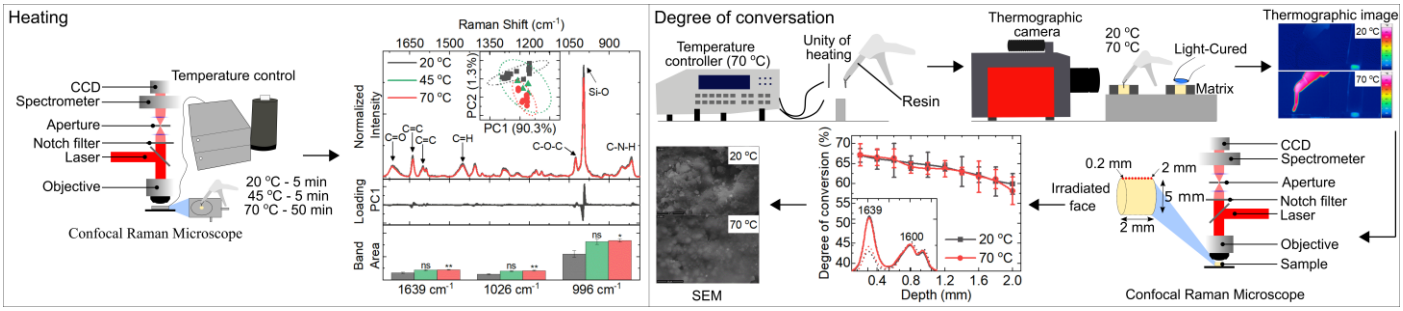

[1] Catalán et al. **Polymer Bulletin**. 2022.

Acknowledgments

The authors are grateful to the Brazilian agencies, CAPES, CNPq, Finep and Fundação Araucária for their financial support in this work and Universidade Estadual de Maringá.

VII Encontro Brasileiro de Espectroscopia Raman
VII EnBraER
05 a 08/12/2022, São Pedro – SP

Synthesis of chitosan/graphene oxide/polyethyleneimine sponges for the treatment of aqueous solutions contaminated by Cu^{2+} and Ni^{2+}

Michel Lopes Franco* (IC)[1,2], Janaína Sobreira Rocha (PQ)[1], Adisom Lucas da Silva Leonardo (IC)[1,2], Thiago A. Moura* (PG)[3], Pierre B. A. Fechine (PQ)[2]

Janaina.sobreira@nutec.ce.gov.br

[1]Gerência de Materiais (GEMAT), Núcleo de Tecnologia e Qualidade Industrial do Ceará – Nutec, Rua Professor Rômulo Proença, s/n – Pici, Fortaleza, Ceará, Brasil; [2]Departamento de Química Analítica e Físico - Química, Universidade Federal do Ceará – UFC, Campus do Pici, Fortaleza, Ceará, Brasil; [3]Departamento de Física, Universidade Federal do Ceará – UFC, Campus do Pici, Fortaleza, Ceará, Brasil.

Palavras-Chave: *Óxido de grafeno, Polietilenoimina, Quitosana, Íons de metais pesados, Adsorção.*

Highlights

A chitosan/graphene oxide/polyethyleneimine sponge was synthesized for the removal of heavy metal ions, where the sponges could be easily collected from the wastewater after the adsorption process.

Resumo/Abstract

Cobre (II) e níquel (II) são metais pesados e, portanto, tóxicos e bioacumulativos. Assim, quando liberados no meio ambiente de forma descontrolada, esses elementos podem causar efeitos indesejáveis à saúde humana e ao próprio ambiente. O óxido de grafeno tem atraído grande atenção em remediação ambiental devido à sua estrutura distinta, muitos grupos tensoativos e alta estabilidade. No entanto, o OG tende a se auto-empilhar ou agregar de forma irreversível em razão de suas fortes interações interplanares, que reduzem sua área de superfície substancialmente e, assim, enfraquecem sua performance de aplicação no tratamento de águas residuais. A polietilenoimina (PEI) contém uma grande quantidade de aminas que são frações ativas facilitam as ligações íon-amida. Neste trabalho, preparou-se scaffolds a partir de OG, PEI e quitosana para remoção de íons Cu^{2+} e Ni^{2+} presente em soluções aquosas. Para a síntese do OG foi empregado o método de Hummer's modificado, que consiste em oxidar o pó de grafite (com tamanho menor que 20 µm / Sigma-Aldrich) utilizando um agente oxidante em meio ácido. Seguidamente, o OG foi funcionalizado com a PEI e realizada a preparação das esponjas fazendo uso da quitosana pelo método de dispersão. Os grupos funcionais presentes OG/PEI servem como sítios de ligação para a complexação de íons de metais pesados. Para caracterizar os grupos funcionais nos componentes e as esponjas resultantes, experimentos de FTIR foram realizados. Para o OG, as bandas dominantes em torno de 3326, 2976 e 1730 cm^{-1} foram atribuídas a uma vibração de estiramento de —OH ou —COOH, —CH_3 e C=O, respectivamente, demonstrando a formação de grupos contendo oxigênio na superfície das nanofolhas. Para GO@PEI, as bandas em torno de 1124 cm^{-1}, relativos ao estiramento C—N, e o desaparecimento em 837, 3293 e 3369 cm^{-1}, correspondente a deformação N—H fora do plano e aos estiramentos NH_2 simétrico e assimétrico, respectivamente, confirmando a funcionalização do nanomaterial. No espectro Raman das amostras de OG e grafite, usado como material de partida, revela a banda em 1330 cm^{-1} associada ao modo vibracional das arestas de grafite que é conhecido como desordem ou banda "D". A banda em torno de 1580 cm^{-1} é conhecida como banda "G" ou banda de grafite. Após a redução do OG pela polietilenoimina, a intensidade da banda "D" aumenta em relação à banda "G" devido à redução do OG. Os resultados de difração de raios-X confirmam o êxito da síntese. Foi realizado os experimentos de adsorção de íons de metais pesados comprovando a capacidade adsorvente para captura de Cu^{2+} e Ni^{2+}.

Agradecimentos/Acknowledgments

This investigation was financed in part by the Conselho Nacional de Pesquisa e Desenvolvimento do Brasil (CNPq).